



University of **HUDDERSFIELD**

University of Huddersfield Repository

Elamin, Fathi

Fault Detection and Diagnosis in Heavy Duty Diesel Engines Using Acoustic Emission

Original Citation

Elamin, Fathi (2013) Fault Detection and Diagnosis in Heavy Duty Diesel Engines Using Acoustic Emission. Doctoral thesis, University of Huddersfield.

This version is available at <http://eprints.hud.ac.uk/id/eprint/19324/>

The University Repository is a digital collection of the research output of the University, available on Open Access. Copyright and Moral Rights for the items on this site are retained by the individual author and/or other copyright owners. Users may access full items free of charge; copies of full text items generally can be reproduced, displayed or performed and given to third parties in any format or medium for personal research or study, educational or not-for-profit purposes without prior permission or charge, provided:

- The authors, title and full bibliographic details is credited in any copy;
- A hyperlink and/or URL is included for the original metadata page; and
- The content is not changed in any way.

For more information, including our policy and submission procedure, please contact the Repository Team at: E.mailbox@hud.ac.uk.

<http://eprints.hud.ac.uk/>

Fault Detection and Diagnosis in Heavy Duty Diesel Engines Using Acoustic Emission

Fathi Hassen Elamin

A thesis submitted to the University of Huddersfield in partial
fulfilment of the requirements for the degree of Doctor of
Philosophy

The University of Huddersfield

November 2013

ABSTRACT

A condition monitoring program applied to diesel engines, improves safety, productivity, increases serviceability and reduces maintenance costs. Investigation of a novel condition monitoring systems for diesel engine is attracting considerable attention due to both the increasing demands placed upon engine components and the limitations of conventional techniques. This thesis documents research conducted to assess the monitoring capabilities used acoustic emission (AE) analysis. It focuses on the possibility of using AE signals to monitor the fuel injector and oil condition.

A series of experiments were performed on a JCB, four-stroke diesel engine. Tests under healthy operating conditions developed a detailed understanding of typical acoustic emission generation in terms of both the source mechanisms and the characteristics of the resulting activity. This was supplemented by specific tests to investigate possible acoustic emission generation due to the piston slap and friction.

The effect of faults on the injector waveform was investigated using the injection system and at one sensor location. To overcome the reflections and injection system configuration effects the method of acoustic emission impedance was used. This enabled the injector signal to be successfully extracted and clearly shows its capability for detecting even minor combustion deviations between engine cylinders.

Comparison between signals and measurement of the oil condition showed both provided useful information about the lubrication processes. Simulation and experimental work have demonstrated the capability of this technique to detect lubrication related faults and irregular lubrication variability between the engine's cylinders.

A review of the AE sources in diesel engines and how to represent the AE signals generated is presented. Three analysis methods were used: time-domain analysis using parameters such as Root Mean Square (RMS), variance, mean and kurtosis; frequency-domain analysis which relied on the amplitudes of the frequency components of the measured signals; and time-frequency domain analysis extracting features so that the energy content of the signals and the frequency components were localized simultaneously.

In this work, data has been obtained from tests on a diesel engine, where the engine load, speed, temperature and the oil lubrication type were changed. The monitored signal and its difference from that obtained for normal engine conditions was noted as a fault signature that could be used for fault detection and diagnosis.

DEDICATION

To my wife, my daughters and my sons, for your patience and absolutely everything with love.

To my brothers and sisters, for their continuous support and encouragement, while I have been away from home.

LIST OF CONTENTS

TITLE PAGE.....	1
ABSTRACT.....	2
DEDICATION.....	4
LIST OF CONTENTS.....	5
LIST OF FIGURES.....	12
LIST OF TABLES.....	17
LIST OF NOMENCLATURE.....	18
LIST OF NOTATION.....	19
DECLARATION.....	23
COPYRIGHT.....	24
AKNOWLEDGEMENTS.....	25

CHAPTER ONE

INTRODUCTION.....	26
1.1 Introduction to Condition Monitoring.....	27
1.1.1 Why Monitor and Diagnose Faults in Engines.....	28
1.2 Motivation.....	30
1.3 Research Topic.....	31
1.4 Implementation of Condition Monitoring System.....	31
1.4.1 Sensor Selection.....	31
1.4.2 Feature Extraction.....	33
1.4.3 Feature Comparison.....	34
1.4.4 Decision Process Determination.....	34
1.5 Introduction to Research Work.....	35
1.5.1 Aims of This Research.....	35
1.5.2 Research Objectives.....	36
1.6 Thesis Structure and Organisation.....	37

CHAPTER TWO

DIESEL ENGINE CONDITION MONITORING.....	39
2.1 Introduction.....	40
2.2 Engine Fundamentals.....	42
2.3 Diesel Engine Sensing.....	43
2.4 A Review of Diesel Engine Condition Monitoring.....	44
2.4.1 Overview of Principal Faults in a Diesel Engine.....	44
2.4.2 Overview of Condition Monitoring Techniques.....	46
2.4.2.1 Vibration Monitoring.....	46
2.4.2.2 Oil / Lubrication Analysis.....	49
2.4.2.3 Cylinder Pressure Monitoring.....	50
2.4.2.4 Instantaneous Angular Speed Monitoring.....	52
2.4.2.5 Airborne Acoustic Monitoring.....	53
2.4.2.6 Exhaust Monitoring.....	55
2.4.2.7 Acoustic Emission Monitoring.....	56
2.5 Summary.....	58

CHAPTER THREE

ACOUSTIC EMISSION MONITORING AND ITS APPLICATION TO DIESEL ENGINES....	60
3.1 Introduction.....	61
3.2 Acoustic Emission Principles and Applications.....	61
3.2.1 Fundamental principles.....	61
3.2.2 Relative Merits of AE, Vibration and Airborne Acoustic Monitoring.....	63
3.2.3 Applications of AE Monitoring.....	65
3.3 AE monitoring of Reciprocating Machinery.....	66
3.3.1 Initial Identification.....	66
3.3.2 Monitoring of Injection, Combustion and Combustion-Related Processes.....	67
3.3.3 Monitoring of Exhaust Valve and Gasket Leakage.....	71

3.3.4	Event Mapping and Source Location.....	74
3.3.5	Monitoring of the piston ring-pack and cylinder liner interface.....	76
3.4	AE Monitoring of Sliding Contact.....	78
3.4.1	Initial Identification of AE Generation from Friction and Wear Source Mechanisms.....	79
3.4.2	AE Monitoring of Sliding Contact in Laboratory Wear Tests.....	80
3.5	Summary.....	89

CHAPTER FOUR

DIESEL ENGINE ACOUSTIC EMISSION SOURCES AND DATA PROCESSING.....		91
4.1	Introduction.....	92
4.2	Diesel Engine Acoustic Emission Generation.....	92
4.2.1	Mechanical Impact.....	93
4.2.1.1	Piston Slap.....	93
4.2.1.2	Valves.....	95
4.2.2	Friction.....	97
4.2.2.1	Piston Liner Assembly.....	98
4.2.2.2	Valve Train System.....	99
4.2.2.3	Engine Bearing System.....	100
4.2.2.4	Auxiliaries.....	102
4.2.3	Other Sources.....	103
4.3	Background Noise.....	105
4.4	Acoustic Emission Processing.....	106
4.4.1	Measurement of Acoustic Emission.....	106
4.4.2	AE Analysis and Signal Processing Techniques.....	108
4.4.2.1	Time-Domain Analysis.....	109
4.4.2.2	Frequency-Domain Analysis.....	113
4.4.2.3	Time-Frequency Domain Analysis.....	114
4.4.3	Feature Extraction and Pattern Recognition.....	115

CHAPTER FIVE

MTHMATICAL MODEL OF PISTON SLAP AND FRICTION IN DIESEL ENGINES.....	118
5.1 General Concepts.....	119
5.1.1 Piston Slap.....	120
5.1.2 Piston Friction.....	121
5.1.3 Characteristic of Piston Assembly Friction.....	123
5.2 Review of Previous Work.....	123
5.3 Piston and Piston Ring Kinematics.....	124
5.4 Governing Equations.....	128
5.4.1 Equation of Motion.....	128
5.4.2 Piston Ring Normal and Friction Forces, F_Q and F_R	131
5.4.3 Wrist-Pin Friction, M_{PP}	131
5.4.4 Cylinder Liner Support, F_T , F_A , M_{TT} , and M_{AA}	132
5.4.5 Skirt-Liner Friction, F_{FT} , F_{FA} , M_{FT} , M_{FA}	133
5.5 Radial Thermal Deformation.....	135
5.6 Cyclic Variations.....	135
5.7 Cylinder Pressure Measurement.....	136
5.8 Effects of Engine Operating Conditions on Piston Liner Friction.....	137
5.8.1 Effect of Engine Speed.....	138
5.8.2 Effect of Engine Load.....	140
5.8.3 Effect of Oil Supply.....	141
5.9 Effects of Piston Parameters on Piston Friction.....	142
5.9.1 Skirt-Liner Clearance.....	142
5.9.2 Oil Supply/Oil Film Thickness.....	143
5.9.3 Surface Finish/Waviness.....	144
5.9.3.1 Waviness vs. Roughness.....	144
5.9.3.2 Parametric Surface Waviness.....	144
5.9.4 Piston-Skirt Profile/Shape.....	145
5.9.5 Piston-Skirt Size.....	146
5.9.6 Piston Ovality.....	147

5.10	Other Considerations.....	148
5.11	Friction Reduction Strategies.....	149
5.12	Summary.....	149

CHAPTER SIX

EXPERIMENTAL TEST FACILITY AND FAULT SIMULATION.....		151
6.1	Test Rig Specification.....	152
6.2	Test Rig Description.....	153
6.3	Measuring Equipment and Instrumentation.....	154
6.3.1	Optical Encoder.....	155
6.3.2	Magnetic Pickup.....	156
6.3.3	Cylinder Pressure Sensor.....	157
6.3.4	Temperature Measurement.....	157
6.3.5	Torque Sensor.....	158
6.3.6	Brüel & Kjær Charge Amplifier.....	158
6.3.7	Analogue to Digital Converter (ADC).....	159
6.3.8	Software: Lab Windows TM/ CVI Version 5.5.....	160
6.4	Data Acquisition Software.....	161
6.5	Acoustic Emission Measurement and Data Acquisition.....	162
6.5.1	Wideband Sensor.....	163
6.5.2	AE pre-amplifier.....	164
6.5.3	AE Data Acquisition System.....	164
6.6	Test Procedures and Fault Simulation.....	167
6.6.1	Test Procedure.....	167
6.6.2	Injection System.....	167
6.6.3	Lubrication Oil Faults.....	169
6.7	Test Rig Recorded Data.....	170
6.7.1	Angular Domain Display.....	170
6.7.2	Frequency Domain Display.....	172
6.7.3	Time-Frequency Domain Display.....	173

CHAPTER SEVEN

DIESEL ENGINE FUNDAMENTAL ACOUSTIC EMISSION CHARACTERISTIC	177
7.1 Introduction.....	178
7.2 Combustion Pressure Event.....	178
7.3 Diesel Engine Acoustic Emission Waveform.....	180
7.3.1 Effects of Operating Condition on the AE Signal.....	182
7.4 Data Analysis Using Statistical Parameters.....	186
7.4.1 RMS Value and Variance as Fault Severity Indicators.....	186
7.4.2 Kurtosis as a Tool for Fault Diagnosis.....	189
7.4.3 Analysis in the Angular Domain.....	190
7.4.4 Analysis in the Frequency Domain.....	194
7.4.5 Analysis in the Angular-Frequency Domain.....	198
7.5 Lubrication Monitoring Using Piston Slap Intensity.....	201
7.5.1 Engine Load.....	203
7.5.2 Oil Temperature.....	203
7.5.3 Engine Speed.....	204
7.5.4 Oil Type.....	205
7.6 Conventional Techniques; Limitations and Drawbacks.....	207

CHAPTER EIGHT

SIMULATION AND MODEL VALIDATION.....	208
8.1 General Concept.....	209
8.2 Influence of Piston Displacement.....	209
8.3 Influence of Piston Sliding Velocity.....	211
8.4 Influence of Cylinder Block Displacement.....	214
8.5 Engine Friction Measurement.....	215
8.5.1 Engine Friction using Conventional Technique.....	215
8.5.2 Brake Specific Fuel Consumption (BSFC).....	217
8.5.3 Friction Measurement Using AE.....	218

8.5.4	IMEP Measurements.....	222
8.6	Lateral Force on Piston.....	224
8.7	Influence of Gas Torque on the Piston.....	228
8.8	Influence of Inertia and Gas Torques on the Piston.....	230
8.9	Lubricant Chemistry.....	231
8.10	Piston and Wrist-Pin Motion.....	233
8.10.1	Lateral Motion.....	233
8.10.2	Tilt.....	234
8.11	Summary.....	235

CHAPTER NINE

CONCLUSIONS AND RECOMMENDATIONS FOR FUTURE WORK.....		237
9.1	Review of Project Objectives and Achievements.....	238
9.1.1	Overview.....	238
9.1.2	Objectives and Achievements.....	238
9.2	Conclusions.....	243
9.2.1	Conclusions Relating to AE Measurements Statistical Parameters.....	243
9.2.2	Conclusions Relating to Time Representation.....	244
9.2.3	Conclusions Relating to Time-Frequency Representation.....	245
9.3	Overall Conclusions Regarding Monitoring Diesel Engine.....	245
9.4	Contribution to Knowledge.....	246
9.4	Recommendations for Future Work.....	246
REFERENCES.....		249

LIST OF FIGURES

Figure 2.1	Diesel engine new technologies.....	41
Figure 2.2	Principal faults in diesel engines.....	45
Figure 2.3	Angular-domain signal of body vibrations of a four stroke diesel engine.....	48
Figure 2.4	Angular-domain of cylinder pressure.....	51
Figure 2.5	Angular-domain of acoustic waveform of two crankshaft revolutions.....	54
Figure 2.6	Angular-domain of exhaust pressure waveform of complete engine cycle.....	55
Figure 2.7	Angular-domain of AE waveform signal of two crankshaft revolutions.....	57
Figure 3.1	Simultaneous in-cylinder pressure ———, RMS AE ——— and acceleration ——— measurements from a gas-fuelled engine.....	64
Figure 3.2	Raw AE acquired from a small, four-stroke engine showing injection/combustion events at areas of maximum pressure, other smaller events appear regularly, AE (———) and in-cylinder pressure (---).....	70
Figure 3.3	RMS AE signals acquired from a large, two-stroke diesel engine, (a) healthy condition and (b) large exhaust valve leak.....	72
Figure 3.4	Raw AE signals acquired from the cylinder head of a small, HSDI engine, (a) propagation around the head, (b) attenuation characteristics.....	75
Figure 3.5	(a) Four hidden signals during a cycle, signal 1 attributed to friction, (b) development of four independent components during test, source.1 attributed to friction.....	77
Figure 3.6	(a) Histogram of cyclic AE energy for normal and no lubricant supply conditions, upper and lower panels at 25% and 50% load respectively, (b) Scatter plot of AE energy versus load with several fault/no fault decision boundaries indicated.....	78
Figure 3.7	AE generation characteristics using a ball and cylinder test-rig for (a) lubricated contact, (b) un-lubricated contact.....	81

Figure 3.8	(a) RMS AE time histories for two different lubrication conditions, (b) linear relationships between integrated RMS AE signals and wear scar volume for different wear regimes.....	83
Figure 3.9	Effect of sliding speed and load on RMS AE level for two different set-ups.....	84
Figure 3.10	Un-lubricated ball and cylinder test rig, cumulative AE versus frictional work, (a) effect of speed (b) effect of loading.....	85
Figure 3.11	Log AE count rate and coefficient of friction versus film parameter.....	87
Figure 3.12	Schematic of the AE monitoring system for a ball on flat sliding cylinder.....	88
Figure 3.13	Induced scuffing at a critical loading.....	88
Figure 4.1	Piston slap phenomenon mechanism.....	94
Figure 4.2	Representative mechanical loss distribution for a diesel engine	97
Figure 4.3	Distribution of valve train friction losses.....	100
Figure 4.4	Schematic of an AE sensor.....	106
Figure 4.5	(a) Examples of AE emission types, (b) typical AE signal acquired from a running engine.....	109
Figure 4.6	Typical time-domain parameters extracted from AE Signals.....	110
Figure 5.1	Stribeck diagram showing the various regimes of lubrication.....	121
Figure 5.2	(a) Schematic of crank-slider mechanism (b) piston primary motion.....	125
Figure 5.3	Schematic of piston cylinder wall system.....	129
Figure 5.4	Schematic of forces and moments acting on the piston.....	130
Figure 5.5	Flow chart for piston frictional force and the piston side force.....	134
Figure 5.6	Pressure torque.....	136
Figure 5.7	Gas pressure acting on the piston crown.....	137
Figure 5.8	Engine speeds acting on the piston.....	139
Figure 5.9	Engine load acting on the piston.....	140
Figure 5.10	Illustration of the dry region.....	141
Figure 5.11	Piston lateral impact velocity.....	142
Figure 5.12	Comparison of aluminium and steel piston designs.....	147
Figure 6.1	JCB444T2 Engine rig.....	152
Figure 6.2	Schematic of the engine test system.....	154

Figure 6.3	Photo of optical encoder position.....	155
Figure 6.4	AC voltage distribution of magnetic pick-up.....	156
Figure 6.5	Kistler type 6125 pressure sensor and specification.....	157
Figure 6.6	K type temperature thermocouple.....	158
Figure 6.7	Torque transducer in position.....	158
Figure 6.8	Charge amplifier-type 2635 (left), back (right).....	159
Figure 6.9	Power 1401 CED analogue to digital converter.....	160
Figure 6.10	Set-up window screen.....	161
Figure 6.11	Data acquisition No: 1 in progress.....	162
Figure 6.12	Wideband type WD acoustic emission sensor and specification.....	163
Figure 6.13	Simple diagram of AE sensor.....	163
Figure 6.14	2/4/6 Pre-amplifier and specification.....	164
Figure 6.15	PCI-2 AE system card.....	165
Figure 6.16	AE data acquisition in progress.....	166
Figure 6.17	PCI-2 Block diagram description.....	166
Figure 6.18	The components of a diesel injector.....	168
Figure 6.19	Arrangement for total misfire.....	169
Figure 6.20	Raw AE signal from a running engine at 0 Nm at 1000 rpm.....	171
Figure 6.21	Frequency spectrum of raw AE signal from a running engine at 0 Nm at 1000 Rpm.....	172
Figure 6.22	Time-frequency domain of raw AE signal from a running engine at 1000 rpm and four different loads.....	174
Figure 6.23	Time-frequency domain of raw AE signal from a running engine at 1000 rpm and four different loads (zoomed).....	176
Figure 7.1	Diagram of cylinder pressure vs. crank angle (0° = TDC).....	179
Figure 7.2	Spectrum of cylinder pressure.....	179
Figure 7.3	Acoustic emission waveform and power spectrum of the diesel engine, AE sensor mounted on the front side of cylinder head (close to cylinder. No.1).....	180

Figure 7.4	AE waveform power spectra of the diesel engine at loads of (a) 50 Nm, (b) 100 Nm, and (c) 150 Nm.....	181
Figure 7.5	Time domain and frequency domain, respectively, of the AE signal from a diesel engine for engine speeds of (a) 1000 rpm; (b) 1000 rpm power spectrum; (c) 2000 rpm; (d) 2000 rpm power spectrum.....	182
Figure 7.6	Time and frequency domain analysis of AE signals from a diesel engine running at 1000 rpm and 2000 rpm.....	183
Figure 7.7	Fourier spectrum of the AE signal from a diesel engine running at 1000 rpm (blue) and 2000 rpm (red) up to 20 kHz upper and 20 kHz to 100 kHz below.....	183
Figure 7.8	AE signals and associated Fourier spectra for the AE from a diesel engine running at 1000 rpm under; (a) zero load; (b) 50 Nm; (c) 100 Nm; (d) 150 Nm.....	184
Figure 7.9	Mean value of AE signal for a diesel engine running at (a) 1000 rpm at four different loads and (b) 2000 rpm at four different loads.....	185
Figure 7.10	AE signals RMS values and the variances (a) 1000 rpm no load and (b) 2000 rpm no load.....	188
Figure 7.11	AE signals RMS values and the variances (a) 1000 rpm under 150 Nm load and (b) 2000 rpm under 150 Nm load.....	188
Figure 7.12	In-cylinder pressures of diesel engine cylinder 1 at 2000 rpm, (a) at no load and (b) at high load.....	189
Figure 7.13	Detection of presence of engine fault using the kurtosis and RMS of the AE signal (Blue) 270 bar, (Red) 235 bar, (Green) 325 bar and (Yellow) blocked injector.....	190
Figure 7.14	AE signals in the angular domain (87% injection pressure).....	191
Figure 7.15	AE signals in the angular domain (120% injection pressure).....	192
Figure 7.16	AE signals in the angular domain (full misfire).....	193
Figure 7.17	Spectra of the AE signals for 87% injection pressure.....	195
Figure 7.18	Spectra of the AE signals for 120% injection pressure.....	196
Figure 7.19	Spectra of the AE signals for full misfire.....	197
Figure 7.20	Angular-frequency representation of healthy and 87% injection Pressure.....	198

Figure 7.21	Angular-frequency representation of healthy and 120% injection Pressure.....	199
Figure 7.22	Angular-frequency representation of healthy and full misfire.....	200
Figure 7.23	RMS value at two speeds.....	202
Figure 7.24	Effects of engine load on amplitude of 1000rpm.....	203
Figure 7.25	Effects of oil temperature on amplitude of the AE signal.....	204
Figure 7.26	Effect of engine speed on amplitude of the AE signal.....	205
Figure 7.27	Effects of engine oil viscosity on amplitude of AE signal.....	206
Figure 8.1	Piston lateral displacement and cylinder lateral displacement.....	210
Figure 8.2	Piston sliding velocity at constant rpm.....	211
Figure 8.3	Piston lateral velocity and cylinder liner response.....	212
Figure 8.4	Displacement and velocity of cylinder block.....	214
Figure 8.5	Engine friction power at different operating conditions with lubricating oils of 20w -50 and 10w-30for both oil.....	217
Figure 8.6	Indicated power vs. speed and load.....	219
Figure 8.7	Friction power vs. speed and load.....	220
Figure 8.8	Friction at two different speeds.....	222
Figure 8.9	IMEP at two different speeds.....	224
Figure 8.10	Piston lateral force, lateral displacement and lateral impact velocity.....	227
Figure 8.11	Cylinder pressure and gas torque.....	229
Figure 8.12	Inertia, gas and resultant torques.....	231
Figure 8.13	Kinematic viscosities vs. oil temperature for the two types of lubricating oil.....	233
Figure 8.14	Stable piston tilt.....	235

LIST OF TABLES

Table 1.1	Major international disasters resulting from lack of proper maintenance.....	30
Table 1.2	Summary of the main sensor parameters.....	32
Table 6.1	Test Engine Specifications.....	153
Table 7.1	Summary of faults seeded into the diesel engine.....	187
Table 7.2	Typical properties of the oils used.....	206
Table 8.1	Indicated power (IP), Brake power (BP) and Friction power (FP) for both oils under prescribed engine operating conditions.....	216
Table 8.2	Percentage reduction of BSFC (g/kWh) of an engine operating at 2000 rpm.....	218

LIST OF NOMENCLATURE

AE	Acoustic emission	IVC	Intake valve closing
ADC	Analogue-digital conversion	IVO	Intake valve opening
ATDC	After top dead centre	I/O	Input/output
BDC	Bottom dead centre	Kur	Kurtosis
BTDC	Before top dead centre	MBPD	Million Barrels per Day
B&K	Brüel & Kjaer	NDT	Non Destructive Testing
BSFC	Break Specific Fuel Consumption	NOx	Oxides of nitrogen
CA	Crank Angle	P	Absolute pressure
CBM	Condition based maintenance	Pdf	Probability density function
CED	Cambridge Electronic Design	PC	Personal computer
CM	Condition monitoring	PCA	Principal Component Analysis
CP	Cylinder Pressure	PM	Particulate matter
CWT	Continuous Wavelet Transform	Psi	Pounds per square inch
DAQ	Data Acquisition	Po	Mean pressure
dB	Decibel	RMS	Root mean square
EV	Exhaust valve	RPM	Revolution per Minute
EVO	Exhaust valve opening	SNR	Signal-to-noise ratio
EVC	Exhaust valve closing	sk	Skewness
FFT	Fast Fourier transforms	STFT	Short-Time Fourier Transform
HSDI	High Speed Direct Injection	TDC	Top dead centre
IAS	Instantaneous Angular Speed	TSA	Time synchronous averaging
IC	Internal Combustion	WT	Wavelet Transform
ICA	Independent Component Analysis	WVD	Wigner Ville Distribution
ICs	Independent Components	Var	Variance
IMEP	Indicated Mean Effective Pressure	σ	Standard deviation
IV	Intake valve		

LIST OF NOTATION

A_{AC}, A_{Ah}	Solid-to-solid contact and hydrodynamic components of bearing areas on anti-thrust side of skirt
A_{TC}, A_{Th}	Solid-to-solid contact and hydrodynamic components of bearing areas on thrust side of skirt
a	Vertical distance from the top of the skirt to the wrist-pin
b	Vertical distance from the top of the skirt to the piston centre of gravity
CL	Horizontal distance between thrust side of liner and liner centreline (cylinder line radius)
C_g	Horizontal distance between piston centre of mass and wrist-pin
C_P	Wrist-pin offset (horizontal distance of the wrist-pin from the vertical axis of the piston)
D	Indication of piston displacement
e_b, e_t	Eccentricities of piston at the bottom and top of the skirt, respectively.
\hat{F}	Connecting rod force
F_A, F_T	Total horizontal normal forces acting on the skirt on anti-thrust and thrust side, respectively.
F_{AC}, F_{TC}	Solid-to-solid contact component of horizontal normal forces acting on the skirt on the anti-thrust side.
F_{Ah}, F_{Th}	Hydrodynamic component of horizontal normal forces acting on the skirt on the thrust side
F_{FA}, F_{FT}	Total friction forces acting on the skirt on the anti-thrust side and thrust side respectively.
F_{FAC}, F_{FTC}	Solid-to-solid contact component of the friction forces acting on the skirt on the anti-thrust and thrust side, respectively.
F_{FAh}, F_{FTTh}	Hydrodynamic component of the friction forces acting on the skirt on the anti thrust side and thrust side respectively.
F_{fr}	Friction force between piston ring and liner.

F_g	Combustion gas force acting on the top of the piston
F_{IC}, \hat{F}_{IC}	Inertia forces due to piston mass
F_{IP}, \hat{F}_{IP}	Inertia forces due to wrist-pin mass
F_{ir}	Ring axial inertia force
F_{pr}	Ring pressure force
F_Q	Normal forces between piston and rings
F_R	Horizontal friction forces between piston and rings
F_S	Piston forces not depending on piston liner contact
f_c	Low pass filter cut-off frequency
f_{sample}	Data acquisition sampling frequency
h	Local oil film thickness
\bar{h}	Mean oil film thickness
h_r	Ring side clearance
I_{PT}	Piston rotary inertia about its centre of mass
L	Piston skirt length
L_T	Ring length in the circumferential direction
l_r	Vertical distances between the wrist-pin axis and rings
M_{AA}, M_{TT}	Moment about wrist-pin due to all the normal forces on the anti-thrust and thrust sides respectively.
M_{AAC}, M_{TTC}	Moment about wrist-pin due to solid-to-solid contact forces on the anti-thrust and thrust sides respectively.
M_{AAh}, M_{TTh}	Moment about wrist-pin due to all the normal forces on the anti-thrust and thrust sides respectively.
M_{FA}, M_{FT}	Moment about wrist-pin due to all the friction forces on the anti-thrust and thrust sides respectively.
M_{FAC}, M_{FTC}	Moment about wrist-pin due solid-to-solid contact friction forces on the anti-thrust and thrust sides respectively.
M_{FAh}, M_{FTh}	Moment about wrist-pin due to hydrodynamic friction forces on the anti-thrust and thrust sides respectively.
M_{IC}	Inertia moment of piston
M_{IP}	Inertia moment of wrist-pin
M_{PP}	Moment about wrist-pin due to wrist-pin friction

M_S	Moments that does not depend on piston liner contact
m_{pis}	Piston mass
m_{pp}	Wrist-pin mass
m_r	Ring mass
PT, PB	Vertical distance from top of cylinder liner to top and bottom of piston skirt respectively.
P_h	Hydrodynamic Pressure
P_w	Wavy contact load per unit length
R	Piston radius
R_p	Wrist-pin radius
t	Time
U	Piston sliding velocity
W_r	Ring width in the radial direction
x^*	Point at which side force on piston changes direction
x^{**}	Point at which piston makes impact with thrust side of liner
X	Horizontal coordinate
Y	Vertical coordinate
β	Coefficient depending on oil coverage of ring
θ	Angular coordinate
μ	Lubricant viscosity
μ_f	Coefficient of friction for solid-to-solid contacts
μ_{oil}	Lubricant viscosity
μ_p	Coefficient of friction for wrist-pin
$\mu_{ring-piston}$	Coefficient of friction between ring and piston
σ	Surface roughness
τ	Hydrodynamic shear stress
Φ	Piston tilt
Φ_x, Φ_y	Pressure flow factors
Φ_s	Shear flow factor
$\Phi_f, \Phi_{fp}, \Phi_{fs}$	Shear stress factors
\emptyset	Connecting rod angle

ψ	Crank angle
Ω	Surface waviness
Δt	Period of engine cycle

DECLARATION

No portion of the work presented in this thesis has been submitted in support of an application for another degree or qualification of this or any other university or other institute of learning.

COPYRIGHT

- i. The author of this thesis (including any appendices and/or schedules to this thesis) owns any copyright in it (the “Copyright”) and s/he has given The University of Huddersfield the right to use such Copyright for any administrative, promotional, educational and/or teaching purposes.

- ii. Copies of this thesis, either in full or in extracts, may be made only in accordance with the regulations of the University Library. Details of these regulations may be obtained from the Librarian. This page must form part of any such copies made.

- iii. The ownership of any patents, designs, trademarks and any and all other intellectual property rights except for the Copyright (the “Intellectual Property Rights”) and any reproductions of copyright works, for example graphs and tables (“Reproductions”), which may be described in this thesis, may not be owned by the author and may be owned by third parties. Such Intellectual Property Rights and Reproductions cannot and must not be made available for use without the prior written permission of the owner(s) of the relevant Intellectual Property Rights and/or Reproductions.

ACKNOWLEDGEMENTS

My research work for this study at the University of Huddersfield was made possible by the will of Almighty Allah (God), then by my academic supervisor, **Prof. Andrew D. Ball**, who gave me the opportunity to start this research, and whose inspiration and guidance made such a valuable experience possible. Prof. Andrew Ball has stood by me and encouraged me throughout my research, providing support when my morale was failing, and who helped me to get my PhD. I thank him for his support and guidance throughout the time of my research.

I am especially grateful to **Dr. Fengshou Gu**, for his sincere and warm-hearted support and encouragement.

Last and always, special thanks are extended to my family: my **wife** and my daughter: **Awaisha**, **and** my Son: **Hisain**, and the lovely young **Maria** for their support throughout the research time. Special and grateful thanks to my **brothers** and **sisters** for their high expectations and love while I am away from home.

I also appreciate the help from all my friends I have met in Huddersfield. They have made my time here both enjoyable and unforgettable.

Finally, I would like to thank all my relatives back home who supported me throughout my study and many thanks to all my friends back home.

CHAPTER ONE

INTRODUCTION

This chapter gives an introduction to the work presented in this thesis. Firstly, the fields of condition monitoring and diagnostic system implementation procedure are introduced. Secondly, the work to be reported in this thesis is introduced; the research work aims and objectives are outlined and the thesis structure is presented.

1.1 Introduction to Condition Monitoring

Due to the growing demands for availability, reliability, cost efficiency and safety, the call for accurate machinery fault detection and diagnosis is becoming increasingly important. Machinery maintenance is often condition based, that is, decisions regarding the repair or replacement of a machine part, overhaul and/or standard maintenance are made on the basis of the measured condition of the machine. Proper machine condition monitoring procedures need to attain high levels of asset availability, reliability and performance whilst minimising unplanned downtime and the cost of maintenance.

Condition monitoring, fault diagnosis and fault detection are terms used to describe similar concepts; detection of any abnormality or deviation from the machine's normal condition. Condition monitoring has the primary aim of assessing the health of a machine or structure, while fault diagnosis identifies the component or process which caused the deviation from the normal condition.

Mechanical signature analysis is, in many aspects, a well-established field of engineering and is widely used, for example, in production quality control. Sensor measurements are employed to determine whether the quality of a manufactured product meets the required specification. Such end-of-assembly tests are becoming common in the manufacture of machines and products, as the market demands ever greater reliability.

Another very important field of application of mechanical signature analysis is condition monitoring. The availability of relatively low-cost digital computers especially designed for industrial applications and the increasing use of digital controllers have given rise to an explosion in the use of diagnostic and monitoring applications over the last two decades.

Acoustic emission (AE) and chemical and physical analysis of in-service lubricating oil, process parameters and thermal images are examples of the variety of technologies utilised in condition monitoring. Traditionally, data as sensed from the object under surveillance is compared with baseline readings taken under normal operating conditions. Today it is possible to combine the data from a number of systems in order to judge the state of the machine or structure [1].

Various signal analysis techniques have been employed in condition monitoring; among these, classical and parametric spectral estimation methods have played a major role. The use of spectral analysis techniques is often dictated by the periodic or repetitive nature of the

motion of most - if not all - machines; defects and incipient failures often manifest themselves in the form of changes in the spectrum of a measured signal whose spectral characteristics are usually easily associated with a physical phenomenon such as the speed of rotation or the repetition rate of a certain motion [1].

Each machine has its own baseline signature expressed in terms of one or more continuously varying parameters. The challenge is to detect any change as soon as the signature begins to depart from normal. The condition of every machine depends on several factors such as the operating environment (quality of fuel, air, water, lubricant etc.), the operating modes (part load running, overloading etc.) and operator skills. All of these are variable, and deviation of any of them from the normal range could lead to a fault developing within the system. In complex systems a fault in any subsystem, if not repaired early enough, can severely affect the performance of the other subsystems.

Thus it is very important to recognise at an early stage that a fault has developed and also to identify the component responsible for that fault. Many existing diagnostic systems belong to a category where the fault is detected after the condition of the machine has deteriorated so badly that visual, audible and olfactory (i.e. smell) signs are already present [2].

1.1.1 Why Monitor and Diagnose Faults in Engines?

Even minor faults can contribute to a reduction in the useful life of high-cost engines, and it is in the self-interest of companies to avoid such potentially unnecessary losses. Faults not only directly reduce the performance of an engine, they can also cause secondary damage to other parts of the engine; this can lead to significant economic loss for the user and in some cases to personal injury [3].

Different predictive maintenance methods and techniques such as vibration, acoustic and acoustic emission monitoring, using time and frequency domains have been developed to detect and diagnose faults, improving maintenance and, hence, the performance of both engines and systems [4]. When the faults are less serious, early detection and diagnosis not only provides information about the nature of the problem but also allows maintenance personnel to plan the necessary corrective action. Thus, the production losses can be minimised. Such an approach will result in lower labour and parts costs, less downtime and more efficient use of maintenance resources [5].

In the past twenty years development of CM techniques, particularly acoustic emission monitoring, has greatly improved the maintenance of rotating machinery. However, over that period, reciprocating machinery such as reciprocating engines has been largely ignored [5]. This is predominantly because the acoustic emission generated during normal operation of a reciprocating engine is impulsive, because of impact forces resulting from the different sources, which makes the diagnosis of problems relatively difficult.

Table 1.1 shows some of the major international disasters which occurred between 1980 and 1989, with their attendant effects. The impact on the environment may be so important that some major incidents must be considered as disasters, even if no human casualties were involved. It is essential to have improved safety in the process industry, up-to-date maintenance information on engine conditions [6]. The fact that the monitoring and control of excessive vibration, noise and temperature levels are now required by law in many countries may provide a significant spur to the introduction of CM techniques [6]. In 1998 alone it is estimated that more than 2000 lives were lost as a result of accidents at sea attributed to weather, fire and explosion, machinery failure, collision/contact, grounding and unknown incidents [3].

Presently diagnostic systems capable of detecting incipient faults in engines are limited due mainly to the extremely difficult task of detecting and interpreting the low level of signal from a fault in its early stages.

Many applications of condition based maintenance (CBM) can provide significant savings [7]. A few examples are listed below:

1. SKF (a CM equipment supplier) claims that in one company, use of CBM reduced maintenance costs by up to 27%, productivity rose by 21%, while unscheduled downtime dropped by 40% and equipment breakdowns were reduced by 74% [8].
2. One study has shown that CBM reduced maintenance costs of one company by more than 30%, increased equipment availability and performance from 2-40%, enhanced safety and reduced energy consumption by up to 10% [7].
3. Adelaide Brighton Cement Ltd: reported savings of 15% (\$5 million) through improvement in plant availability and avoiding 6-10 unplanned shutdowns per year. \$125,000 per year was saved by reducing time-based maintenance schedules. Reduced spare parts inventory resulted in saving of approximately \$130,000 per year [9].

Table 1.1 Major international disasters resulting from lack of proper maintenance [6].

Year	Location	Causes	Effects
1980	North Sea (UK)	Oil rig capsize	123 killed
1984	Bhopal (India)	Toxic release	2700 killed and about 10 times as many injured
1984	Ixhuatepec (Mexico)	LPG explosion	500 killed
1988	North Sea (UK)	Piper Alpha explosion	167 Killed
1986	Chernobyl (USSR)	Nuclear reactor fire	31 killed and 135000 residents were evacuated
1989	USSR	Gas pipe explosion	500 killed

1.2 Motivation

In the last century, the development of heavy duty diesel engines achieved a high level of success. Today diesel engines are complex and have numerous components that could potentially fail. In order to avoid failure and to maintain high efficiency it is essential to monitor the engine condition continuously. Thus there has been an increased interest in engine condition monitoring because of the potential advantages to be gained from reduced maintenance costs, improved reliability, increased engine availability and reduction of the risk of main engine failure. Nowadays, the essential issue for diesel engine condition monitoring in most industries is inadequate and accurate fault detection and diagnosis. One of the most promising approaches to condition monitoring is to use AE signal analysis [10]. Hence, the motivation of this research is the efficient detection and diagnosis of faults in a heavy duty diesel engine using AE techniques. The motives behind not building in such user oriented diagnostic systems into domestic equipments (cars included) are fairly transparent. However, major machinery failure causing damage to life and property can never be justified.

1.3 Research Topic

The topic of this research is “Fault Detection and Diagnosis in Heavy Duty Diesel Engines Using Acoustic Emission”.

The main challenge to diesel engine fault detection and diagnosis is the improvement of diagnostic accuracy based on the information collected. In order to use effectively the collected information, the significance of every parameter or feature needs to be considered. This research will study the possibilities of improving diesel engine fault detection and diagnostic accuracy based on AE measurements. Measurement techniques are widely available for dealing with uncertainly problems and AE measurements are included in this type of problem.

The use of AE for detecting diesel engine faults is most useful when [11];

1. The fault is incipient (fault symptoms are not clear).
2. Fault information is not precise (in some cases) because of the background noise;
3. The boundaries between different failure modes are not clear or overlap making it difficult to identify specific faults.

1.4 Implementation of Condition Monitoring System

To implement a successful condition monitoring system the following four procedures should be carefully considered [1]:

1. Sensor selection.
2. Feature extraction.
3. Feature comparison.
4. Decision process determination.

1.4.1 Sensor Selection

An insight into the underlying science of any particular machinery is essential when selecting the type of sensor to be used in applications associated with that machinery. Sensors designed to respond to one particular physical variable are often influenced to some extent by other

variables. This knowledge helps in eliminating disturbances from other variables. The major parameter for sensor selection is summarised in table 1.2.

Table 1.2 Summary of the main sensor parameters

Range	Max minus Min value of the measured stimulus
Resolution	Smallest measurable increment in measured stimulus
Sensing frequency	Max frequency of the stimulus which can be detected
Accuracy	Error of measurement, in% full scale deflection
Size	Leading dimension or mass of sensor
Opt environment	Operating temperature and environmental conditions
Reliability	Service life in hours or number of cycles of operation
Drift	Long term stability (deviation of measurement over a time period)
Cost	Purchase cost of the sensor

It is vitally important to pay appropriate attention to the communication channel through which the signals from the sensors are processed. It is the extraction of specific features from the signals that are important, and it is good practice to use knowledge gained from experience to maximise the signal-to-noise ratio. These insights are generally more valuable than relying solely on the unthinking application of advanced signal processing strategies and can often turn the detection of a deviation from normal into meaningful information about the machine under examination.

Having decided on the types of sensors suitable for the detection of relevant phenomena, it is important to recognise that the sensors, and parts of the communication channel, are not always entirely reliable. Accommodating faults in the detection system is traditionally achieved by distributing sensors and associated hardware components around the system under consideration in order to ensure against defects or damage in any one localised channel.

Such arrangements are typically configured in a triplex or quadruplex arrangement with the outputs from the channels compared for logical consistency, with small variations between them being ignored. Such an approach is often called hardware redundancy although the concept is often extended to include analytical processes, in which case parallel redundancy is a more appropriate term [1]. When building hardware redundancy into a system it is vital to remember that identical sensors tend to have similar life expectancies, and hence a malfunction in one sensor is likely to be closely followed by faults in others. This limitation is overcome by using dissimilar sensors responsive to different process variables.

1.4.2 Feature Extraction

Early detection of the onset of any deviation from normal is an important application of industrial diagnostics. The concept of feature extraction can be represented in simple terms as:

$$z(t) = a(t) + x(t) + \sigma * y(t) \quad (1.1)$$

Where $z(t)$ is the output of the sensor, $a(t)$ is the normal condition signature, $x(t)$ and $y(t)$ are the signals associated with the background noise and the signal arising from the onset of an anomaly respectively. The operator σ has a value of zero when there is no anomaly present and unity otherwise. The task in detecting the occurrence of an anomaly is to estimate when the operator is sufficiently removed from zero and close enough to unity to constitute the indication of the onset of an anomaly [1]. In practice this means making a decision, as will be discussed in the following two subsections (1.4.3 and 1.4.4).

At this stage it is necessary to select a suitable feature extraction strategy. It is usual to collect sample records over significantly long periods of operation in order to establish a base line defined as normal operation. The standard derived in this way is often called a historical standard. Historical standards are widely used in industrial applications because they are relatively easy to establish although uncertainties arise in any resulting decision making process.

1.4.3 Feature Comparison

Sample records establish a base line performance which extraction strategies use to detect an actual departure from normality, so confidence in the fault detection system would be enhanced by additional information on the long term statistical nature of base line data.

One method that is used is to test prototypes of key elements of a system under consideration for the whole of their life expectancy in order to generate signals arising during failure of the element and establish base line data over very long periods. Standards established by prototype testing generally have wide acceptance amongst operators of industrial systems. However, in some simple situations, it is possible to establish a comprehensive theoretical standard by rigorous mathematical analysis.

1.4.4 Decision Process Determination

The ultimate aim in any fault detection system is to provide an unambiguous indication of the onset of fault conditions as soon as possible and do so with utmost reliability. The criteria for assessing the quality of the decision include:

1. The time T taken before an indication of fault conditions is reached.
2. The probability, P_s , of generating a spurious indication of a fault.
3. The probability, P_m , of missing the onset of fault conditions.

These three criteria are interrelated, which necessitates consideration of the trade-offs involved in designing any particular application.

Suppose that the extraction of a feature from a system operating under 'normal' conditions results in a Gaussian probability density function (pdf) with zero mean value. The onset of a fault is assumed to shift the mean value of the feature to a new non-zero value [1].

It is to be expected that as the averaging time T , over which the features are estimated, is increased, the overlap between the two pdfs decreases. T determines the speed of response of the diagnostic system to a fault condition. The choice of T is thus determined by the maximum time allowable in any practical situation. In any system with a high risk of severe damage as a result of the escalation of an undetected fault, such as a nuclear reactor, T would be defined to be around one-half of one second. The automatic detection of a fault requires the

setting of a decision boundary which when crossed in feature space initiates the indication of the fault condition [1].

The reliability of the decision making process can be improved by using more than one feature extracted from the signal, providing, of course, that the features are independent. A simple example of multiple features would be the simultaneous use of an amplitude probability function with the power within a defined frequency band. The optimal threshold could be set and decision rules specified, ranging from the signal exceeding both thresholds simultaneously, to either threshold alone being exceeded. The former having the same philosophical base as the parallel redundancy discussed above.

1.5 Introduction to Research Work

The diesel engine is a complex machine and as such it provides a challenging environment to test ideas on fault detection and diagnosis. When operating in a healthy condition it can give thousands of hours of uninterrupted service. However, if a fault develops, the growth can be fairly rapid. For this reason developing a sensitive condition monitoring system capable of detecting a fault in its early stages before break-down happens is important.

In this research, AE data collected from a JCB 444T2 diesel engine is used for the detection and diagnosis of specific developing engine related faults.

1.5.1 Aims of This Research

The thesis uses AE as a CM technique for the study of predictive maintenance of a direct injection diesel engine. The aim of this research is to develop a more accurate and sensitive fault detection and diagnosis tool that can be used with internal combustion engines (static engines only).

This will be achieved by analysing the AE data from the one sensor and developing a MATLAB based post-process computational analysis tool. Time, frequency and frequency-time domain analyses will be used for CM and their suitability compared and discussed. The thesis will present an overall methodology of diagnostic system development, which requires source identification, dynamic modelling, signature recovery, fault signature identification, and diagnostic system design. Each of the main chapters of this thesis is a major component

of the proposed methodology, in the order in which one would expect to proceed when developing a diagnostic system.

The thesis will also develop a mathematical model to represent the specific component of a diesel engine. The model includes the secondary motion of the piston, because secondary motion has significant implications for oil transport past the piston ring-pack and engine friction. The model predictions of system behaviour will be tested against the experimental results.

1.5.2 Research Objectives

In this work, AE measurements acquired from external surfaces of diesel engines are investigated under the premise that these measurements can reveal information about the operation of critical processes and mechanical events within the engine. This is because the capital investment and life cycle costs of such machines are significant and the applications are critical in terms of safety as well as business profitability and operational reliability in a HD environment.

Objective 1: To review condition monitoring of diesel engines.

Objective 2: To review the diesel engine's principal faults and practical condition monitoring techniques used to monitor and evaluate these faults.

Objective 3: To study diesel engine AE sources and to investigate what information can be extracted from AE measurements regarding engine operation. This necessitates an evaluation of AE signals acquired from the AE sensor with the aim of correlating features in the AE signals to actual events occurring within the engine.

Objective 4: To study specifically AE signals arising from the condition of the lubrication, which is a key element of engine operation and impacts upon engine performance, emissions and reliability and, importantly. There is no suitable lubricant monitoring tool even though a number of techniques (structure-born noise, acoustic, oil analysis etc.) have been used in the past. The influence of other engine parameters such as engine speed, load and temperature will also be investigated in order to develop understanding of the source mechanisms responsible for AE generation, and thereby of the aspects of interfacial behaviour which can be monitored.

Objective 5: To apply signal processing methods and techniques (time, frequency and time-frequency domain analyses) to extract fault features for early fault detection and to compare their performance.

Objective 6: To develop a mathematical model of the diesel engine to be used for condition monitoring. The experimental results will be used to verify the model predictions.

Objective 7: To introduce specific quantified faults into the engine and both measure and predict the effects on engine performance.

Objective 8: To allow the advanced CM techniques investigated and developed in this thesis to be used for demonstration in educational and training purposes concerning diesel engines.

Objective 9: On the basis of the investigation conducted in this work to provide useful information to guide future research in this field.

1.6 Thesis Structure and Organisation

In this section a brief introduction is given to the contents and relative emphasis of the chapters of the thesis.

Chapter 1: A brief introduction to condition monitoring is presented, as well as the aims and objectives of this work.

Chapter 2: A brief introduction to diesel engine condition monitoring methods, advantages, performance and faults are presented.

Chapter 3: Outlines the principles of AE and gives a brief review of the growing range of applications and presents a review of the developments to date concerning AE monitoring of diesel engines and other reciprocating machinery. Previous work on AE monitoring of sliding contact is examined in detail for a variety of applications including; laboratory wear tests, hard disk drive operation and the meshing of gears.

Chapter 4: Investigates sources of AE in diesel engine. Details are given of diesel engines AE sources including mechanical impact (piston slap, valve impact and injector tick), friction and other sources (gas flow, fluid flow, crack formation and wear) and background noise (noise not related to the engine sources). Introduce the fundamentals of AE measurement, AE data processing techniques and recognised AE analysis parameters.

Chapter 5: Develops the mathematical model of the behaviour of the four-stroke diesel engine, including a dynamic model of the piston mechanism. The aspects of the model are combined into a set of non-linear differential equations developed using MATLAB.

Chapter 6: Describes and explains relevant aspects of the diesel engine test rig. It then briefly describes the transducers used in this work, the experimental procedures and the fault simulation. Test engine specification is briefly introduced. Details are given of the AE, temperature, speed, load (torque), and cylinder pressure sensors. It also describes data acquisition.

Chapter 7: Investigates the fundamental characteristics of the diesel engine AE signals, using time-domain, frequency-domain, time-frequency-domain and other statistical analyses of acoustic emission data collected by the AE sensor. AE signals for a range of loads and speeds are considered in order to provide a baseline for normal engine characteristics.

Chapter 8: Shows how the model developed in chapter five is implemented. The mathematical equations are solved numerically in the MATLAB environment to give impact force between piston skirt and cylinder wall friction forces. It describes the initial implementation of the model, including quantifying physical parameters. It then briefly explains how the simulation was implemented and comparison of model predictions and system behaviour are made.

Chapter 9: Summarises the achievements of the research work described in this thesis and relates each one to the objectives given in Section 1.5.2. The key findings of the work are listed as conclusions and those aspects of the thesis which are novel and where the author has made a contribution to knowledge are given in some detail. Finally, suggestions for further research are presented.

CHAPTER TWO

DIESEL ENGINE CONDITION MONITORING

This chapter provides a general introduction to the diesel engine. Firstly, engine fundamentals are discussed and then an overview is given of diesel engine condition monitoring. The principal faults occurring within the engines are presented and relevant measurement procedures for condition monitoring are briefly discussed.

2.1 Introduction

The diesel engine has found wide application as the main power supply system in a variety of road vehicles, merchant ships and emergency generation units, and is a mainstay that serves a variety of industries. Within the last decade, the use of the diesel engine became even more widespread as high-speed direct injection diesel engines became realistic alternatives to the gasoline engine for the modern passenger car, because it's due to the economy of operation and decrease of greenhouse gases, especially of CO_2 . Carbon dioxide is a major source to the greenhouse effect, which leads finally to global warming. The overall sales of diesel vehicles in the EU roughly doubled between 1994 and 2002, with much of the growth occurring in the latter years; diesel vehicles reached 44% of the new car market sale in 2003 [12] and 53.3% in 2010 according to Schmidt's Diesel Car Prospects to 2015 [13].

Diesel fuel consumption world-wide in 2005 was expected to be 22.8 MBPD: with on road vehicle consumption 12.6 MBPD (of which freight trucks consumed 74%, and buses and light duty vehicles 13% each) and off-road 10.2 MBPD [2]. It has been estimated [2] that, world-wide, on-road diesel demand will grow at an annual rate of a proximately 3% per year, double that of gasoline. Such a growth would result in worldwide demand for diesel fuel for on-road vehicles of 16.6 MBPD by 2015.

The diesel engine possesses many advantages over spark ignition engines (SIE), but ever since its invention it has been associated with the emission of oxides of nitrogen (NO_x) and harmful particulate matter (PM), which have many negative health and environmental effects [14]. Of course, the degree to which these harmful emissions are generated by a diesel engine is strongly dependent on the engine maintenance. Because European legislation is set to impose further restriction on the level of emissions that are permitted from diesel engines together with targets for greater fuel efficiency [14], the diesel engine manufacturer has the task of producing suitable power train systems that meet or exceed such directives.

To meet these proposed standards, the engineer has to develop new techniques and processes that can be integrated with existing engine sub-systems to reduce pollutant output. Figure 2.1 presents newer technologies which have been introduced into diesel engines in order to fulfil engine performance and emission requirements.

The fuel injection system is a sub-system that has lent itself to improvement in engine performance and emission quality, and will play a vital role in the development of improved diesel engines for the foreseeable future. New injector technology will allow small and precise will help quantities of fuel to be injected into the combustion process faster, and more precise control of the cooled exhaust gas re-circulation and catalysts equipment will help to meet the lower NOX emission level requirements, while new filters will retain some or most of the particulates [15]. This thesis investigates and analyses a new type of CM for diesel engines, capable of detecting engine failures and faults which have harsh/negative impact on the engine.

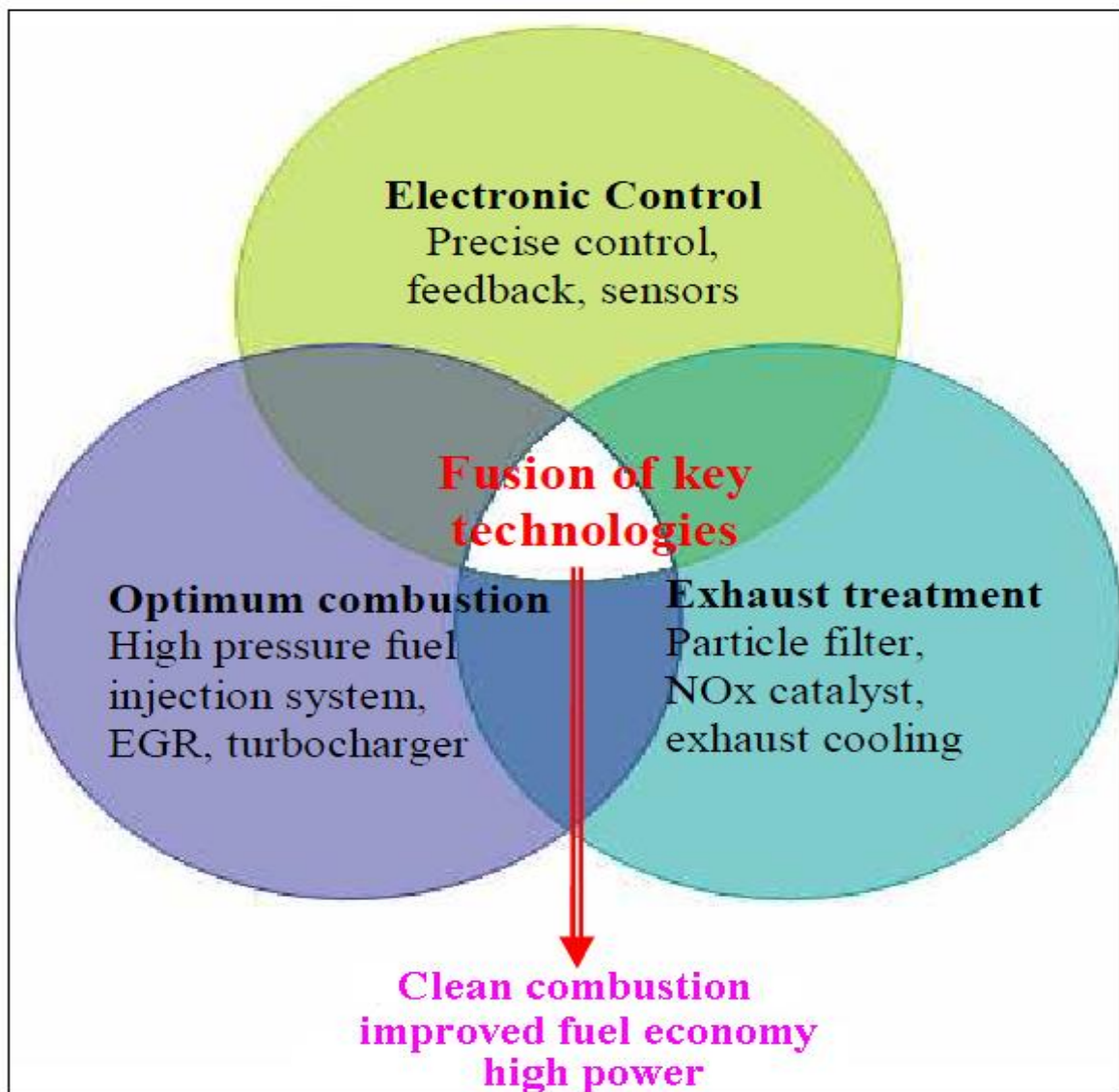


Figure 2.1 Diesel engine new technologies [16].

2.2 Engine Fundamentals

A diesel engine is the power source of many machines. It generates the necessary drive power to overcome the resistance of loads by burning fuel and converting the energy content of the inlet mixture to mechanical motion. Internal combustion (IC) engines are commonly classified according to the type of fuel they use; the two principal categories are diesel and petrol. Diesel engines and petrol engines are also categorized as compression ignition and spark ignition, respectively. There are many different types of diesel engines. In marine and stationary engines, a two-stroke turbo charged configuration is most frequently used, while in smaller engines a four-stroke cycle is more common, two and four refer to the number of piston strokes occurring during any one cycle of events. Diesel engines are often larger and more rigidly built than spark-ignition engines because of the higher stress levels due to the higher pressure in the combustion chamber.

For injection of the diesel fuel into the combustion chamber there are two main techniques, direct-injection and indirect-injection. In the direct-injection method, fuel is injected directly into the cylinder, where it is mixed with air. For an indirect-injection, the engine has an auxiliary injection combustion chamber where the fuel is mixed with air. This technique is used when a faster fuel-air mix is needed, i.e. small engines operating at high speed. For fuel economy and power density the direct-injection system has a clear advantage and is therefore state of the art in passenger cars [16].

In contrast to spark-ignition engines, diesel engines do not use spark plugs. Here, the fuel-air mix is compressed by the piston which results in a temperature rise. This temperature rise is large enough for the gas to self-ignite.

Most commercial vehicles are invariably powered by the diesel engine because of its superior thermal efficiency and higher fuel efficiency and reduced CO_2 emission. The diesel engine is an essential contributor in the construction, transport, agriculture, electrical generation, marine and other sectors. For that reason, diesel power plays an essential role in the economic growth of a nation and pollution of the environment.

From a maintenance viewpoint, the engine is the major cost item in most common sources of power, both for vehicles and for static equipment and the most complex component requiring fault detection and diagnosis. Not only are most failures hidden they can also involve several

aspects: mechanical, chemical, electrical, thermal or any combination of these. At the same time, any single failure symptom can be caused by several failure sources. For instance, an overheating engine can be traced to mechanical, electrical and/or thermal causes.

Traditional maintenance practices mean that most engine failures prove catastrophic. There is little advance warning of the engine malfunction so failures are expensive and accompanied by secondary damage. The main performance indicators on most common diesel engines are engine temperature and oil pressure. There is an increased tendency to move from preventive (time-based) maintenance to one dependent on engine and component conditions. Condition monitoring is used to detect abnormalities of the engine and incipient failure, and plays a significant role in improving economic efficiency and in preventing dangerous accidents from occurring.

2.3 Diesel Engine Sensing

The vibration signal gives a global representation of the diesel engine signature, with almost every moving part of the engine and the associated stiffness contributing to the signal. It is often difficult to interpret the vibration signals in any but the simplest diesel engines. Vibration excitation of diesel engines is largely caused by movement of mechanical components (mass effects). Motions of liquid and gas, with their lower inertia forces, are not easily monitored using vibration signals. AE with its sensitivity to high frequency stress waves and insensitivity to low frequency, whole body movements, offers a potential complementary alternative sensor technology.

Acoustic emission is the term used to describe stress waves emitted by certain mechanical and fluid phenomena. Typical phenomena, which generate AE, include plastic deformation, sliding contact, mechanical impact, turbulent flow and cavitation. Many of these processes occur in diesel engines and the main challenge is to use signal processing to monitor these processes effectively to determine the engine condition; whether using time-domain, frequency-domain or time-frequency-domain features extracted from the CM signal.

2.4 A Review of Diesel Engine Condition Monitoring

Abnormal running conditions for a diesel engine can vary widely in severity and consequences from slightly affecting an engine's performance to catastrophic equipment failure. These events can be expensive, sometimes dangerous, and occasionally cause environmental, and health and safety issues. Good CM can ensure the engine provides the required power under safe conditions with less fuel consumption, lower emissions and lower maintenance cost. Detecting faults and diagnosing the underlying problem as quickly as possible and providing assistance to correct the problem are the goals of engine abnormal situation prevention.

Condition monitoring of diesel engines can be assessed on a continuous or periodic basis from observation or measurement of selected parameters. The application of CM and fault diagnosis strategies to a diesel engine is a well-recognised method of increasing its operational efficiency and reducing consequential damage, spare parts inventories and breakdown maintenance.

The main job of most monitoring systems is to obtain information about the engine in the form of primary data and, through the use of modern signal processing techniques, to provide vital information to the engine operator and the engine control system, before any failure occurs with the engine in service. Good monitoring systems for diesel engines can achieve at least the following benefits:

- Improved decision making capability for selection of optimum engine operation conditions.
- Only defective equipment or assemblies are replaced, reducing time and cost of maintenance.
- Effective prediction and planning of maintenance operations. Time scheduled for maintenance can be used effectively since the nature of the fault is known in advance and both spare parts and labour can be organised accordingly.
- Reduction of engine emissions and fuel consumption.

2.4.1 Overview of Principal Faults in Diesel Engines

This section presents the principal faults within a diesel engines and then outlines monitoring techniques used in engine condition monitoring.

Diesel engines are widely employed nowadays where high power production is necessary such as in heavy power generators, heavy road vehicles, most long-distance locomotives and most road vehicles have diesel engines also. In the 1950s and 60s diesel engines became increasingly

popular for use in vans and taxis, however it was not until the sharp increases in oil prices in the 1970s that serious attention was paid to the small passenger car market [17]. The last few years have seen the use of small diesel engines grow, largely due to better fuel economy and longer operating life, until nowadays all main European car producers offer at least one diesel engine model [17]. The diesel engine when operating normally can give thousands of hours of uninterrupted service. However, if a fault develops, the growth of the fault tends to be fairly rapid and can lead to major failure which can cause loss of life, damage to property and incur high costs when it occurs in, for example, commercial transport vehicles or ships. This why, it is essential to implement reliable and sensitive engine condition monitoring techniques.

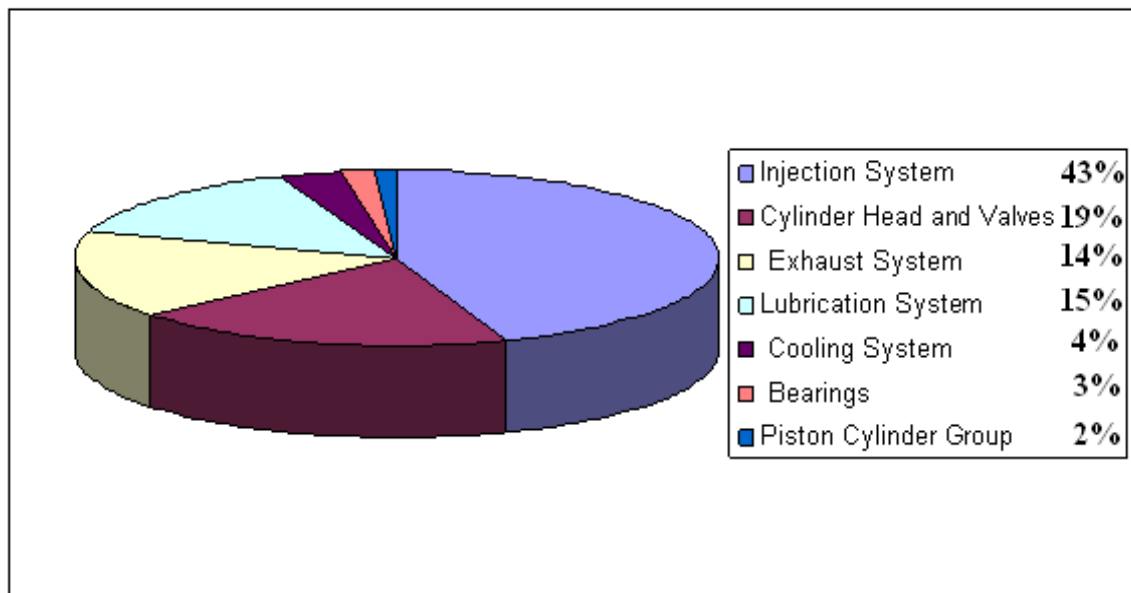


Figure 2.2 Principal faults in diesel engines

Diesel engines use high compression ratios, generating a sufficiently high pressure and temperature to cause spontaneous ignition of the injected fuel. Also the speed of engine rotation is 3000 rpm or more. The high speed, high pressure and high temperature increase the risk of faults occurring within the engine. Figure 2.2 shows classification of faults according to engine systems and components [18].

One of the most important elements is fuel injection system malfunction, which is responsible for about 43% of the engine faults [18]. These system faults can also directly affect engine efficiency, exhaust emission, engine noise and other parameters.

Another important element is the lubrication system malfunction account for a high percentage of the engine faults. The lubrication system faults can directly affect the engine power, emission and other performance parameters, this is why it worthwhile to study this element of the system and associated faults.

2.4.2 Overview of Condition Monitoring Techniques

Nowadays engine performance together with high economy is a very important operating characteristic, and CM is being used to ensure that this characteristic is not only maintained but optimised. The conventional attitude to engine upkeep has been to follow a fixed routine maintenance program based on the engine manufacturer's instructions. This approach has two disadvantages.

1. The maintenance schedule is based only on past experience of similar engines. There is no guarantee that an individual component would be in perfect condition throughout this interval.
2. The component is sometimes still in good condition even after the elapsed interval and it would be a waste of time and money to repair or replace a perfectly healthy component.

Many techniques are being used for machines condition monitoring; this subsection explains the use of some of these techniques for fault detection and diagnosis in diesel engines.

2.4.2.1 Vibration Monitoring

Vibration monitoring is one of the most important methods employed for identifying faults and predicting engine failures. This method, in particular, is becoming progressively more accepted as a predictive maintenance method and for engine maintenance decisions. This is why the understanding of vibration methods is of enormous significance to maintenance engineering. Vibration monitoring collects the vibration signals generated by an engine and analyses them to decide the engine's condition. There are numerous reasons for the wide application of this type of monitoring and one of the main reasons is that each engine produces vibrations of different types

whilst working. The second reason is that the vibration system of the common engine and its structures are theoretically well-understood, making it possible to predict the features of the vibration signals detected using special instrumentation such as wide band transducers and convenient analysers. The third reason is that one can avoid considerable expense, for instance by avoiding the acquisition of an engine or the possible sudden loss of power output. Furthermore, improvements in computation and vibration signal processing methods have added to its large number of applications. Difficulties in using vibration monitoring might occur due to the mixture of various noise and vibration sources, both non-linear and non-stationary, and the influences of numerous different transmission paths [19]. Nevertheless, vibration monitoring is not yet adequate to provide all-purpose condition monitoring of the diesel engine as it provides mostly vibration information which is related to the firing sequence of the engine.

While types of failures such as wear might not make significant changes to the vibration signal, vibration-based CM has evolved as a key method which employs transducers to measure the vibration at a point, and the point where the transducers should be placed is where the signal detected is dependent upon the failure (fault) to be diagnosed. It is particularly useful for analysing rotating machinery because it is normally easy to use in such circumstances and relatively cheap. Various methods exist for processing and saving of signals produced during vibration analysis some of which are:

1. Most simply, using peak, peak to peak or RMS values of signals to establish the mechanical condition of an engine.
2. Spectrum analysis which transforms the time-domain input signal using Fourier processes. This is used mainly for tendency analysis and diagnosis, with particular frequencies related to particular components [20];
3. Envelope analysis, or high frequency resonance technique (HFRT), restricts the signals to those frequencies that are necessary to be monitored. It suppresses undesired background vibrations, and allows the envelope near the signal to be analysed, cancelling unwanted low frequency vibrations; and
4. Cepstrum analysis is employed to identify a sequence of harmonics (or sidebands) in the spectrum and to estimate their relative strength. This is done by taking the logarithm of the amplitudes and reconstructing one or more spectrums using these latest values. This has the effect of increasing the comparative significance of the component of lowest frequency. Usually the power Cepstrum is a frequency analysis of a frequency analysis.

Vibration method is an obtrusive method and this is a common problem with its use because transducers have to be fitted onto the engine in several places to collect relevant vibration data. However this technique has remained rather limited in its application to diesel engines, essentially because of the complexity of the vibration signals that are involved, see Figure 2.3, because the superposition of the contributions of different vibratory sources modified by their respective transmission paths. These sources originate from several internal phenomenons in the engine and excite the natural modes of the engine. The vibration is amplified at the natural frequencies of the engine. Therefore, the produced vibration and the noise radiated from the engine result from the combination of the excitations and the dynamic response of the structure.

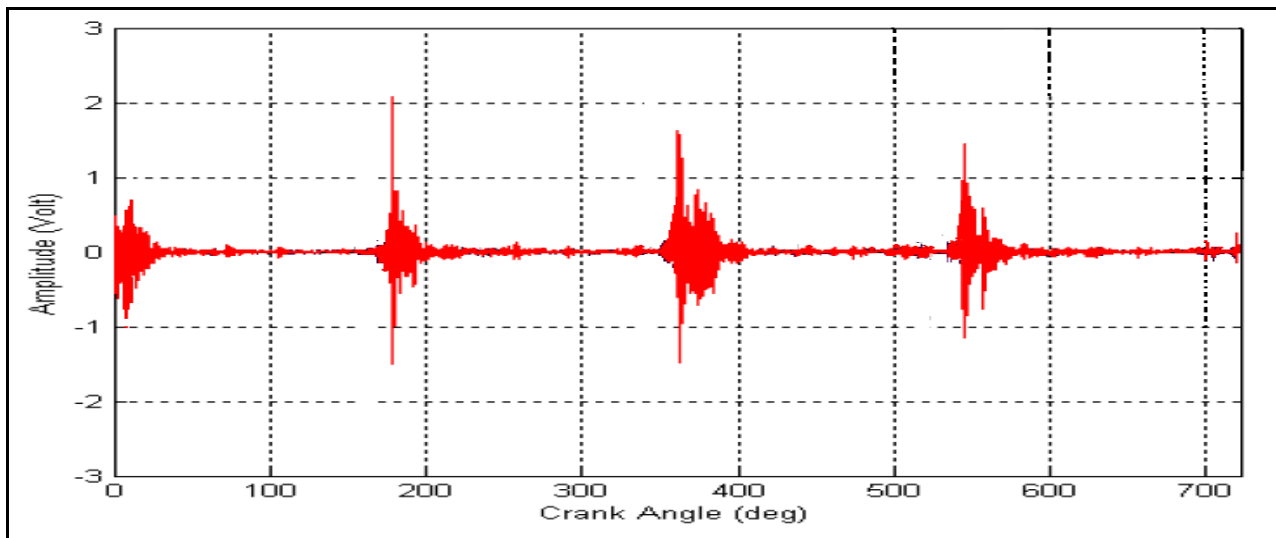


Figure 2.3 Angular-domain signal of body vibrations of a four stroke diesel engine

It was quickly realised that any effective approach dedicated to diesel engines would have to cope with the highly transient nature of their vibrations. Gu, et al., [20] demonstrated that common injector faults change the vibration energy of the injection pulses, and on this basis, the monitoring of an injector via the comparison of monitored pulses with a baseline is described [21].

Molinaro and Castain [22] have performed signal processing pattern classification on sensor-based vibration signals to improve knock detection in spark ignition engines. They applied a classical four-step technique to the modelled vibration signal, consisting of: feature extraction (e.g. energy, amplitude distribution, statistical parameters and cepstral coefficients), selection of

the most representative features, identification of the ‘elements’ characterised by the features, their vectors and their relationships, and, finally application of classification rules (i.e. with and without knock). Although they only used the vibration signal, the accuracy of the fault detection was 100% at a speed of 1500 rpm, while, at higher speeds the result was less good; i.e. the accuracy was 75% at 5500 rpm. Thomas, et al., [23] have also used a pattern recognition technique to detect engine knock, again using the vibration signal.

Grimmelius and Meiler [24] have developed a feature extraction and pattern recognition algorithm to detect cylinder mis-fire in a diesel engine by applying a base-level fluctuation signal analysis and torsion peak value analysis on the crankshaft torsion signal.

2.4.2.2 Oil / Lubrication Analysis

The analysis of oil is widely employed in CM and this is due to the fact that the contents (debris) of the oil provide a superior indication of the condition of the engine. This is because the oil comes into contact with the majority of the moving parts in the engine. Unfortunately, until now oil analysis has generally been applied only in the CM of marine diesel engines. Oil analysis is particularly useful where it is not easy to apply the vibration technique, but it does have its own advantages. Different methods of oil analysis that have been employed are:

1. Viscosity determination by a simple experiment can give an indication of the change in chemical structure of the oil. Due to oil dilution by fuel the degree of contamination of the oil will be indicated by the flash-point of the oil.
2. The magnetic chip detector method utilises a magnetic plug fitted into the lubrication system and directly into the oil. The size and number of particles attracted to the magnet indicates engine wear, particularly of components such as cylinder liners.
3. Ferrography is a relatively simple and valuable method similar to magnetic chip detection, but in this case a magnetic field is used to separate the particles by their size instead of attracting them together. The shape and size of the particles provide information on different failure mechanisms such as abrasion, fatigue and corrosion.
4. Spectrography uses various methods to determine different particle concentrations in the oil. In some methods a sample of oil is atomised using a spark and the amount of energy emitted/absorbed at particular wavelengths correspond to the concentration of particular elements present in the oil.

Oil analysis gives an indication of the engine's suitability for sustained use and provides significant results about the condition of the individual components in the engine. Physical and chemical tests of lubricants can be employed for efficient diagnosis and detection of imminent mechanical failures in the engine. Conventionally, oil analysis has been very hard to carry out on line. Beck and Johnson [25] reported the use of ferrography to monitor particles present in the lubricant of a diesel engine over thirty years ago. Since then there have been many reports on the application of ferrography and oil spectrometry to many kinds of diesel engines. Yan Liu, et al., [26] developed a system for on-line wear condition monitoring for a marine diesel engine. This system consisted of: particle detection, lubricant quality assessment and measurement of shaft torque moment and instantaneous rotation velocity. This system detected wear particles in lubricant with on-line ferrography so as to judge wear condition of the diesel engine. Oil analysis methods can also be carried out for gear boxes and many other machines.

2.4.2.3 Cylinder Pressure Monitoring

In diesel engines, cylinder pressure can be considered to be the pulse of the engine, and the most commonly used parameter used to study combustion. Cylinder pressure, as a function of crank angle for both the compression and expansion strokes of the engine cycle, has been used to obtain quantitative information about the combustion process. The pressure history and peak pressure inside the engine cylinder give an indication of the timing and quality of the combustion and heat release rate.

Analysis of the energy released by the air to fuel mixture shows that it is a function of the variation of pressure in the cylinder and so the latter is directly related to the engine's torque and work output. Studies of pressure variation as function of crank angle as well as cylinder volume are commonly used to monitor diesel engine combustion.

The crank angle at which the peak pressure occurs is very important for the combustion process and gives information about ignition and injection timing which are very important parameters for combustion optimisation, and CM of internal combustion engines. Detailed knowledge of the pressure, and crank angle at which peak pressure occurs, could be part of a powerful diagnostic technique. Cylinder pressure is a direct indication of combustion performance and is used to estimate air to fuel ratio [27, 28], and estimate of ignition timing in engines [29]. Air to fuel ratio estimation is very useful for transient engine control, and Galley and Powel [27] estimated the air

to fuel ratio of a petrol engine by using the crank angle history in conjunction with inlet manifold pressure and engine speed. Leonhardt, et al., [30], used cylinder pressure to monitor fuel injection pump performance. They measured cylinder peak pressure, temporal location of peak pressure and engine speed. These fed into a neural network which was used to evaluate a function they called the "centre of gravity of pressure waveform" to predict mass of injected fuel and crank angles at which the fuel was injected into a four cylinder diesel engine. By comparing the predicted values with the ideal, they were able to detect anomalies such as misfire or poor combustion in the cylinder. Fog, et al., [31] developed a system, which predicted cylinder pressures from strain gauge measurements at the cylinder head. A feed forward neural network time series representing ten past histories of strain gauge readings was trained to predict the next instance of strain as well as cylinder pressure. It was conjectured that the cylinder pressure record predicted in real time could be used for fault diagnosis.

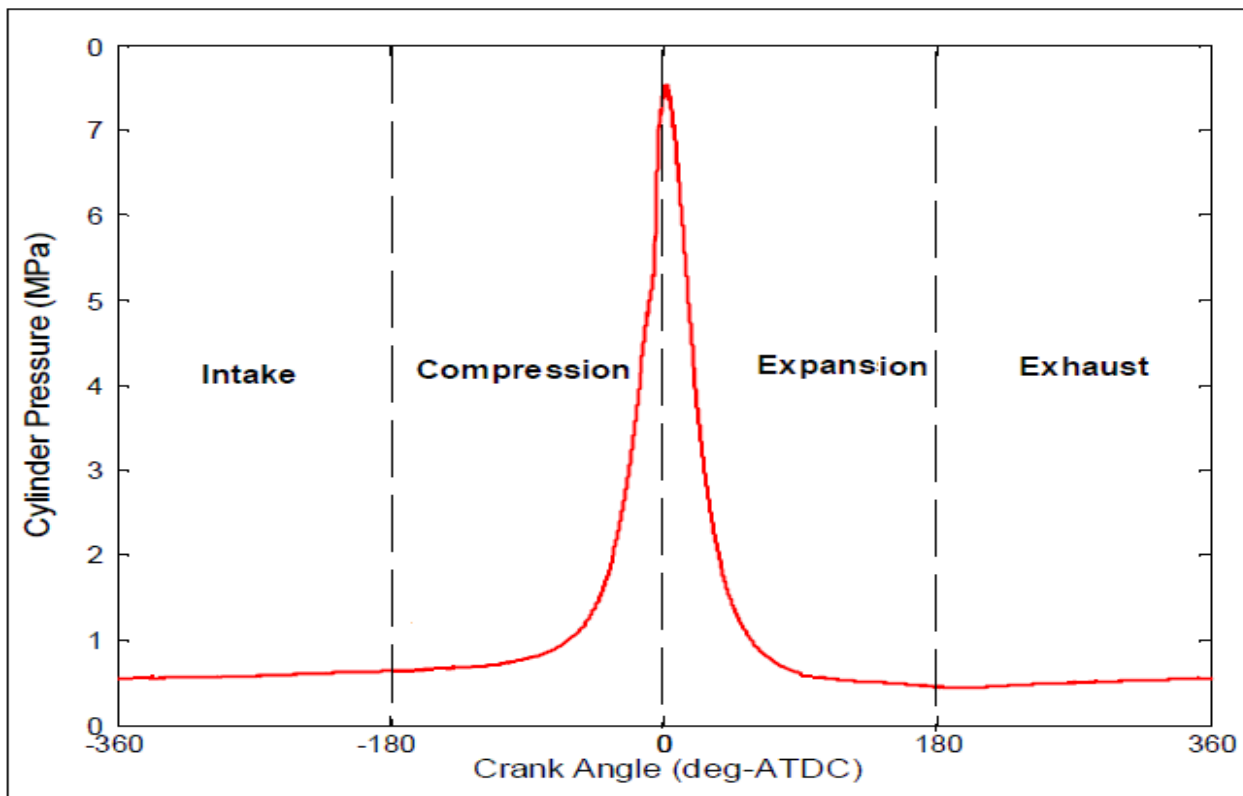


Figure 2.4 Angular-domain of cylinder pressure [16].

Gassenfeit and Powell [28] used a similar approach incorporating the ratio of the cylinder pressure before and after combustion. Cylinder pressures have also been used for direct engine control by Anastasia and Pestana [29], Kawamura, et al., [32] and Pestana [33]. Russell and Haworth [34] show how combustion noise can be measured by analysing the rate of change of pressure in each cycle.

Figure 2.4 shows direct cylinder pressure measurement made with a flame-front piezo-electric transducer. Several measurement techniques available for direct in-cylinder pressure measurement are not suitable for use within in-service engines because they are expensive, unreliable, not sufficiently robust and not easy to maintain or calibrate. Cylinder pressure indirect measurement techniques are not suitable for the use on small automotive engines, because they are only suitable for the use on engines with individual cylinder heads and exposed to the combustion process are subjected to large thermal shock and typically require water cooling. They are also fragile making them unsuitable for use outside of a laboratory environment.

2.4.2.4 Instantaneous Angular Speed Monitoring

Flywheel instantaneous angular speed (IAS) of a diesel engine contains a lot of information about in-cylinder pressure. This technique has been used to detect faults within fuel injection systems and combustion processes. It is based on the fact that the IAS of the flywheel increases as the cylinder fires and decreases with subsequent cylinder compression. This technique again requires the use of speed sensors such as encoders fitted onto, say, the crankshaft of the flywheel and if we mounted more sensors, we will get more accurate results.

Cylinder to cylinder variations are identified from frequency domain harmonics, with dominant harmonics at the cylinder firing rate, and sub-harmonics indicating cylinder differences. Many of the frequencies noted, but not related to cylinder firing were shown to be caused by engine accessories [35].

Statistical methods were employed by Sood, et al.,[36] to extract features from measured flywheel speed data. Waveform cross-correlation analysis enabled the classification of waveform data into faulty and healthy cluster vectors. This method was shown to give a high diagnostic success rate. A parameter estimation approach was also adopted by Sood, et al.,[37]. They showed that an analysis model and parameter ratio classifier can give highly successful diagnosis. Function approximation was carried out using regression coefficient feature vectors.

Kim, et al.,[38] examined pattern recognition diagnostic techniques using flywheel speed data sampled at a very high rate. Three bases were used for the investigation: minimum distance, auto regression and principle component analysis. Of these methods, it was shown that principle component analysis is very capable in detecting misfiring and it was demonstrated that its implementation in an ‘on-the-engine’ processor was quite straightforward.

Jianguo, et al.,[39] developed a dynamic model for simulating the IAS on a small four cylinder diesel engine. It was found that the gas pressure and the vertical unbalanced inertial force, calculated based on the proposed model, had a great influence on the IAS. The characteristic parameters for detecting faults relating to the in-cylinder pressure were successfully obtained.

Gu, et al.,[40] used neural networks and fuzzy logic to process the IAS to detect diesel engine faults. Ben Sasi, et al.,[35] extracted the IAS from the diesel engine alternator output voltage to detect exhaust valve clearance faults. To date the research on IAS has shown that this technique, while useful for confirming the identification of faults detected by other methods, is not yet able to diagnose faults. However, in the near future it is expected to show considerable success with advances of on-board computational technology.

2.4.2.5 Air-borne Acoustic Monitoring

This technique focuses on the analysis of acoustic or noise signals generated from engines. Faults within machines could be diagnosed in 1950 using a ‘Bin-Aural’ engineer’s stethoscope. This simple tool had two probes, one for vibration with a solid contact pointer (called the ‘tectoscope’), and the other for sound with a non-touching conical earpiece (called the ‘Tectophone’) [41]. Fault detection using this tool depended very much on the ability of the operator to remember what he had heard previously when the machine was operating correctly. Perhaps those were the days of the ‘skilled’ operator’ which still exists in the medical field, where the use of a stethoscope is used to identify the early signs of human body failure, such as faulty heart valves (a swishing noise), etc.

In the early 1960s considerable success was claimed at the Boeing Company in the USA for the detection of faults in an aero-engine using an acoustic analyser. This was followed by similar work in UK with Rolls-Royce and Bristol Siddeley Engines including the Spey, Dart and Olympus engines. This engine research had the objective of being able to monitor such parts as bearings, blades, shafts and gears using one or more carefully placed microphones; the engine

frequencies being recorded at idling speed. No significant differences were detected between a ‘good’ engine and one with artificial fault included. The primary problem was that the difference between any two ‘good’ engines was greater than the difference caused by the fault. The conclusion at the time was that “acoustic diagnosis is not easily achieved when applied to complex rotating machinery” [42]. Figure 2.5 shows a microphone output representing the acoustic waveform signals of two crankshaft revolutions of the engine test rig.

Acoustic analysis is not nearly so widely used as vibration monitoring in the CM of diesel engines. This stems from the difficulties associated with extracting useful information from signals having a high noise content, and the fact that the transducer is so easily influenced by the local environment.

Cyclic combustion noise variation was used in fault diagnosis by Schmillen, et al.,[43]. Aouichi, et al.,[44] investigated the internal mechanisms causing diesel engine noise and described how noise levels are likely to change with fault condition, and Izumi, et al.,[45] compared combustion noise and vibration information. Chaudhri [46] showed that sound measurement is more useful in the detection of faults which cause considerable changes in noise output but little or no change in vibration signals.

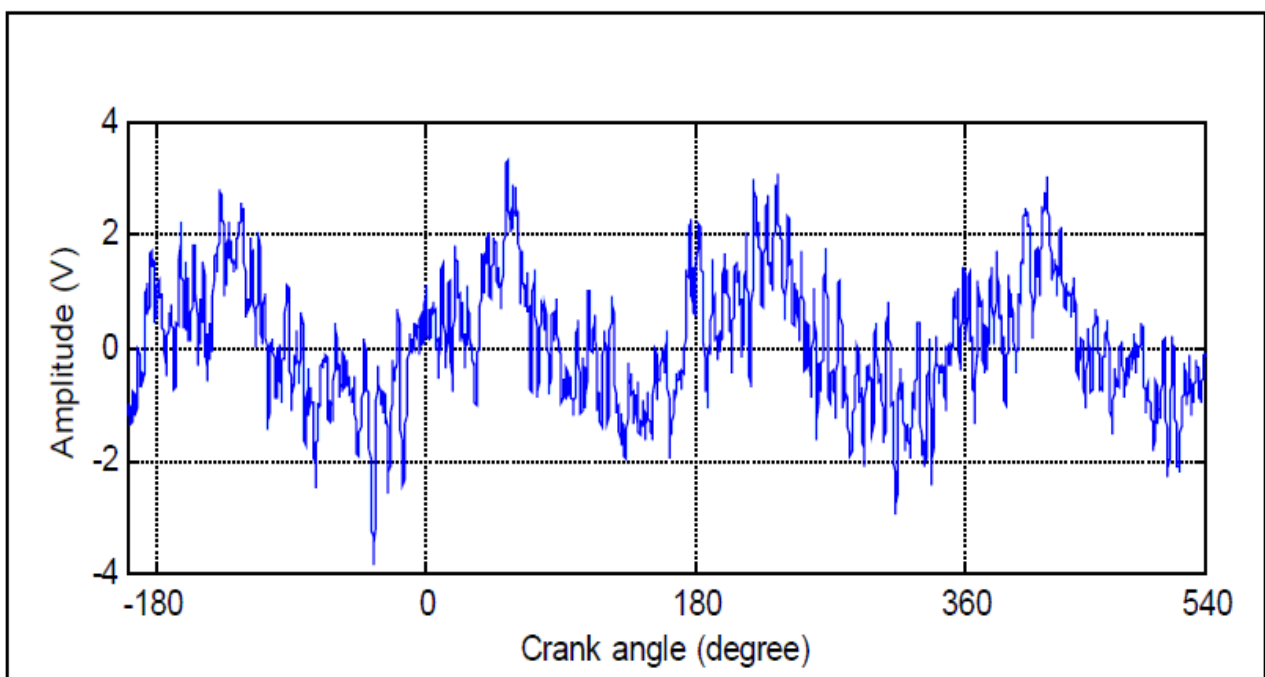


Figure 2.5 Angular-domain of acoustic waveform for two crankshaft revolutions [47].

The most considerable advances were achieved by Ball, et al.,[47] and by Gu, et al.,[48], when it was found possible to eliminate background noise by digital filtration, and the pseudo-Wigner-Ville distribution (SPWVD) and Continuous Wavelet Transform (CWT) were used to detect and diagnose incipient faults in diesel engines.

2.4.2.6 Exhaust Monitoring

Diesel engine exhaust quality contains information related to combustion, injection and lubrication. Through exhaust monitoring it is possible to reveal defects including injector faults, misfiring, bore wear, valve leakage and lubrication degradation, it is also possible to make an estimation of overall engine performance. In addition, exhaust emissions measurement also serves as statutory safeguard for the environment.

The extraction of condition monitoring information from diesel exhaust can be achieved in two ways: chemical analysis of exhaust (emission) gases (including HC , CO , NO , NO_2 , CO_2 and H_2O), and the physical measurement of particles, colour, temperature, mass flow rate, noise, etc. Figure 2.6 shows a shape of the pressure wave for a complete engine cycle measured from the engine exhaust pipe.

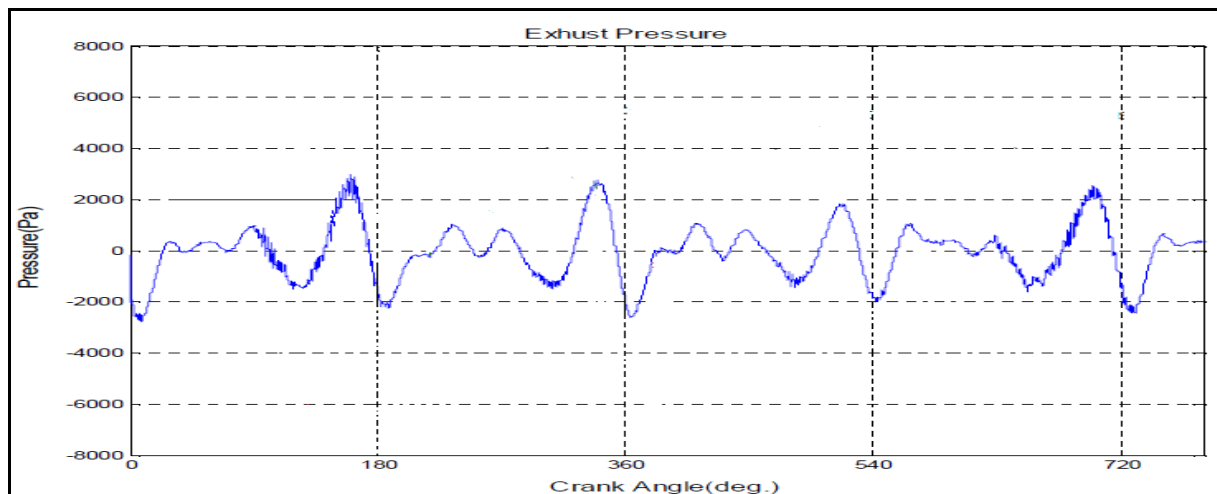


Figure 2.6 Angular-domain of exhaust pressure waveform for complete cycle [16].

Hadden, et al.,[49] reported a technique for the CM of diesel engines based upon the measurement of exhaust pressure pulses, and defect identification from smoke colour was documented in Highway and Heavy Construction. More recent developments tend to focus on the

derivation of an accurate relationship between performance and emissions: Gill [50] and Khair [51] both reported on the passive control of a diesel engine using a particulate trap and catalytic converter. Hartman, et al.,[52] reported the development of an in-cylinder optical sensor for active emission control. Another attractive measuring approach was monitoring of particle dynamic behaviour using laser light reported by Klingen [53], Corcione [54] and Smallwood, et al.,[55].

Of particular interest is the exhaust monitoring technique proposed by Soliman, et al.,[56] because this involves both emission control and routine condition monitoring to detect misfire and some other combustion related faults. The technique is based upon tailpipe pollutant concentration, and engine deterioration criteria for preventive maintenance are explored.

2.4.2.7 Acoustic Emission Monitoring

Acoustic emission has been widely applied to, amongst other things, pipeline testing, evaluation of ageing aircraft, transformer testing, rocket motor testing, production quality control, inspections of valves in steam lines, wind turbine monitoring, ship hull monitoring and earthquake prediction.

AE is defined as mechanical waves, naturally generated by an abrupt release of stored energy within a material, which can be observed in rupture processes such as the snapping of dry twigs and the cracking of rocks. AE measurement techniques involve the detection of the stress waves, usually within a range of 100 kHz to 1 MHz. This frequency range is relatively high and has the useful consequence that a better signal to noise ratio can be achieved than with vibration signals or acoustic signals. AE is the predominant technique for detection of microscopic changes in material where the atomic rearrangement in a material during cracking and deformation generates elastic waves. By using piezoelectric transducers, the waves travelling through the material can be detected. AE is also sensitive to phenomenon such as cavitation, impact and turbulence [56].

An AE is an acoustic wave generated by a material and an AE signal is the electrical signal produced by a sensor in response to this wave [57]. Burst type AE signals are often represented by a decaying or damped sine wave. The mathematical model of such a signal is described in Equation 2.2.

$$V(t) = V_0 \exp(-Bt) \sin(\omega t) \quad (2.2)$$

Where,

$V(t)$ = Output voltage of the AE sensor,

V_0 = Initial maximum signal amplitude,

B = Damping factor / decay constant (greater than 0),

t = time (variable),

$\omega = 2\pi f$, is the angular frequency.

Basically, there are two types of AE signals, burst and continuous signals.

1. Discrete or burst emission: this is high amplitude, energy emission where the individual stress waves representing definite activity in a process can be observed. Phenomena such as crack growth can be observed with burst emission.
2. Continuous emission: this is low amplitude, low energy emission useful for continuous observation such as monitoring leaks in processes and dislocation in metals.

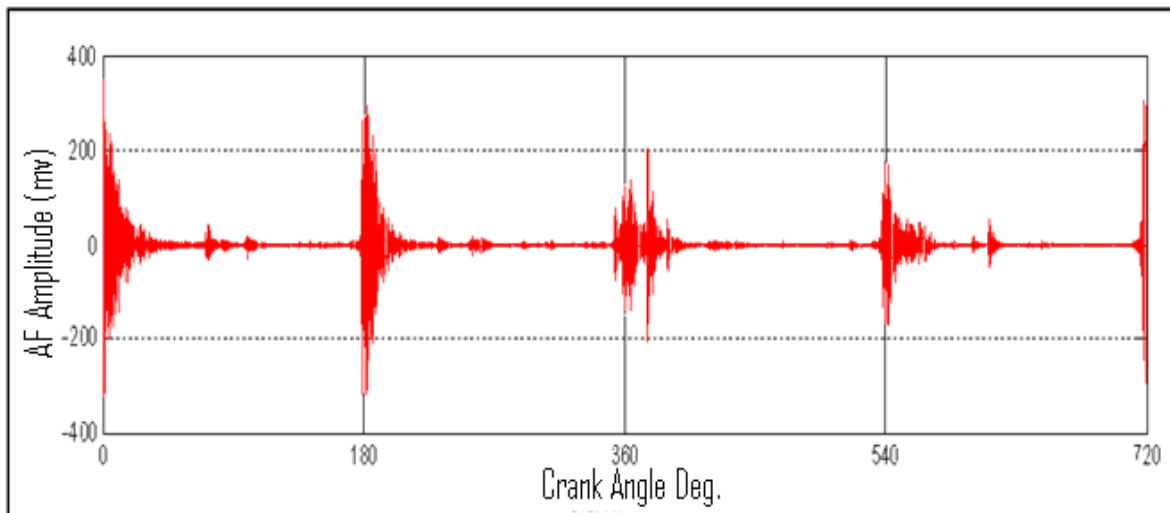


Figure 2.7 Angular-domain of acoustic emission waveform signal of two crankshaft revolutions

Figure 2.7 shows a AE sensor output representing the AE waveform signals for two crankshaft revolutions. AE can be generated by a wide range of possible impulsive sources which, in reciprocating machinery, can include combustion, piston slap, valve clatter, gas flow and many other mechanical and fluid events. Such sources also produce acoustic noise and vibration, although acoustic waves and lower frequency vibrations can both suffer from the difficulties of interfering sources (e.g. wind noise, structural vibration), which make the diagnostic information

from the sensor signal more difficult to extract. For this reason, AE has great potential for revealing the internal operating characteristics of the machine, whilst using non-intrusive sensors. Current diagnostic systems normally involve an automatic analysis of the acquired signal. Feature extraction and pattern recognition algorithms are often used for analysing signals, and a class, which is determined by the diagnostic results, is assigned. In the simplest form, each class indicates a condition such as normal/faulty, or a more specific condition like a leaking cylinder head gasket. The classification is achieved by matching features of the signal, or even the complete acquired signal, with a set of reference data corresponding to known conditions. Fog, et al.,[58], have successfully applied principle component analysis to AE signals to detect exhaust valve leakage in a large marine diesel engine. El-Ghamry, et al.,[59] used various statistical features and pattern recognition techniques such as the mean and the variance of AE signals to identify diesel engine faults such as cylinder head gasket leakage.

AE Advantages

1. High sensitivity,
2. Non directional technique,
3. Insensitive to structural resonances and mechanical background noises,
4. Real time capability volume monitoring approach,
5. Early and rapid detection of defects, faults, cracks, and
6. Minimization of plant downtime for inspection, no need for scanning the whole structural surface.

AE Disadvantages

1. Highly specialised sensors and signal processing is required,
2. Signals weaker than vibration signals, and
3. Rapid attenuation of signal during propagation requires the AE sensors to be very close to the source.

2.5 Summary

The shift to predictive maintenance strategies has created a requirement for more revealing diagnostic information than currently available.

As regards the former, a wide range of novel monitoring techniques have been investigated by different authors, with some proving more successful than others. Of these, analysis of vibration

signals appears the most promising due to the non-intrusive nature of the measurements, the rich information content of the signals and recent advances in signal processing techniques. Furthermore, it appear that more diagnostic information is contained in the higher-frequency emission range and therefore monitoring based upon significantly higher-frequency AE measurements is anticipated to offer even greater capabilities. Previous work in this area shall be reviewed in the following chapter.

CHAPTER THREE

ACOUSTIC EMISSION MONITORING AND ITS APPLICATION TO DIESEL ENGINES

This Chapter provides an understanding of three areas of AE monitoring that are central to the research work presented in this thesis. Firstly, the principles of AE are outlined, which includes discussion of AE sources, and a brief review of the growing range of applications. Secondly, developments to date concerning AE monitoring of diesel engines and other reciprocating machinery are reviewed. Finally, previous work on AE monitoring of sliding contact is examined in the context of application to laboratory wear tests. This provides the opportunity to examine relationships between variables that govern sliding contact and any resulting AE activity.

3.1 Introduction

Acoustic Emission or stress wave emission is phenomena whereby transient, high-frequency elastic waves in the range 100 kHz to 1000 kHz are generated by the rapid release of strain energy from a localised source within or on the surface of a material or a certain process. A number of source mechanisms in machine operation, are recognized to generate AE such as sliding contact, wear, mechanical impacts and certain types of fluid flow. The signals resulting from AE can be measured at the surfaces of a machine using a suitable sensor and can be analysed in different ways to extract the required information, the most important of which is signal characterisation with regard to performance of the machine being studied [59]. While AE sensors are mounted on the surface (externally) the technique is non-intrusive. In addition, AE signals are associated with the degradation of real operational processes, while other monitoring techniques are often intrusive and typically measure degradation symptoms [60]. The many benefits associated with AE monitoring are such that research into its applications has increased in the last decade and a number of engineering disciplines have become associated with commercial AE based monitoring systems [61].

3.2 Acoustic Emission Principles and Applications

AE monitoring, also referred to as stress wave monitoring, is the practise of characterising and evaluating AE signals in order to investigate material or component behaviour. It is inherently a passive Non Destructive Testing (NDT) technique that relies on energy being released from a material. This is distinctly unlike conventional ultrasonic NDT inspection techniques, where the effects of introducing external, artificial waves of a known type are monitored.

The purpose of this section is to provide an understanding of the foundations of AE monitoring; how AE is generated, how AE can be measured, methods to process AE signals in order to provide information for condition monitoring, and how AE monitoring fares when evaluated against comparable techniques.

3.2.1 Fundamental Principles

AE is the term given to describe transient, elastic waves of surface displacement that occur within the approximate frequency range 100 kHz to 1000 kHz due to changes in the microstructure of materials. Phenomena which cause these impulsive releases of energy and which conform to the classical definition of an AE source, i.e. they occur due to mechanical deformation of a stressed

material, include crack growth, movement and creation of dislocations, and slip, twinning and grain boundary sliding in metals. In essence, any form of atomic level material dislocations can generate AE and it has been claimed that displacements as small as 1/1000th of an atomic radius can produce well-distinguished AE signals [61]. There are a number of other mechanisms that either give rise to AE that occur in the absence of any deformation process, these are sometimes termed pseudo or secondary sources, and in terms of machinery operation include mechanical impacts, sliding contact, turbulent fluid flows and fluid cavitation.

AE generated waves radiate in all directions, propagating throughout the material in a variety of forms; as compression, shear and Lamb waves, and ultimately manifesting themselves as Rayleigh surface waves. As the waves propagate they suffer a loss of amplitude with distance. Pollock [62] identified four reasons for this attenuation; geometric spreading of the wave front, internal friction, dissipation of energy into adjacent media and velocity dispersion.

Geometric spreading of the wave from a point source inevitably results in attenuation since the wave has a fixed amount of energy which must be distributed over an ever larger wave front. The wave amplitude will decrease inversely with distance in three-dimensional solids and inversely as the square root of the distance in two-dimensional structures such as plates and shells. This form of attenuation has been noted as being dominant close to the source, i.e. in the near field [62]. Internal friction involves the conversion of elastic wave energy into thermal energy through various damping mechanisms. This results in exponential attenuation with distance that becomes dominant at greater distances from the source, i.e. the far field.

Further signal distortion takes place when material boundaries are encountered as wave reflection, refraction, transmission and mode conversions can all occur. Therefore, for complicated structures that feature, for instance, intricate geometries, cavities and contain fluids, wave propagation will be considerably more complex than for simple plates and strips. These effects generally cause a reduction in wave amplitude with distance although local constructive or destructive interference effects may also exist. Wave dispersion is a further form of attenuation which causes different frequency components of a signal to propagate through a material at different velocities. The outcome is that a signal of initially short duration spreads out as it travels and loses amplitude accordingly.

In effect this means that by the time measurement of the signal is possible at the material surface the waveform will merely be a representation of the original source excitation. Nevertheless, significant information is still available, and it is typically the variation of the measured signal, either with time or distance, which is of interest. The benefit of AE propagation is that, given a source of sufficient energy, external remote investigation of material behaviour can be achieved. This is a significant advantage when the area of interest is at an inaccessible location or is one which prohibits the use of other monitoring techniques.

3.2.2 Relative Merits of AE, Vibration and Air-Borne Acoustic Monitoring

The source mechanisms that produce AE are generally also responsible for vibration and audible air-borne acoustic waves. All can be exploited as non-intrusive condition monitoring techniques, although it has been claimed that AE has significant advantages over the other two.

The principal benefit of AE is that far greater signal-to-noise ratios can be achieved for signals relating to the most important mechanisms and processes. Because of the very high frequency content of AE the lower-frequency background noise, which can be troublesome for vibration monitoring, has little bearing on the AE signal. Accelerometers monitor surface motion up to approximately 50 kHz using the most modern transducers. However, operational noise and machine resonances are also prevalent in this region and because this background vibration is often orders of magnitude greater than any fault-induced vibration then early, accurate detection of faults can be difficult. Consequently, when abnormalities in the vibration signal are detected the machine or component is usually close to failure, or failure has already occurred. AE monitoring on the other hand is of such sensitivity that it can be used to detect the degradative processes that lead to failure rather than the consequences. A further benefit of high-frequency AE is that the temporal and spatial resolutions are significantly greater than for vibration monitoring. Again, this is because high frequency waves attenuate much quicker with regards to both time and distance. The monitoring of air-borne acoustics via instrumentation located away from the material surface is a further step down in diagnostic capabilities where additional acoustical environmental effects have to be considered.

Numerous investigations have directly compared AE and vibration monitoring, and to a lesser extent air-borne acoustics for machinery diagnosis. These have included experimentation on rolling element bearings [63, 64, 65], reciprocating engines and compressors [66, 67, 68], centrifugal

pumps [69] and the meshing of gears [70-72]. In each of these cases AE monitoring was shown to be the more effective for fault detection and performance monitoring. One aspect where AE monitoring shows a particular improvement on vibration monitoring is an increased sensitivity to fluid flows, both for normal and faulty operation [63, 69, 71].

The improvement offered through AE monitoring is emphasised in Figure 3.1, which shows simultaneous in-cylinder pressure, RMS AE and RMS accelerometer measurements acquired from the cylinder head of a running gas-fuelled engine [67]. It is evident that the vibration signal lacks clear correlation with the timing of the valve activity (denoted in Figure 3.1 as IVO and IVC for inlet valve opening and closing, and EVO and EVC for exhaust valve opening and closing) whereas the AE signal displays more information with transient AE events generated at each valve action. In this case the accelerometer measurements appear to show a particular lack of information as other researchers have reported that valve impacts within engines are identifiable from vibration signals [73, 74, 75].

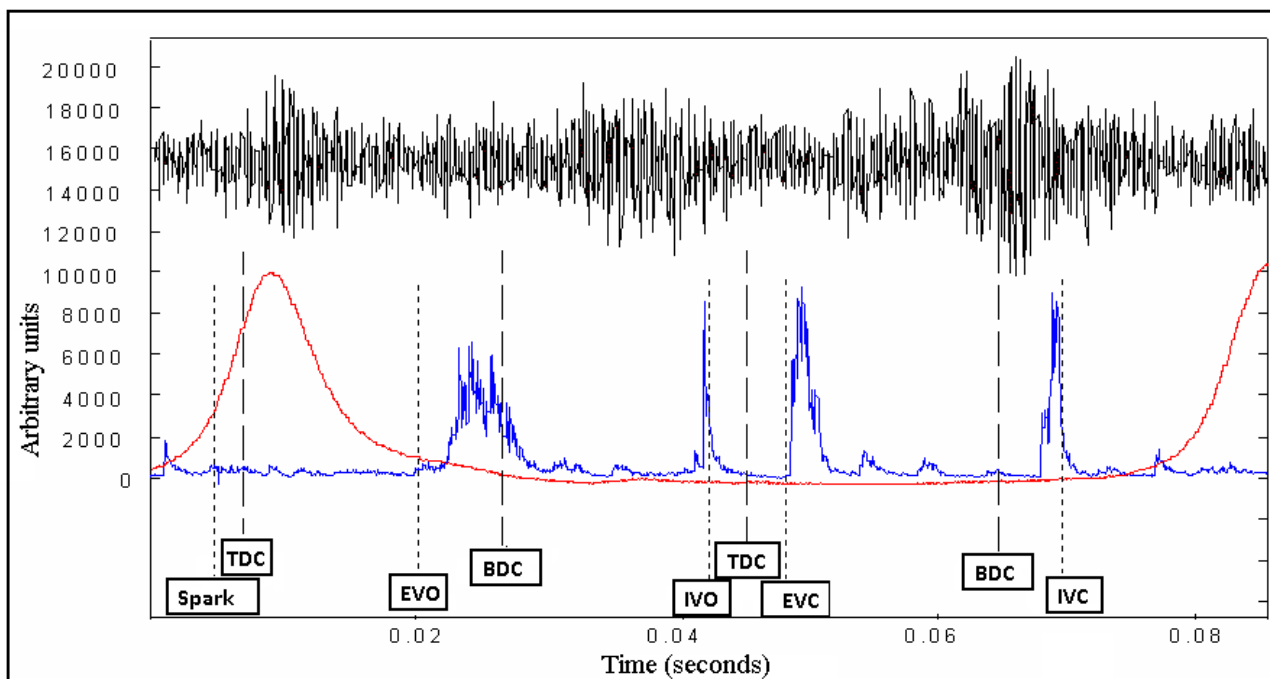


Figure 3.1 Simultaneous in-cylinder pressure—, RMS AE — and RMS acceleration — measurements from a gas-fuelled engine [67].

Vibration monitoring does possess some advantages when compared to AE monitoring. Accelerometers can be mounted so to measure the vector components of acceleration thereby

providing a 3-dimensional account of whole-body surface movement. This is in contrast to the 1-dimensional measurements available through AE measurements. Absolute measurements of acceleration can be obtained; hence data can be compared on a quantitative basis. This has resulted in vibration monitoring being widely-used, well-understood and industrially accepted. Currently, AE monitoring is not as widely-understood or as accepted although it is quickly gaining in recognition as a condition monitoring technique [67].

3.2.3 Applications of AE Monitoring

The benefits of AE monitoring are sufficient for it to become an established technique in a number of engineering disciplines with a number of bespoke AE-based commercial monitoring systems available for specific applications. This is particularly true in the field of pressure vessel proof testing where the non-destructive nature and high sensitivity to cracks and fluid flow through confined spaces make it a valuable tool for structural assessment and defect location [61, 76]. AE analysis has proven to be particularly well suited to be the monitoring of crack initiation and propagation [77]. This has been ascertained through applications as varied as the monitoring of cables in suspension bridges [78] and of the structural integrity of historical statues [79].

On a smaller scale, laboratory materials research is a further successful application. The generation of AE from microscopic material disturbances has allowed material properties, damage mechanisms and resulting material behaviour to be investigated in detail using insight that may not be available through other means.

Condition monitoring of machinery via AE measurements is an expanding area of active research where AE monitoring of bearings is perhaps the most advanced, probably as a result of the regularity of bearing faults occurring in industry and the relative ease of investigation. Other components investigated include gearboxes, turbines and reciprocating engines. Progress to date in monitoring of reciprocating engines shall be detailed in the following section.

Recent developments in computational and data acquisition capabilities have permitted further investigation into these established research themes as well as opening up additional research possibilities. These have been in fields as diverse as orthopaedic diagnostics, where friction during bending of human knees has been detected [80], and botany, where phenomena such as flora cavitation have been studied [81].

3.3 AE Monitoring of Reciprocating Machinery

The purpose of this section is to provide a review of achievements to date regarding AE monitoring of reciprocating machinery; this primarily involves diesel engines, both large and small, but also includes work on reciprocating compressors. The use of non-intrusive AE analysis in engine diagnostics is a relatively recent development that has centred primarily on research institutions, although the progression into commercial use has of late been observed, with at least one AE-based engine diagnostic system currently available [82].

This monitoring method is based on the premise that the mechanical and fluid events and processes occurring within engines, e.g. valve activity, injector operation, piston motion, fuel combustion and exhaust, generate AE which can then be measured with suitably placed external sensors. Therefore, with appropriate signal analysis there is the possibility to monitor aspects of machine operation and detect associated faults. Details shall be given as to what has been investigated and also the analytical techniques that have been employed. A thorough review of this topic is also provided by Steel and Reuben [61].

3.3.1 Initial Identification

To the author's best knowledge the first published work concerning AE acquisition from engines was reported by West, et al., [83]. However, these works made no attempt to understand the AE generated during engine operation, rather, they were largely exercises in signal-processing with the aim being to extract a digitally embedded burst-type AE signal, relating to a micro crack, from background AE acquired from a lawnmower engine. Nevertheless, it was recognised that certain aspects of engine operation could result in AE generation: "We are looking at scenarios where the AE signal is buried in strong interference (which could be periodic) due to a mechanical motion, like the movement of a piston in an engine" [84].

Much of the AE in this case was regarded as noise which was dominated by frequencies below 30 kHz. This is below the typical AE frequency band lower limit, and it is not clear what, if any, pre-processing filtering steps were taken. Hence this observation may simply be a consequence of unfiltered AE acquisition.

Gill, et al., [85] were the first to report on the possibility of engine diagnosis via AE measurements. This study focused in particular on the combustion process, with RMS data acquired from sensors

located close to the combustion chambers of small, four-stroke high speed direct injection (HSDI) diesel engines. Information about the timing and sequence of mechanical operation within the engine was used to map the events in the AE signals acquired during normal operation to their respective origins. This showed that events were generated from combustion or combustion-related processes as well as from valve activity for all four cylinders. The presence of these events was found dependent upon sensor location with signals from other positions on the engine noted as being more complex containing contributions from other engine driven components.

Two induced fault conditions were investigated; fuel starvation through disconnection of the fuel-feed pipe to an individual cylinder, and reduced injection discharge pressure. Under fuel starvation conditions a simple comparison revealed that the events purported to relate to the combustion process in normal operation were absent. To characterise a progressive reduction in injector discharge pressure the authors used a simple technique whereby the energy in a time-windowed section of the signal was calculated and compared as conditions varied. It was also found practical to use the signal averaged over 10 cycles so that a time-averaged, time-domain signal was obtained, which provided a better overall representation of the AE signature at a particular running condition. The signal energy in a window corresponding to the combustion process was found to increase with a reduction in discharge pressure. It was reasoned that this was due to an increase in combustion harshness as a result of poorer fuel atomisation. Analysis of event timing was also found to be useful for fault detection. The initial event, postulated to be combustion-related occurred earlier in the cycle with decreasing injection pressure. This was consistent with the premise that the event was injection related since the lower delivery pressures would be achieved by the fuel pump earlier in the cycle.

3.3.2 Monitoring of Injection, Combustion and Combustion-Related Processes

Gill, et al., [86] expanded their earlier work [85] to investigate more detailed raw AE signals acquired from the fuel injector body of a small, HSDI diesel engine operating under reduced injection discharge pressures. To provide a thorough evaluation of injector operation the AE data were supplemented by measurements of injection pressure, needle lift and in-cylinder pressure. As in the previous study, the relatively small size of the engine meant that AE originating from all four cylinders of the engine propagated to the sensor location, with the most prominent events found to relate to fuel injection and combustion in the cylinder closest to the sensor.

The level of temporal resolution offered through AE monitoring permitted the injection AE signature to be separated into its constituent events. The authors suggested that the initial AE burst was due to the sudden increase in fuel pressure whilst the main AE burst was generated due to the injector needle attaining the fully open position and subsequently impacting with the injector body. Importantly, these observations were validated through comparison with the needle lift measurements.

Again, similar to [85], the timing of injection events was observed to advance for a reduction in injection discharge pressure. This was found consistent both cyclically and also over all engine speeds and loads considered. The authors also report that for the lowest pressure the duration of the whole injection/combustion AE event was extended compared to the normal condition by a period of low amplitude AE. This was thought to be related to coarse fuel atomisation which would require a longer combustion period. Validation of this suggestion was not provided, and would have been difficult to achieve, but it does illustrate that examination of AE activity may reveal further insights than needle lift and fuel pressure monitoring.

Several other research groups have investigated AE relating to injection and combustion processes [67, 87-93]. Berjger [87] confirmed that operation of a fuel injector without combustion was indeed a source of AE. Fuel was injected into a combustion chamber of a four-stroke engine filled with inert gas thereby inhibiting fuel ignition and combustion and leaving only the injection events, namely the pressure increase in the injector body, the resulting needle movements and high-pressure fuel flow, as possible AE sources. Analysis presented in this work was limited but AE events were noted and attributed to injector operation, with the amount of activity dependant on both the quantity and diameter of the nozzle orifices. The proposed use of such knowledge was for injector nozzle diagnostics in ship injection systems.

Bialkowski, et al., [88] performed similar tests on a common-rail diesel injection system again finding that significant AE activity was generated by injector operation in the absence of combustion. In this case, AE activity was found to increase with both injection pressure and fuel pre-heating.

Godinez, et al., [89] reported that injector cavitation and detonation could be diagnosed from analysis of time-domain AE characteristics. These claims were corroborated through simultaneous acquisition of other engine data, in this case load measurement from the rocker. Time-domain analysis of windowed injection/combustion events was also found to be a suitable method for

identification of operating conditions over varying load by Frances, et al., [90]. Eleven statistical features were extracted from a window corresponding to the combustion AE events for a 3.8 MW, medium speed, four-stroke engine, namely; signal energy, mean, standard deviation, variance, skewness, kurtosis, maximum amplitude, peak start location, peak ignition location, peak end location and power spectral density ratio. Principal Component Analysis (PCA) was used to identify and eliminate redundant features and a neural network was then applied to differentiate between operating conditions. The results of this process showed that engine loading condition could be reasonably identified, although not with complete confidence. Further frequency-domain analysis showed that engine loading could not be determined through analysis of frequency content but could be distinguished through wavelet analysis.

Chandroth, et al., [91] described a data acquisition system which acquired AE measurements alongside vibration and in-cylinder pressure data for the detection of combustion-related faults in a small, four-stroke diesel engine. This was expanded upon by Sharkey, et al., [92] who applied neural networks to assess the value of each measurement technique for the detection of these faults. Selective pre-processing methods were employed, in the case of AE data this consisted of frequency-domain analysis. The authors reported that the best performance in terms of generalisation, i.e. when one dataset is tested against validation data, with a value of 97.7 %, was from the AE measurements. This compared with 94.0 % and 88.7 % for the vibration and in-cylinder pressure data respectively, providing further evidence of the usefulness of AE measurements in engine diagnostics.

Other combustion-related features have been investigated. The possibility of using AE measurements to infer fuel-to-air ratios in an 8-cylinder, 430 kW, four-stroke gas engine was investigated by El-Ghamry, et al., [67]. For this work a window of raw AE data corresponding to the combustion period in the cylinder closest to the transducer was extracted from the rest of the signal. Simple features were then calculated such as the mean, peak, peak to mean ratio, standard deviation and variance over 10 individual cycles acquired at various running conditions.

The amount of AE activity was observed to increase for both lean and rich running conditions compared to the reference normal condition, with variance noted as the most distinct parameter. The changes in fuel supply were also evident, although to a lesser degree, from inspection of in-cylinder pressure data.

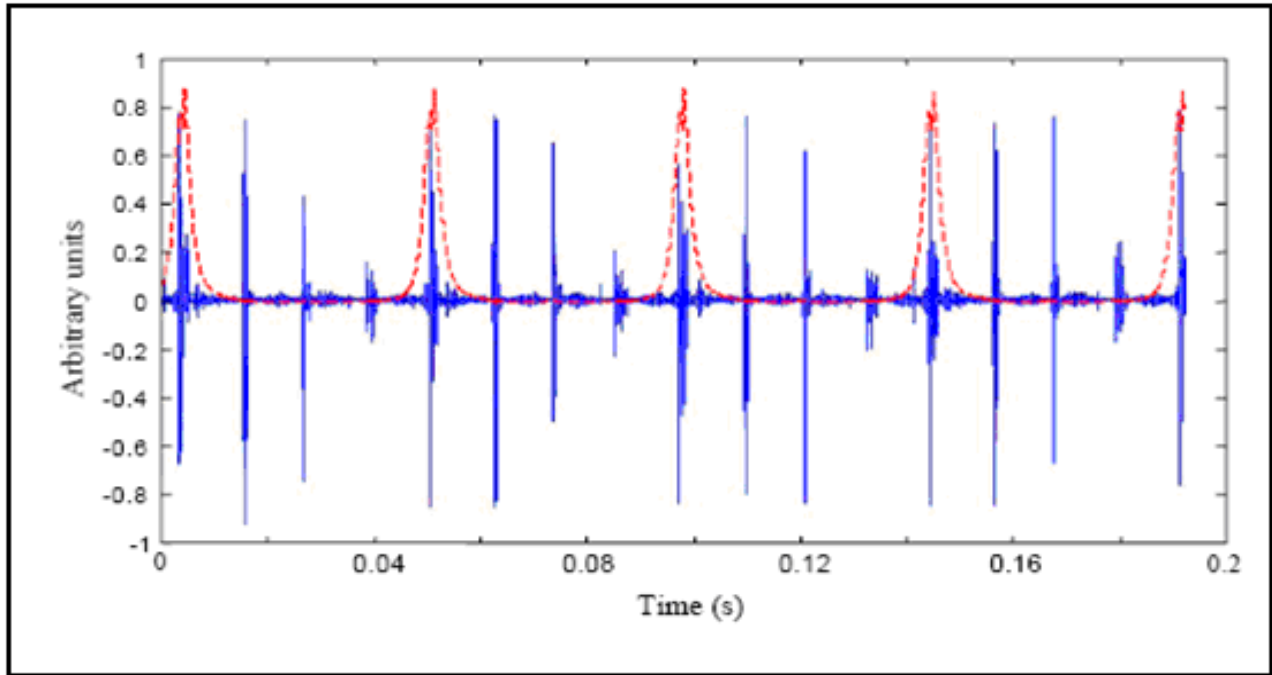


Figure 3.2 Raw AE acquired from a 430 kW, four-stroke engine showing injection/combustion events at areas of maximum pressure, other smaller events appear regularly, AE (———) and in-cylinder pressure (-----) [93].

El-Ghamry, et al., [93] further outlined a technique whereby the in-cylinder pressure trace could be reconstructed from the AE signal over the compression/expansion period. This would be similar to others who attempted reconstruction of the in-cylinder pressure trace using vibration [94-96] and IAS measurements [97, 98, 99-104] to diagnose combustion deficiencies. Although this work centred on the combustion period, data were presented, see Figure 3.2, which showed a number of other events, both large and small in relation to the prominent injection/combustion events, and these appear regularly during the cycle and are cyclically consistent.

3.3.3 Monitoring of Exhaust Valve and Gasket Leakage

Much use has been made of the sensitivity of AE to gas flow excitation to investigate the monitoring of fluid flows within engines, including normal processes and leakages from both exhaust valves and gaskets.

El-Ghamry, et al., [67] reported that for a 0.5 MW gas engine AE was generated at times coincident with valve movements; the specific example given was of exhaust valve opening, which was observed to be accompanied by a broad, high-amplitude AE event. It was reasoned that the AE generated during valve opening may be indicative of the gas flow properties through the exhaust port, and thus this activity would be affected by such factors as in-cylinder pressure, valve leakage and deposition. The authors also noted that the AE signals were much more defined and responsive to these valve actions than simultaneously acquired vibration measurements.

Fog, et al., [66, 71, 105] detected exhaust valve leakage in a large, two-stroke diesel engine using AE measurements, again finding this more effective than acceleration, in-cylinder pressure or temperature measurements. For this work in addition to the normal case the exhaust valve was degraded by cutting a groove in the valve face, with two leakage areas, 4 and 20 mm². It was found that due to the large size of this engine the cylinder-by-cylinder analysis was simpler than for small engines because the propagation distances and signal attenuation were such that cross-cylinder interference was minimal. This allowed for easier isolation of events, and using knowledge of the engine cycle the AE events were then related to mechanical actions within the engine, Figure 3.3 shows such events labelled as XVO, XVC, IJS and IJE which relate to exhaust valve opening and closing and the start and end of the injection process, respectively. A further pre-processing step was the resampling of the data, which effectively related one AE sample to one pulse of the shaft encoder signal thereby overcoming signal non-stationarity over varying operating conditions. Furthermore, it greatly reduced the amount of data per cycle which permitted the easier application of higher statistical analysis techniques.

RMS AE signals acquired from the exhaust valve housing of the engine operating under normal conditions and with a large exhaust valve leakage are given in Figures 3.3(a) and 3.3(b) respectively. It is clear that with the leak there is a significant increase in AE activity. As might be expected, this occurs during the compression and expansion phases and increases in amplitude with in-cylinder pressure. This leakage activity was also observed to increase in proportion to the leakage area.

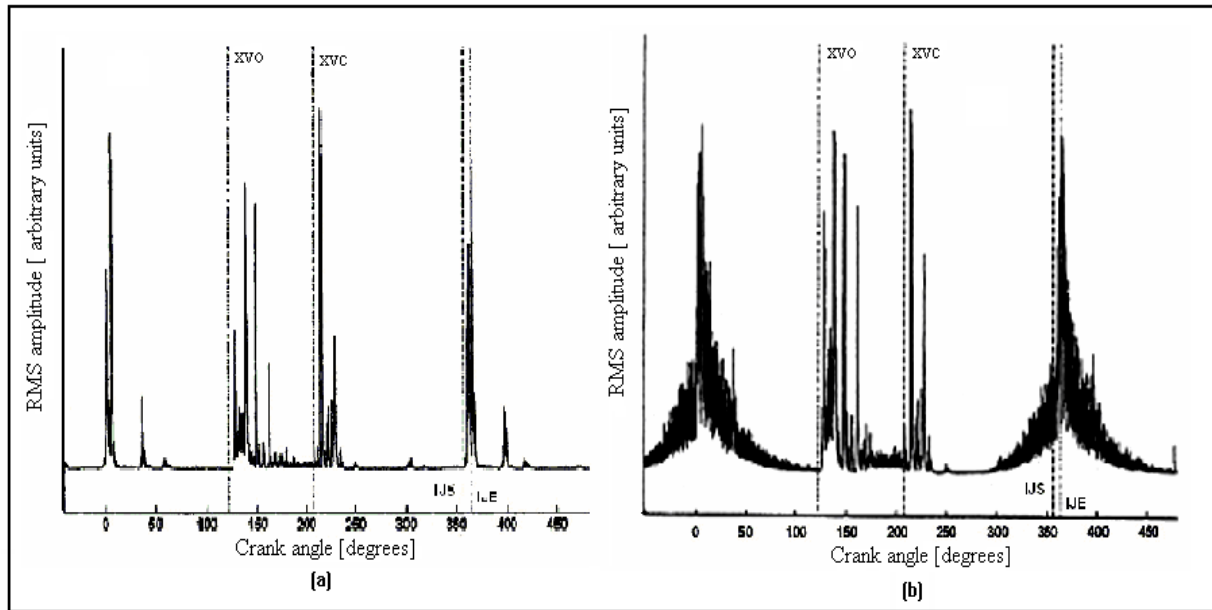


Figure 3.3 RMS AE signals acquired from a large, two-stroke diesel engine, (a) healthy condition and (b) large exhaust valve leak [66].

Friis-Hansen and Fog [106] investigated the same dataset and found that a simple calculation of the mean value in a windowed region relating to the compression stroke, 300 to 350 degrees after TDC, was sufficient to distinguish between leakage sizes with only a small percentage of misclassifications. This window was chosen carefully to avoid signals relating to injector and valve sources. The possibility of monitoring injector misfire was also investigated, not through analysis of AE generated during the injection process but through the consequences on combustion, i.e. the in-cylinder pressure and related leakage levels. Detection was proposed through comparison of AE energy during windows of the AE signal before and after TDC. Ratios above and below unity were found to be suitable for distinguishing between normal operating and complete misfire conditions. However, it was not clear whether this method would work under no leakage conditions.

Monitoring of head gasket leakage in a small, four-stroke diesel engine was investigated by El-Ghamry, et al., [107]. As with others who have considered AE generation from small engines a high level of cylinder cross-talk was observed, hence sensor positioning was important in order to target specific engine areas. When gasket leakage was induced AE activity during the compression/expansion phase increased significantly, in a similar manner to that observed previously by Fog, et al., [66, 73, 105], for exhaust valve leakage. An algorithm based upon signal

thresholding and statistical quantifiers was developed to automatically identify this gasket leakage feature. Frances, et al., [108] also reported that the energy content of a windowed section of the signal varied when a fault was introduced to the exhaust manifold gasket of a small, four-stroke engine. However, although a change was generally observed between fault and no fault conditions the difference was not systematic over varying engine speeds and loads.

Variability of AE signals over several cylinders of a medium-speed, four-stroke diesel operating under normal conditions was evaluated by Frances, et al., [109]. For each cylinder statistical parameters were calculated over a number of cycles for a windowed area of the signal containing the compression and expansion phases. In each case the AE energy content was found to be cyclically consistent; however, substantial variation was observed between cylinders. One cylinder displayed a significant increase from the normal variance, and tests over varying loads indicated that the additional AE activity was related to the in-cylinder pressure. Frequency analysis showed that it contained energies at higher frequencies and although this was not investigated further this led the authors to suggest that the additional AE activity was indicative of leakage.

AE measurements have also been successfully used to monitor normal and faulty valve processes and associated leakages in reciprocating compressors, Gill, et al., [68, 103]. AE signals acquired from the cylinder head of a small, two-cylinder compressor during normal operation showed all mechanical activities of inlet and exhaust valves [110]. In this case, the valves were of the plate variety and their operation was therefore dictated by the pressure differential between the cylinder and exhaust manifold. Several faults were induced. For both a grooved discharge valve seat and an unseated discharge valve. Additional AE features relating to gas leakage were evident in addition to changes in event timing brought about by variations in pressure balance. Analysis of event timing also permitted the detection of a weakened valve spring.

Testing on a large scale, industrial, ethylene compressor [68] further demonstrated the sensitivity of AE monitoring to valve actions and fluid flows. Valve opening and closing events were readily identifiable. A further source was identified as fluid flow in and out of the cylinder; in addition to being active at valve opening this also generated a low-amplitude feature around mid-stroke positions. Data acquired immediately prior to an overhaul, with 'real' faults in place, showed that significant AE activity resulted from leakage past the valves and also from leakage through the stuffing box to the sump.

3.3.4 Event Mapping and Source Location

The task of relating AE events to their respective mechanical and fluid-mechanical sources within an engine, termed ‘event mapping’, has been described in a number of papers and reports. Event mapping is, effectively, the source location of a sequence of AE events aided by knowledge of the processes that constitute an engine cycle and which may be anticipated to give rise to AE. Acquisition of other engine signals can also be useful, engine timing signals are particularly valuable as they provide calibrated timing references; also, needle lift measurements have proved effective in understanding AE generation during fuel injector operation [86]. Even when further engine information is unavailable the processes of varying engine operating conditions and inducing faults will generally bring about changes to the cyclic AE signature which can then be used to understand the original source mechanisms.

It has been demonstrated that the temporal resolution of AE signals acquired from engines is of an extremely high order, due to burst-type events usually being of a relatively short duration. Therefore, this allows the events to be separated and mapped in the time, or angular, domain to a precise level. This is particularly true for large, low-speed engines where interference between events is often minimal.

Nivesrangsan, et al., [111-114] conducted a thorough investigation into the mapping of AE events generated within the cylinder head of a small HSDI diesel engine. In doing so they introduced techniques for spatial reconstitution [113] and source location [114] using multi-sensor arrays. The motivation for developing such techniques was to provide focused monitoring of specific components and/or processes and thereby improve the diagnostic capabilities of AE. This is particularly relevant for small, multi-cylinder engines as the small propagation distances and material attenuation properties results in AE from all cylinders contributing to the AE measured at a single point. This is exemplified in Figure 3.4(a) which shows raw time-domain AE data acquired from sensors located on the cylinder head adjacent to cylinders 1, 2 and 4 [112]. The windowed firing period for each cylinder is also indicated and immediately it is clear that the main events are associated with the injection/combustion processes, and that the amplitude of these events are greatest for the sensors located closest to the cylinder in question.

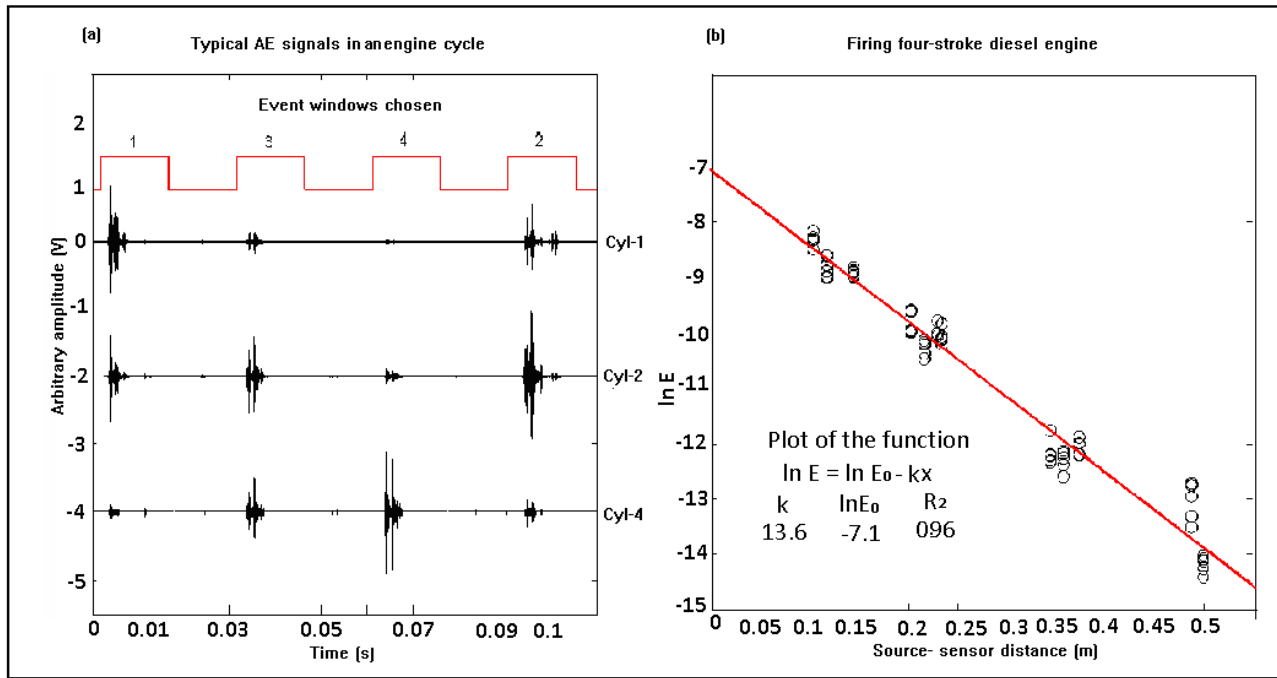


Figure 3.4 Raw AE signals acquired from the cylinder head of small, HSDI engine, (a) propagation around the head, (b) attenuation characteristics [112].

A systematic reduction in energy is evident as the AE propagates to other sensor positions; see Figure 3.4b which shows AE energy level versus injector-sensor distance. In order to develop techniques for application on a running engine the authors first investigated AE propagation characteristics, i.e. source-sensor attenuation, wave arrival time differences and frequency modulation, using Hsu-Nielsen simulated sources and a nine sensor array located around the cylinder head [112, 113]. Nivesrangsan, et al., then applied the knowledge gained from these tests to reconstituting the source AE characteristics, in terms of timing and amplitude, for events associated with injector operation and exhaust valve opening [113]. Good results were reported from the reconstitution process, thereby offering more accurate information regarding event timing and amplitude that could be used as the basis of a diagnostics system. However, the events considered were noted as being the dominant features in the signals, which opens the question as to how this process would fare for lower-strength sources. Further difficulties were noted when an event was itself a composite of multiple sources.

Accurate source location of events was also demonstrated using triangular sub-arrays taken from the nine-sensor array [114]. Triangulation methods based upon wave arrival, time-of-flight difference and relative energy content were investigated, with the former found successful for burst-

type events and the latter for events which contained multiple sources. A prerequisite for application of these techniques was that the signals should contain strong, well-defined events, with filtering suggested to improve performance for weaker sources. The success of this work opens the path towards complete automatic spatial decomposition of signals using multi-sensor arrays. A possible application could be to precisely locate the source of events that may be indicative of a fault, such as events that may originate due to scuffing in large engine cylinder liners.

3.3.5 Monitoring of the Piston Ring-Pack and Cylinder Liner Interface

Pontoppidan and co-workers [115-120] have investigated AE monitoring of the piston ring-pack and cylinder liner interface. The different published papers used some of the same datasets. Here the interest lay with developing advanced signal processing techniques for the detection of changes in signals rather than on fundamental interpretation and understanding of the signals. RMS AE data were acquired at 20 kHz from sensors positioned on the cylinder cover and liner of a large, two-stroke diesel engine running at several loads, and under normal and no lubricating oil supply conditions. Again, the inherent non-stationarity of the signals was overcome through resampling the data to a constant number of samples per engine cycle via the TDC and shaft encoder signals. Techniques such as ‘event alignment’ were also developed to account for variations in the timing of injection events due to load changes [116-118].

Statistical techniques such as Independent Component Analysis (ICA) and PCA were used to investigate the data and it was found that changes in lubricating oil condition could readily be identified [119, 120]. Further work [115] applied a variant of ICA to effectively separate the RMS AE signature into four components, or ‘hidden signals’. Three of these signals modelled characteristics of AE generation at three different loads whilst the remaining signal was identified as being representative of friction and wear. These four signals are shown in Figure 3.5(a), with Signal 1 the friction related signal, and data presented from BDC to BDC (300° shown in figure). The authors noted that features in the friction signal could be related to the engine operation; the amplitude was lower at the beginning and end of the cycle which was thought possibly due to improved lubricating conditions at around BDC as the cylinder may have received oil indirectly via the common air intake. Figure 3.5(b) shows the level of each hidden RMS AE signal present as the test progressed. Changes in the three load-related signals corresponded with the load changes.

The friction-related signal emerged just after the lubricating oil supply was shut down and increased throughout the experiment until the supply was restored. This resembles what would be expected, and appears to verify to a degree the existence of a friction contribution to the overall AE signal.

Sigurdsson, et al., [116] further showed that AE generation was greater during operation with no lubricant supply than for normal conditions. In this case a simple feature was extracted, the total AE energy generated during an engine cycle, and this was found sufficient to discriminate between lubrication conditions at constant load. Figure 3.6(a) depicts this feature clearly for two engine speeds.

However, AE energy was observed to also increase with load, therefore values for fault and no-fault conditions coincide over varying loads, implying that a single overall threshold cannot be used for fault detection.

The authors suggested models, founded on supervised and unsupervised learning and with engine load as an input, which could counter this problem by providing non-linear threshold functions, as shown in Figure 3.6(b).

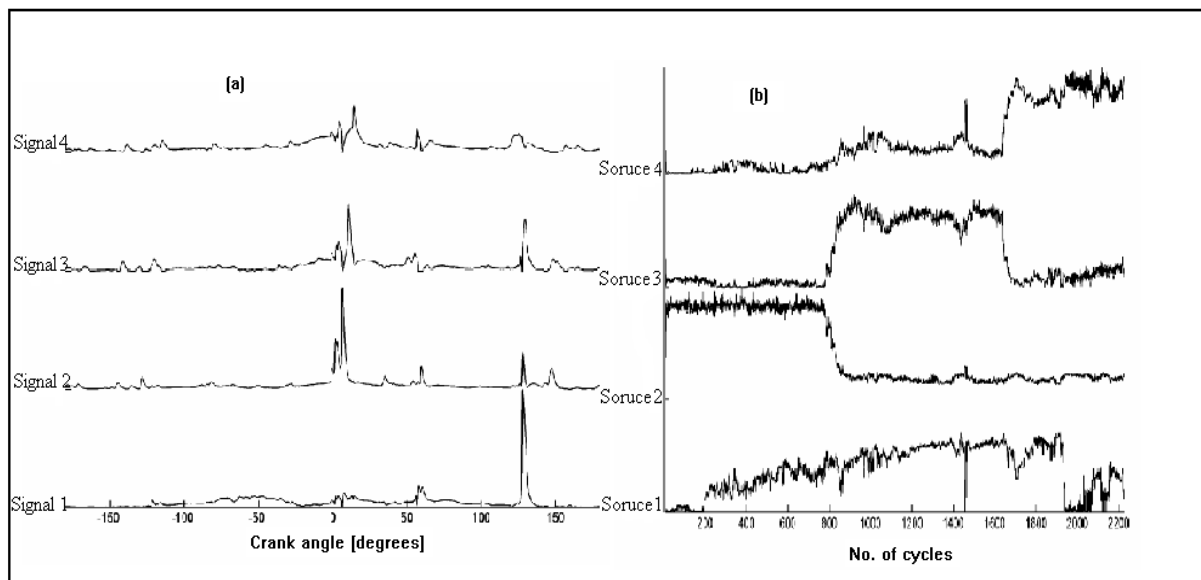


Figure 3.5 (a) Four hidden signals during a cycle, Signal 1 is attributed to friction and wear. (b) Development of four independent components during test, source 1 attributed to friction [115].

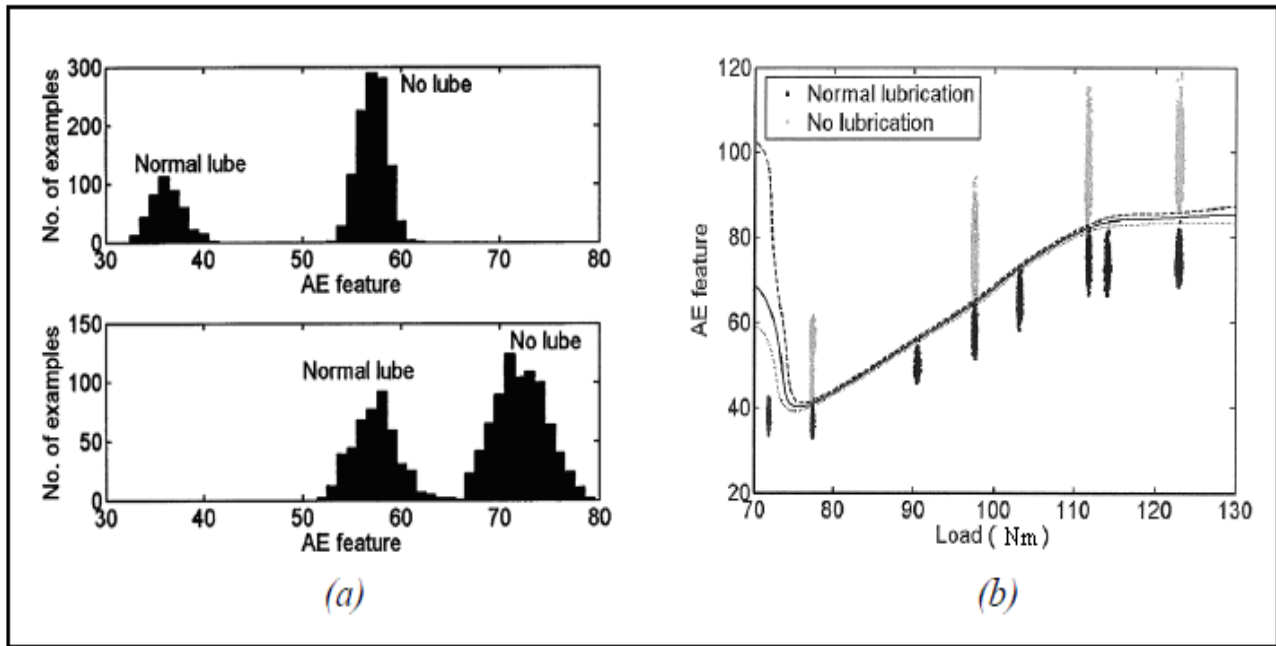


Figure 3.6 (a) Histogram of cyclic AE energy for normal and no lubricant supply conditions, upper and lower panels at 25% and 50% load respectively, (b) Scatter plot of AE energy versus load with several fault/no fault decision boundaries indicated [114].

Carlton [121] alluded to the commercial use of an AE monitoring system to address the problem of cylinder liner scuffing. Although no further information was revealed, and no results or case studies were presented, it can be assumed from the context that this was in relation to large marine engines.

3.4 AE Monitoring of Sliding Contact

As has already been stated one of the major objectives of this work is to investigate AE generated from the sliding friction of piston assembly and cylinder liner. To provide a foundation for this it is necessary to review the body of work which has considered AE monitoring of sliding, or interacting, surfaces.

The study of sliding contact encapsulates the topics of lubrication, friction and wear. When two contacting surfaces move relative to each other than a resistance to motion occurs. This resistance, or friction, is due to a combination of various mechanisms such as asperity deformation i.e. (deformation through rubbing), adhesion and ploughing by hard asperities or entrapped wear particles, and results in surface and sub-surface deformations, dislocations and fractures which dissipate strain energy in a variety of thermal, kinetic and elastic forms. Monitoring of these effects

therefore presents the opportunity to gain insight into tribological behaviour since they are intrinsically related to the friction mechanisms.

One component of the elastic energy released is in the form of radiated stress waves, including AE.

The possibility of using AE to infer tribological behaviour has been investigated and developed in numerous published works covering various applications. Precursor to more detailed studies was the initial understanding that AE arises from frictional processes that occur during manufacturing operations such as turning, grinding and forming [122-128]. Fundamental friction and wear characteristics have been investigated on standard wear testing laboratory equipment [129-142]. These have identified systematic relationships between AE activity and the various parameters which govern friction and wear. Further investigations have focused on applying AE monitoring to a range of industrial situations where interfacial conditions are problematic. This has included a significant body of work on the monitoring of hard disk drive magnetic storage devices [143-162] and also industrial applications such as gearboxes, mechanical seals and bearings [163-176].

3.4.1 Initial Identification of AE Generation from Friction and Wear Source Mechanisms

AE monitoring was initially identified as a technique that could prove useful for investigation of friction and wear phenomena through studies of material cutting and forming processes conducted to investigate whether tool or cutting process condition could be ascertained. The concept behind this is that in order to remove or form material a considerable amount of power is expended in the form of plastic deformation of the material. This is inevitably accompanied by friction acting at the interface of tool and work piece, and chip in the case of machining processes, the consequence of which is gradual wear of the tool surface that is detrimental to the quality of the work piece surface finish.

AE generated during turning of aluminium alloy was investigated by Grabec and Leskovar [122]. The spectral content of the signal was examined with audible frequency emissions observed to be discrete whilst emissions in the ultrasonic range, including AE, were continuous. The influences of various cutting parameters were evaluated and although the continuous signal was related to the friction at the tool/work piece interface no correlation could be identified between tool wear and AE activity, though the possibility was not dismissed. Tool condition monitoring via AE measurements was also considered by Iwata and Moriwaki [123]. They again focused on the spectral content and

reported that features up to 350 kHz were related to the tool wear condition, it was also suggested that AE count parameters may be indicative of tool condition.

Numerous further studies followed these initial works and these have firmly established the effectiveness of AE monitoring of tool condition for manufacturing processes including turning [124, 125], milling [126], grinding [127] and forming [128]. In all of these examples characteristics of AE generation have been related to friction and wear. A number of researchers have associated burst-type AE events to occurrences such as tool fracture and chip break-off whilst continuous AE emissions have been linked to continual shearing and friction. This material is not reviewed in detail here but is used to highlight the role that this research has had in establishing the use of AE monitoring towards understanding interfacial behaviour.

It is appreciated that the material deformation energies associated with manufacturing processes may be considerably greater than for normal wear processes. Nonetheless, it has also been recognised that small energy level deformations generate AE, for instance, Dornfeld, et al., [177] proposed the use of AE to detect the onset of slip between surfaces. Their work consisted of blocks of varying materials and surface roughness pulled in a stick-slip motion against a reference aluminium base block, with pulling speed and normal load varied. For all materials except lucite plastic a burst-type AE signal was observed upon the onset of motion, i.e. the transition from static to kinetic friction, with the basis for AE generation identified as deformation of surface asperities in contact. For the plastic material it was thought that there was no AE generation due to a combination of low surface roughness and characteristically poor AE generation capabilities. For steel blocks the AE amplitude was observed to increase with speed whilst an increase in normal load was found to result in increased AE activity for rough surfaces and reduced activity for smoother surfaces. A further application was given of a robotic gripper where burst-type AE signals were observed upon contact of gripper arm with the object and again upon the slipping release.

3.4.2 AE Monitoring of Sliding Contact in Laboratory Wear Tests

To investigate the relationship between AE generation and the friction and wear of sliding contact systems a number of studies have been performed using laboratory test-rigs on which simple test pieces are loaded against each other in relative motion. These test-rigs can take several forms such as a stationary ball on rotating cylinder or reciprocating pin on stationary disc, and typically the speed of relative motion and the applied load can be altered so as to provide a range of wear

characteristics. Such tests are routinely used in tribological studies and represent an ideal base for investigation of AE activity from friction and wear. Furthermore, these test-rigs allow other friction and wear parameters to be readily obtained, for instance, measurements of friction force or wear scars, and these can aid interpretation of AE activity and correlation to tribological behaviour.

One of the first investigations of this kind was conducted by Belyi, et al., [129] who examined friction and wear behaviour of polymers sliding against steel using AE and observed that AE parameters could be used to distinguish between different wear mechanisms. Surface roughness of specimens was increased which caused a transition from adhesive and fatigue wear regimes to abrasive wear, and this was found to be accompanied by an increase in AE count rate. This was explained by a greater number of AE generation sites as wear debris surface area increased. A linear relationship between cumulative AE count and wear volume was presented.

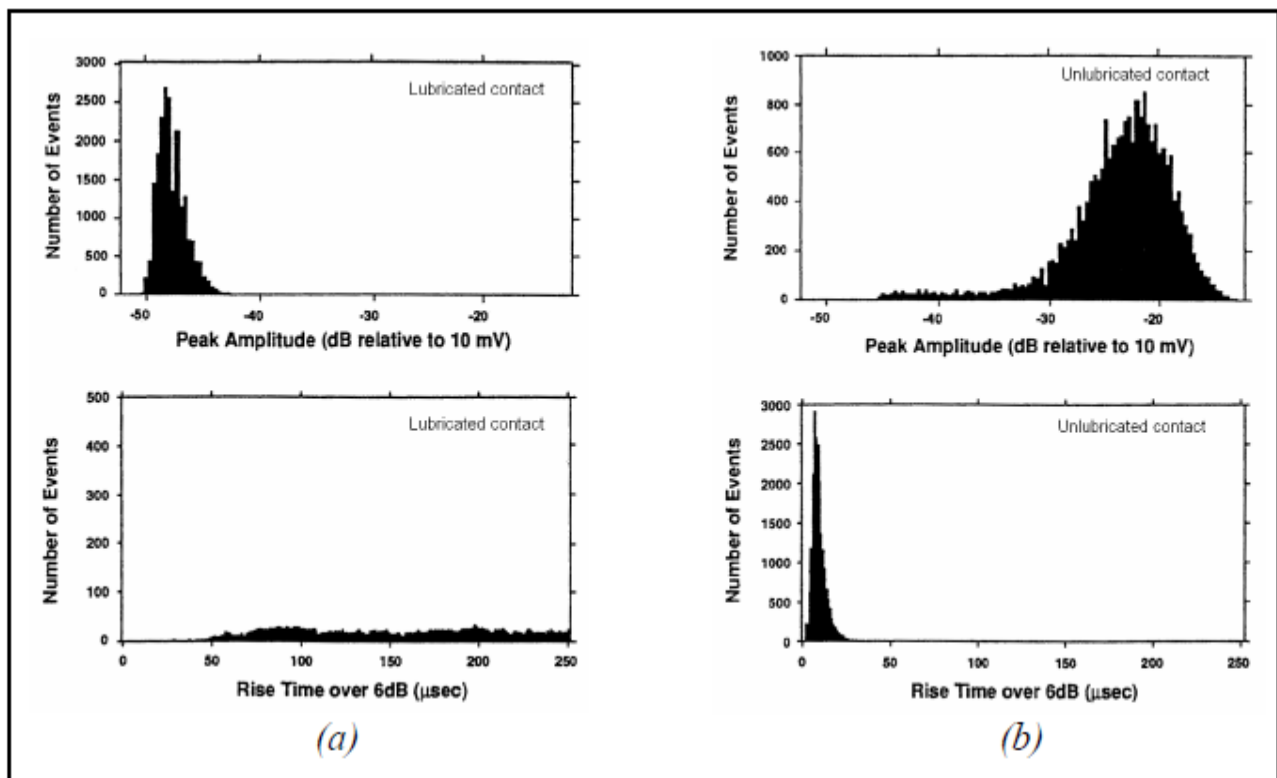


Figure 3.7 AE generation characteristics using a ball and cylinder test-rig for (a) lubricated contact, (b) non-lubricated contact [130].

McBride, et al., [130] generated a body of work which investigated AE generation during rotation of a steel cylinder loaded against a stationary steel ball with both lubricated and unlubricated contact considered. The AE peak amplitude and the rise time for each AE signal were extracted from time-series AE parameters. Clear differences were observed between lubricated and non-lubricated conditions for each parameter; Figure 3.7(a) shows lower but more consistent peak AE values and no particular rise-time characteristic, whilst Figure 3.7(b) shows greater peak AE values with increased spread for non-lubricated contact and a distinctively sharp event rise-time characteristic.

These observations were correlated to the wear inflicted upon the ball and cylinder surfaces. The non-lubricated contact produced a distinct wear scar with evidence of material transfer and wear debris, which led the authors to conclude that the non-lubricated AE characteristics were indicative of micro-fracture and material removal. Theoretical analysis of the contact zone indicated that mixed lubrication conditions would exist and the lubricated case, however, showed smooth wear scars with significant plastic flow. The authors therefore attributed the AE generation characteristics in this case to asperity contact.

Work in this area was taken forward by Boness, et al., [131] who, using a similar set-up also found that AE generation was greater from unlubricated contact than lubricated. They were also able to distinguish between different wear mechanisms. Common features in the time-history for lubricated and unlubricated conditions emerged after the data were presented in log-log format as shown in Figure 3.8(a). An initial peak observed for both cases was attributed to the initial removal and gross deformation of original asperities. This was followed by a second peak of gradually increasing amplitude. Scanning Electron Microscope (SEM) examination of the surfaces at this point revealed transference of debris from the rough cylinder to smooth ball hence this secondary phase was attributed to adhesive wear. The erratic behaviour exhibited by the unlubricated case after about 200 seconds was attributed predominantly to abrasive wear. It was further proposed that for each mechanism; initial contact, adhesion and abrasion, a linear relationship between wear scar volume and integrated RMS AE signal could be established. This is shown in Figure 3.8(b) for the initial contact and adhesive wear periods for contact lubricated with two grades of paraffin.

This concept was further investigated for lubricated contact by Boness and McBride [132] who reported differing behaviour between a reference lubricated sample and one containing a wear-

reducing additive, the latter exhibited less AE generation and a reduced wear volume. Furthermore, they could also distinguish between different concentrations of added aluminium particles to accelerate wear. AE activity was observed to increase with particle concentration, and this concurred with increased wear as quantified through examinations of wear scars.

Other authors [133-135] have verified the capability of AE measurements to detect changes in wear regimes during unlubricated sliding. Jiaa and Dornfeld [133] studied long-distance unlubricated sliding using a pin-on-disk set-up. Through analysis of time-series RMS AE, and substantiation by SEM examinations, they identified distinguishing features for three different wear regimes; running-in, steady-state and self-acceleration. Tests to investigate break-in behaviour after the removal of wear particles indicated a close relationship between AE activity and energy lost through frictional work. Additionally, the response of AE generation to varying sliding speeds and loads was evaluated.

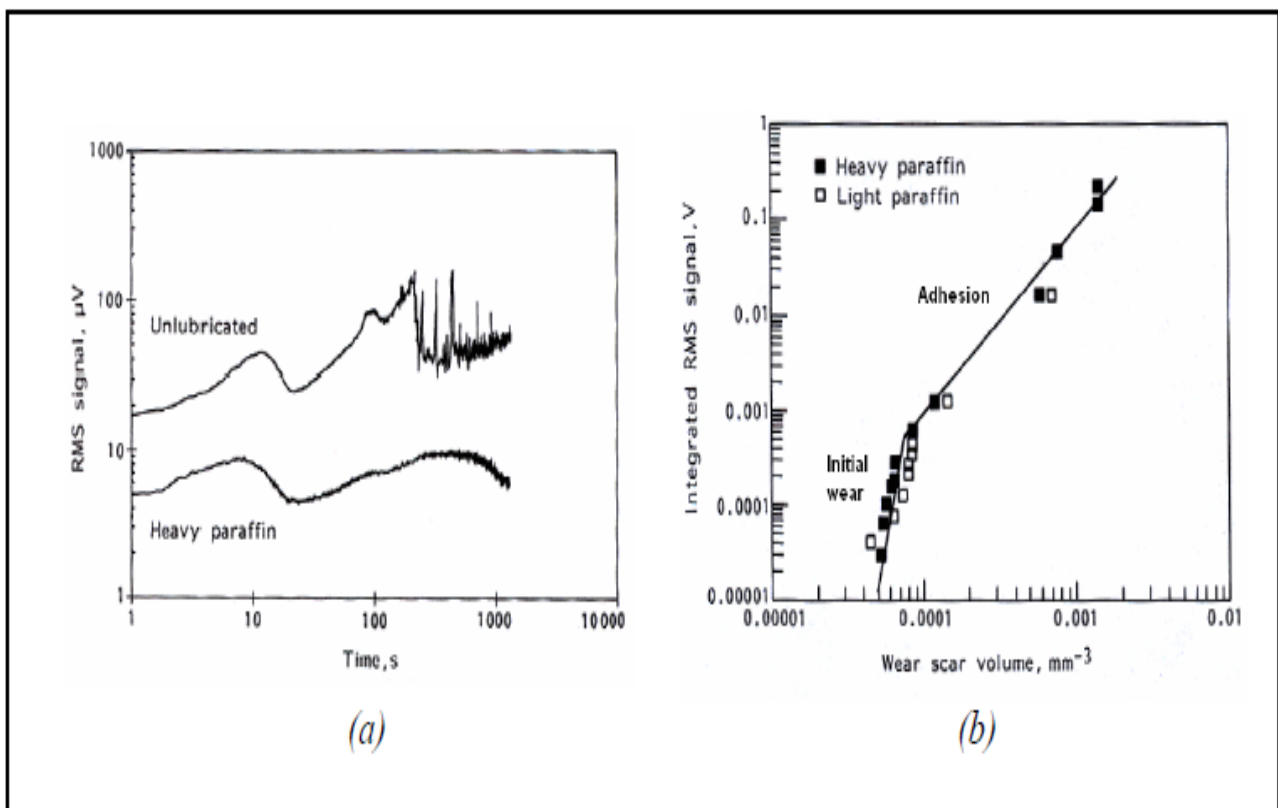


Figure 3.8 (a) RMS AE time histories for two different lubrication conditions, (b) linear relationships between integrated RMS AE signals and wear scar volume for different wear regimes [131].

The mean RMS AE level during the steady-state wear region was found to be proportional to both, as shown in Figure 3.9 for data scaled to the same range from two different AE measurement arrangements and material pairs. The authors stated that their results were in agreement with a power function relation between RMS AE and the rate of frictional energy dissipation given by Diei [136].

Similarly, Hamchi and Klamecki [134, 135] investigated the use of AE monitoring to discriminate between different wear mechanisms acting at an unlubricated pin-on-disc interface. Various loads and speeds were considered as well as several pin materials. For most materials the AE count rate and energy content were found to parallel the variation of wear rates across the mild-severe wear transition. It was also found that the different methods of energy dissipation associated with adhesion and micro-cutting (abrasion) wear regimes produced different peak AE amplitude distributions. However, it was noted that the results were dependent upon the material properties, with inconclusive results from tests with a copper pin.

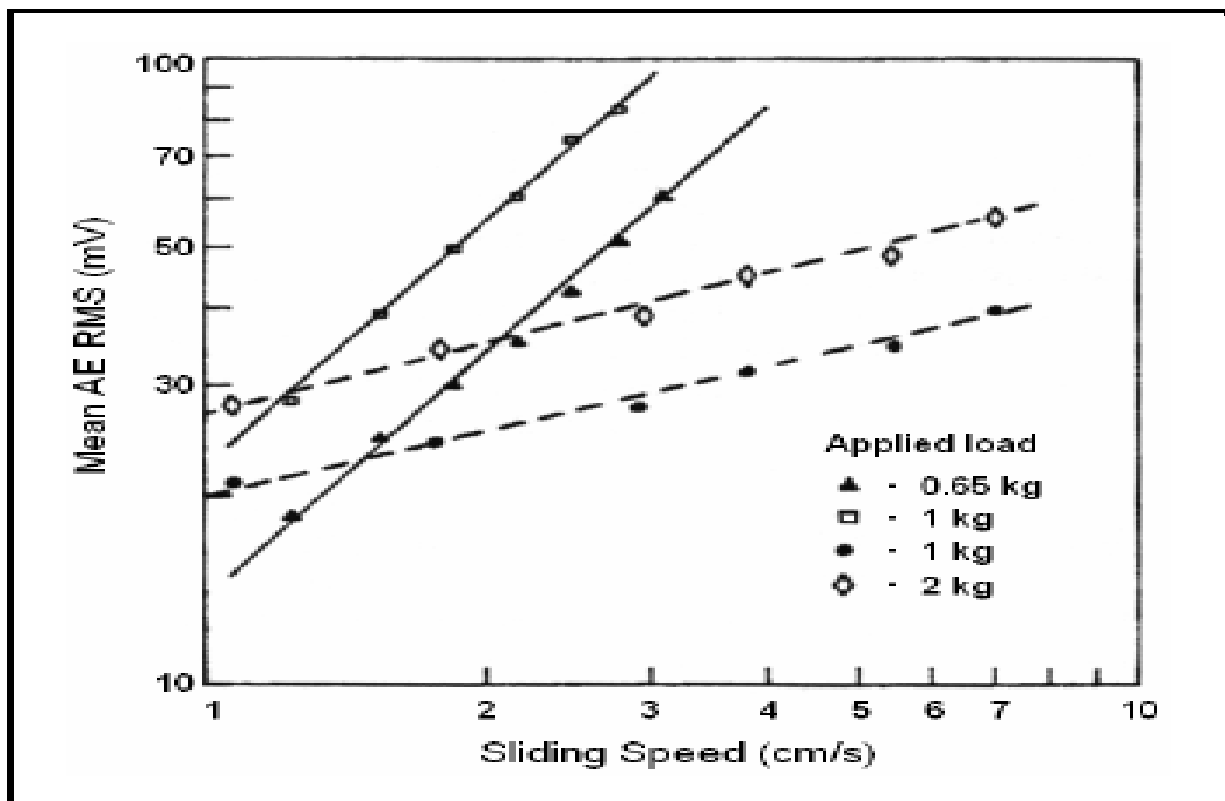


Figure 3.9 Effect of sliding speed and load on RMS AE level for two different arrangements [134].

Lingard and Ng [137] investigated AE generation during unlubricated sliding of a rotating disk loaded against a stationary disk. Again, a range of disk materials, loads and speeds were investigated with torque friction measurements and wear scar dimensions recorded to aid interpretation of the AE data. Significant AE activity was observed with AE event count rate and cumulative event count extracted as parameters. No discernible relationships emerged when these were evaluated against measures of wear such as wear rate and volume, although the possibility was not discounted. Instead, relationships were identified between frictional work and cumulative AE event count for all the material pairs examined. Relationships for varying speeds and loads are as shown in Figures 3.10(a) and 3.10(b) respectively whilst a further factor was found to be the materials of the pairs used.

The form of these relationships were noted as being similar to the power law relationship between the amount of AE generated and the rate of frictional work given by Diei [136] and referenced by Jiaa and Dornfeld [133].

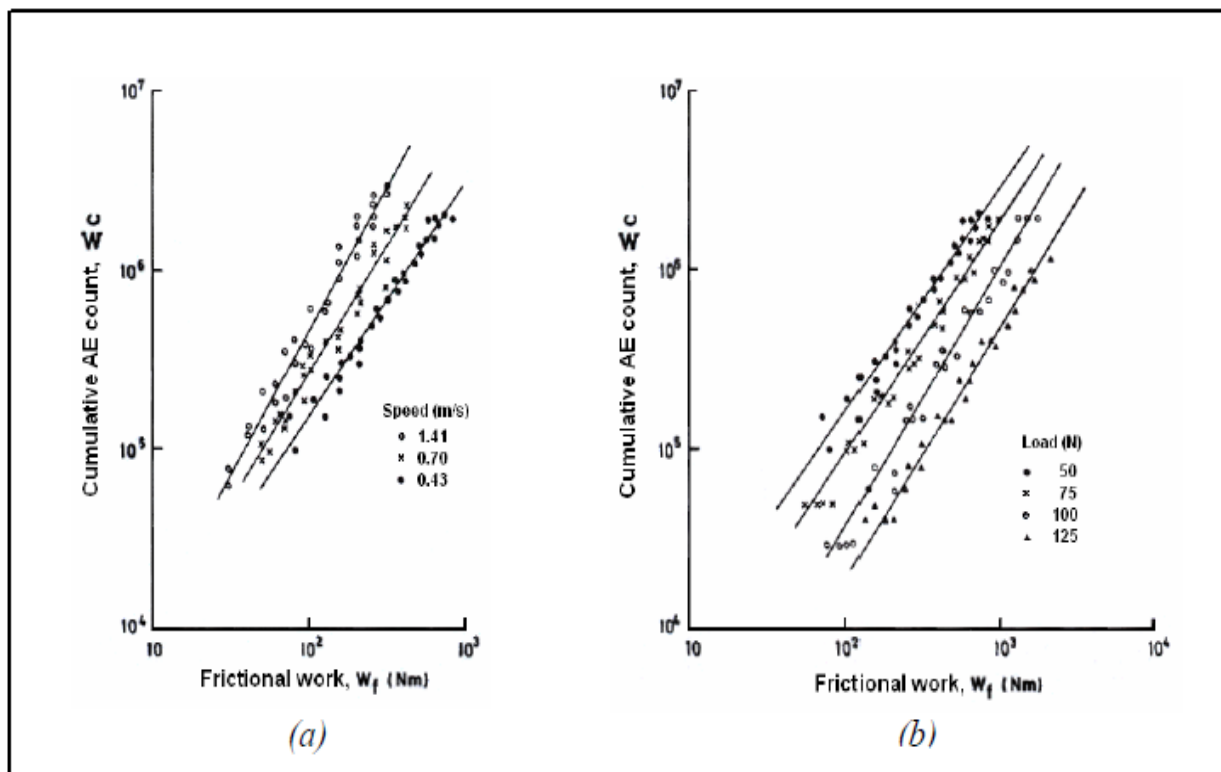


Figure 3.10 Unlubricated ball and cylinder test rig, cumulative AE versus frictional work, (a) effect of speed (b) effect of loading [137].

The authors also provided an explanation as to why AE generation would be related to frictional forces rather than parameters of wear. They reasoned that Archard's theory of adhesive wear indicates that only a small proportion of asperity interactions produce a wear particle, whereas all such events contribute to the frictional force.

Further work by Lingard, et al., [138] led the authors to state that AE output appears to be more sensitive to contact conditions than measurements of either friction force or of the wear rate. Frequency domain analysis showed that certain peak frequencies were associated with different material pairs.

Recent work by Mechefske and Sun [139] considered AE generation from lubricated sliding contact using a ball-on-disk test-rig and a non-contact laser vibro-meter. The lubricant contained an anti-wear additive, zinc dialkyldithiophosphate, which was noted as increasing in effectiveness with greater sliding speeds. Similar to other work, their results showed that the peak AE and RMS values increased in accordance with sliding speed and wear surface strain rate. They also reported that AE count rate, in terms of sliding distance, reduced when sliding speed was increased and they related this to the effectiveness of the lubricant and hence wear rates.

AE generation during elastohydrodynamic lubrication has been investigated [131, 138]. Boness, et al., [131] reproduced these conditions by using a polished surface on a ball-on-cylinder test-rig and noted that for these conditions the RMS AE level was no greater than the base noise level of the equipment. This further confirmed the authors' view that asperity contact was the primary AE source in their work. Lingard, et al., [138] also reported that AE activity was a sensitive indicator of lubrication condition. They observed that when lubricant was introduced to a disc-on-disc interface the AE activity reduced significantly, a reflection of the much reduced wear rates. Moreover, they found that as conditions were altered so to increase the elastohydrodynamic effect, quantified by the film parameter Λ in Figure 3.11, the AE count rate systematically reduced.

Several research groups have indicated that scuffing, severe adhesive wear, can be identified through AE monitoring. Boness [140] investigated normal operation and scuffing inducing conditions using a ball-on-cylinder test rig, with jet fuel and clay-treated jet fuels as lubricants and tests at various loads in both air and nitrogen environments. For both environments an initial peak in the AE activity was observed which was believed to indicate interaction of major asperities during initial wear. For the air environment, under non-scuffing inducing conditions, both AE levels

and wear scar diameter gradually increased till the end of the test. Under the same conditions the nitrogen environment case showed no further increase in wear scar or AE level thus indicating that a further oxidative wear mechanism was present for the air environment case.

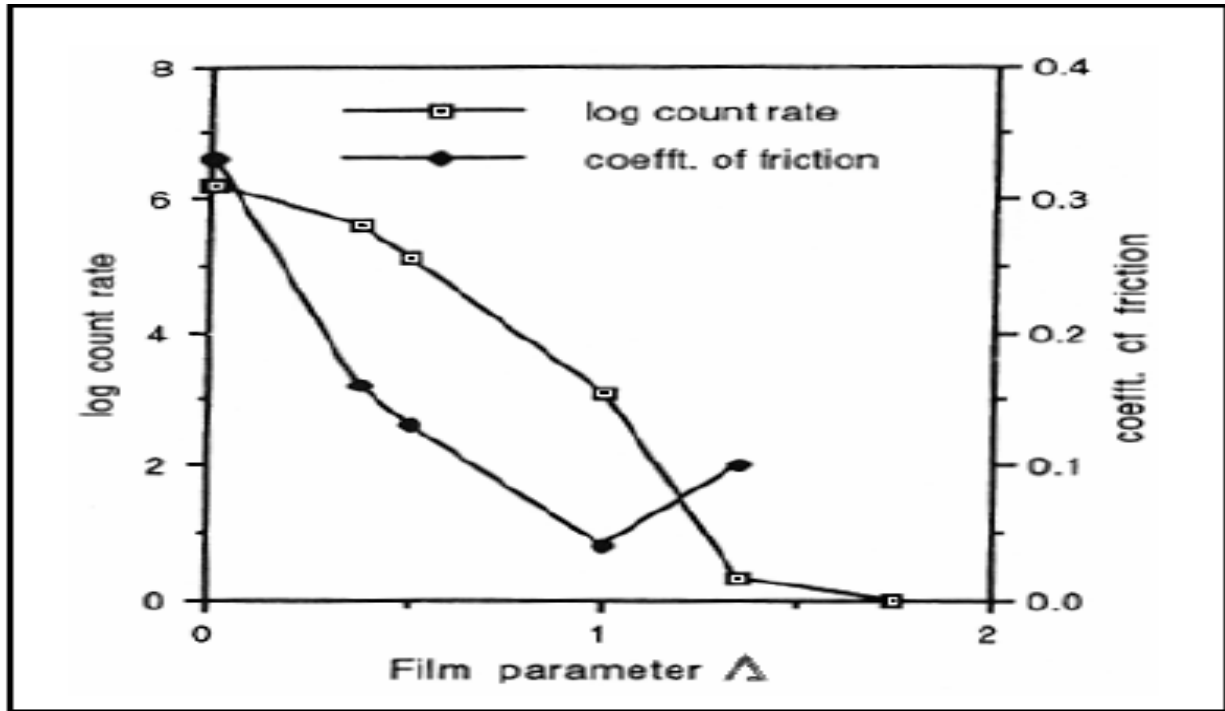


Figure 3.11 Log AE count rate and coefficient of friction versus film parameter [138].

Regarding scuffing, this could be induced at a critical load in the nitrogen environment, and could be identified through wear scar examination. At this critical load the clay-treated fuel samples exhibited greater AE levels than untreated fuel, as shown in Figure 3.12. Further examination of the wear scars showed that at this critical load the initial adhesive damage in some cases led to progressive deterioration and subsequent failure, i.e. scuffing, which was accompanied by constant high AE levels, labelled as ‘scuffed’ in Figure 3.12. For others, the surface recovered with both wear and AE levels reduced for the remainder of the test, labelled as ‘incipient scuff’ in Figure 3.12.

An interesting observation regarding the stability of AE monitoring was made by both Boness, et al., [131] and Lingard, et al., [138]. Using different test-rig and material arrangements both research groups showed that if a test was interrupted and then restarted, the AE RMS activity resumed at its previous level. This bodes well for the robustness and repeatability of AE monitoring.

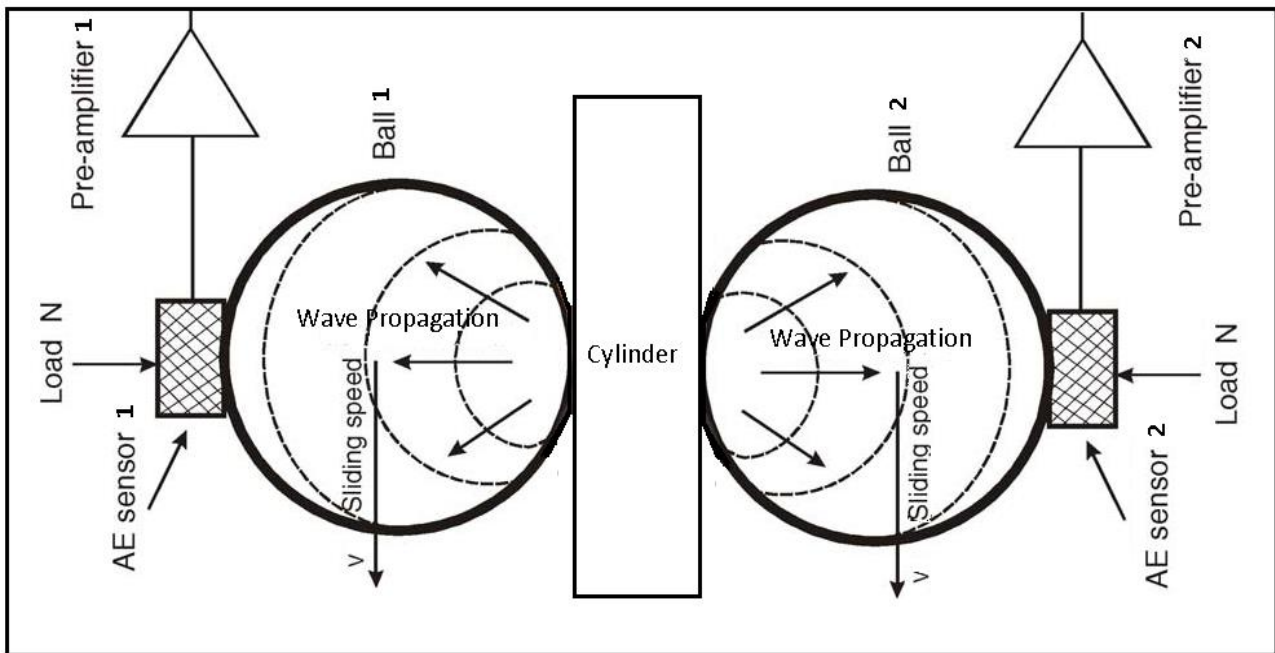


Figure 3.12 Schematic of the AE monitoring system for a ball on flat sliding cylinder.

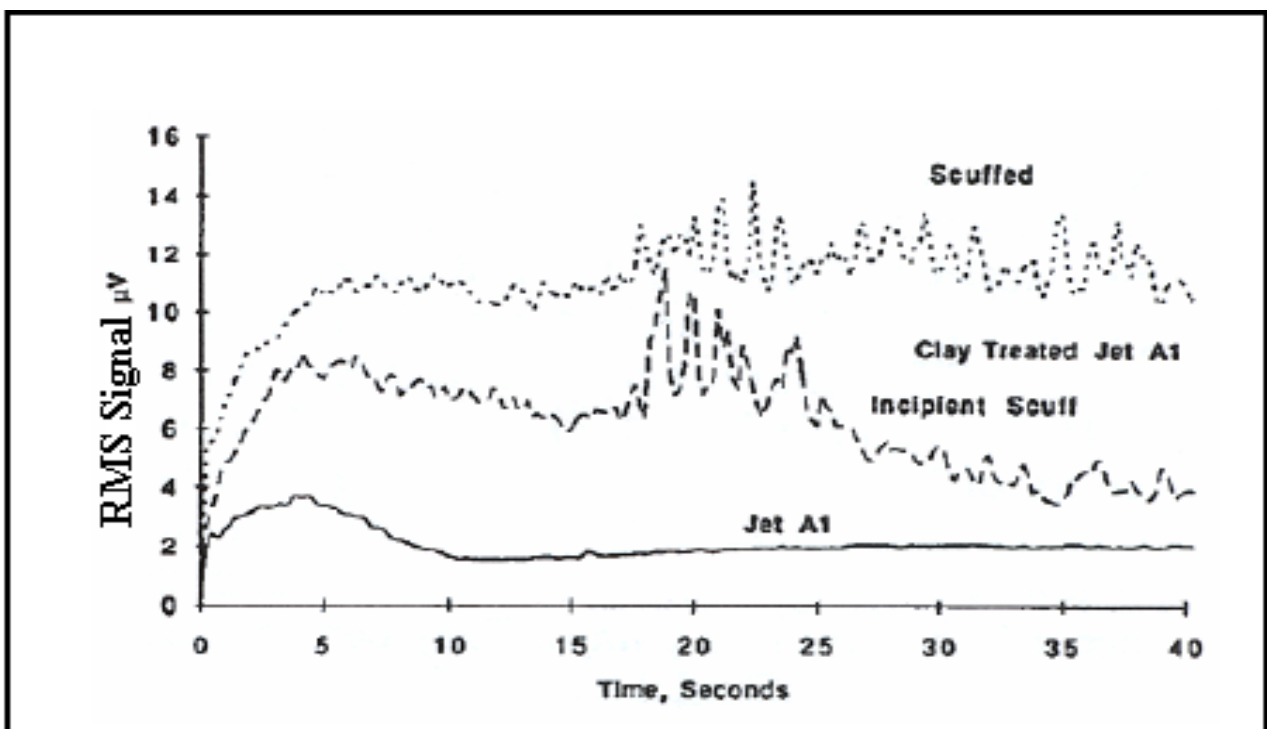


Figure 3.13 Induced scuffing at a critical loading [140].

3.5 Summary

This section has reviewed AE generation and how it can be measured and analysed to provide information useful for condition monitoring. The measured AE signal is generally dependent upon three main factors; the source generation characteristics, the transmission path from the source to the sensor, and the sensor response characteristics. A variety of processing techniques can then be applied to the measured signal, from the extraction of simple waveform and statistical parameters to complex algorithms.

The use of AE as an engine condition monitoring measured has been found to offer greater diagnostic capabilities than comparable techniques, due to higher level temporal and spatial resolutions, increased sensitivity and improved signal to noise ratios. It has been established that the mechanical and fluid-mechanical events and processes occurring within engines, e.g. valve contacts, fuel injection, combustion and exhaust, are AE generating sources from which diagnostic information can be garnered. Findings which suggest AE monitoring can be applied towards determining the lubrication condition are particularly relevant to the work in this thesis.

The majority of investigations into engine AE generation have used similar analytical procedures, at least for the initial processing steps. Raw or RMS AE data has been typically been converted from the time-domain to an angular base to overcome sign non-stationary. In many cases RMS AE has been found adequate; however, to best exploit the extreme temporal resolution available then raw measurements are necessary. The signals are then usually interpreted through mapping of AE events to the mechanical and fluid-mechanical actions occurring within the engine. Simplistic and advanced signal processing techniques have been used to characterise signals, many researchers have found simple statistical parameters to be sufficient, calculated either from the whole engine cycle or from windowed areas, although improvements have been reported using advanced statistical techniques.

AE monitoring has also proved to be effective for gaining insight into the tribological behaviour of sliding contacts, particularly for evaluation of contact dynamics and frictional behaviour during boundary lubrication conditions. This has been ascertained over several different applications where factors governing contact have been varied and corresponding effects on AE activity related, including; sliding speed, load, time, surface topography and lubricant characteristics. Various

qualitative relationships have been proposed and in some cases these have been found transferable across applications. Tests where hydrodynamic conditions were induced showed little or no AE activity above background noise levels. A variety of primarily time-domain AE parameters have been used to characterise the AE activity, although frequency-domain analysis has also been shown useful. The potential benefit of this work in terms of condition monitoring is that it demonstrates that it may be possible to obtain an on-line measure of friction without the need for direct, intrusive measurements.

CHAPTER FOUR

DIESEL ENGINE ACOUSTIC EMISSION SOURCES AND DATA PROCESSING

This chapter investigates and discusses acoustic emission sources in diesel engines; including mechanical impact (for example piston slap, valves impact, injector tick, etc.), friction sources, other sources (gas flow, fluid flow Crack formation and wear), turbo noise and background noises. Secondly the fundamentals of acoustic emission measurement, acoustic emission data processing techniques and recognised AE analysis parameters are introduced.

4.1 Introduction

Development of modern heavy duty diesel engines is driven by three major factors: fuel economy, pollutant engine-out emission, and customer satisfaction. To satisfy these requirements, advanced technologies are needed for all aspects of engines, including lubrication oil, fuel and engine components. The performance of the engine is directly affected by the friction, wear, blow-by gas flow (one of the important sources of AE) and oil consumption, which are in turn closely related to the listed three factors. Therefore, a detailed understanding of acoustic emission sources is crucial for developing advanced condition monitoring of diesel engine.

4.2 Diesel Engine Acoustic Emission Generation

The AE signals encountered on diesel engines are mostly stress waves travelling on the surface of the engine. Mechanical events that generate AE include impacts and crack formation; in addition, fluid and gas flows also generate AE [178]. The propagation of the acoustic emission waves through the engine is very complex; with non-uniform wave dispersion/attenuation, reflection/transmission needing to be considered.

Neill, et al., [179] and Fog [180] have shown that for AE measurement, the distance between sensor and source should be reduced as much as possible so that AE signals are far more localised, i.e., virtually coming only from the source where they are generated. This means, however, that differential damping of different sources will be crucial in sensor location considerations due to material interfaces along the signal path [181]. Of course, it is necessary to ensure good signal conductivity from the surface to the sensor.

Virtually all the theory and knowledge from vibration monitoring can be applied to AE since the two types of signal are generated by the same events, e.g., impacts and frictional movement, both lead to small movements of the structure (vibration), and micro cracking inside the material. The magnitude of AE signals are functions of the amplitude of the forces and wear involved, and thus many of the phenomena that have been used for monitoring vibration also appear in AE but because of the frequency ranges involved with less contaminating noise – and noise has always been the most significant problem with vibration measurement.

A review of an engine's AE sources shows that the generation of engine AE involves many different sources and mechanisms and that makes the AE signals very complex, in addition AE wave propagation in a real structure is additionally complicated by factors including internal damping, reflection, refraction, conversion mode and diffraction [182]. These AE signals contain not only stationary waveforms but also non-stationary transients, pulses and embedded noise.

4.2.1 Mechanical Impact

The impact sources in diesel engines will be related mainly to collisions between mechanical parts: e.g. piston slap, injector tick and valve movement [183, 184]. The following sections will describe both of these in detail.

4.2.1.1 Piston Slap

It is well known that the impacts between piston and cylinder may contribute significantly to the AE generated from diesel engines in a specific frequency range. Reducing diesel engine piston slap effects will reduce not only AE events, but also reduce impacts and wear of the piston and cylinder, and hence enable better operation of the diesel engine.

Piston slap, see Figure 4.1, is common to all reciprocating engines, and has been the focus of considerable interest over the past decade or so. This interest has been stimulated by:

1. The effect of waterside attack on diesel engine cylinder liners.
2. The excessive wear on pistons, cylinder liners and piston rings.
3. The contribution this phenomenon makes to the overall level of AE generated by reciprocating engines.

Piston slap is mechanical in nature and is responsible for a considerable portion of the diesel engine's overall AE events. The crank-slider mechanism of an engine between piston and cylinder inner wall has a very small clearance which is large enough to allow the piston's secondary motion. Piston slap is the impact between the piston and the cylinder wall and represents one of the more prevalent sources of AE among the mechanical impact sources present in a diesel engine when compared with other sources such as the injection system, impacts in bearings, the valve train and the auxiliaries [185,186]. Piston slap occurs because of sudden variations in the forces acting on the piston in the radial direction of the cylinder liner. These radial forces are a function of the inertial forces acting on a piston and

connecting rod. When the impact occurs between piston and cylinder liner kinetic energy is transferred to the cylinder, and transmitted through the structure of the engine as an AE, and radiated away from the engine's surface in the form of noise.

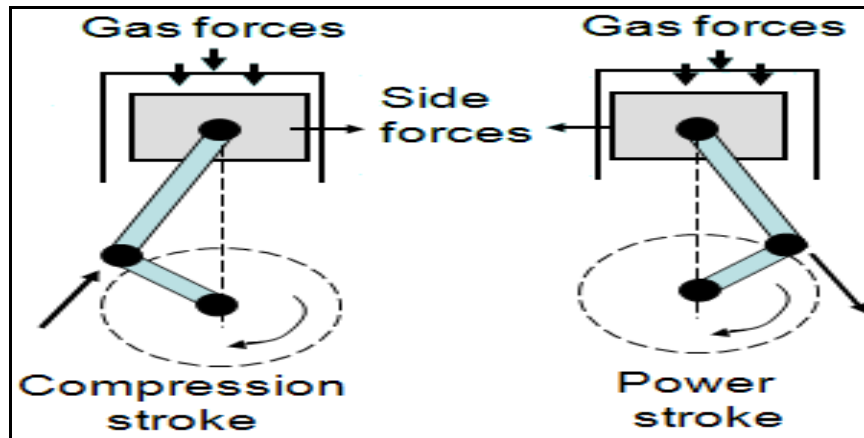


Figure 4.1 Piston slap phenomenon mechanism

Many research activities in the last few years have been focused on piston slap. The investigations have addressed the dynamic behaviour of the piston assembly and studied the influence of radial clearance, engine speed and properties of lubricant on piston slap and associated phenomena.

Griffiths and Skorecki [187] identified the final speed of the piston as a useful parameter with the purpose of calculating the kinetic energy of the impact, assessing the reduction in noise produced for different geometric-constructive configurations of the engine. They concluded that piston slap predominates in the low frequency range below 5 kHz, while Fielding and Skorecki [188] showed experimentally that the effects can extend to 5 - 10 kHz.

Haddad, et al., [189, 190] showed that piston slap could become one of the major sources of noise in internal combustion engines with an optimized combustion chamber. This study analysed the measured vibration from piston slap and investigated the effects of load, speed and temperature, different operating conditions, and the use of different lubricants.

Ungar and Ross [186] studied experimentally the effects of the impacts of the piston in alternating machines, confirming that they constitute an important part of the engine total noise. They

developed a theoretical description to calculate the crank angle at which piston slap occurs and to predict the AE.

In 2000 D'Agostino, et al., [191], proposed a computer program for the determination of the fluid film force between piston skirt and cylinder wall due to the hydrodynamic lubrication mechanism. The finite element method has been applied by other authors to analyse the impact force. However, these models are sufficient only to estimate the impact forces.

To eliminate noise generated by piston slap attention should be directed towards:

1. Preventing the change of the side force by offsetting the crankshaft from the axis of the cylinder by an amount greater than the crank radius, but this rather drastic change in engine design is hardly likely to be acceptable.
2. Close control of the piston-cylinder liner clearance as a practical solution to elimination of piston slap.

The thickness of the oil film in the cylinder clearance plays a very important role in reducing piston slap and AE.

4.2.1.2 Valves

A multi-cylinder diesel engine has many intake and exhaust valves. Closing and opening of these valves is achieved by a camshaft and valve springs operating in precise synchronisation. AE events from the valves in a diesel engine arise from two sources of distinctly different origin and character, namely:

1. Impact between colliding surfaces, in particular those of the valve and valve seat, and of the rocker arm with push rod or valve stem. Valve impact is considered to be the predominant source of AE.
2. Aerodynamic noise created by gas passing between the valves and their seating, and gas flow over the valve face.

The valve is loaded by a spring and the cylinder pressure, which varies periodically during engine operation. The valve impacts on the valve seat on valve closure, and the degree of impact depends

on the valve closing velocity, which is controlled by the dynamic behaviour of the valve train, particularly the force exerted on the valve by the valve spring.

The bending of the valve cone results in a sliding motion, improper contact and valve/seat interface wear, which affects engine performance. Valve wear has been a problem to engine designers and manufacturers for many years. Work carried out previously to isolate the fundamental mechanisms of diesel engine intake and exhaust valve seat wear experimentally [192, 193] has shown that recession originates from two processes: impact of the valve on the seat on valve closure, and sliding of the valve against the seat as the valve head deflects and wedges against the seat as combustion occurs in the cylinder. These processes produce characteristic wear features on valves and seats. Impact on valve closure leads to the formation of a series of ridges and valleys on the valve seating faces and surface cracking on seat insert seating faces. Radial scratches were seen on seat insert seating faces as a result of sliding at the valve/seat interface.

Studies of wear have focused on the effect of engine operating conditions such as temperature and load [194]. Little work has been carried out to investigate the effect of design parameters, material properties, valve closing velocity and the effect of reducing lubrication at the valve seat interface on wear.

Research work on diesel engines has tended to place greater emphasis on investigating exhaust valve wear than on intake valves. Modelling approaches, used until now for predicting valve wear [195,196], have been simplistic and have focused mainly on the sliding contact between the valve and seat under the action of the combustion pressure, taking no account of the impact of the valve on the seat on valve closure. Most only enable a qualitative analysis rather than providing a quantitative prediction of valve recession.

Most investigations dealing with diesel engine AE discuss the amount of AE generated by the valve but have been limited to showing the contribution the valve makes to the overall AE events by comparing the condition when the valves are operating normally with that when the valves are inoperative; this type of work is reported by Bradbury [197] and Mercy [198].

4.2.2 Friction

Many researchers have studied the frictional contributions and tribological characteristics of each engine component through both theoretical and experimental studies.

The engine frictional losses can be classified into four main components: piston/ring assembly, valve train system, bearing system, and auxiliaries (water pump, oil pump, alternator, etc). Figure 4.2 shows the general proportions of the frictional loss of each engine component, although these proportions can be changed according to engine speed, load, and the type of engine.

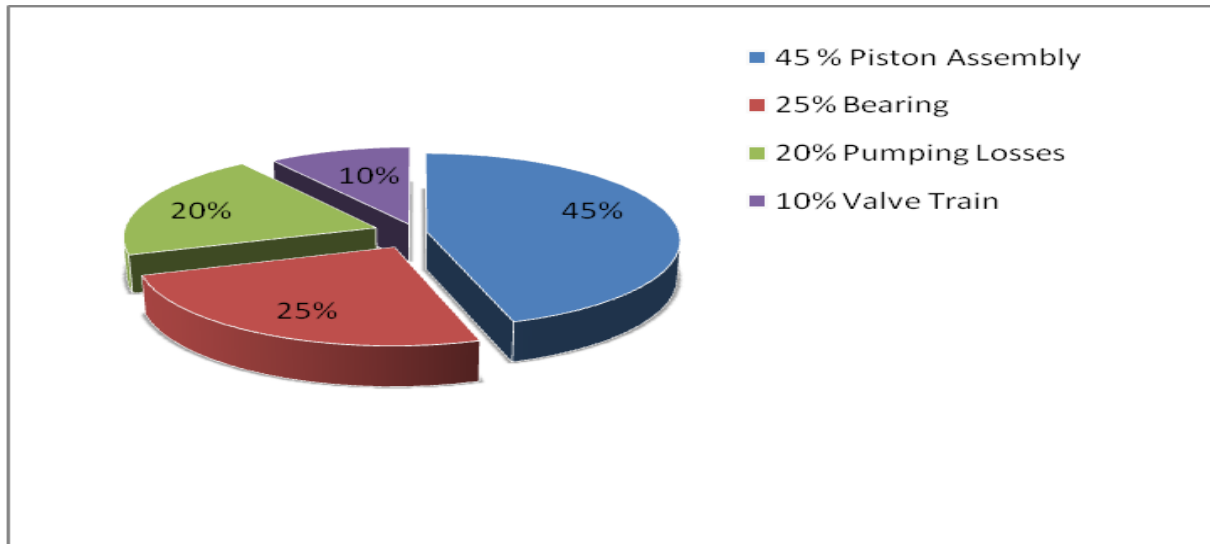


Figure 4.2 Representative mechanical loss distributions for a diesel engine [199].

From Figure 4.2, it can be said that most of the engine friction losses are from the piston assembly. Therefore, it is necessary to attack the piston assembly friction to achieve low engine friction since the piston assembly (piston skirt, piston rings and piston pin) accounts for about half of total engine friction for motoring conditions, and an even higher fraction of total engine friction for firing operation. Many researchers have made a great effort to understand the tribological phenomena and reduce the frictional losses of the piston assembly. However, the friction reduction of the piston assembly still remains a challenging area due to the complexities of the tribological phenomena and the interrelations among friction, emissions, durability, noise and vibrations, oil consumption, blow-by, etc. The friction characteristics of the diesel engine are related to the type of lubrication. The main friction sources in diesel engines are:

4.2.2.1 Piston Liner Assembly

The frictional forces associated with the piston liner assembly usually consist of:

1. Ring friction.

2. Piston skirt friction. This type of friction is strongly dependent on two factors:

- a) Whether the skirt contacts the cylinder bore, and
- b) How the skirt shears the oil

3. Rod bearing friction.

McGeehan [199] reviewed the literature for piston and ring friction and quoted sources [200, 201] that suggested that piston assembly friction could account for 58 % to 75 % of the total mechanical friction of the internal combustion engine. However, these papers were written before 1980. Recent literature and experience at Cummins Engine Company suggests that the total friction due to pistons, rings, and rods will contribute only 40 to 55 % [202-204], which is a measure of the progress made in the last three decades.

Friction can be measured by motoring teardown engine tests which are commonly used and probably the simplest technique to evaluate engine friction [205, 206]. This test involves rotating the engine with a motoring dynamometer and recording the torque required to maintain a constant speed. By removing components from the engine it is possible to determine their contribution to friction. There are also other friction sources in the engine, but these contribute only a small amount compared to the total engine friction. There are recommendations and contributions made in the literature from various companies for reducing friction.

1. Ford Motor Co. [202, 204, 207] methods to reduce friction:

- . Reduce ring tension (44 % reduction in tension causes a 22 % reduction in ring friction),
- . Reduce mass '25 % reduction causes a 0.1 psi MEP',
- . Coated top ring,
- . Ring materials and coatings,
- . Reduce the number of rings (4 % reduction for 2 rings rather than 3 rings),
- . Optimized ring face profiles,
- . Low friction skirt and roller follower coatings '8 %'.

2. Cummins Piston Ring Division [208, 209]:

- . More conformable low tension oil ring,
- . Reduced compression ring cross-section,
- . Connecting rod guided by piston (constrain the rod from moving along the axis of the engine with the piston rather than between the crank throws), and
- . Reduce the piston mass,

3. Southwest Research Institute [210]:

- . Reduce oil ring tension,
- . Reduce windage or percent of oil in the air, and
- . Reduce maximum cylinder pressure.

Almost every company surveyed claimed that reducing ring tension (oil ring in particular) and top ring width would reduce friction.

Efforts to reduce piston skirt friction yielded mixed results. Some said that reducing the contact area of the piston skirt would reduce friction while others said it would not. Increasing skirt clearance was another way to reduce friction but it was noted that this might increase cavitation problems. Reduced mass of the piston was cited by many as a way to reduce friction.

4.2.2.2 Valve Train System

The elements that are responsible for most of the valve train friction are:

1. Cam / tappet interface,
2. Cam journal bearings,
3. Rocker arm /pivot, and
4. Oscillatory interfaces.

Valve train frictional losses typically account for 7 to 15% of the total mechanical losses of a diesel engine, and are generally about a quarter of that for piston assemblies. However, at low engine speeds their relative importance is much more equal. However, it is in terms of wear and the consequent reliability and durability problems that the valve train has proved to be the most difficult to design and lubricate effectively [211]. The design and tribological performance of the cam and follower have therefore historically been based on the choice of materials, specification of the lubricant additives and calculation of Hertzian stress. It is widely accepted that there is significant surface contact between the cam and follower resulting in boundary lubrication. However, in more recent times the role of thin film lubrication, predominantly elastohydrodynamic lubrication, has been recognized [211]. Figure 4.3 shows the distribution of friction losses.

It is well known that at the start of the cam/follower event the friction is dominated by rolling and then subsequently by sliding of the surfaces in the presence of lubricant as the cam nose is neared.

Apart from the cam/follower interface, the camshaft bearings, follower/guide and valve/guide interfaces also contribute towards drive train friction losses. Ball, et al., [212] measured the valve train friction of diesel and gasoline engines and found that the form of the camshaft drive torque variation with crank angle was largely dictated by the cam profile and valve spring forces.

Baniasad and Emes [213] adopted a similar approach using novel strain gauge camshaft drive pulleys to study the effect of engine speed and temperature on average camshaft drive torque. There are many possible ways in which valve train friction measurement can play a vital role. For example, in the design and development of cam profiles and geometry, valve timing, valve spring rate and lubricant formulation. It can also provide validation data for predictive mathematical models and provide guidance as to their further development.

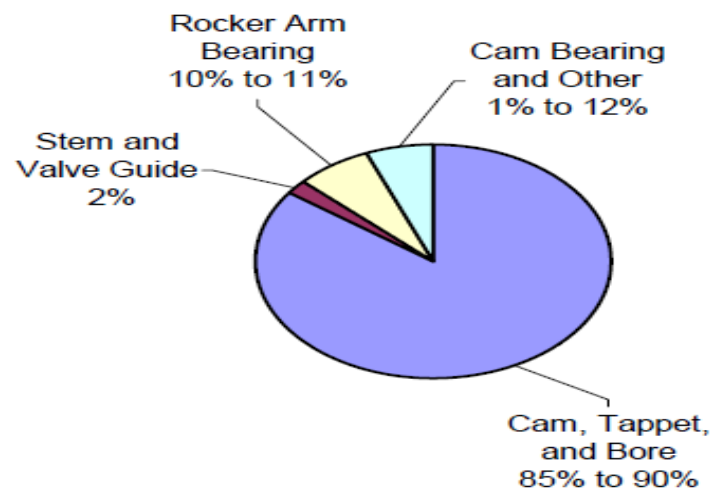


Figure 4.3 Distribution of valve train friction losses.

4.2.2.3 Engine Bearing System

Bearing friction contribution makes the second largest contribution to engine friction followed by losses from the valve train, which comes from many different sources including the crankshaft main bearings, connecting rod big-end bearings, connecting rod small-end bearings, camshaft bearings, and rocker arm bearings. Engine bearings typically represent 20 to 30% of the total engine frictional losses. Of the many different bearings in a diesel engine none are more critical or highly stressed than the connecting rod big/small-end bearings and the crankshaft main bearings.

At low engine speeds, the engine friction loss is more dominated by boundary lubrication than mixed lubrication, whereas shear loss becomes important at higher engine speeds and under such conditions lubricant viscosity plays an important role in defining these losses. Engine journal bearings operate mostly under hydrodynamic lubrication, apart from during stop/start or under very high loads where elastohydrodynamic lubrication and mixed lubrication can become important. A journal bearing consists of a shaft rotating within a stationary bush as with an engine main bearing, whereas in big-end bearing the bush also has angular velocity. The hydrodynamic film generated between the journal and bush surfaces supports the load. This feature is normally called bearing load-carrying capacity and is related to the bearing durability.

Most of the reported engine bearing friction data has been calculated through the measurement of lubricant temperature and oil film thickness. A number of experiments have been performed to measure oil film thickness in a big-end bearing using the total capacitance technique [214–218]. Bates, et al., and Spearot [219] and Murphy [220] also measured oil film thickness by the total resistance method to investigate bearing performance. Suzuki, et al., [221] and Choi, et al., [222] measured minimum film thickness using the total capacitance method and compared the data with the predicted results. Choi, et al., [223] carried out evaluation of friction in engine bearing from crankshaft temperature measurement. Cho, et al., [224] measured the big-end bearing film thickness by using the total capacitance method and a scissor-type linkage called a grasshopper linkage to bring the wiring out of the engine crankcase. Irani, et al., [225] used capacitive measurement technique to measure hydrodynamic lubricating oil film thickness in the middle main bearing of a heavy-duty six-cylinder diesel engine. Measurement of oil film thickness as a function of the crank angle was carried out with a variation of the engine speed, load, and oil temperature. Masuda [226] measured the bearing film pressure distribution on a test rig using semiconductor-type pressure transducers. Schilowitz and Waters [227] successfully measured the oil film thickness in the main bearing of an engine in an operating vehicle. Mihara, et al., [228] successfully used a thin-film pressure sensor made of manganin to measure oil film pressure during engine operation.

Helena, et al., [229], on a test rig, measured oil pressure in a journal bearing using an optical sensor. Warrens, et al., [230] used a relatively new, commercially available dynamically loaded journal bearing rig to study the effect of different viscosity modifiers on friction performance. Mufti, et al., [231, 232], on a custom made rig, measured oil film thickness in a journal bearing using eddy current sensors. Tanaka [233] successfully used a transparent bearing to study the effect of oil cavitation on a test rig. Cerrato, et al., [234] modified the main bearing of a single cylinder engine,

extensively modifying the bearing housing, to measure the frictional performance. Similarly, other researchers like Syverud [235], Sinanoglu, et al., [236], Sorab, et al., [237], Tseregounis, et al., [238], and Unlu and Atik [239] have carried out interesting experiments on test rigs, looking at details such as the effects of temperatures, pressures, oil film thickness, etc. on journal bearing performance.

From the above review, it is clear that oil film measurements have been carried out by numerous researchers but none have measured engine bearing friction in a real firing engine without any major modification to the bearing housing.

4.2.2.4 Auxiliaries

Engine auxiliaries comprise about 20-25% of the total engine friction losses. Engine auxiliary power losses come from such built-in accessories as turbo, pumping losses (coolant pumps, oil pumps and fuel injection pumps) as well as those that are external such as fans, generators, air conditioning, and power-steering pumps. Of these components the oil pump will be the focus since the fuel pump, whether inline or distributor type, are cam driven against roller followers and the basic friction losses are closely related to those covered in the valve train friction section, while the power to drive the coolant pump is rather low in comparison.

The report by Steward and Selby [240] shows a number of examples of how reducing oil viscosity will reduce engine friction. But it was also shown that reducing the viscosity could cause significant increase in wear. However, cases were also shown where different additives to the oil could lessen or eliminate the effect of the low viscosity on wear.

As the reports above indicate, lower viscosity oils may lead to increased wear. In particular, wear will increase around Top Ring Reversal of the cylinder bore. This increase in wear may be reduced by:

1. Improving the design of the piston and ring,
2. Improved oil formulations, and
3. Material which have a high resistance to wear.

4.2.3 Other Sources

Fluid and gas flow are also common sources for AE in diesel engines. The most significant gas flow restriction in a diesel engine is the flow through the intake and exhaust valves, which plays an essential role in determining residual gas fraction which have an important influence on fuel consumption and emissions, and the important fluid flow is that through the injector. Turbulence generated in a diesel engine is defined anisotropic and an AE signal generated by the turbulent or cavitating flow through the orifice can be detected by AE sensors. The gas flow processes into, through, and out of a diesel engine is all unsteady - that is the pressure, temperature and gas particle velocities vary with time. Both large-scale and small-scale turbulence have a drastic result on combustion, flow-mixing and heat-transfer in an engine [241]. The major source of energy for turbulent velocity fluctuations is shear in the mean flow, e.g. jets [242], but the velocity gradient at the wall in the boundary layer produces large vortices which are unstable inside the chamber and eventually break down into additional turbulent motion.

The fluid flow through the orifice of the injector is associated with four components:

1. Pressure build up in the injector (this includes a small impact between needle and valve seat before the needle is fully open).
2. Needle lift (mechanical impact between needle and its backstop and fluid flow through injector nozzle).
3. Needle closing (mechanical impact between needle and its seat and fluid flow through injector nozzle).
4. Back pressure fluctuations in the fuel line (repeated reflections of back pressure between needle and plunger of the fuel injection pump in the fuel delivery line after needle has closed).

Typically, the injection process is a combination of needle impacts and the high pressure fuel flow within the injector body. Gu and Ball [243,244] have studied needle dynamic behaviour in the diesel engine injection process and have developed a dynamic model for the needle motion of a typical single-stage, hole-type injector of a direct injection diesel engine and compared it with experimental results for the vibration response from an injector body. They describe the vibration characteristic of injectors by three series of transients during an injection cycle; fluid excitation beginning prior to needle opening impact, needle opening impact and needle closing impact. Gill, et al., [245] also have observed the injection process using AE and vibration methods and found that

AE detected activity starting with the build-up of fuel pressure in the high-pressure pipe prior to the opening of the needle valve, which did not appear in the vibration signal.

Crack formation is also a source of acoustic emission in diesel engines. Crack formation appears after many repetitive cycles of use and can affect even high-strength materials. The onset of crack formation can be the result of surface impact due to relative motion. The impact factor could be from residual stresses in the component due to the impact, the stress concentration associated with the shape of the impact stem and incipient micro-cracks formed during impact, or plastic work in the material or distortion of the microstructure. Cracks in the bearing (connecting rod bearing) could be the effect of cavitation and crack formation in the liner may be reduced by ensuring the piston had a low coefficient of friction, experienced only small impacts, or high strength materials were used [246].

Wear is inevitable for engine parts in sliding contact. The amount of wear depends on material pairs, surface topography, working conditions and chemical effects of the environment. It is impossible to completely prevent wear, but since it leads to large economical losses it is the subject of much research in many disciplines. Any empirical relation is difficult to develop because the relevant factors are not predictable. Seventy five percent of the wear in an engine occurs during the heating up period, because of the poor lubrication at that time. The lubricant normally forms a thin film to prevent metal–metal contact. When the engine is not in operation, the lubricant drains to the bottom, and it takes time to form a complete film after starting up. Since the hardness of the surface is higher and the roughness is less effective wear at this stage is expected to be less.

The most severe wear occurs on the cylinder surfaces in diesel engines. On the upper portions of the cylinders, lubrication is poorer comparing to other regions, because the lubricant that reaches here is then partly burnt. Pistons, valves, and piston rings are the other elements subjected to severe wear. The wear in cylinders is the result of the physical and chemical effects of combustion, cooling, friction, and lubrication. To eradicate or at least to reduce the wear at the cylinder-piston-ring system, the surface of the cylinder tube is continuously lubricated.

The primary reason for wear is the failure in lubrication. During the engine's operation, on the one hand the cylinders are continuously lubricated; on the other hand the rings strip off the oil, and cause metal–metal contact. Abrasive wear particles on the cylinder form deep grooves on the surface. The wear rate is not the same on all parts of the cylinder. The most severe wear occurs at

regions near top dead centre (TDC), the least lubricated region because the flame removes the lubricant and constitutes thermal shocks. The regions near to bottom dead centre (BDC) are the least worn regions because these regions are least exposed to the flame and are best lubricated.

4.3 Background Noise

Background noise is unwanted signals picked-up from sources that are not relevant to the source being monitored and can have electrical and/or mechanical origins. Precautions against such interfering noise should always be taken, even though enormous progress has been made since the early use of AE technology. In diesel engines AE events will almost certainly be generated from more than just the source of interest and will be a complex combination of combustion, impact and flow generated AE. These AE signals must be identified or eliminated in order to discriminate them from the signals of interest generated by the engine.

A basic starting point for eliminating these unwanted signals is the selection of an appropriate frequency range for the application. Background noise coming from longer distances usually consists only of frequency components below 20 kHz, and so has only a small influence on the measurements higher than 20 kHz. It has been found that 100 kHz to 1MHz is a suitable range for the study and monitoring of diesel engines. Further studies are needed to narrow the range and improve the accuracy of AE monitoring. Noise elimination could be a key factor to successful use of AE inspections in some difficult industrial applications such as on-line monitoring of welding and the detection of fatigue crack growth in flying aircraft [247, 248].

Electrical noise problems can be eliminated by using differential sensors or sensors with built-in preamplifiers and selecting proper thresholds.

4.4 Acoustic Emission Processing

4.4.1 Measurement of Acoustic Emission

There are several methods of measuring absolute surface displacement which involve capacitive, electromagnetic and laser-optical measurement techniques. However, practical difficulties in applying these methods in an industrial environment have meant that the vast majority of AE monitoring has used resonant transducers based on piezoelectric elements. These sensors have proven to be suitably sensitive and robust to the extent that they have become accepted as the norm. The material used for the active element is most usually lead zirconate titanate (PZT), a

piezoceramic; although it has been shown that it is equally feasible to use other piezo-active materials such as polyvinylidene difluoride (PVDF) [249].

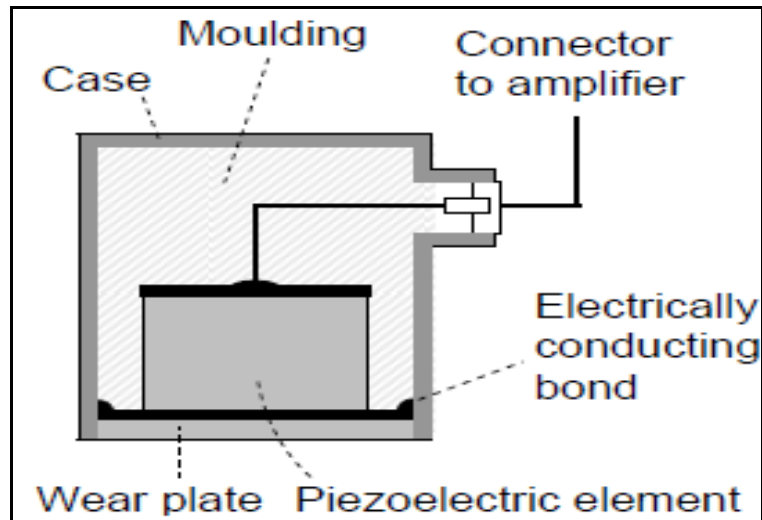


Figure 4.4 Schematic of an AE sensor [10].

The construction of a piezoelectric AE sensor is shown schematically in Figure 4.4. These sensors rely on the fact that a voltage is generated in proportion to the compression of the piezoelectric element; hence nanometre surface displacements are converted into an electrical signal. However, the output of most piezoelectric sensors is not an accurate description of the surface movement under inspection. Rather, the AE signal, i.e. the sensor output, is the sensor's response to the forcing transient waves.

This is influenced by the sensor construction and consequent frequency response, the amplitude sensitivity and associated self-resonance (ringing after initial excitation), and also by whatever means the sensor is coupled to the material.

The sensor response characteristics are determined by the geometry of the piezoelectric element. These can be manufactured in a variety of forms so as to offer a range of resonance frequencies and sensor sizes for various applications, although for sensor selection there is usually a compromise between bandwidth and sensitivity. If prior information is known about the source frequency characteristics then narrowband sensors can be selected to provide high sensitivity, conversely, if source characteristics are unknown then broadband sensors with lower sensitivity are available. With regards to monitoring of machinery the AE sources of interest have typically broad and varied

frequency contents and therefore broadband sensors are generally required if all mechanical and fluid processes are to be considered. Moreover, since most of these sources are of reasonably high amplitude the loss of sensor sensitivity is less important than the broadness of the frequency response. A further factor in sensor selection is the anticipated source to sensor transmission distance. Given that higher frequencies suffer from greater attenuation they have an inherently smaller detection distance and therefore the spatial range of a sensor is indirectly determined by its resonance frequency.

The use of resonant sensors incurs further distortion of the original source AE, but this is tolerable, and somewhat unavoidable, since these transducers represent the most practical means of measuring emissions in the upper frequency range. Although the impact of this may be minimal for comparative work when a consistent set-up is used, it can be a problem when absolute measurements are required. Furthermore, the lack of a universally accepted, and applied, method of signal calibration means that quantitative comparison of test results obtained from different detection systems is highly questionable.

Attempts have been made to overcome this problem through signal normalisation and characterisation of AE sensor response to reproducible broadband sources such as pencil-lead breaks [250], glass capillary breaks [250, 251] and helium gas jets [252]. However, there are problems with this approach, particularly since the generated waveforms are reproducible only at a single point on a given structure and even then although the structure can generally be well-defined the amplitude is dependent upon the source energy. As a result these methods are not universally employed in practice; rather they tend to be used as a check to ensure the functionality of the AE detection system and to confirm the quality of sensor coupling. A further use for these reproducible sources is to investigate AE propagation in structures, in which case the acquired signals are required to be normalised as a function of the source energy.

There are several other essential components in an AE measurement system. Signal amplification is necessary and is provided either integral to the sensor or externally via a pre-amplifier. Filtering of the signal is necessary to eliminate unwanted frequency components and background noise. The range of this filtering can typically be varied to suit the application although a prerequisite is the removal of any low-frequency energy and this lower limit varies from 20 to 100 kHz. Analysis of the frequency content via conventional spectrum analysers, rather than time-series data, was also much used.

RMS averaging of the raw signal used to be commonly used in the acquisition of AE data. This significantly reduces the required sampling rate thus allowing the use of less sophisticated data acquisition equipment. However, this was at the expense of information loss, both of the fine detail of the raw AE waveform and of the associated spectral content. Some researchers use specific circuitry which does not acquire and store data for future analysis but instead analyses the signal in real-time through the extraction of waveform features.

Today Analogue to Digital converters continuously digitise raw AE signals at full bandwidth, i.e. at sampling rates up to several MHz, and store this data for future analysis. Prior to this, digitised acquisition of raw AE was limited to small data batches that for many applications were insufficient to permit a full investigation.

4.4.2 AE Analysis and Signal Processing Techniques

There are two basic types of AE signal. The first is burst-type emission, where the signal consists of clearly defined ‘events’ as shown in Figure 4.5(a). These events are characterised by amplitude significantly larger than the background level, distinct sharp signal rises and close to exponential decays, and individual pulses can be well-separated in the time-domain. The second type is continuous emission; this occurs when burst generation is so rapid that the signal appears continuous and resolution of individual events is not possible.

Typically, signals acquired from machinery will be a combination of both to varying degrees, for example, Figure 4.5(b) shows a raw AE signal measured from the surface of a running engine in which a number of overlapping burst- and continuous- type events of varying amplitude are evident.

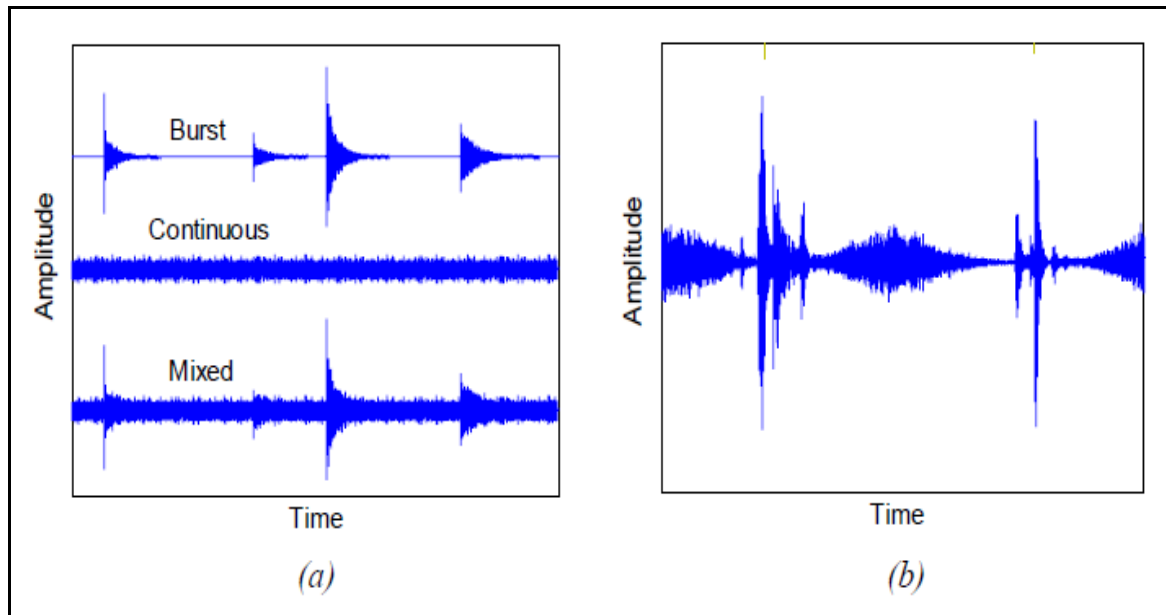


Figure 4.5 (a) Examples of AE emission types, (b) typical AE signal acquired from a running engine.

4.4.2.1 Time-Domain Analysis

There are various means by which AE signals can be processed and evaluated in order to extract information useful for condition monitoring, the most fundamental being the characterisation of signals with regards to the behaviour of the object under observation. The most common method for achieving this is time-domain characterisation of burst-type events through extraction of waveform parameters. This typically involves monitoring the sensor output continuously for activity that exceeds a predefined threshold level. When this occurs an event is registered and the signal is then processed to extract parameters such as those identified in Figure 4.6, these include; peak amplitude, event rise time, event decay time, signal duration, AE event count and AE count rate.

Of all the waveform descriptors, the measure of threshold crossing counts has probably been the most widely used, likely due to the simplicity of measurement system required and the applicability for both burst and continuous type emissions. However, there are disadvantages associated with the sole use of count parameters to describe AE signals.

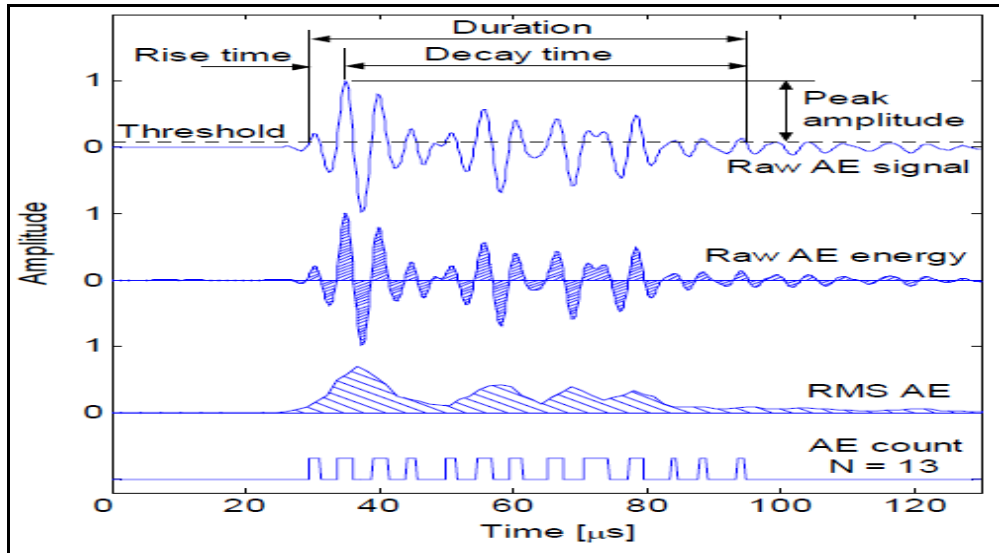


Figure 4.6 Typical time-domain parameters extracted from AE Signals [252].

These were outlined by Beattie and Jaramillo [252] who stated that firstly, AE count rate considers the amplitude of a signal only indirectly in that a large amplitude signal will usually persist for a longer time than a low amplitude signal, thus producing more counts. Secondly, for two signals of equal amplitude and duration, the one with the higher frequency content will register most counts. They suggested that a more quantitative measure is desirable, with the most obvious being the amount of AE energy emitted.

A further problem with applying threshold-based analysis to machinery monitoring is that burst type activity is often accompanied by a high level of continuous signal. If the burst activity is generated from a fault-related source, such as the early signs of wear, then this may effectively be buried in the continuous signal, which can make identification via threshold-analysis difficult. Therefore, to fully preserve the possibility of incipient fault detection and to better understand AE generation from machinery, continuous and mixed AE should be analysed by other means.

AE energy is a measurement parameter used extensively in AE monitoring. However, the calculation of energy is open to interpretation. The energy is taken as the area under the absolute of the signal, as defined in Equation 4.1; this is in contrast to a number of researchers who define AE energy as the area under the square of the signal.

$$E = \int_0^t |v(t)| dt \quad (4.1)$$

Where $|v(t)|$, is the absolute amplitude of the AE signal in volts, t is time in seconds and E is the AE energy in V.s.

A point to note regarding Equation 4.1 is that although it is presented in relation to time this does not preclude the use of other bases. For instance, for AE acquired from rotating equipment the AE signal is often transformed from a time-domain waveform to one which is a function of angular displacement. The resulting AE energy is then also an angular-domain parameter and the integration limits may be angular positions, as defined in Equation 4.2.

$$E_{\theta} = \int_a^b |v(\theta)| d\theta \quad (4.2)$$

Where $|v(\theta)|$ is the absolute amplitude of the angular-domain AE signal, θ is angular position in degrees, E_{θ} is the angular-domain AE energy, and a and b are angular positions.

A further parameter widely used to indicate energy is the Root Mean Square (RMS) value of the raw AE signal, calculated using Equation 4.3.

$$RMS = \sqrt{\frac{1}{N} \sum_{i=1}^N x_i^2} \quad (4.3)$$

Where x is the data value at a discrete point in time and N is the total number of data samples in the selected time period. Root Mean Square (RMS) of a signal can be measured also using this equation:

$$V_{RMS} = \sqrt{\frac{1}{T} \int_{t_0}^{t_0+T} v(t)^2 dt} \quad (4.3a)$$

Where $v(t)$, is the instantaneous value of the signal at time t and V_{RMS} is the RMS value of $v(t)$ for the time period T .

This can be applied as post-acquisition processing in which the RMS value for each successive time window is calculated, as shown in Figure 4.6 for a burst-type event. Otherwise, a signal averaging circuit can be in-built into the acquisition equipment which continually calculates the RMS value over a sliding time period. This allows data acquisition at a lower, more conventional rate thereby

bringing about a significant reduction in data size. This can be beneficial when analysis of many hundreds or thousands of lengthy acquisitions is considered as analysis of raw waveforms can be extremely computationally intensive.

Further simple statistical parameters are commonly used to describe signals such as the mean, \bar{x} , standard deviation, σ , and variance, σ^2 , as defined in Equations 4.4, 4.5 and 4.6 respectively. These can be applied to a whole signal, to sections, or windows, of a signal, or to determine variation between sets of signals.

$$\bar{x} = \frac{1}{N} \sum_{i=1}^N x_i \quad (4.4)$$

$$\sigma = \sqrt{\frac{1}{N-1} \sum_{i=1}^N [x_i - \bar{x}]^2} \quad (4.5)$$

$$\sigma^2 = \frac{1}{N-1} \sum_{i=1}^N [x_i - \bar{x}]^2 \quad (4.6)$$

Other statistical indicators often used are the skewness and kurtosis [253] as well as crest, impulse, clearance and shape factors. Kurtosis and skewness are statistical parameters that can be used to describe the graphical representation of the AE signal population. Kurtosis characterises the relative peakedness or flatness of a distribution compared to the Gaussian distribution. Positive kurtosis indicates a relatively peaked distribution. Negative kurtosis indicates a relatively flat distribution. Kurtosis is defined as

$$Kur = \frac{\frac{1}{n} \sum_{i=1}^n (x_i - \bar{x})^4}{RMS^4} \quad (4.7)$$

Skewness characterises the degree of asymmetry of the distribution around its mean. Positive skewness indicates a distribution with an asymmetric tail extending towards more positive values. Negative skewness indicates a distribution with an asymmetric tail extending towards more negative values. The Gaussian distributions produce a skewness of zero.

$$S_k = \frac{E[(x_i - \bar{x})^3]}{RMS^3} \quad (4.8)$$

4.4.2.2 Frequency-Domain Analysis

Frequency-domain analysis offers further options for investigation of AE signals, and is a proven technique for machinery diagnostics. This has been established through a long association with vibration monitoring where spectral analysis is considered one of the principal analytical tools and is used in many commercial monitoring packages.

Since AE is regarded by some as an extension of vibration monitoring, in that both are measurements of surface motion as a function of time, the transfer of many diagnostic principles from the latter to the former has been accomplished.

In general, frequency analysis involves the decomposition of time-series data into the frequency domain; this is typically achieved as an estimate through an algorithm known as the Fast Fourier Transform (FFT). For many applications this method alone is sufficient to describe the signal. However, other algorithms have been developed which implement the FFT in order to estimate the distribution of the signal energy in the frequency domain, the principal methods for this are known as the Power Spectral Density (PSD) and Welch's PSD estimate [254].

Regarding condition monitoring, analysis of frequency spectra can be similar to time-domain analysis, in that deviations from the expected normal condition may be indicative of faults. Some frequency parameters are directly associated with aspects of normal machine operation such as running speed or resonance, however, the development of faults may result in the emergence of discrete frequencies which can be related to the physical behaviour of individual machine components, and AE spectral analysis is used to distinguish between different types of source mechanism which is of benefit when investigating events of unknown origin.

A further approach commonly used is to filter the signal to separate it into its constituent parts. If the filter is carefully constructed then this can then allow increased focus on specific events through enhanced signal-to-noise ratios.

There are some problems in using frequency domain analysis and the common one is the energy leakage and the low resolution. This energy leakage can be reduced by employing a window function, such as a Hanning window.

4.4.2.3 Time- Frequency Domain Analysis

Time- frequency domain analysis is an attractive approach which analyses AE signals in the time-frequency domain. This is useful because many acoustic emissions are transient signals whereas stationary characteristics are assumed by the classical Fourier approach. For transient AE signals, the early parts of an event can often provide more information concerning the AE source than the main stream because the latter is often distorted by the effect of multiple reflections during propagation. The significant progress made in time-frequency analysis in the past twenty years provides tools to investigate the characteristics of frequency in these transient processes.

The most widely used time-frequency methods include the Short-Time Fourier Transform (STFT), Wavelet Transforms (WT) and Wigner-Ville Transform (WVT). The Wigner-Ville Distribution (WVD) was first successfully used to analyse transient AE signals for condition monitoring by [255] Newland at the University of Manchester.

The STFT can be defined as:

$$S_x(t; \tau) = \int_{-\infty}^{\infty} x(t) \omega(t - \tau) e^{-j2\pi f t} dt \quad (4.10)$$

It employs a moving window $\omega(t - \tau)$ to the measured AE signal $x(t)$ when performing the Fourier transform. If the time window is narrow enough, a good time resolution can be achieved, but at the cost of reduction in frequency resolution. This will not be troublesome in the analysis of AE signals because high frequency resolution is not often necessary for such high frequency signals. This technique will be used to analyse the AE signals acquired during the experiments.

Wavelet transforms are techniques introduced in the 1980s to process transient signals, particularly to reveal local disturbance, and have been applied by many researchers to the field of fault diagnosis. The pioneering work was carried out by Newland [255,256] who introduced the wavelet transform into the analysis of mechanical vibrations. It has been widely recognised that the wavelet transform is an effective technique for machinery fault diagnosis. In the past 10 years, numerous studies have been published in the field of condition monitoring and fault diagnostics which have included signal processing in the time-frequency domain for the detection of transient signals and extraction of fault feature or weak signal components [257].

Wavelet transform has been used to process AE signals. Qi [258] demonstrated the effectiveness of wavelet-based AE analysis to characterise fracture behaviour in composite materials. Jeong [259]

applied a Garbor wavelet to analyse the AE event generated in anisotropic composite laminates and found it an effective tool to analyse the wave propagation in a dispersive medium. Ding, et al., [260] used a wavelet packet transform to accurately estimate the arrival time of AE events based on the decomposition of the AE signal. These studies show the effectiveness of wavelet transform in the analysis of AE events, particularly single burst AE. No paper has been found in the literature that has applied this technique to the analysis of a continuous AE signal or a train of burst-type acoustic emissions.

4.4.3 Feature Extraction and Pattern Recognition

A number of other approaches exist for AE signal processing which do not involve applying a threshold, which are applicable for burst and continuous type emissions, and for both time- and frequency- domain information. Although the work in this thesis does not apply these techniques it is considered worthwhile to provide a brief review.

Many of these methods are considered attractive to condition monitoring as they introduce some form of automation to the analysis process and therefore lend themselves well to real-time monitoring. Also, they can be adapted to quickly handle large amounts of data and to identify changes in signals, or signal features which do not conform to the expected case. A further point is that many of these processes are purely statistical in nature, and require minimal interpretation of the complex AE signals with regards to the material or component behaviour. Hence, they are generic and transferable over applications as is borne out in the wide range of data processing problems to which they have been applied, such as speech recognition, machine vision, medical diagnostics and financial market analysis.

One technique used for isolating significant features from large and often complex datasets is Principal Component Analysis (PCA). This is a form of higher-level statistical analysis whereby variance is analysed and a simplified description of the data is returned which preserves as much statistically relevant information as possible. The removal of redundant features is deemed desirable, especially for the large datasets which AE monitoring usually generates, as it permits the application of further statistical classification and diagnostic aids.

Independent Component Analysis (ICA) is a further signal isolation technique, and is considered an extension of PCA. It assumes that the measured signal is a composite of separate signals which can be resolved using ICA algorithms based upon the assumption that the source signals are statistically

independent. The outcome is the source signals and also a measure of their separation effectiveness, i.e. how strongly they appear in the measured signal. This technique is especially useful for extracting low-level or hidden signals, which may otherwise be obscured by dominant sources.

Pattern recognition techniques are extensively used in condition monitoring applications, either using simple time-domain parameters, or in combination with feature extraction or other analytical processes. The overall aim with pattern recognition is to ascertain the condition of an item through comparison of measured signal parameters against a reference bank in which signals over varying conditions are mathematically and statistically well-defined. A best-match is identified and the acquired signal is then classified as representative of that particular condition. One drawback with this process is that in order to minimise misclassifications prior knowledge is required of all conditions that may be encountered. This may be impractical due to the many different operating conditions and fault scenarios; hence the pattern recognition process may, in application, be limited to differentiating between normal and abnormal conditions.

Neural networks have regularly been used to recognise and classify complex fault patterns without requiring a great deal of prior knowledge about the process, the signals, or the specific fault patterns. Neural networks are structured in layers of interconnecting processing elements (neurons), with the behaviour of the network determined by the weights associated with each connection. These weights can be adaptively trained using example signals to associate a particular input pattern to an output classification. Hence, if something similar to that pattern is presented again then the network will recognise it and return the appropriate output. Many output possibilities can be programmed in this manner and it is not unusual to have several processing layers in order to achieve an output classification. Neural networks are adept at handling large amounts of data in a short period of time and are therefore useful for real-time analysis and for data fusion, i.e. the amalgamation of information obtained from a variety of sensory inputs.

Further generic signal processing tools include fuzzy logic and expert systems. Fuzzy logic is a technique used when fault threshold values for conventional time-domain and frequency-content analysis are felt too rigid to suit the complex nature of mechanical condition monitoring. Expert systems is a term used to describe the application of knowledge-based procedures and programs that are the equivalent to the knowledge, or reasoning processes, that would be expected from human experts in a particular field.

CHAPTER FIVE

MATHEMATICAL MODEL OF PISTON SLAP AND FRICTION IN A DIESEL ENGINE

In this chapter a mathematical model is developed for the numerical simulation of the behaviour of the four-stroke diesel engine used in the test rig, and subsequently for predicting the impact and friction forces between piston assembly and cylinder wall responsible for piston slap signatures and friction. The model consists of a piston displacement equation, piston acceleration equation and piston motion equation. In addition, a hydrodynamic lubrication model is developed for piston slap phenomenon and friction.

5.1 General Concepts

This chapter describes a mathematical model developed to simulate the work cycle of a healthy four-stroke diesel engine, and to simulate the consequences of piston slap and piston friction. The fundamental idea is that piston slap is initiated when the connecting-rod side force changes direction either due to changes in the connecting-rod angle, or the connecting-rod force (from compression to tension or vice versa). The piston's impact against the cylinder bore and friction are significant sources of AE events and energy loss and can lead to cavitation wear on the cooling side of the liner, while its motion along the cylinder bore generates friction and transports oil, thereby affecting wear of the piston, rings and liner, and contributing to oil consumption.

Factors effecting the piston slap and friction are [261]:

1. Cylinder liner temperature,
2. Oil film thickness between piston skirt and cylinder liner,
3. Lubricant viscosity,
4. Engine speed,
5. Piston skirt profile,
6. Piston skirt size,
7. Piston skirt waviness,
8. Piston skirt roughness,
9. Skirt-liner clearance, and
- 10 Wrist-pin offset.

Piston skirt lubrication is provided by lubrication oil which is, in general, picked up from the oil sump and thrown onto the cylinder bore by the motion of the crankshaft. In some engines, lubrication oil is also sprayed onto the underside of the piston or other locations within the power cylinder system. The lubrication is then transported along the cylinder bore by the motion of the piston, piston rings and gravity. Lubrication oil is also transported around the system when it is entrained in blow-by gases. The lubrication oil leaves the cylinder bore in three ways: oil returns to the sump: oil entrained in the blow-by gas leaves the system via the crank case: or oil is consumed in the combustion chamber.

The engine process is the basis for the model simulating piston slap and friction AE events but due to the complex nature of oil transport within the system and inaccessibility for experimental confirmation, it is often impossible to accurately predict the location and thickness of oil films within the system.

5.1.1 Piston Slap

As stated, piston slap is caused by changes in direction of the piston side force. This event occurs many times in an engine cycle; however, major piston slap has been found to occur near TDC during firing. This is due to the fact that at this time the impact energy is greatest due to the high pressures in the cylinder chamber [262]. While high levels of engine noise have warranted in major changes in diesel engine design geometry, piston slap is reduced simply by changing the geometric parameter of the piston known as wrist-pin offset [263, 264, 265, 266]. Offsetting the piston has the effect of reducing slap impact since movement of the piston from one side of the cylinder to the other occurs prior to peak cylinder conditions, and thus with less impact energy. This has generally been used for reduction of AE events caused by piston slap in diesel engines and has proved to be successful, relative to other event source levels.

Without wrist-pin offset the piston simply traverses from the anti-thrust side to the thrust side, when the side force on the piston changes direction. This usually occurs near peak cylinder pressure conditions, which causes a steep piston side force curve, and in turn, causes higher impact intensity. The effect of wrist-pin offset is to cause the piston to tilt when the cylinder pressures become significant, in an orientation such that the bottom of the piston makes initial contact with the thrust side of the cylinder liner. As stated, this occurs before peak pressure conditions, and thus the intensity of impact is minimised. The reaction force due to contact at the bottom of the skirt combined with the change in direction of side force causes the piston to tilt in the opposite direction, causing another minimal impact between the top of the piston skirt with the cylinder liner. This two phase impact technique of lowering piston slap impact intensity has proven to be effective in low-noise engine design.

However, with the development of high speed, low weight engines, more study is needed of the dynamics of piston slap and the factors affecting it, rather than the quick answer of varying wrist-pin offset. Limited studies on the engine conditions affecting piston slap in diesel engines have been undertaken, including engine load and speed effects [267], and clearance effects at low speeds [268]. In addition, studies of the dynamics of the piston using displacement measuring techniques have also been accomplished [269, 270]. However, there is need for a more complete picture of the dynamics of the piston during piston slap, and the engine conditions and parameters affecting its intensity. Also, there has been little understanding of the role of the oil film in damping the impact, since prediction of the oil film is extremely difficult, and there are no adequate ways of measuring this parameter.

5.1.2 Piston Friction

The diesel engine frictional losses can be classified into four main components: piston assembly, valve train system, bearing system, and auxiliaries (water pump, oil pump, alternator, etc). Figure 4.2 shows the general proportions of the frictional loss for each engine component, although these proportions will change according to engine speed, load, and the type of engine [270].

From Figure 4.2, it can be said that most of the engine friction losses are from the piston assembly (piston skirt, piston rings and piston pin) which accounts for nearly half of the total engine friction for motoring conditions, and an even higher fraction of total engine friction for firing operation. Thus, it is necessary to attack piston assembly friction to achieve low engine friction. Many researchers have made a great effort to understand tribological phenomena to reduce the frictional losses of the piston assembly. However, the friction reduction of the piston assembly still remains a challenge due to the complexities of the tribological phenomena and the interrelations between friction, emissions, durability, noise and vibration, oil consumption, blow-by, etc.

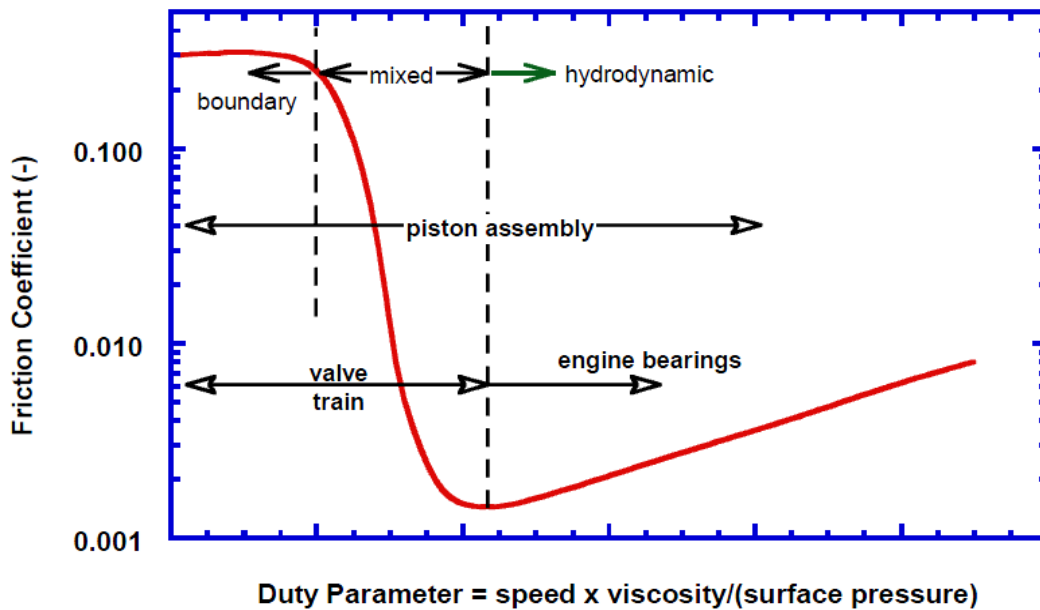


Figure 5.1 Stribeck diagram showing the various regimes of lubrication [263].

In general the characteristics of the lubrication phenomena in the piston assemblies can be explained using the Stribeck curve. Figure 5.1 shows a general Stribeck diagram representing the various lubrication regimes. The Stribeck diagram classifies the lubrication regime into three regions: boundary lubrication, hydrodynamic lubrication, and mixed lubrication. In the boundary

lubrication region, the asperities between two rubbing surfaces come into contact and become dry friction. Surface properties and lubricant additives affect the friction losses in this region and the friction coefficient is independent of lubricant viscosity, surface speed, and load. In the hydrodynamic region there is no direct contact between the two surfaces. The lubricant film separates the two surfaces completely and friction losses in the hydrodynamic region mainly come from shear forces of the fluids moving at different velocities between the two surfaces. The mixed lubrication region lies between these two extremes.

Basically the main functions of the piston ring assembly are to seal:

1. The high pressure combustion chamber from the crankcase, and
2. The oil in the crankcase from the combustion chamber.

Optimized piston/ring pack designs should fulfil these functions with minimum friction losses and wear. That is, the tribological characteristics such as friction, lubrication and wear of the piston/ring assembly are equally important. However, in this study the main concern will be concentrated to the friction losses of the piston assembly.

The lubrication phenomena of piston rings are extremely complicated due to the variation of piston speed, piston ring dynamics and interactions of the cylinder gas and lubricant film between the ring, ring groove, and the cylinder liner. Many researchers have made progress in analysing the lubrication phenomena of the piston assembly. The results of their research have proven that the basic frictional mechanism of the piston assembly is the combination of boundary, mixed and hydrodynamic lubrication.

As the oil viscosity, piston speed, and load are changed, the lubricant regime of the piston assembly also changes. As the piston approaches TDC and BDC, the piston speed becomes zero momentarily and the duty parameter (the x-axis) in the Stribeck curve approaches zero. Therefore, the lubrication regime near the TDC and BDC positions becomes boundary lubrication. At the mid-piston stroke, the piston speed is a maximum value and hydrodynamic lubrication becomes dominant. Mixed lubrication occurs during the transitions between hydrodynamic and boundary lubrication. On the up-stroke, the squeeze film effect of the oil can delay the transition to mix and boundary lubrication. In addition to the complicated friction mechanism of the piston/ring, the friction reduction of the piston/ring is also interrelated with oil consumption, blow-by, wear and other engine durability problems. Therefore, it remains a challenging problem to reduce the piston assembly friction losses. Recently however, the AE technique as developed at Huddersfield University will be used in

monitoring piston slap intensity and piston assembly friction, and will thus provide an understanding of the impact forces.

5.1.3 Characteristics of Piston Assembly Friction

The friction measurement of the piston assembly under engine firing condition is still a challenging problem. This is why in this research the piston assembly friction measurement under firing condition was done by using the AE technique.

Engine friction can roughly be divided into: coulomb friction (dry friction) which occurs when asperities between two surfaces moving relative to each other come into contact, and fluid friction which develops between adjacent layers of fluid moving at different velocities. The actual degree of friction in and between engine components can seldom be put neatly into either of these categories, but instead will lie somewhere between these two extremes because the load on, and velocity of, engine friction surfaces always vary when the engine is operating.

This means that there is a continuum between dry friction and fluid friction and the place on this continuum is dependent on such factors as: component geometry, surface roughness, relative velocities of the moving surfaces, normal loads and various rheological properties of the lubricant. This continuum approach is exemplified by what is commonly known as a Stribeck curve. Figure 5.1 shows a generic example of this curve.

5.2 A Review of Previous Work

Early work in this area [186-190] was focused on reducing engine noise and vibration and began with rigid body, frictionless models of the piston-cylinder system based on idealised joint constraints and a variety of additional simplifications. These models were initially used to solve for the crank angles at which the lateral force on the piston is reversed, causing piston slap to occur and to develop an idea of which parameters were likely to affect piston motion. They were later developed into more sophisticated models that were used to investigate the effect of variations in piston-cylinder bore clearance and wrist-pin offset. Experimental results obtained by Skorecki [187] confirmed that piston slap is a significant source of engine noise, particularly in the range of 2 kHz to 4 kHz and were used both to confirm the trends predicted by the model simulations and to investigate the effect of varying lubrication conditions on piston slap.

In 2000 D'Agostino et al [191] proposed a computer program for the determination of the fluid film force between piston skirt and cylinder wall due to the hydrodynamic lubrication mechanism. The finite element method (FEM) has also been applied by other researchers to analyse the impact force. However, the models as well as the FEM were not sufficient to estimate the impact forces. This is because the basic mechanism associated with the piston slap is related to the mechanical elements of engine block in a non-simple way.

More recent work has emphasised modelling of the oil film. The average Reynolds equation developed by Patir and Cheng [271] was used by Zhu et al [272, 273] to take into account surface roughness and waviness, and models have been extended from essentially two-dimensional kinematic models to quasi-three-dimensional models which make use of the two-dimensional Reynolds equation, which was applied over a variable circumference by Dursunkaya et al [262].

5.3 Piston and Piston Ring Kinematics

Fundamental to piston and piston ring operation are the piston and piston ring dynamics, which comprise the primary and secondary piston motions, radial and axial ring motions and ring twist. These motions influence all facets of piston and ring operation; the formation of oil films, the resulting friction between ring and liner, friction between piston and liner, slap between piston skirt and liner, wear of the components and blow-by across the ring pack.

The primary motion of the piston is equal to that of the piston rings. This can be determined as a function of the crank angle when the geometry of the crank-slider mechanism is known; a schematic of this assembly for a trunk-piston engine is shown in Figure 5.2a. Thus, expressions can be derived for piston displacement, velocity and acceleration, and these are given in Equations 5.1, 5.3 and 5.5 respectively.

The piston displacement, velocity and acceleration during a four-stroke engine cycle, with a connecting rod/crank radius ratio, n , of 2.6, are shown in Figure 5.2b.

If the crankshaft is rotating at constant angular speed, ω as shown in the Figure 5.2, we can calculate the position of the piston in terms of the crank angle θ [274]:

$$x = r[(1 - \cos\theta) + n(1 - \cos\alpha)] \quad (5.1)$$

Where: α is the angle the con-rod makes with the vertical, and it can be seen that:

$$l * \sin\alpha = r * \sin\theta \quad (5.2)$$

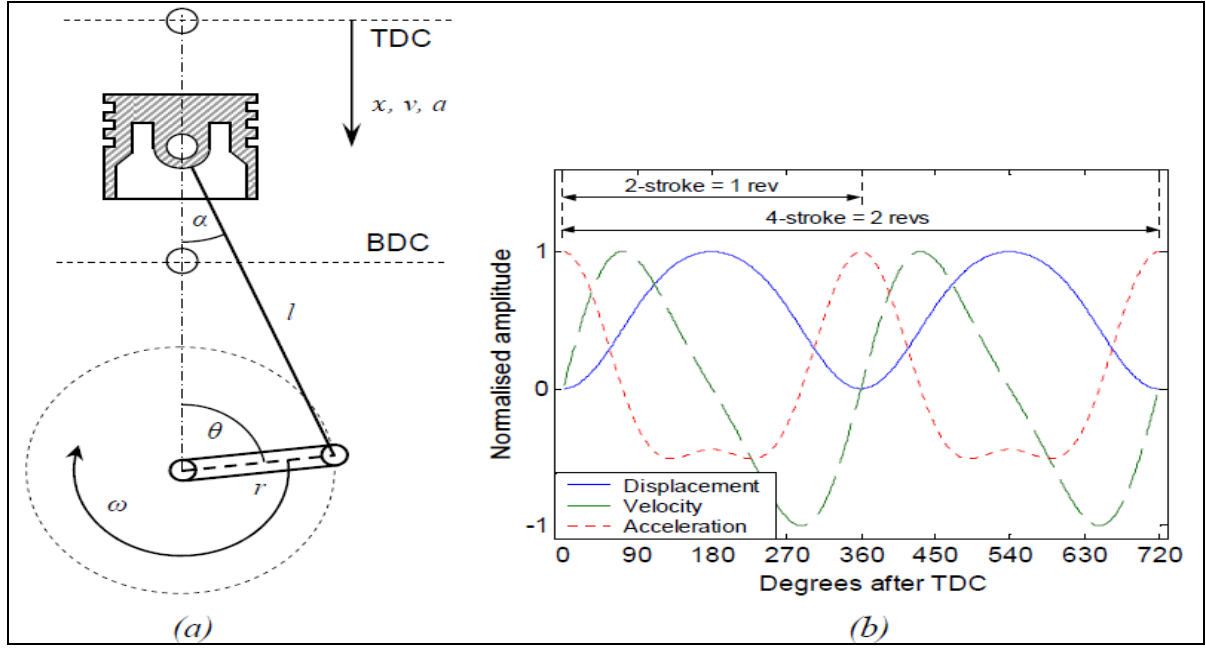


Figure 5.2 (a) Schematic of crank-slider mechanism, (b) piston primary motion [275].

From Eq. 5.2 we got:

$$\sin \alpha = \frac{r}{l} \sin \theta$$

$$\sin \alpha = \frac{1}{n} \sin \theta$$

Where $n = l/r$

By using the trigonometric identity of:

$$\cos \alpha = \sqrt{1 - \sin^2 \alpha} = \sqrt{1 - \left(\frac{r}{l} \sin \theta\right)^2} = \sqrt{1 - (n * \sin \theta)^2} \quad (5.3)$$

By substituting Eq. (5.3) into Eq. (5.1), we obtain

$$x = r \left[(1 - \cos \theta) + n \left(1 - \sqrt{1 - \left(\frac{1}{n} \sin \theta\right)^2} \right) \right] \quad (5.4)$$

In another form

$$x = r \left[(1 - \cos \theta) + (l/r) \left(1 - \sqrt{1 - \left(\frac{1}{n} \sin \theta\right)^2} \right) \right] \quad (5.5)$$

With respect to time, the mean crankshaft angular speed:

$$\omega = \frac{2\pi * rpm}{60}$$

If the angular velocity is constant, then

$$\theta = \omega t$$

Differentiating:

$$\frac{d\theta}{dt} = \omega$$

$$\frac{d^2\theta}{dt^2} = 0$$

The piston position with respect to crank angle is simply x and the piston speed is:

$$v = \frac{dx}{dt} = \frac{dx}{d\theta} * \frac{d\theta}{dt}$$

$$v = \frac{dx}{d\theta} * \omega \quad (5.6)$$

$$v = \omega r \left(\sin \theta + \frac{\sin 2\theta}{2n} \right) \quad (5.7)$$

The piston acceleration is the differentiation of the piston velocity. The acceleration with respect to crank angle is x'' :

$$x'' = \frac{d^2x}{d\theta^2}$$

$$x'' = -r * \cos \theta - \frac{r^2(\cos^2 \theta - \sin^2 \theta)}{\sqrt{l^2 - r^2 \sin^2 \theta}} - \frac{r^4 \sin^2 \theta \cos^2 \theta}{(\sqrt{l^2 - r^2 \sin^2 \theta})^3} \quad (5.8)$$

The acceleration with respect to time and the angular velocity of piston derivatives then:

$$a = \frac{dv}{dt} = \frac{d^2x}{dt^2}$$

$$a = \frac{d}{dt} * \frac{dx}{dt}$$

$$a = \frac{d}{dt} \left(\frac{dx}{d\theta} * \frac{d\theta}{dt} \right)$$

$$a = \frac{d}{dt} \left(\frac{dx}{d\theta} \right) * \frac{d\theta}{dt} + \frac{dx}{d\theta} * \frac{d}{dt} \left(\frac{d\theta}{dt} \right)$$

$$a = \frac{d}{dt} \left(\frac{dx}{d\theta} \right) * \left(\frac{d\theta}{dt} \right)^2 + \frac{dx}{d\theta} * \frac{d^2\theta}{dt^2}$$

$$a = \frac{d^2x}{d\theta^2} * \left(\frac{d\theta}{dt} \right)^2 + \frac{dx}{d\theta} * \frac{d^2\theta}{dt^2}$$

$$a = \frac{d^2x}{d\theta^2} * \omega^2$$

$$a = x'' * \omega^2$$

$$a = \omega^2 r \left(\cos \theta + \frac{\cos 2\theta}{n} \right) \quad (5.9)$$

Where x is piston displacement from TDC, r is the crank radius, θ is the crank angular displacement from TDC, n is the ratio of connecting rod length to crank radius (i.e. l/r), v is piston velocity, ω is the mean angular speed of the crankshaft and a is piston acceleration. Piston secondary motion also affects ring operation. This is caused by clearance between the piston and liner which allows lateral movement and rotation of the piston about the piston pin according to the forces and moments acting upon it. Piston rings also exhibit secondary motions; again including lateral movement and ring rotations and, additionally, ring lift and ring twist. These arise from the various forces acting on the rings. These include; inertial forces from piston acceleration and deceleration, forces owing to the pressure difference across the ring, oil film damping forces, and friction forces from shearing of the lubricating film and contact pressure at the ring/liner interface.

5.4 Governing Equations

5.4.1 Equation of Motion

The equations of motion for the piston have been well developed [276,277]; however, modifications were made here in consideration of wrist-pin moment inertia, M_{IP} , wrist-pin friction M_{PP} , and friction and normal forces on the piston from the three rings, F_{R1} and F_{Q1} for the top ring, and F_{R2} and F_{Q2} for the second ring and F_{R3} and F_{Q3} for the third ring (see Figures 5.3 and 5.4). Also, the forces and moments due to oil film support were broken down into four forces and four moments. Each side of the cylinder liner has a normal force, friction force, a moment due to the

normal force, and a moment due to friction force. For the thrust side, this corresponds to F_T , F_{FT} , and M_{TT} , and. M_{FT} For the anti-thrust side, this corresponds to F_A , F_{FA} , and M_{AA} , and M_{FA} [276].

Equilibrium of forces in the y-direction yields:

$$\sum F_y = F_g + \hat{F}_{IP} + \hat{F}_{IC} + \tilde{F} \cos \phi + \sum_{j=1}^3 F_{Qj} + F_{FT} + F_{FA} = 0 \quad (5.10)$$

Where F_g corresponds to the force due to the gas pressure on the top of the piston, and \hat{F}_{IC} and, \hat{F}_{IP} correspond to axial inertial forces due to the piston, and wrist-pin (along with part of the connecting rod), respectively. The connecting rod force is given by \tilde{F}

Equilibrium of forces in the x-direction yields:

$$\sum F_x = F_{IP} + F_{IC} - \tilde{F} \sin \phi + \sum_{j=1}^3 F_{Rj} + F_T + F_A = 0 \quad (5.11)$$

Where F_{IP} and F_{IC} correspond to the horizontal inertia forces due to the piston, and wrist-pin, respectively. The third equilibrium equation balances moments about the wrist-pin and yields:

$$\begin{aligned} \sum M_{Wrist\ pin} = & M_{IC} + M_{IP} + M_{PP} + M_{TT} + M_{AA} + F_g C_P + F_{IC}(a - b) - \hat{F}_{IC} C_g + \\ & M_{FT} + M_{FA} + C_P \sum_{j=1}^3 F_{Qj} + \sum_{j=1}^3 F_{Rj} l_j = 0 \end{aligned} \quad (5.12)$$

Where M_{IC} corresponds to the rotary inertia due to the wrist-pin, C_P and C_g correspond to the wrist-pin offset and horizontal distance between the wrist-pin axis and centre of gravity, respectively, and a and b correspond to the vertical distance from the top of the skirt to wrist-pin and centre of gravity, respectively. Elimination of \tilde{F} from equations (5.10) and (5.11) yields:

$$-F_{IP} - F_{IC} = F_S + (F_{FT} + F_{AT}) \tan \phi + F_T - F_A \quad (5.13)$$

Rewriting equation (5.12) yields:

$$-M_{IC} - M_{IP} - F_{IC}(a - b) = M_S + M_{TT} + M_{AA} + M_{FT} + M_{FA} \quad (5.14)$$

Where F_S and M_S are the forces and moments that do not depend on piston-liner contact:

$$F_S = (F_g + \hat{F}_{IP} + \hat{F}_{IC} + \sum_{j=1}^3 F_{Qj}) \tan \phi + \sum_{j=1}^3 F_{Rj} \quad (5.15)$$

$$M_S = M_{PP} + F_g C_P - \hat{F}_{IC} C_g + C_P \sum_{j=1}^3 F_{Qj} + \sum_{j=1}^3 F_{Rj} l_j \quad (5.16)$$

Frictional losses from the second ring are relatively small, and, as a result, most friction reduction strategies focus on the top and oil control rings. The horizontal inertia forces and moment are defined in terms of piston eccentricities, e_b and e_t and can be calculated as:

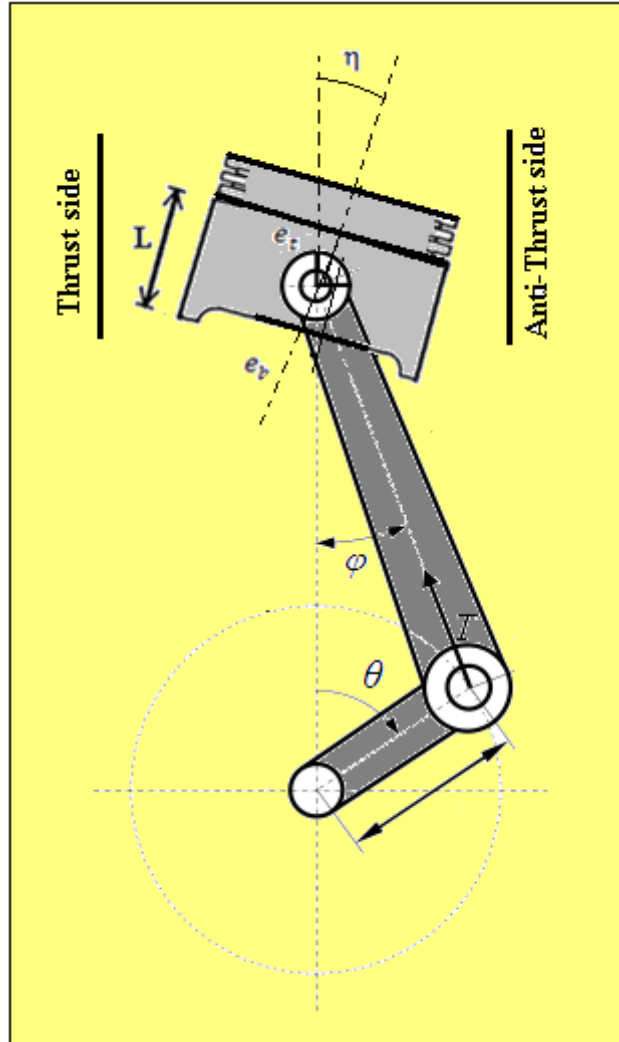


Figure 5.3 Schematic of piston cylinder wall system [276].

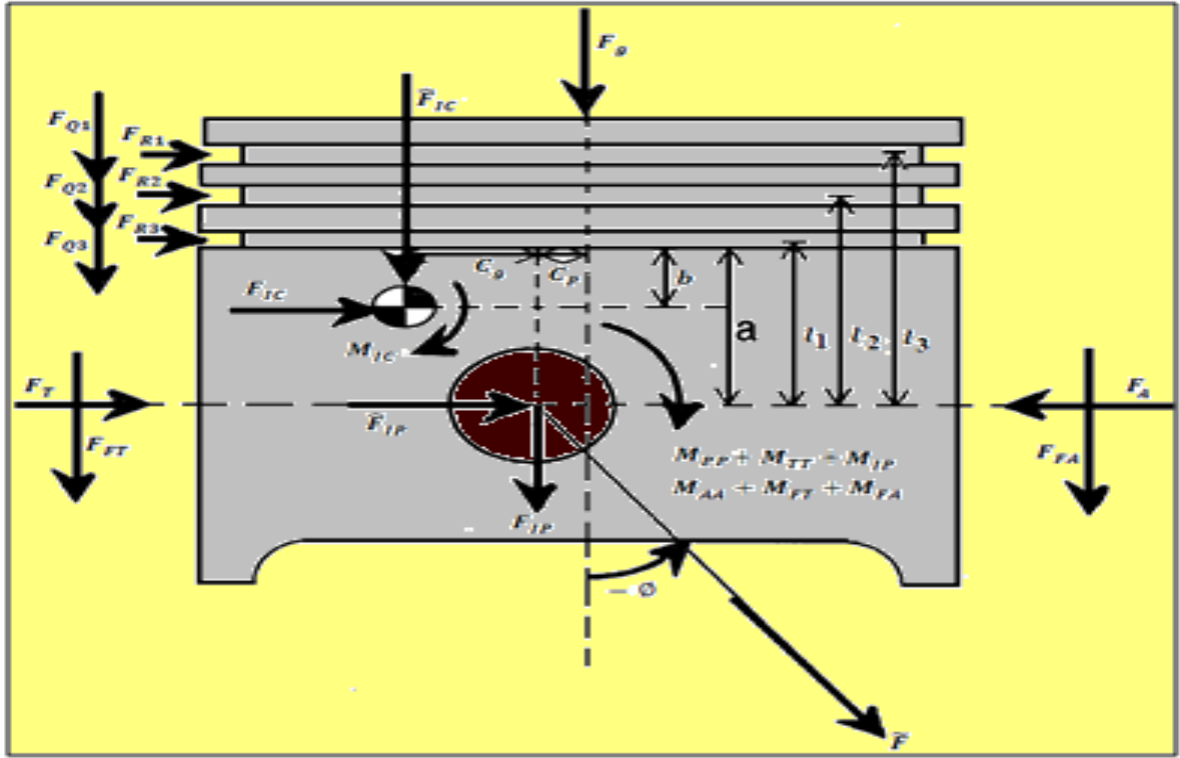


Figure 5.4 Schematic of forces and moments acting on the piston [276].

$$F_{IP} = -m_{PP}[\ddot{e}_t + \frac{a}{L}(\ddot{e}_b - \ddot{e}_t)] \quad (5.17)$$

$$F_{IC} = -m_{pis}[\ddot{e}_t + \frac{b}{L}(\ddot{e}_b - \ddot{e}_t)] \quad (5.18)$$

$$M_{IC} + M_{IP} = -\frac{I_{PT}(\ddot{e}_t - \ddot{e}_b)}{L} \quad (5.19)$$

From Newton's law in matrix form:

$$[F] = [m][a] \quad (5.20)$$

Thus, equations of mass and acceleration define the equations of motion for the piston; the procedure for determining the terms in the force matrix depends on the piston contact.

$$\begin{bmatrix} F_S + (F_{FT} + F_{FA}) \tan \phi + F_T - F_A \\ M_S + M_{TT} + M_{AA} + M_{FT} + M_{FA} \end{bmatrix} = \begin{bmatrix} m_{PP} \left(1 - \frac{a}{L}\right) + m_{pis} \left(1 - \frac{b}{L}\right) & m_{PP} \frac{a}{L} + m_{pis} \frac{b}{L} \\ \frac{I_{PT}}{L} + m_{pis}(a - b) \left(1 - \frac{b}{L}\right) & m_{PP}(a - b) \frac{b}{L} - \frac{I_{PT}}{L} \end{bmatrix} \begin{bmatrix} \ddot{e}_t \\ \ddot{e}_b \end{bmatrix} \quad (5.21)$$

5.4.2 Piston Ring Normal and Friction Forces, F_Q and F_R

The piston normal forces have been calculated assuming solid-to-solid contact between ring and groove, and using forces calculated by a model similar to Namazian [277]. F_{pr} , F_{fr} and F_{ir} correspond to the pressure force, friction force between the ring and liner, and ring axial inertia force, respectively. The ring's equation of motion is obtained by considering these forces [263]:

$$m_r \frac{d^2 h_r}{dt^2} = F_{pr} + F_{fr} + F_{ir} - F_{Q1} \quad (5.22)$$

Where m_r , is the ring mass, and h_r is the top ring side clearance. The force between the piston and ring is given by Namazian as:

$$F_{Q1} = -\beta \mu_{oil} L_r \frac{dh_r}{dt} \left(\frac{W_r}{h_s}\right)^3 \quad (5.23)$$

Where L_r , is the ring length in the circumferential direction; W_r is the ring width in the radial direction, and β (critical shear rate) depends on area covered with oil (assumed as 0.1). Substituting equation (5.23) into (5.22) yields:

$$F_{pr} + F_{fr} + F_{ir} - \beta \mu_{oil} L_r \frac{dh_r}{dt} \left(\frac{W_r}{h_s}\right)^3 = m_r \frac{d^2 h_r}{dt^2} \quad (5.24)$$

This can be solved for h_r to obtain the normal force due to the top ring. A similar analysis was done for the second and third rings.

The horizontal friction force can be calculated since the normal force is known:

$$F_{R1} = \mu_{ring-piston} F_{Q1} \quad (5.25)$$

Where $\mu_{ring-piston}$ is the friction coefficient between the piston and ring.

5.4.3 Wrist-Pin Friction, M_{PP}

The wrist-pin frictional moment M_{PP} is modelled as [254]:

$$M_{PP} = (\sin \Phi) \mu_p R_p F \quad (5.26)$$

Where R_p , is the radius of the wrist-pin, and F represents the normal force on the wrist-pin. The sign changes with change in piston tilt.

5.4.4 Cylinder Liner Support, F_T , F_A , M_{TT} , and M_{AA}

The cylinder liner support is divided into a force and moment on both the thrust and anti-thrust side [261]. The two sides are decoupled by use of the piston tilt equation:

$$\tan \Phi = \frac{e_t - e_b}{L} \quad (5.27)$$

Where, Φ is the piston tilt, see Figure 5.4, and the side support due to hydrodynamic lubrication is given by an averaged Reynolds Equation based on average flow factors [261].

$$\frac{\delta}{\delta x} \left(\Phi_x \bar{h}^3 \frac{\delta P_h}{\delta x} \right) + \frac{\delta}{\delta y} \left(\Phi_y \bar{h}^3 \frac{\delta P_h}{\delta y} \right) = 6\mu U \left(\frac{\delta h}{\delta y} + \Omega \frac{\delta \Phi_s}{\delta y} \right) + 12\mu \frac{\delta h}{\delta t} \quad (5.28)$$

Where Φ_x and Φ_y are the pressure flow factors, and Φ_s is the shear flow factor. These flow factors are based on surface waviness, Ω and surface roughness, σ . The $\frac{\delta h}{\delta t}$ term is dependent on piston skirt thermal distortions, machined profile, elastic deformations and geometry. With the proper boundary conditions for the Reynolds Equation, the normal force due to hydrodynamic pressure and its moment about the wrist-pin is found by the following integrations: (for the thrust side):

$$F_{Th} = R \int A_{Th} P_h(\theta, y) \cos \theta d\theta dy \quad (5.29)$$

$$M_{TTh} = R \int A_{Th} P_h(\theta, y) (a - y) \cos \theta d\theta dy \quad (5.30)$$

Where A_T and A_A are the total bearing areas on the thrust and anti-thrust side, respectively, found by iteration.

If the distance between the piston skirt and cylinder liner become small enough so that the hydrodynamic assumption is invalid, a contact pressure and friction force result. The contact pressure is determined by calculating the normal pressure for one wave, then integrating over the area to find the total normal pressure, and consequent force and moment. The coupled local wavy contact pressure, \bar{P}_W , and wavy contact deformation, δ equations defined by Zhu et al [273] are solved via adaptive step control numerical method, the following normal force and moment result (for the thrust side

$$F_{Tc} = R \int A_{Tc} P_W(\theta, y) \cos \theta d\theta dy \quad (5.31)$$

$$M_{TTc} = R \int A_{Tc} P_W(\theta, y) (a - y) \cos \theta d\theta dy \quad (5.32)$$

Thus, by combining the contributions from the hydrodynamic and constant normal forces and moments, the following total normal force and moment result (for the thrust side):

$$F_T = F_{Th} + F_{Tc} \quad (5.33)$$

$$M_{TT} = M_{TTh} + M_{TTc} \quad (5.34)$$

5.4.5 Skirt-Liner Friction

The frictional forces and moments caused by hydrodynamic lubrication are also given by Zhu et al [273] for a rough piston skirt. The shear stress is given as:

$$\tau = -\frac{\mu U}{\bar{h}}(\Phi_f + \Phi_{fs}) + \Phi_{fp} \frac{\bar{h}}{2} \frac{\delta P_h}{\delta y} \quad (5.35)$$

Where Φ_f, Φ_{fs} and Φ_{fp} are the average shear stress factors dependent on surface waviness and roughness. Thus, the hydrodynamic friction force and moment is given as (for the thrust side):

$$F_{FTh} = R \iint A_{Th} \tau(\theta, y) d\theta dy \quad (5.36)$$

$$M_{FTh} = R \iint A_{Th} \tau(\theta, y) (R \cos\theta - C_p) d\theta dy \quad (5.37)$$

In the case of contact, friction is given by (for the thrust side):

$$F_{FTc} = -R \frac{|U|}{U} \iint A_{Tc} P_w(\theta, y) \mu_f d\theta dy \quad (5.38)$$

$$M_{FTc} = R \frac{|U|}{U} \iint A_{Tc} P_w(\theta, y) \mu_f (R \cos\theta - C_p) d\theta dy \quad (5.39)$$

Thus, by combining the contributions from the hydrodynamic and constant frictional forces and moments, the following total forces and moment result (for the thrust side):

$$F_{FT} = F_{FTh} + F_{FTc} \quad (5.40)$$

$$M_{FT} = M_{FTh} + M_{FTc} \quad (5.41)$$

This summarized the theory behind the piston slap model which will be used and compared with the experimental results.

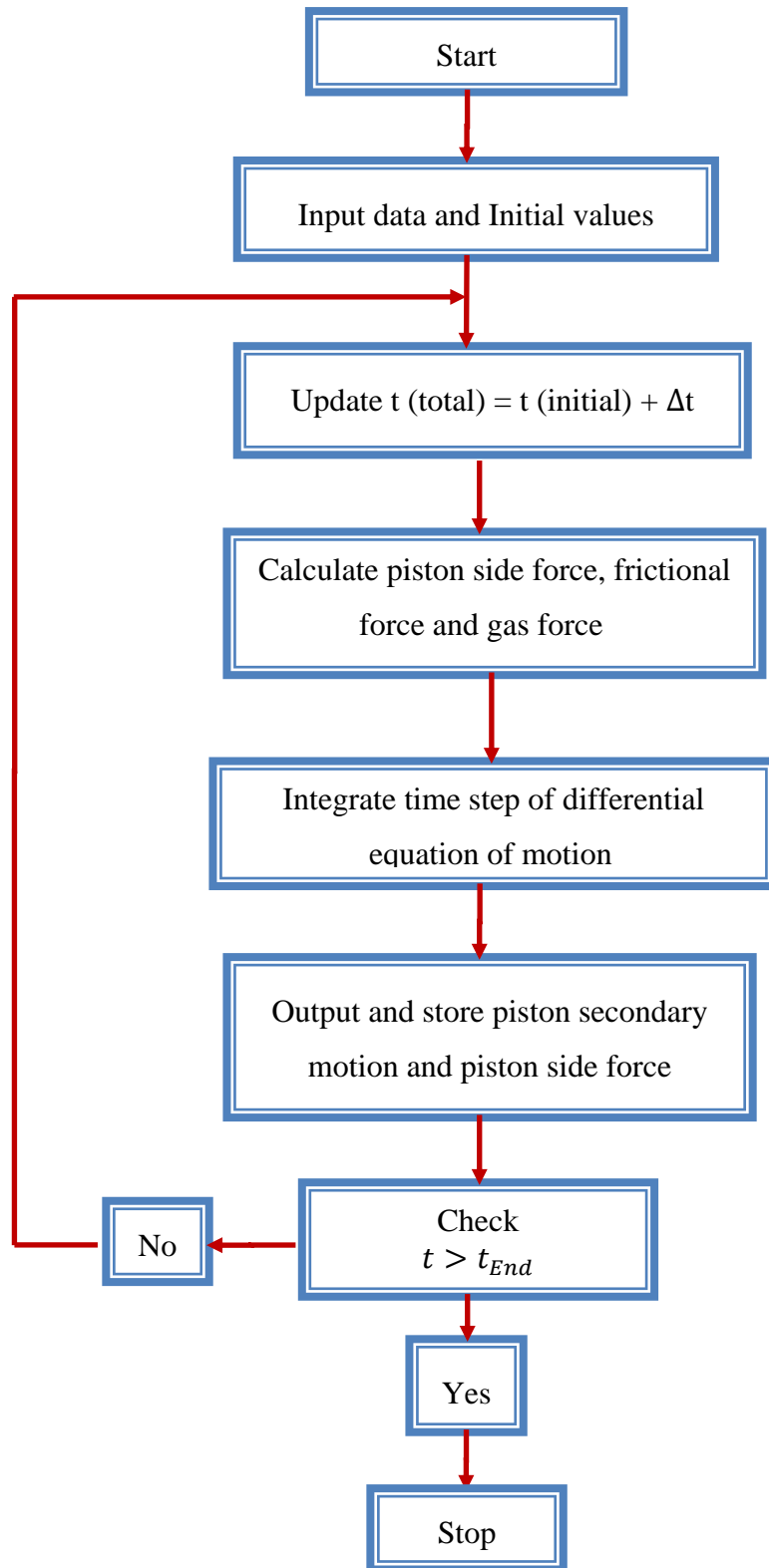


Figure 5.5 Flow chart for piston frictional force and the piston side force.

5.5 Radial Thermal Deformation

During combustion, the piston crown and top land are exposed to combustion gases, resulting in heat transfer to the piston and crown temperatures of about 200°C . The top ring(s) seal the combustion chamber and there is significant clearance between the piston and the cylinder bore at the pin axis, so in general the piston skirt is not exposed to significant amount of the combustion gases. The piston skirt temperature is therefore predominantly determined by conduction of heat from the crown, and typically varies axially through $60\text{-}100^{\circ}\text{C}$. Depending on the material and structure of the piston, and whether any cooling oil is supplied to the underneath of the piston, temperatures within the piston can vary significantly. These temperatures and the corresponding thermal expansion, which is of the same order as the piston cylinder bore clearance, vary over time with running conditions from cold shape at start-up, to a significantly larger shape at steady-state, high load and speed. It is considered for the purposes of this study that we have fully warmed engine I assume steady state warm thermal behaviour.

5.6 Cyclic Variations

As the cylinder pressure changes from minimum to maximum value, the piston assembly friction is influenced by the cylinder pressure variation. Thus, in addition to the friction force, it is valuable to determine the range between maximum and the minimum of the friction force during the measured engine cycles. The cylinder pressure variation and gas torque is shown in Figure 5.5.

As expected, the piston assembly friction is dependent on the cylinder pressure variation. The variation of the second peak of the friction forces is very dependent on that of the peak cylinder pressure. The crank angles at which the friction forces become maximum or minimum are coincident with that of maximum pressure or minimum pressure, respectively.

The gas torque signal exhibits an offset sine wave shape. The amplitude of the combustion related torque oscillations is clear. The phase of the torque output main component is within a few crank angle degrees of cylinder pressure. This is observed at the peak values of torque; however the torque is a distorted sine wave which can be observed in the bottom lumps between the combustion events. This is largely due to inaccuracies in the reciprocating masses and valve train.

Fuelling, igniting and combustion relate cylinder to cylinder torque fluctuations. Due to uneven air charges, fuel injections, poor ignition repeatability and/or combustion instability, the engine torque output is never completely even, especially at low speeds. Logically, the frequencies characterizing these phenomena are lower than the firing frequency.

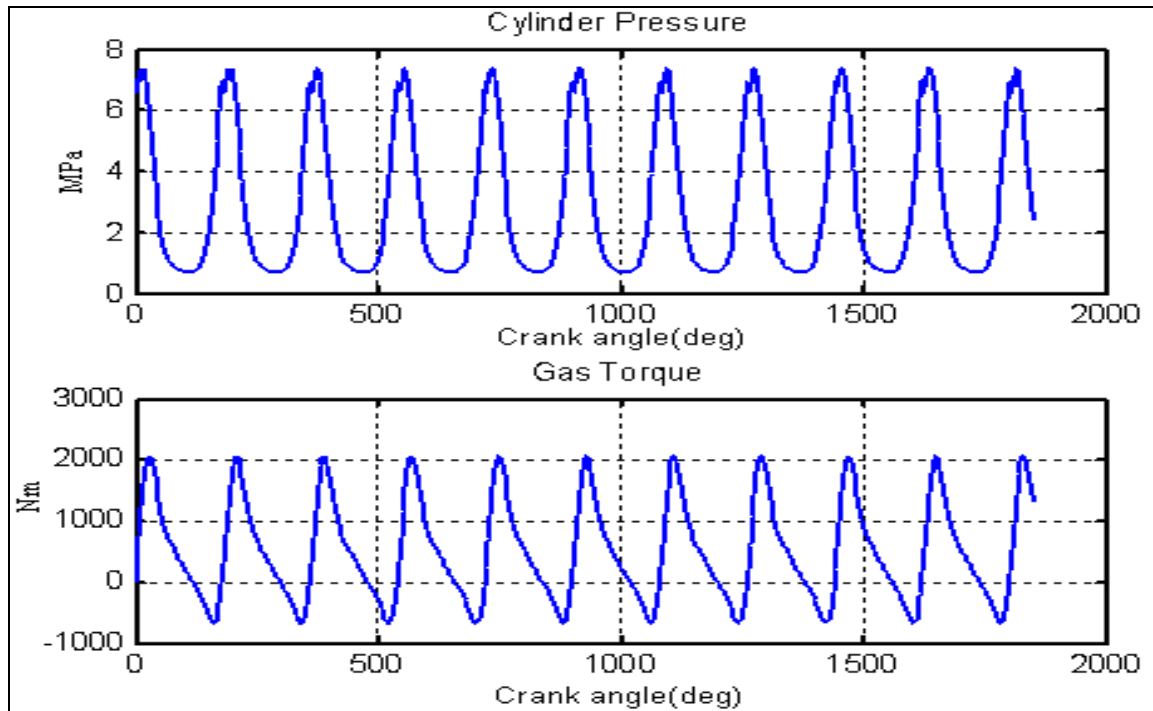


Figure 5.6 Measured diesel engine pressure and gas torque

5.7 Cylinder Pressure Measurement

The oil viscosity at 90°C is just about 5% of that at 30°C [276]. The smaller value of viscosity yields an increased possibility for boundary and mixed lubrication between the piston and the liner. At elevated oil temperatures, the oil film thickness between the piston assembly and the liner could be less than the mean length of metal asperities at some piston positions, and thus there could be more possibility of metal-to-metal contact between them during the engine operation.

That is, the lubrication regime could be boundary and/or mixed lubrication near the TDC and BDC positions in which the cylinder pressure is high and the piston speed is low. Figure 5.6 shows the measured cylinder pressure at an oil temperature of about 90 °C. The region of most significance of pressure is the region around TDC of compression stroke, as this is where transducer is located.

The trend of pressure force variation as the engine speed increases is the same as that for low oil temperature. However, the absolute value of cylinder pressure at high oil temperature is less than that at low oil temperature due to the difference in volumetric efficiency. Since the air densities trapped in the cylinder become lower and the volumetric efficiencies are lower at

high oil temperature, the cylinder pressure at high oil temperature is lower than that for low oil temperature at the same engine speed.

From figure 5.6 (lower one) the measured engine speed fluctuations between two speeds, the increased moment of inertia of the angle-brake set up leads to very large engine non-uniformity and thus limited speed fluctuations. Nonetheless, the greater speed droops of the friction are apparent.

Note that the firing stroke is within the crank angle range from 10 to 190 degree ATDC. The maximum pressure shown here is around top dead centre.

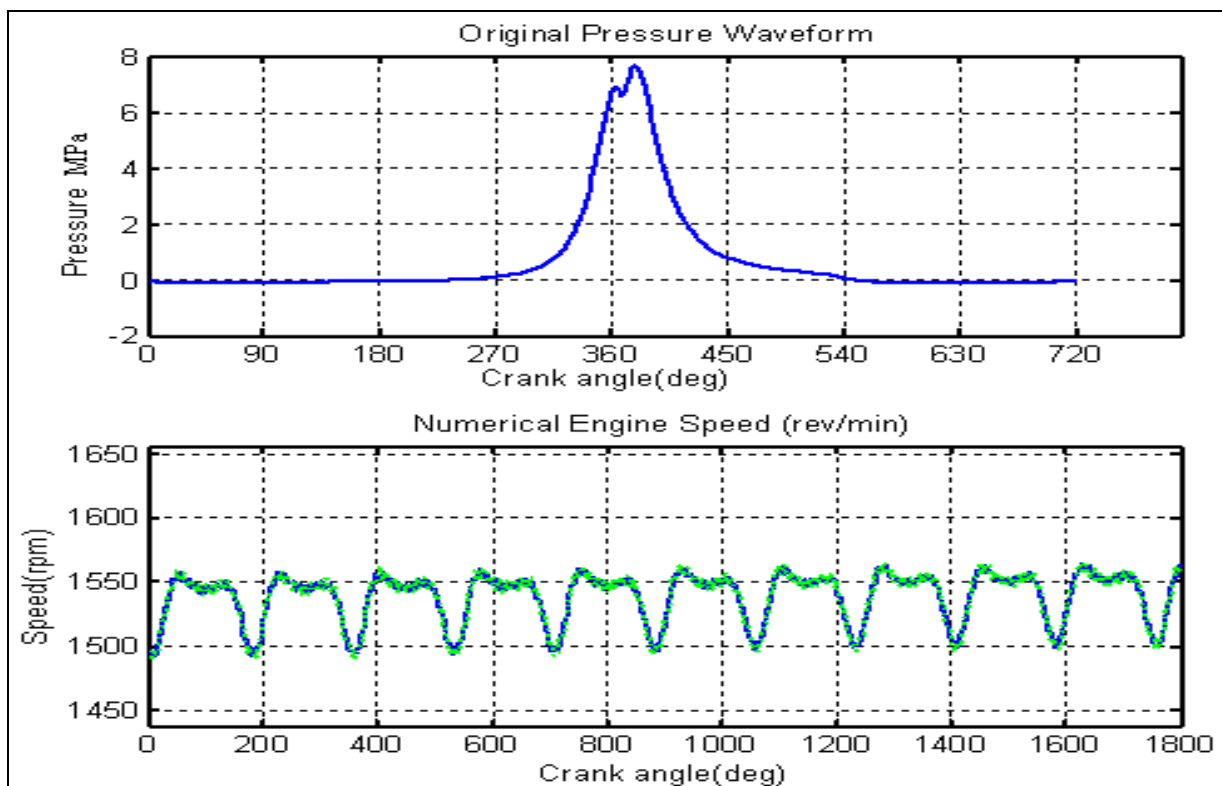


Figure 5.7 Gas pressure acting on the piston crown

5.8 Effects of Engine Operating Conditions on Piston Liner Friction

Modern diesel engines operate in a variety of speed and load conditions depending on their application. In small vans and heavy duty trucks, loads and speeds will vary considerably due to the variety of operating conditions encountered. Some passenger car engines typically operate at high speeds and high loads. Stationary power generation engines operate in high load, low speed

conditions because high load generates more power and the low speed is needed to interface with the electric generator and the power grid.

Both engine speed and load affect the friction generated between the piston and the liner. In addition, oil supply plays a very important role in piston assembly liner lubrication.

5.8.1 Effect of Engine Speed

With increasing engine speed, combustion characteristics and corresponding pressure trace change; altering fuel injection timing and increase fuel mass (because the piston speed is directly related to the rotational speed of the crankshaft). Also the engine temperature increases with increased engine speed, and correspondingly the thermal deformations of the piston and cylinder bore increase. Both the piston and cylinder bore temperatures and thermal deformations increase with axial height, and the location of the coolant chamber affects the temperature distribution and any reinforcements can restrict thermal deformation.

Figure 5.7 shows piston axial velocity (Eq. 5.7) and lateral force (Eq. 5.13) behaviour for the JCB engine. It can be seen that the piston axial velocity increased with increasing engine speed and the piston lateral trust force is only slightly influenced by increasing speed. The speed of the piston is zero at both TDC and BDC as seen in Figure. By comparison with the Stribeck curve of Figure 5.1 the lubricant would be in the boundary regime and some asperity contact would presumably occur. Also the coefficient of friction will increase during this phase resulting in increased friction forces [276]. Therefore, it is likely that high strength AE will be produced at these angular positions. Moreover, at TDC the lateral forces are much higher than at BDC because of combustion and the resulting AE should be stronger. The high forces seen at (0, 720 and 1440 deg.), because gas pressure variation is greatest value around firing TDC (negative value denote piston movement towards the BDC), whereas during compression, and inlet and exhaust strokes, its magnitude is much lower.

Other factors such as the number of piston rings; piston ring profiles, width, tension, piston skirt length and profile are all capable of influencing piston ring assembly friction but it is clear that these factors serve only to superimpose themselves on the effects inherent to the nature of the piston ring assembly's reciprocating motion (relative velocity) and in-cylinder pressure fluctuations due to combustion (load).

As the speed increases the instantaneous piston speed at mid- stroke also increases. At higher piston speeds the lubricant is in the hydrodynamic region, higher fluid pressure will develop in the oil film formed by the hydrodynamic lubrication and friction force will increase. Friction forces at both

dead centres are different because at the BDC the area of contact between piston and cylinder wall is smaller due to the opening of the transfer port located at BDC. At the middle of the stroke, the opening of the exhaust port also reduces the contact area between piston and wall, because of the max piston speed at middle (low oil viscosity, the shear rate depends directly on the piston speed, and the viscosity is controlled by the shear rate).

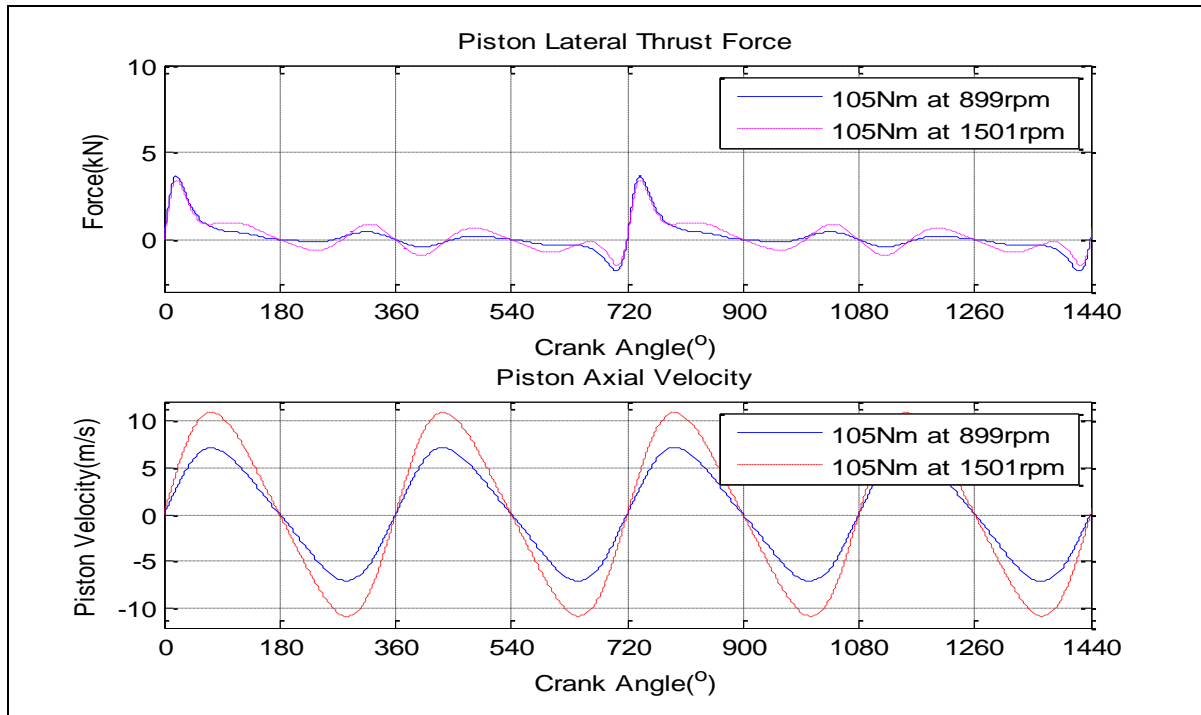


Figure 5.8 Engine speed and effect on the piston

The lateral force after compression TDC decreases as the engine speed increases as seen in Figure 5.7. However, in contrast to the period of time after cold starting the engine, the friction force near the mid-stroke does not change a lot. This is basically due to the low oil viscosity at high oil temperature. At high speeds, the measured friction forces are more influenced by the increased signal noise that occurs at higher speeds. The friction forces decrease slightly near compression TDC as the engine speed increases and increase near mid piston stroke even if the differences are small. However, in contrast to expectations, the friction force peak near compression TDC at high speed is greater than that for low speed.

5.8.2 Effect of Engine Load

The effect of engine load on friction is less straightforward. In order to maintain constant engine speed when the load on the engine increases, the amount of air and fuel brought into the cylinder to be compressed and burned during combustion must be increased. As a result, higher peak pressures are reached in the cylinder.

The engine load acting on the piston (force and velocity) is illustrated in Figure 5.8 as a function of the crank angle. As seen in the figure the piston lateral force was increased by increasing the load and there is no significant change in piston axial velocity with increasing load. The friction generated by the piston is significantly affected by the pressures reached in the cylinder throughout the engine cycle.

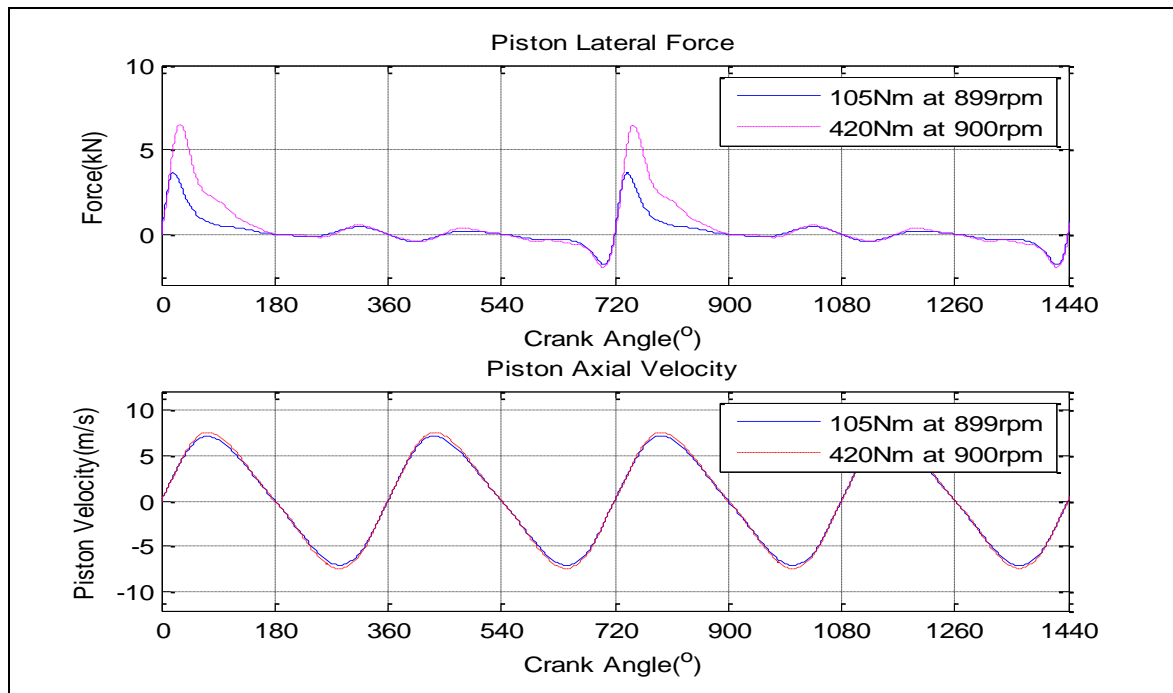


Figure 5.9 Engine load acting on the piston

The cylinder pressure controls the top land pressures, which affect the piston dynamics and therefore the lubrication conditions encountered by the rings throughout the engine cycle. Although in general, the contribution of friction as a percentage of the engine's indicated power output reduces as load increases, because the piston lateral force is increased as seen in Figure 5.8, major

changes in load may result in a change in the type of piston liner friction that dominates in different parts of the cycle.

5.8.3 Effect of Oil Supply

The amount of oil supplied to the piston throughout the engine cycle has a significant effect on the friction and lubrication conditions between the piston and the liner [276]. The presence of oil between piston and liner should significantly reduce the friction force, as the side load is partially supported by hydrodynamic pressure, thereby reducing the extent of asperity contact. This may affect the piston tilt to a small degree, but is not common to have a significant effect on lateral motion. Also the presence of oil does not change the timing of the start of piston slaps, but provides cushioning, slowing the piston's travel across the cylinder bore once contact with the oil is made, and reducing oscillations due to bouncing and tilt. The lateral motion is reduced due to the fact that the incompressible oil physically reduces the available clearance and can only be squeezed out in a finite amount of time.

Note that there is no oil on the liner in the region above TDC of the oil control ring in the first cycle. This is because the oil control ring can never travel above its own TDC position, and there is thus no direct oil supply to the upper rings between TDC of the oil control ring and TDC of the top ring. As a result, the only source of oil to this part of the liner is what is brought into this region by the top ring or the second ring in subsequent cycles. There is therefore much less oil supply to this section of the liner as can be seen in Figure 5.9.

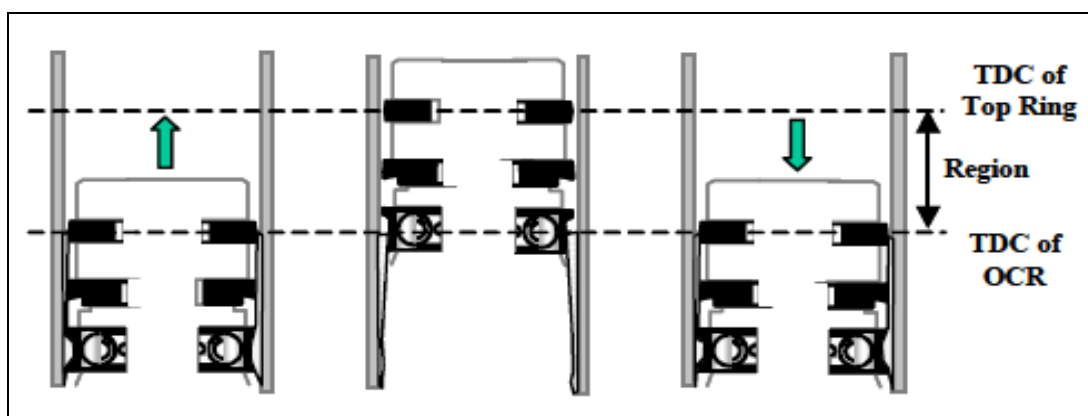


Figure 5.10 Illustration of the oil dry region at top of cylinder [276].

5.9 Effects of Piston Parameters on Piston Friction

5.9.1. Skirt-Liner Clearance

As the piston travels up and down in the cylinder, it also rotates (at low speed about 10 rpm) and moves transversally in a secondary motion, due to changing gas pressures and inertias [276]. Instead of travelling along the axis of the cylinder, the piston presses against one side of the liner as it moves towards the combustion chamber, then moves to the other side as it travels down. When the piston moves from one side to the other a “slap” occurs, which is when the piston hits the liner and oscillates briefly before remaining pressed against it. The impact velocity of this slap affects the amount of noise produced by the engine as well as the piston frictional losses as seen in Figure 5.10. The skirt/liner clearance directly affects the impact speed of the piston slap. A larger clearance allows the piston to accelerate over a larger distance, resulting in a faster impact speed at the slap. Large impact velocities lead to large impact forces, which lead in turn to large contact friction losses. Thus, skirt/liner friction should be reduced as clearance is reduced. This should be for larger oil thicknesses, but for thinner oil films a minimum point should occur where friction begins to increase again when clearance is decreased.

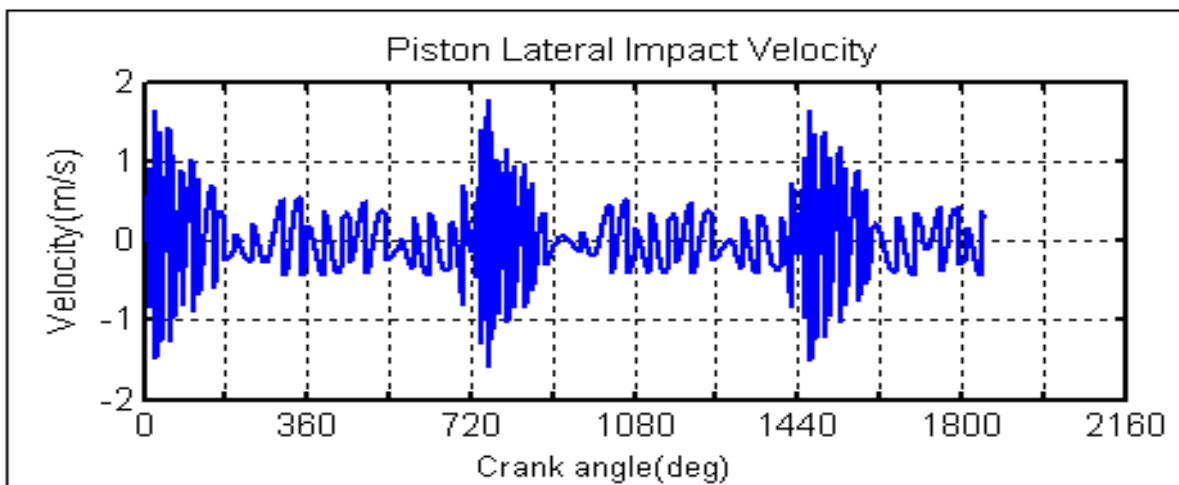


Figure 5.11 Piston lateral impact velocity

This minimum point results from asperity contact occurring at tight clearances, which increases friction, by bringing the skirt and liner surfaces closer together for low oil film thicknesses. For large clearances the slapping velocity dominates and friction decreases as clearance decreases, while for very small clearances asperity contact becomes important and friction begins to rise while

clearance is decreased. There is almost no change in hydrodynamic friction with clearance, what causes change in the friction is a largely change in asperity contact. The ideal skirt-liner clearance provides sufficient space for the oil but is not large enough to produce significant impact. Insufficient clearance produces excessive contact friction, while excessive clearance produces excessive impact.

5.9.2. Oil Supply/Oil Film Thickness

Oil film thickness, which is controlled by oil supply, has a direct impact on friction but the mechanisms of oil distribution between the piston and liner are not fully understood. A very thin oil film enables the skirt to easily push the oil aside and contact the liner, leading to boundary friction. On the other hand, a thick oil film tends to encourage hydrodynamic lubrication by providing more contact between the film and the piston surface, thereby enabling the lateral force to be spread over a larger area.

As the film thickness is increased to a certain point, it reduces boundary contact friction to a very small value, which minimizes net friction work loss. If film thickness is increased beyond this critical point, however, no further reduction in boundary friction occurs, and hydrodynamic friction increases due to an increase in wetted area. Thus, increasing film thickness beyond the critical point can actually increase net friction.

The oil film thickness has a much greater impact on boundary friction than hydrodynamic. The boundary friction is increased rapidly as film thickness is decreased, this is due to an increase in the amount of boundary contact that occurs as the piston and liner surfaces are brought closer together. When the film thickness is increased sufficiently the boundary contact friction component is very small (can be neglected), and further increases in film thickness increase hydrodynamic friction loss. There is only a small change in hydrodynamic friction throughout the range of film thicknesses.

The oil film thickness has a much larger effect on piston friction than skirt/liner clearance. The main effect of the clearance is to control friction during the “slap” period of the piston transition, while the film thickness affects skirt/liner contact throughout the cycle.

When its effect on friction is clear, the lubricant film thickness may also affect other engine parameters. For example, a thicker oil film can serve to cushion engine slap, reducing engine noise and vibration as well as friction. However, if the film is too thick, oil consumption may become a problem.

5.9.3 Surface Finish/Waviness

The piston skirt is typically machined so that it is covered by circumferential grooves, as well as smaller scale “roughness” asperities [276]. The grooves behave as oil reservoirs, supplying oil for hydrodynamic lubrication. The customary measure of groove size is waviness, which is the “amplitude” (i.e., half of the peak-to-valley depth) of the groove.

The liner also affects oil flow and retention. In typical diesel engines, liners have a honing pattern that serves much the same purpose as the waviness pattern on the piston: the grooves retain oil by surface tension and serve as an alternate supply, and they also provide flow paths for oil. Unlike the piston, in which grooves are machined circumferentially, the grooves in the liner are often oriented at an angle relative to the horizontal. The honing angle has a modest impact on friction. Shallow honing angles (relative to the horizontal) encourage oil to flow laterally rather than move up or down the liner, which would be undesirable.

5.9.3.1 Waviness vs. Roughness

Surface roughness refers to the natural deviations of an actual surface from a geometrically smooth shape. Any metal shape has natural surface roughness that is related to the method of manufacture, degree of polishing, and other factors. In a ring surface, surface roughness plays an important role because it serves much the same purpose as waviness on a piston surface: the valleys serve as oil reservoirs, and the gaps between the peaks provide flow paths for oil. In a piston, however, the waviness amplitude should be greater than the roughness amplitude, often by an order of magnitude. Thus, although roughness would be expected to play an important role in a piston with a nominally smooth (un-honed) surface, roughness only slightly modifies the effective amplitude of the waviness peaks in typical pistons. Therefore, roughness amplitude is expected to have a negligible effect on friction. The changes in roughness had little impact on net friction.

5.9.3.2 Parametric Surface Waviness

The friction losses decrease as surface waviness decreases, largely due to a decrease in boundary friction. For availability of oil, a piston with deeper machined grooves has more volume to contain the oil – that is, the lubricant can be trapped within the machined grooves instead of staying between the piston and liner. When it is contained within the grooves, the oil is not useful as a lubricant or to support hydrodynamic pressure, and asperity contact occurs. Conversely, when the

oil cannot escape into deep machining grooves and is compressed between the piston and liner, hydrodynamic pressure is generated and the piston load can be fully supported on the oil film.

The relation of friction to surface waviness suggests dependence not only on waviness height, but on the relation of the waviness to oil availability. A smoother piston should require less oil to support hydrodynamic lubrication, while a very wavy piston should require more.

There is a nearly linear relationship between waviness, film-thickness ratio and piston friction. Thus, in cases where very little lubricant is available to the piston a low waviness is preferred, whereas in cases where a large film thickness is possible, a smooth piston is still preferred but a wavier surface is allowable. However, a very smooth piston is always undesirable.

Although skirts with low waviness values appear to produce the lowest friction, extremely smooth surfaces can lead to high friction, wear and sometimes seizure. Extremely smooth surfaces do not retain oil well, so that direct solid-solid contact, if and when it occurs, can be very poorly lubricated and quite severe. Also, the contact surface area may be larger in cases of very smooth surfaces, further contributing to friction and wear. Therefore, friction can be minimized by selecting small but nonzero waviness values, to prevent scuffing.

In addition to the waviness, the effect of the roughness is dominated by the macroscopic waviness. Since the characteristic length of waviness (i.e., the depth of the machined grooves) is typically an order of magnitude greater than roughness, the effect of waviness on friction loss dominates.

5.9.4 Piston-Skirt Profile/Shape

Changing the “flatness” of the skirt changes both the hydrodynamic and boundary friction of the piston. A flatter skirt should show both a larger wetted area and a thicker oil film. The thicker oil film indicates that separation between the piston and liner is increased, decreasing boundary contact or possibly eliminating it entirely. An increase in wetted area size and film thickness tends to lead to an increase in hydrodynamic friction losses, but this also results in lower average and peak oil pressures, which could help reduce hydrodynamic friction. The increase in wetted area and oil film thickness (skirt/liner clearance) is sustained throughout the stroke.

The skirt-liner clearance for sharper profiles drops significantly below the waviness height for a large portion of the cycle, meaning that substantial boundary contact is occurring and high friction forces created. For flatter profiles, skirt/liner clearance drops below the waviness height briefly, and only by a small amount, indicating that much less metal-metal contact is taking place. A piston with a flatter profile experiences more wetting during the entire engine cycle, so that the change in hydrodynamic lubrication is the same throughout.

The change in skirt/liner clearance with piston profile suggests that a sharper profile experiences much more boundary friction than a flatter one. This confirmed that a flatter piston profile causes a large reduction in boundary friction, along with a slight increase in hydrodynamic friction. Changing the piston profile has a substantial effect on the amount of boundary friction generated, with metal-metal contact almost entirely eliminated for the flattest profile. The small increase in hydrodynamic friction for flatter profiles is much smaller than the corresponding change in boundary friction. In two different oil viscosities, the piston Friction Mean Effective Pressure (FMEP) decreases for flatter profiles, with boundary contact decreasing substantially with smaller increases in hydrodynamic friction. For both oil viscosities the proportion of the changes in hydrodynamic and boundary friction is different for the two cases.

5.9.5 Piston-Skirt Size

The size of the piston skirt is an important parameter in piston design. For example, a steel piston requires a dramatically different design from an aluminium piston because steel is a much denser material. Steel offers a stiffer structure that can handle much higher in-cylinder pressures but, if it is not designed carefully to reduce weight; it will require much larger connecting rods and other supporting structure, which could nullify any potential advantages. In a typical steel piston design, much of the material is removed, especially in low-stress areas like the periphery of the piston skirt. Figure 5.11 illustrates the difference in skirt size by comparing aluminium and steel pistons, which were both designed for heavy-duty engines. (Obviously, it is simplistic to change the skirt size without modifying the profile, stiffness, or other characteristics.)

The effect of skirt size on friction can be understood by observing that smaller skirts must distribute the lateral load over a smaller area (i.e., have higher average and peak pressures), so they tend to have more boundary lubrication and less hydrodynamic lubrication. Indeed, there is a dramatic increase in boundary friction as the skirt size is reduced, but a slight decrease in hydrodynamic lubrication as the skirt gets smaller. On balance it seems best to make the skirt as large as possible.

In actual piston designs, the tendency of smaller skirts to operate in the boundary lubrication regime can be offset by other design changes. For instance, the ovality can be adjusted to spread the load horizontally. Also, the profile can be adjusted to spread as much pressure in the centre region as possible. Most of the pressure is borne in the centre of the skirt. Since the steel piston spreads the load horizontally across its width, it does not incur significant friction disadvantages by reducing skirt height.



Figure 5.12 Comparison of aluminium and steel piston designs [276].

5.9.6 Piston Ovality

The piston ovality is designed not just to minimize friction, but also to minimize wear, reduce seizing, enhance guidance, etc. Piston ovality is essentially a piston profile oriented in the horizontal direction, and it fulfils several of the same purposes as the profile.

When the engine is in operation, the piston skirt deforms in response to pressures stemming from lateral force on the connecting rod and inertial forces. Just as smooth, flattened profiles distribute pressure more evenly and thereby promote hydrodynamic friction, pistons with less ovality have the potential to reduce friction by conforming more closely to the liner.

However, the caution that must be exerted regarding the profile also applies to ovality: the system must be evaluated after the piston has been deformed by operational temperature and lateral pressure.

Ovality is analogous to profile shape because both modify the effective clearance between the piston and liner. The objective of both is to facilitate a relatively flat oil film with gradual gradients in order to distribute the lateral force over as large an area as possible. This promotes hydrodynamic lubrication and reduces wear. The ovality is adjusted so that it closely matches the shape of the liner, particularly at points in the cycle when the lateral force is high.

Since reducing the ovality (i.e., making the piston more round) enables it to better conform to the liner surface, it is predicted that reducing ovality will reduce contact friction, thereby reducing net friction as well. However, it is important to not completely eliminate ovality (i.e., make a perfectly circular piston). The lateral pressure is highest along the thrust and anti-thrust lines, so these areas

will deform the most. A perfectly round piston will thus deform preferentially along the thrust and anti-thrust lines, leading to “negative ovality,” or a concave shape that shifts pressure away from the thrust/antitrust lines. This could cause instabilities and produce undesirable high-pressure patches. Since ovality can be adjusted independently of the piston profile, the two parameters can be jointly optimized to achieve ideal results. The profile is difficult to optimize because the piston rotates during the stroke especially near the TDC effectively changing the profile. The ovality does not change as much, however, since the piston does not rotate significantly about the thrust/anti-thrust axis. Therefore, in principle, the ovality can be optimized more precisely than the profile. Ideally, the two can be jointly optimized to minimize boundary contact friction while also achieving other objectives, such as smooth guidance throughout the stroke.

5.10 Other Considerations

In addition to frictional losses, wear of the piston and liner must also be taken into account. Piston-liner wear leads to leakage of combustion gases out of the engine cylinder (“blow-by”) and a corresponding reduction in efficiency and increase in engine emissions. Limiting this degradation of engine performance and avoiding the need to service and replace parts, requires that piston-liner wear be controlled.

The actual wear of the piston and liner is a complicated and not well-understood phenomenon, and wear predictions have not been included in this study. Wear factor can be calculated, which takes into account two main contributors: asperity contact pressure and sliding distance. The wear factor is a mean factor for an engine stroke, and can be calculated as the integral of the contact pressure multiplied by the piston speed, integrated over the stroke distance.

The wear factor increases as mean lubricant viscosity is reduced, because the amount of asperity contact occurring increases. Wear increases strongly even as frictional losses remain low—the minimum FMEP at a viscosity corresponding to a high wear rate. This means choosing an ideal lubricant viscosity which represents a balance between friction and wear considerations, and the desire for low friction must be balanced against the need for low wear. It is possible to decrease wear slightly by controlling viscosity changes during the engine cycle. Maintaining high viscosity near dead-centres can reduce asperity contact in the end-stroke regions, decreasing wear.

5.11 Friction Reduction Strategies

Piston friction arises from a complex combination of design characteristics, material and surface features, oil properties, and engine operating conditions. The piston skirt contributes as much friction as the ring-pack to the engine's mechanical losses. Like the ring-pack, its friction can be reduced if asperity contact is reduced. The piston experiences both hydrodynamic and boundary lubrication, with the dominant lubrication regime changing during the engine cycle. While the hydrodynamic frictional losses from the two sides are approximately equal and occur throughout the stroke, boundary contact is only observed on the major thrust side, during the expansion stroke. This results from the high gas pressures present after combustion, as well as the piston "slap" as it moves from the minor to the major thrust side. The boundary friction generated in this region of the stroke contributes a significant amount of total piston skirt friction.

Several piston parameters have been discussed above including design parameters such as the skirt profile and waviness, and other factors including lubricant viscosity and skirt-liner clearance, with the goal of reducing friction. The most important parameters identified were oil film thickness and skirt waviness, which can both be manipulated to reduce friction by reducing skirt/liner asperity contact.

There are some issues which have not been addressed and are significant in friction reduction. These parameters are practical design parameters which offer the greatest potential for near term implementation, viz. mechanical design of the piston itself such as piston skirt ovality, the physical dimensions of the piston skirt, and optimizing the lubricant parameters for pistons of certain geometrical and material designs. Also there is another important parameter, which is skirt stiffness. The author expects that more flexible skirt can reduce friction, by increasing wetted area and decreasing contact friction.

5.12 Summary

The results presented in this chapter are for heavy duty diesel engine. The degree to which conclusions drawn from these results can be applied to other engines is sometimes limited, particularly when there are significant differences in the combustion pressure - inertia balance, piston - cylinder bore relative stiffness or oil supply conditions.

The model analysis demonstrated the piston's lateral motion is essentially driven by the combustion pressure, component axial inertias and angular position of the connecting rod. Piston cylinder bore friction and wrist-pin friction were not play a significant role in determining the side force acting on

the piston. The connecting rod angular inertia and rate of change of momentum do not play a large role in determining the magnitude of the side force but can significantly affect the mid-stroke piston slap timing. The side force acting on the piston, and driving lateral motion, is relatively unaffected by oil film thickness.

The lateral motion of the piston is constrained by the cylinder bore and oil film, and is therefore essentially a function of the piston – cylinder bore clearance, oil film thickness, side force, and piston deformation (and cylinder deformation as well). There is large effect that oil film thickness can have on lateral motion if there is sufficient oil supply, significantly reducing lateral motion and impact velocities, and damping out oscillations.

Each of the parameters (Piston Ovality, Piston-Skirt Size...etc), which mentioned above has the potential to affect friction, but they offer varying benefits. Obviously, the improvements are not additives, if the waviness is excessive, profile curvature will no longer have much of an effect on friction. In order to reduce friction, the piston should be designed to provide a relatively even skirt-liner clearance in order to enhance hydrodynamic lubrication and avoid boundary lubrication. This can be achieved by using a relatively flat profile, adjusting piston ovality to match the liner shape, and reducing waviness peaks so they do not contact each other. Moreover, selecting the lubricant such as the viscosity excessive drag is also crucial to controlling friction. A key take away from this study is that the piston liner system is highly-integrated, and changing one variable affects many other parameters.

CHAPTER SIX

EXPERIMENTAL TEST FACILITIES

AND FAULT SIMULATION

This chapter discusses test-related issues including the test rig, instrumentation, and test procedures. Firstly a brief description of the test engine characteristics and specifications is given. Secondly details of the test systems and instrumentation are presented, with further information concerning the acoustic emission instrumentation as it is of crucial importance in this work. The data acquisition, test procedures, software and fault simulation strategies are described in the final section.

6.1 Test Rig Specification

The test-bed for this project used as a source of AE data, was a JCB 444T2 diesel engine, 4.4 litre, four-cylinder, four-stroke, 16-valve, in-line, direct injection and turbocharged, as seen in Figure 6.1 and Table 6.1). This engine test setup is available within the Automotive Laboratory, Huddersfield University, UK. This type of diesel engine is chosen as a test bed in this study, because it's a heavy duty diesel engine and used as a power supply in different equipments, such as wheel loaders, excavators, soil compactors, electric generators, etc.,

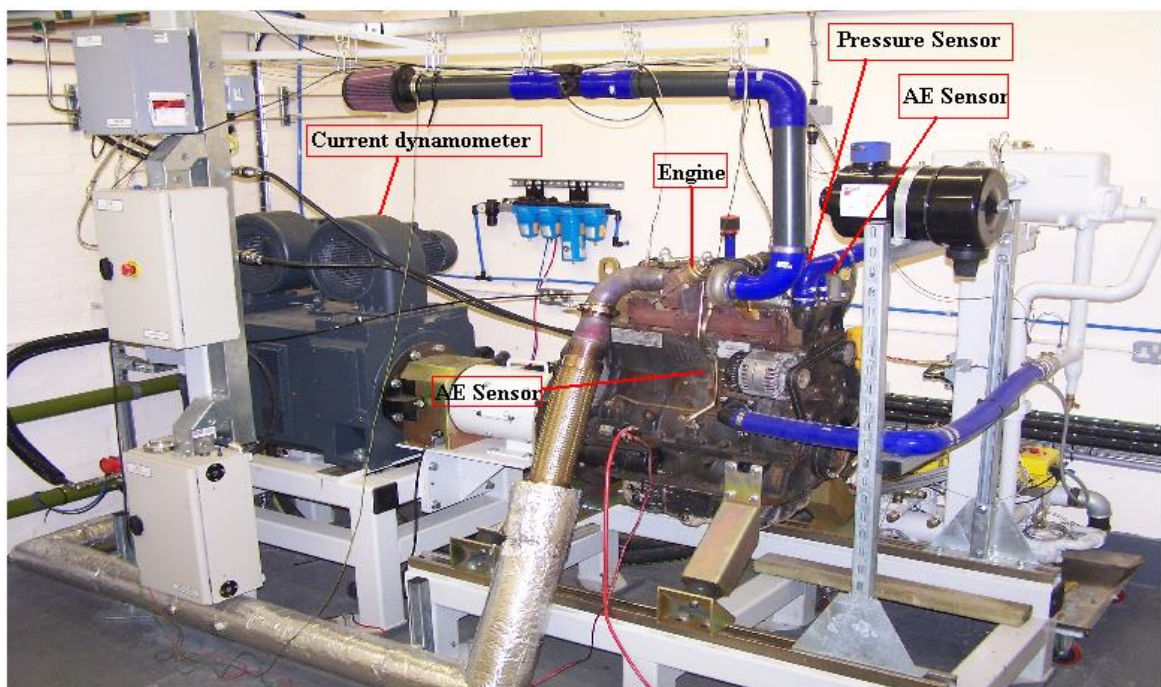


Figure 6.1 JCB444T2 Engine rig

The diesel engine was connected to an eddy current dynamometer which exerted a braking force and was rated to handle an engine of a maximum power of 210 kW and a maximum torque of 501 Nm. The test cell holding the dynamometer has a ventilation system to maintain room temperature and an exhaust extraction system. Also the rig is controlled by a panel control outside the room which is used to start/stop the engine, adjust engine speed and fuel supply, and monitor the engine temperature. Figure 6.1 is a photo of the test engine in situ. The four cylinders were numbered 1-4, with cylinder 1 at the front.

Table 6.1 Test Engine Specifications [specification catalogue]

Type of engine	Turbocharged diesel engine
Number of cylinders	4
Bore	103mm
Stroke	132mm
Inlet valve diameter	36.5mm
Exhaust valve diameter	33.2mm
Compressor inlet diameter	60mm
Compressor outlet diameter	60mm
Turbine inlet diameter	100mm
Turbine outlet diameter	80mm
Compression ratio	18.3:1
Number of valves	16
Injection system	Direct injection
Displacement	4.399 litre
Cooling system	Water
Maximum power	74.2 kW @ 2200 rpm
Fuel injection pump	Rotary mechanical
Injection sequence	1-3-4-2

6.2 Test Rig Description

The test rig, as seen in Figure 6.1, consists of two main parts; the JCB 444T2 diesel engine (firing sequence of 1-3-4-2) and AC dynamometer. There is one AE sensor and other instrumentation mounted on the test engine. The charge amplifiers and power supply units are cited in the front of the engine. The outputs from all sensors are sent to the data acquisition system and operating computer. The exhaust noise was reduced by adding exhaust mufflers to the silencer. The load was applied by attaching an AC dynamometer to the engine shaft.

The AE signals are amplified and sent to the AE data acquisition system, whereas the other signals are sent to the CED power 1401 data acquisition system (see Fig. 6.9) and then to the computer, for

analysis and storage. An optical encoder was also fixed to the crankshaft to give a trigger pulse once per revolution in order to synchronise data collection.

6.3 Measuring Equipment and Instrumentation

Figure 6.2 shows the schematic for the test rig and instrumentation used in this work. In addition to the AE measurements made by AE sensor, five different types of transducers have been installed on the test rig to collect data on: combustion pressure in cylinder one (transducer was fixed in cylinder one, because AE sensor was mounted in cylinder one as well), speed, top dead centre position, engine coolant temperature and load. These signals were collected using the following different types of transducers:

1. Optical encoder,
2. Magnetic pickup,
3. Cylinder pressure transducer,
4. Thermocouples, and
5. Torque sensor.

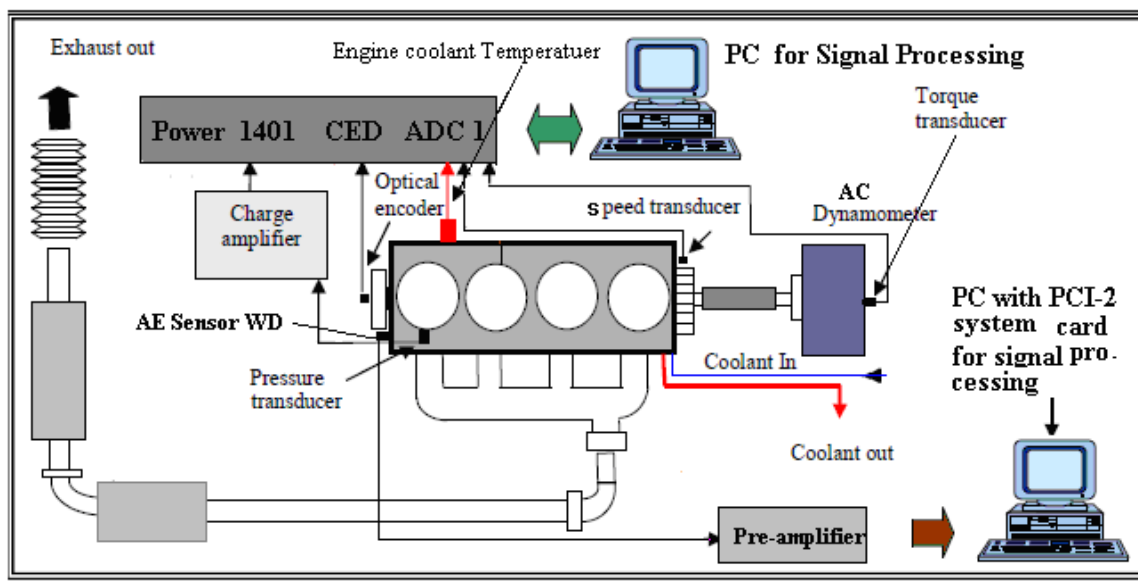


Figure 6.2 Schematic of the engine test system.

Before the pressure sensor signals were fed to the Analogue-to-Digital Converter (ADC), they passed through a B&K type 2635 charge amplifier to condition the signal. The charge amplifier compensates for the reduction in transducer sensitivity due to the use of long cables, filters out

unwanted signal components and amplifies the signal. The charge amplifier also converted the high-impedance output signal into a low-impedance voltage signal.

Speed and load channels were directly fed to a Cambridge Electronic Design (CED) Power 1401 multifunctional data collection interface. This ADC has sixteen 16-bit input channels and sixteen digital I/O ports. Five programmable clocks, clock inputs and event (clock start) connections are also provided for specific applications.

The in-cylinder pressure signal used to monitor combustion conditions was obtained from a Kistler type 6125A piezoelectric pressure sensor from cylinder one as mentioned.

The flywheel TDC trigger signal is used to set the start time of data collection so that each data segment is measured at an exact crank position. This is to ensure accurate time domain averaging and rearrangement of data segments. A second trigger signal, from the flywheel gear encoder, is used to measure engine speed, and from which a given number of pulses were sent out every revolution.

The external load is measured with a torque sensor, which was fixed behind the AC dynamometer.

6.3.1 Optical Encoder

A reference point is required to compare data collected from the test rig, or to time average the signals. This was achieved by using an HED-6000 optical encoder, which is fixed to the crankshaft (in front of engine) as shown in Figure 6.3.

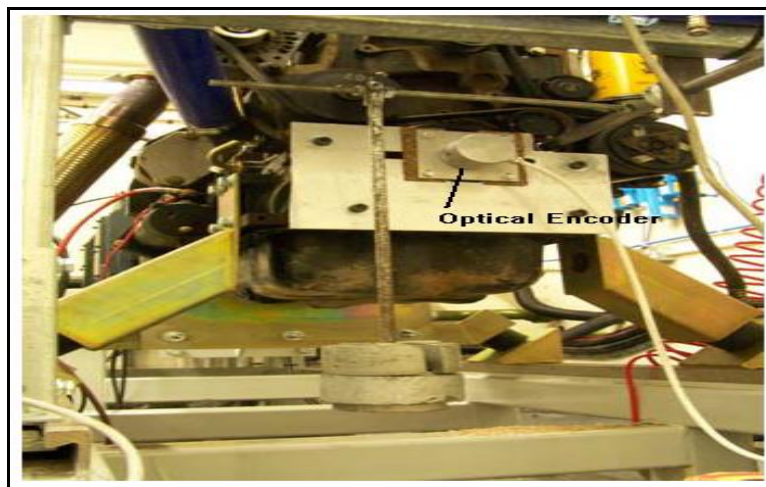


Figure 6.3 Photo of optical encoder in position.

This device consists of a rotating disk, a light source, and a photo detector. The encoder enabled data collection to commence at precisely the same crank angle position in each cycle, and also gave a pulse for each complete rotation of the crankshaft, it allowed time domain averaging to be performed over the same period.

6.3.2 Magnetic Pickup

Engine speed and the number of crankshaft revolutions play a large role in cycle process analysis and in determining engine conditions, so it is important to measure this parameter as accurately as possible. For this measuring task miniature magnetic pick-ups are suitable. This type of sensor consists of a permanent magnet, yoke and coil. A magnetic pick-up is mounted in close proximity to the gear teeth of the engine flywheel because the distance between the gear teeth and the pick-up coil is critical, see Figure 6.4. An electric impulse is produced by the sensor's internal coil every time a gear tooth passes its tip. Since there are 126 teeth on the flywheel, every 126 impulses will indicate one complete revolution of the crankshaft, and the number of teeth detected per second is proportional to the speed of the engine.

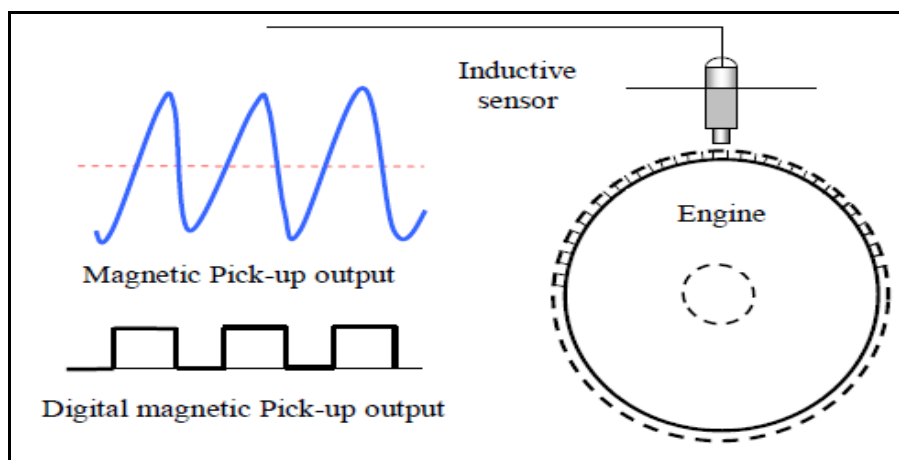


Figure 6.4 AC voltage distribution of magnetic pick-up [16].

The magnetic pick-up sensor acts essentially like a small generator, producing a current as lines of magnetic flux are cut. These magnetic pick-up sensors come in non-powered and external-powered varieties. The two wires to carry the AC voltage are twisted and shielded to prevent electrical interference from disrupting the signal. It is remarkable that these transducers supply a high signal

output in spite of their small size and this has enabled their use where many conventional sensors cannot be fitted. Hence these transducers are used in a wide range of sensing applications.

A RS-4652 magnetic pick-up speed sensor was used to measure the speed of the engine. It was fixed on the engine using a small bracket so that its tip was at a distance of approximately 2 mm from the flywheel.

6.3.3 Cylinder Pressure Sensor

In-cylinder combustion pressure was measured by a Kistler type 6125A piezoelectric pressure sensor, see Figure 6.5. The sensor was fixed in the combustion chamber of cylinder number 1. The sensor is made of polystable quartz elements, and ground insulated to avoid electrical interferences due to ground loops, and does not require additional cooling. It has also been specially designed to work at high temperatures and for precision measurement in internal combustion engines. The specifications of the sensor are summarised in Figure 6.5.


	Parameter	Value
	Pressure range	0 – 25 MPa
	Sensitivity	-15.8 pC/bar
	Linear error	± 0.2 FSO
	Temperature range	-50° up to 350 C°

Figure 6.5 Kistler type 6125 pressure sensor and specification [16].

6.3.4 Temperature Measurement

Temperature measurements were taken in order to monitor the lubricating oil, cooling water, by means of thermocouples installed at the oil sump and cooling water (water way out from the engine). AE data is very dependent upon the engine temperature, and measurement and collection of this data ensured repeatability of measurements (chosen of AE sensor location is very important). Also temperature monitoring ensured the safe operation of the other sensors and the engine itself. The thermocouples used in this test were K-type; see Figure 6.6, with a linear response from -20°C to 220°C .

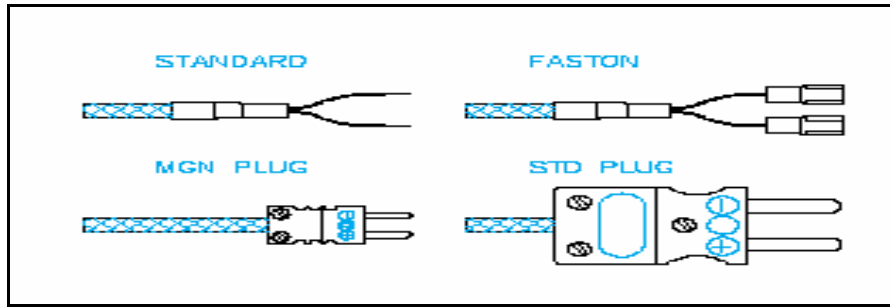


Figure 6.6 K-type, Cr-Al thermocouple.

6.3.5 Torque Sensor

The torque sensor was a force transducer which converted applied force into an electrical signal. A torque sensor type Heidenhain used in this project was attached to the back of the AC dynamometer to measure the load applied by the latter to the engine, see Figure 6.7.



Figure 6.7 Torque transducer in position

6.3.6 Brüel & Kjær Charge Amplifier

The output from the cylinder pressure transducer was connected to a B&K Charge Amplifier Type 2635 to amplify the weak output signal, which gives an output voltage proportional to input charge. This type of amplifier is a comprehensively equipped charge conditioning amplifier intended for different applications, its output can be routed to portable tape recorders and level recorders, electronic voltmeters, measuring amplifiers and frequency analyzers [278]. It can be powered from internal batteries or external DC power supplies, making it useful both in the field and in the

laboratory see Figure 6.8. An overload detector, test oscillator and power supply unit are also included. The overall gain of the type 2635 is adjusted in the input and integrator amplifiers in order to provide a rated output level switchable between 0.1mV/unit and 1V/unit in 10 dB steps. With these nine positions, the output signal level can be adjusted to best utilize the limited dynamic range of tape recorders and to match the various input requirements of recorders, voltmeters and analyzers [278].



Figure 6.8 Face of B&K charge amplifier type 2635 (left), back (right) [278].

6.3.7 Analogue to Digital Converter (ADC)

All the signals collected from the test rig, as explained in previous sections, needed to be converted from the original analogue form to digital. Except for the AE signal this was achieved using a Cambridge Electric Design (CED) Power 1401 ADC interface between the transducers and the computer, see Figure 6.9. The CED Power 1401 is able to record waveform data, digital (event) data and marker information, and can generate waveform and digital output simultaneously for real-time, multi-tasking experimental system using its own processor, clocks and memory, under the control of the host computer. The Power 1401 features a 16-bit internal microprocessor and an on-board memory to facilitate high speed accurate data capture and complex on-line analysis, freeing

valuable time for the host computer to perform other tasks, such as updating the display and writing the data to hard disk.

Technical data of the Power 1401 CED

1. 16 digital input/output channels and 500MHz bandwidth,
2. Rear panel BNC socket for clock inputs and event (clock start) connections,
3. Interface adapters available for PC (ISA or PCI bus), and
4. 5 programmable clocks.



Figure 6.9 Power 1401 CED analogue to digital converter [77].

6.3.8 Software: Lab Windows TM/ CVI Version 5.5

National Instruments Lab Windows / CVI Version 5.5 is an interactive development environment written in the programming language C, to create virtual instrumentation applications [279]. It includes a large set of run-time libraries for instrument control, data acquisition, analysis, and user interface. Building an application in Lab Windows / CVI begins with the user interface, and a graphical user interface (GUI) editor is included. The Lab Windows / CVI development environment contains many measurement specific features that make developing C based measurement applications much easier than in traditional C development environments by, e.g. offering automatic code generation.

6.4 Data Acquisition Software

The data acquisition software is based on a windows operating system and has the ability to perform on-line data sampling, record and monitor engine parameters as it is running, such as speed, load and temperature. The software package has a separate set-up page to allow the user to choose the

required settings such as channel numbers, sampling frequency, data length and filenames. Figure 6.10 shows the set-up window used to select the sampling frequency, channel points and the other important factors and parameters. The sampling frequency is set at 80 kHz. This enables embedded very high frequency band signals (up to about 40 kHz) such as transient pressures and temperatures to be collected. The data length is set at 8192 samples so that one complete combustion cycle (720° crank angle) is included even at the low speed of 1000 rpm. Time Synchronous Averaging (TSA) was used for six segments collected continuously at the same speed and load, and each segment is acquired at exactly the same crank angle as a reference position. Figure 6.11 shows the progress of the data acquisition process. On this screen multiple channels of data are being collected. One of which is cylinder pressure and one channel is coolant temperature.

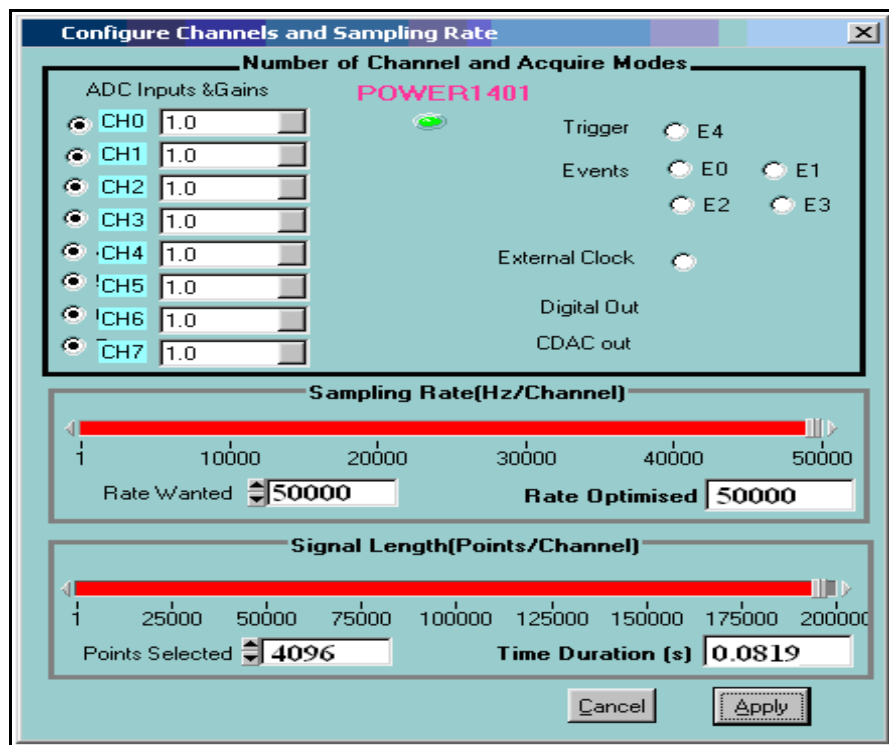


Figure 6.10 Set-up window screen

Other parameters such as speed, load, sampling rate, and data length are automatically saved in binary format to the hard disk. The measured data is analysed offline using the MATLAB package. All the results and figures resulting from the experimental work and discussed in later chapters of this research work were generated directly from the MATLAB environment.

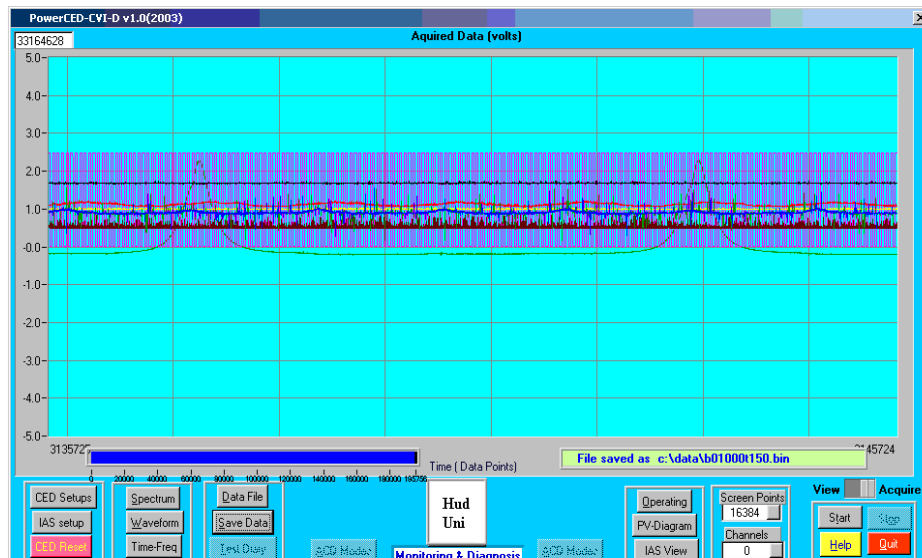


Figure 6.11 Data acquisition in progress.

6.5 Acoustic Emission Measurement and Data Acquisition

AE measurements are based on the use of an AE sensor to convert the motion of a point on a surface generated by elastic waves into an electrical signal in which the variations of voltage mimic identically, or are analogous to, the variations in motion. During AE measurements the operating environment of the engine was noise controlled, e.g. the door was closed (room door) and the other engines in the laboratory switched off to minimise contamination of the AE signal.

AE sensors used for accurate AE measurement need to be sensitive, stable, capable of high temperature operation, have good frequency response and be able to operate over a very wide range of AE levels. To obtain the required accuracy this project used a wideband sensor as this is most commonly used for precision measurement.

6.5.1 Wideband Sensor

The AE sensor used in this research were of the commercially available piezoelectric element type, based on the ceramic, lead zirconate titanate (PZT). These generate small voltages in relation to nanometre amplitudes surface waves and can be manufactured so as to provide different bandwidth responses and sensitivities to suit a variety of applications.

The AE signals were measured using a Physical Acoustics Corporation Wideband sensor model WD as shown in Figure 6.12. This type of sensor has a differential output to decrease the influence of noise. The Wideband sensor was chosen because it has a frequency range suitable for most engine events, good sensitivity, high temperature operation and is of small size.


AE Wideband Sensor Model WD 	Parameter	Value
	Operating frequency range	100 kHz-1000 kHz
	Dimensions (dia x ht) mm/inches	18 x 17 / 0.7 x 0.65
	Operating temperature	-65 to 177 °C

Figure 6.12 PAC WD acoustic emission sensor and specification [280].

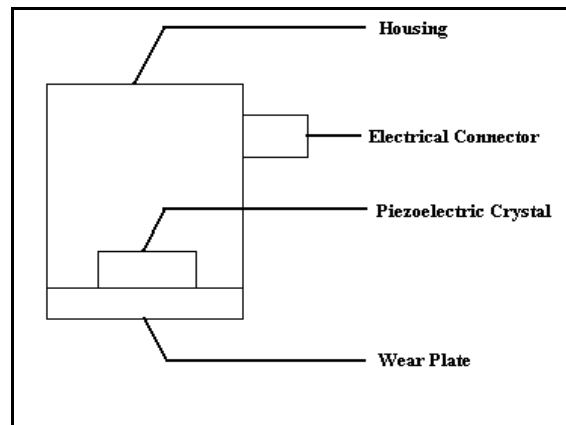


Figure 6.13 Simple diagram of AE sensor.

A schematic diagram of the AE sensor is given in Figure 6.13. Essentially it consists of a crystal which is housed in an appropriate enclosure with a wear plate and a connector. The sensor moves due to the stress wave impinging on its face, and it delivers an electrical signal to a preamplifier. The preamplifier can be fixed inside the sensor enclosure to prevent signal loss. To ensure good transmission of the AE signal, a thin layer of high vacuum grease was applied between the sensor face plate and the holder surface.

6.5.2 AE pre-amplifier

Amplification of the raw AE signals were generally provided by a PAC model 2/4/6 preamplifier chosen for maximum compatibility to get best results. This type of preamplifier can work with either a single ended or differential sensor, and provide 20, 40 or 60 dB gain and also band-pass filtering within the range 100 to 1000 kHz. The power is supplied using the output signal BNC. Figure 6.14 shows the pre-amplifier and its specifications.

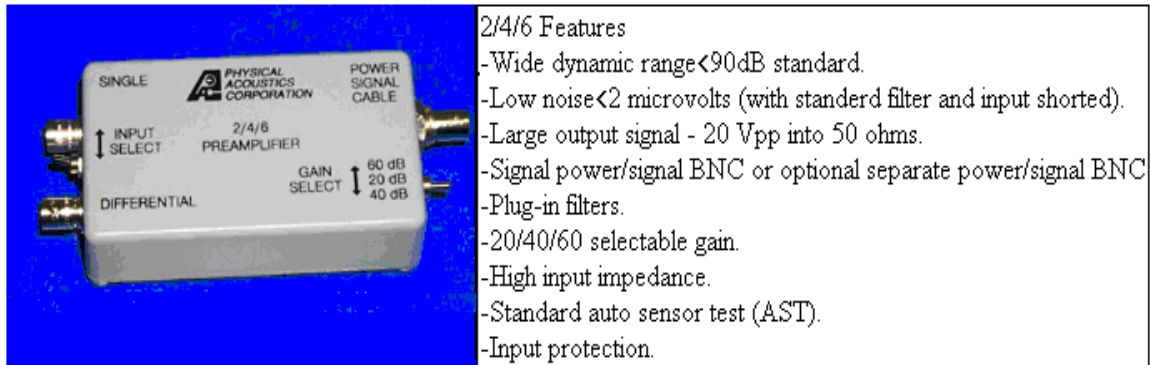


Figure 6.14 PAC model 2/4/6 pre-amplifier and specification.

6.5.3 AE Data Acquisition System

The typical frequency of AEs is in the range of 100 kHz – 1MHz. The recent development of data-streaming methods makes it possible to continuously sample and save such high frequency signals. Data streaming is able to maintain a steady high-speed data flow within a computer so that the data can be transferred to a storage medium continuously using such devices as the PAC PCI-2 board, shown in Figure 6.15. This board is connected to the computer through an industry standard high-speed (138MB/sec) PCI bus and the sampled AE waveforms can be continuously transferred to the hard disk up to the capacity of the hard disk.

The AE measurement system developed in this research is based on the PAC PCI-2 card, which was specially designed for high-speed data acquisition of AE signals.

The stored data can be shown on screen and characterised using all of the waveform features and statistical parameters discussed in Section 4.5.2, or processed using advanced digital computing methods in MATLAB through the interface software developed by this author. All the AE signals presented in the following chapters were processed using the software developed in MATLAB.

Figure 6.16 shows the progress of the AE data acquisition process. In this screen two channels of data are being collected. The sampling rate and length are automatically saved. The data files are saved in binary format to the hard disk. The measured data is analysed offline using MATRLAB package.

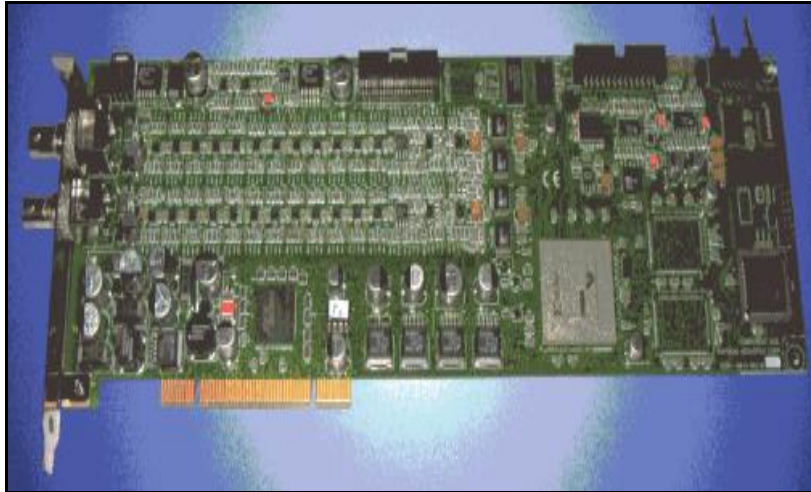


Figure 6.15 PCI-2 AE system card [280].

The system has two AE channels and two parametric channels with 16-bit A/D converters.

For the AE channels, as shown in Figure 6.17, the PCI-2 card provides selectable anti-aliasing filter circuitry with 4 high pass filter selections (1 kHz, 20 kHz, 100 kHz and 200 kHz) and 6 low pass filter selections (100 kHz, 200 kHz, 400 kHz, 1 M Hz, 2 MHz and 3 MHz) allowing the configuration of different filter strategies. The data-streaming function enables AE waveforms to be recorded on the hard disk of the computer continuously at a rate of up to 10 M samples/sec.

The first parametric channel can be connected directly with the output of sensor and can provide measurement configurations such as gain control, offset control and filtering options. The second parametric channel only provides a straight +/- 10 volt input for conditioned sensor output. The sampling rate for these two parametric channels can reach up to 10,000 readings/ sec.

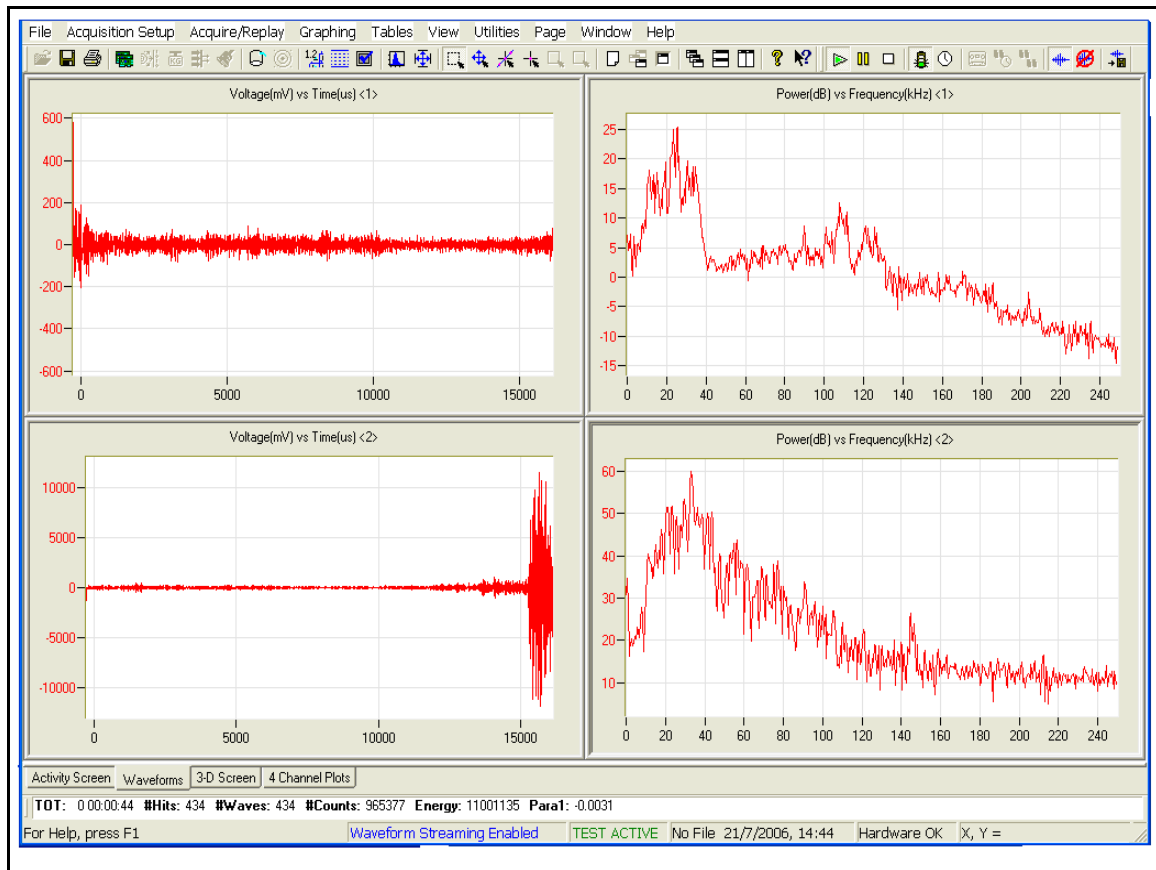


Figure 6.16 AE data acquisition system in progress.

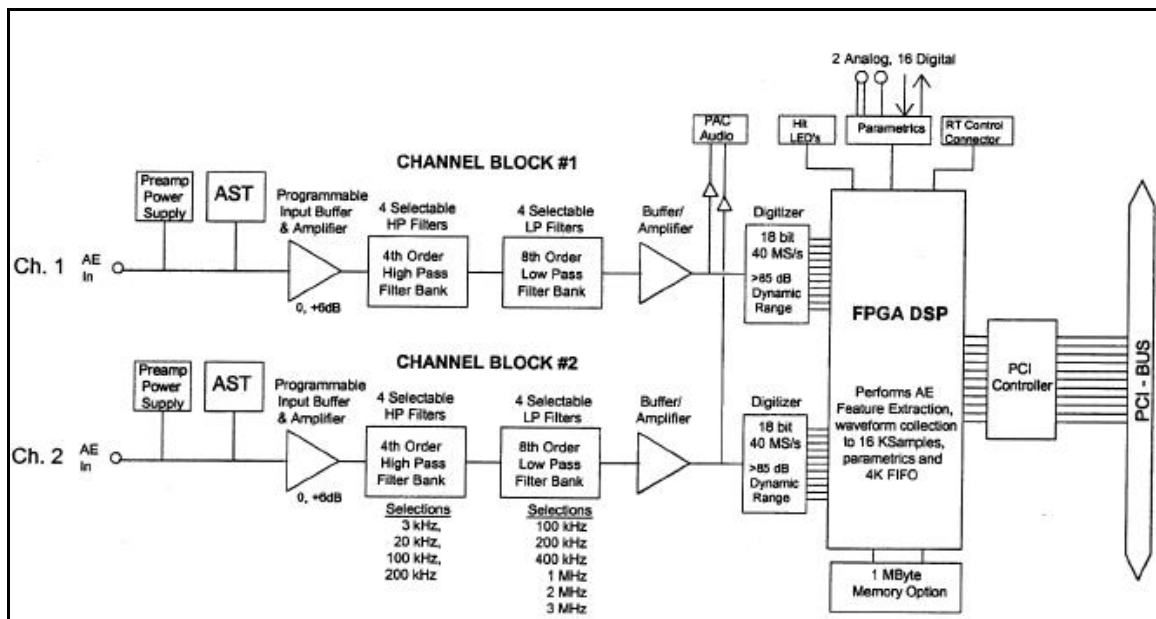


Figure 6.17 PAC PCI-2 block diagram [280]

6.6 Test Procedures and Fault Simulation

Two types of faults were simulated and seeded into the engine. The engine was tested at two speeds (1000 and 2000 rpm) and four different loads, which will see in the following chapters. Data were collected from the engine while it was running under these faulty conditions, these faults were:

1. Injector related faults, such as injection pressure reduction, injection pressure increase and injector disconnected (full misfire).
2. Lubricating oil related faults such as friction, piston slap and changes in viscosity.

6.6.1 Test Procedure

Before starting the engine, to avoid health risks the ventilation system should be checked to determine it was working properly. This system works by sucking-up the exhaust emission of the engine and taking it outside the laboratory (engine room). The valves for the fuel, the cooling water for the engine, and the dynamometer were also opened manually before starting the engine. The emergency engine switch-off is fixed on the control panel. The oil supply indicator was checked to ensure a suitable and adequate oil supply during test. The engine temperature was checked periodically to ensure it never exceeded 90°C .

The key objective for this study was to acquire real data from the test rig and to develop an understanding of how to apply signal processing methods to AE data for diesel engine CM. First the engine was tested under different loads: zero Nm, 50 Nm, 100 Nm and 150 Nm, and at speeds of 1000 rpm and 2000 rpm. In these tests one AE sensor was fixed inside the holder and the holder mounted on the cylinder head of the engine by ceramic glue (for injector fault) and the holder mounted (sensor inside the holder) on the cylinder block for lubricating oil condition monitoring. High vacuum grease was applied between the sensor and holder to give good signal conductivity between them.

6.6.2 Injector System

The fuel injection system is possibly the most important part of a diesel engine, and faults in the fuel injectors causes many engine failures which is why it was decided to seed faults into the fuel injectors. Not only is the injector responsible for delivering the right quantity of fuel to the cylinders, but this fuel must be delivered at the right time and at the right rate. In addition to this, the fuel must be finely atomised and effectively distributed throughout the cylinder to allow the complete combustion of the air and fuel.

There is one injector for each cylinder of the engine; this injector is fixed inside the cylinder head. The introduction of fuel into the combustion chamber in a finely atomised spray is controlled by the injector.

The internal components of the injector were accessible and these can be seen in Figure 6.18. From left to right the figure shows the nozzle tip, the check valve stop, the check valve spring, the washer assembly and the injector body.



Figure 6.18 Components of a diesel injector.

One of the most important factors affecting the condition of the injection process is the fuel breaking pressure. Any change in the fuel breaking pressure will change the injection time and therefore affect the combustion process and degrade engine performance. In this work, the injector breaking pressure was decreased by reducing washer thickness, see Figure 6.18 (a thinner washer assembly was created) so that more fuel was injected; as a consequence the injector breaking pressure was reduced from 270 to 235 bar (as a result, earlier injection was expected) and by increasing the thickness of washer (a thicker washer assembly was created) the injector will inject less fuel and the start of injection will be later (breaking pressure was increased from 270 to 325 bar).

The last seeded fault was to disconnect the fuel injector from the fuel line (full misfire), this means that air will be compressed and injected into the chamber without any fuel, which means that there will be no combustion. Figure 6.19 shows the fuel pipe disconnected from the injector and the pipe

connected to fuel container to avoid fuel spillage in the room. For comparison a set of experimental data was collected using a healthy condition injector at 1000 rpm and different loads.



Figure 6.19 Arrangement for total misfire.

6.6.3 Lubrication Oil Faults

The lubrication system is one of the most important part of a diesel engine, and problems in the lubricants causes many different engine failures (wear, cylinder, crankshaft, bearing etc.), which is why it was decided to study lubricating oil condition and quality. The data expected from oil analysis is dependent upon many factors. Primarily, the size of the engine will affect the data.

Viscosity is one of the most important oil properties, which determines whether the lubrication oil can still effectively lubricate at operating temperatures. Viscosity is directly relates to the condition of the lubrication oil, as the measure of how viscous the oil is relates to how well the oil can maintain its lubricating properties in the cylinder and outer parts under high temperature and pressure. High or low viscosity can also indicate further problems, where high viscosity could suggest high particulate load, or that the oil level is no less important, would indicate that, if too low, this can cause significant problems often resulting in engine failure (increase friction, wear etc.). Depending on the environment in which the engine operates. Also if the oil level is too high, this can make many different problems such abnormal running.

6.7 Test Rig Recorded Data

6.7.1 Angular-Domain Display

The measured amplitude of the signals from the healthy engine was displayed in the angular-domain. Angular-domain analysis was expected to reveal the overall signal amplitude and cyclic features, while frequency-domain analysis gave spectral information of the AE. These methods were applied to study the AE generation mechanisms and to give the individual features of the sources.

Figure 6.20 shows the AE waveform recorded in a laboratory environment without any special consideration or precautions. It displays the raw AE time-domain signal acquired from one working cycle (two complete revolutions) of the engine as a function of crank angle at engine speed of 1000 rpm with no load. The mechanical events corresponding to crank angle are shown along the bottom of the figure. IV and EV refer to intake and exhaust valves respectively, 1, 2, 3 and 4 refer to the cylinders and INJ refers to the injector.

The main feature extracted from the AE waveform shown in Figure 6.20 is that it exhibits four peaks corresponding to the engine firing sequence and each peak is caused by combustion in one of the cylinders of the engine, from left to right, cylinders 1, 3, 4, and 2. The waveform consists of numerous frequency components superimposed on each other due to the numerous AE sources.

The thin vertical lines indicate TDC for each cylinder in the order they fire: 1-3-4-2. As can be seen from Figure 6.20, the largest AE signals are associated with injection events and occur just after TDC for each cylinder. Smaller amplitude events are also associated with exhaust valves opening. The highest AE amplitudes are, as would be expected, observed for the cylinder closest to the sensor, since the magnitude of the signal will decrease with distance from sensor. Thus the highest amplitude signal detected by the AE sensor is, as can be seen from the figure, due to events occurring in cylinder one. This is because the sensor is mounted closest to cylinder one.

The major mechanical events in the engine cylinder head are injection, fluid excitation, exhaust valve opening and its mechanical impacts (impact between valves and seats, injector needle impact and rocker arm with valve stem impact).

Figure 6.20 shows that the dominant event follows the fuel injection and that exhaust valve closing is the most significant valve event, which is associated with the engine exhaust valve and differs from those associated with the intake valve. The intake valve movement involves lower kinetic

energy and the pressure differences across it might be expected to generate lower inherent signal energy, and this almost certainly explains the non-appearance of clear AE events for the exhaust valve closing (EVC).

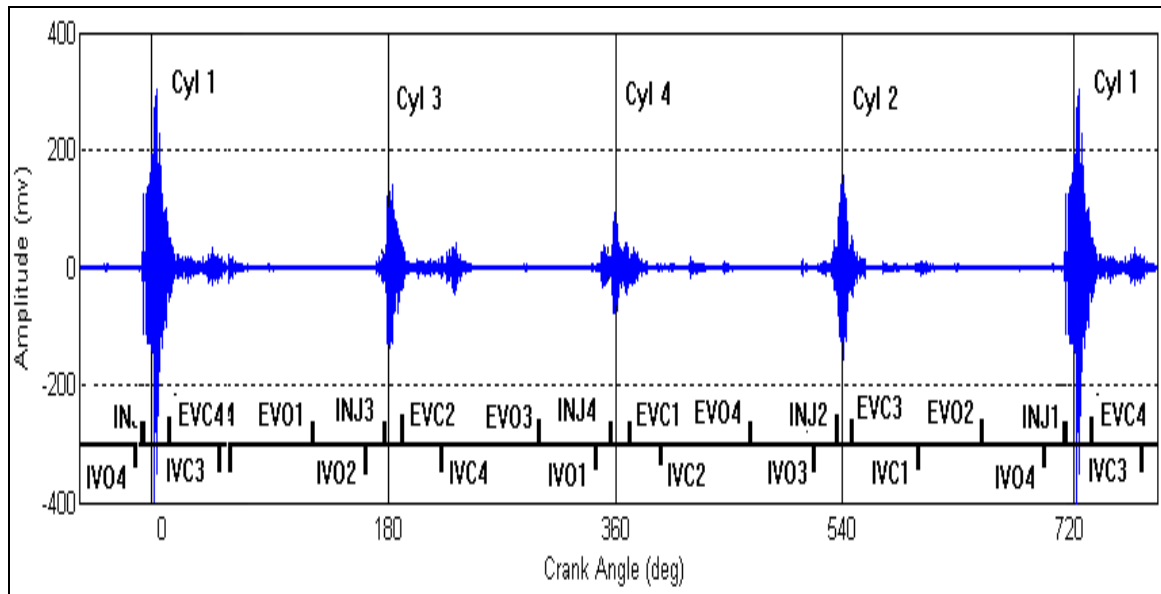


Figure 6.20 Raw AE signal in angular-domain from engine running at zero load and speed of 1000 rpm

The injector events for each cylinder occur at crank angles of around 0° , 180° , 360° and 540° , consistent with the firing order of 1-3-4-2. However, it is possible that the valve events include a number of related events associated with impacts of the rocker arm with the push rod or valve stem. It is also evident in the AE data that the actual timing of events can be slightly different. The difference in energy between cycles - e.g. the kinetic energy between the two potential impact points at push rod and valve stem - is relatively random, depending on exactly the position of the rocker from the previous cycle. There are also apparent inconsistencies between cycles, e.g. the exhaust valve opening events show differences between the various running conditions. This is due to the exhaust valve opening energy changing with the force the hot products of combustion exert on the face of the valve, an effect whose magnitude will depend on running conditions.

6.7.2 Frequency-Domain Display

Frequency-domain analysis gives spectral information of AE signals by transforming them from the time-domain to the frequency-domain. The common, obvious characteristics in the spectrum of AE signals are the firing frequency and its harmonics.

Here the recorded AE data is plotted as amplitude of AE response against frequency, and the constancy between AE and engine load should be more distinct than in the angular-domain. The demonstration in the frequency-domain is frequently more important because the frequency rates of AE and their relationship to the dynamic features of a system are clearer, as mentioned previously in section (4.4.2.2). The frequency spectrum or frequency domain can be achieved by using the digital Fast Fourier transform of the time waveform.

Figure 6.21 shows the spectrum of the raw AE data at 1000 rpm with no load and we can see the first peak in the AE spectrum occurs at a frequency of about 20.0 kHz. It is also clear there is a single main peak in the spectrum extending from about 10 kHz to about 40 kHz. This is somewhat surprising, given the frequency response of the sensor, and confirms the importance of the peak.

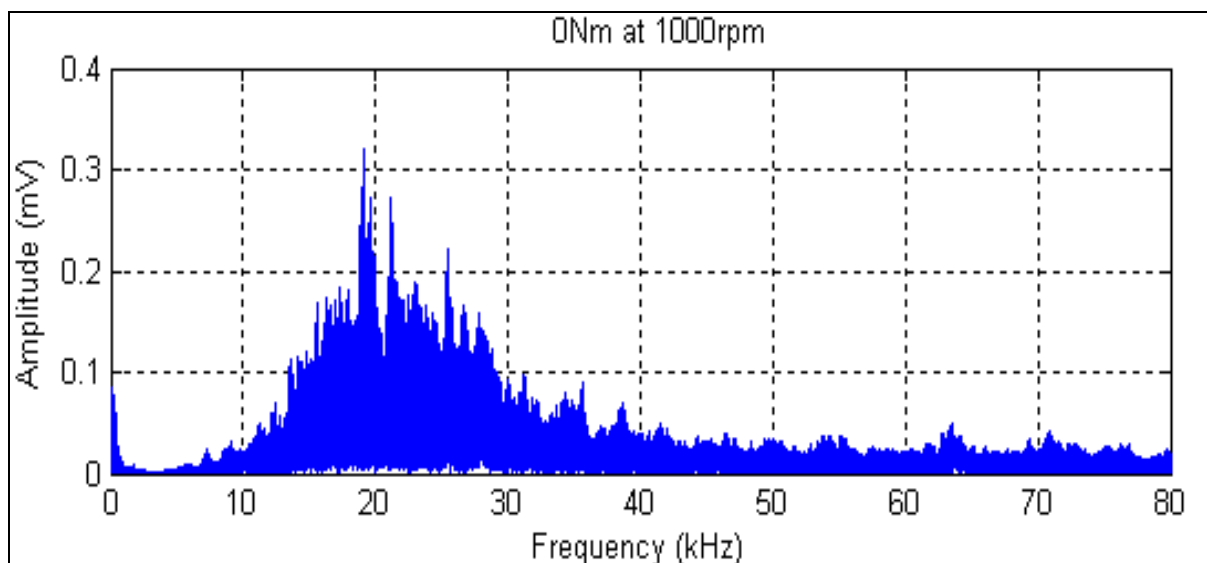


Figure 6.21 Frequency spectrum of raw AE signal from engine running at 1000 rpm with no load

As can be seen from the Figure 6.21, there are two main frequency bands, low and high (below and above 40 kHz). The low frequency band is generally continuous and dominates the signals, and is

thought to be associated with the mechanical activity of moving parts around the cylinder head. The higher frequency components can be measured around TDC for each cylinder.

These components are thought to be associated with fluid flow, including fuel flow in the injectors and gas flow over the valves. Fog et al [58] and El Ghamry et al [59] observed that the high frequency components in AE signals appear to be associated with fluid-flow activity for a number of sources such as exhaust valve leakage on a two-stroke large marine diesel engine and a cylinder head gasket leak on a four-stroke, high-speed diesel engine respectively. Also gas flow across turbine is very important source of AE.

6.7.3 Angular-Frequency Domain Display

Conventional spectral analysis using statistical parameters and Fourier transforms for the study of periodic, stationary and deterministic signals cannot accommodate the temporal variation of the spectral characteristics of a non-stationary signal.

The Fourier transform does not take time information into account, it simply identifies all frequencies contained in the signal, but it does not provide information regarding the time when those spectral components are present and when they are not. The Fourier transform is not a suitable technique for non-stationary signals, and transient signals which are important in diesel engines are, by their nature, normally highly non-stationary,

In order to accurately represent the frequency information contained in non-stationary signals, a technique that presents both time and frequency information needs to be used, producing a signal spectrum in the time-frequency domain.

Angular-frequency analysis is a signal processing method that makes it possible to see both the time and frequency information at the same time. It displays the combined results from time and frequency analyses in a three-dimensional way which plots the amplitudes against time and frequency axes as shown in Figure 6.22.

Using this technique to analyse AE signals generated by a diesel engine enables us to link every event observed in the time-frequency plane to a single excitation source. It is then possible to measure the energy of each event and to quantify the part each excitation mechanism plays in the AE signals measured on the surfaces of the engine.

To describe this temporal variation of engine AE signals, an evolving spectral analysis must be performed by using time-frequency methods. Such methods are a good tool for describing the spectral contents of transient signals as a function of time: they enable several patterns superimposed in time and/or in frequency, within the same transient signal, to be located and separated in the time-frequency plane [281].

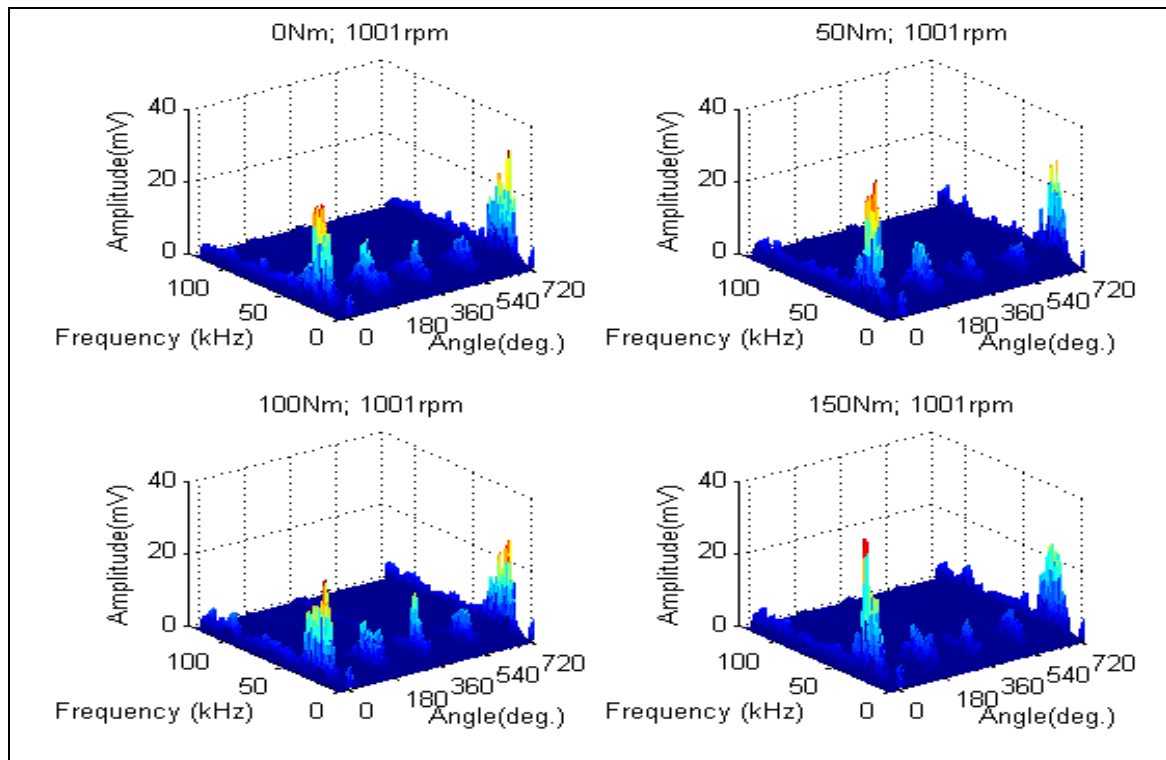


Figure 6.22 Time-frequency domain of raw AE signal from engine running at 1000 rpm with four different loads: 0 Nm, 50 Nm, 100 Nm and 150 Nm.

Time-frequency analysis of such signals should make it possible to separate the responses associated with each source of excitation and consequently lead to a better understanding of, for example, the mechanisms of combustion, associated shocks and the transmission of resulting AE signals to the external structure of the engine.

An efficient time-frequency method should allow us to:

1. Locate at each point of the structure the responses inherent to each source of excitation,
2. Analyse the frequencies associated with each source of excitation, and

3. Measure the contribution of each source of excitation in terms of energy.

This should make it possible to quantify the contribution of generated AE signals from each of the sources.

The time-frequency method is very useful in that most engine AE signals are related to events such as combustion and valve operations which have fixed occurrence times determined by the crank mechanism. By performing time-frequency analysis these events can be identified according to their occurrence in both time and frequency [281].

The most common current method for obtaining the time-frequency distribution is the short-time Fourier transform (STFT). The STFT is a linear time-frequency transformation which maps a signal onto the time-frequency (scale) plane and is sensitive to transient signals. The STFT used in this work processes a signal by decomposing the signal into short blocks (or windows) and computing the spectrum of each block. Different types of windows can be used to reduce spectral leakage, but usually a Gaussian window is used. It is common to have a certain overlap of blocks to reduce information loss due the window function.

For the AE engine, angle frequency analysis in which time is replaced by the crank angle is more useful and has been used in this study. Figure 6.22 shows the AE waveform of the diesel engine in the joint angle-frequency domain for an engine speed of 1000 rpm and four different loads (0 Nm, 50 Nm, 100 Nm, and 150 Nm). From the STFT representation we can clearly see four peaks representing the combustion events of the engine cylinders in the firing order from left to right (1, 3, 4, 2 and 1).

In the angular -frequency spectrum with no load shown in Figure 6.22, a large AE peak occurs at crank angles integer-multiples of 180 degrees, when the piston of each cylinder reaches TDC and immediately afterward during combustion. The AE levels at these angles are significantly larger in the 20 to 50 kHz frequency domain and last for about 10 degrees especially for cylinders 3 and 4, which is temporal stretching due to transmission distance. Lower frequency AE components, due probably to the motion of the pistons and other moving parts, are present and discernible particularly away from TDC positions and reach a maximum frequency around 50 kHz. It is expected that an increase of crankshaft and piston bearing gaps particularly affect these lower AE events. The spectrum analysis shows that the major part of the energy is located in the lower

frequencies (below 50 kHz), this can be seen more clearly in the STFT representation, and also we can see that the peak of the STFT extends to a low frequency range. The heights of the combustion peaks are proportional to the engine load and confirming that the engine AE signals are load dependent.

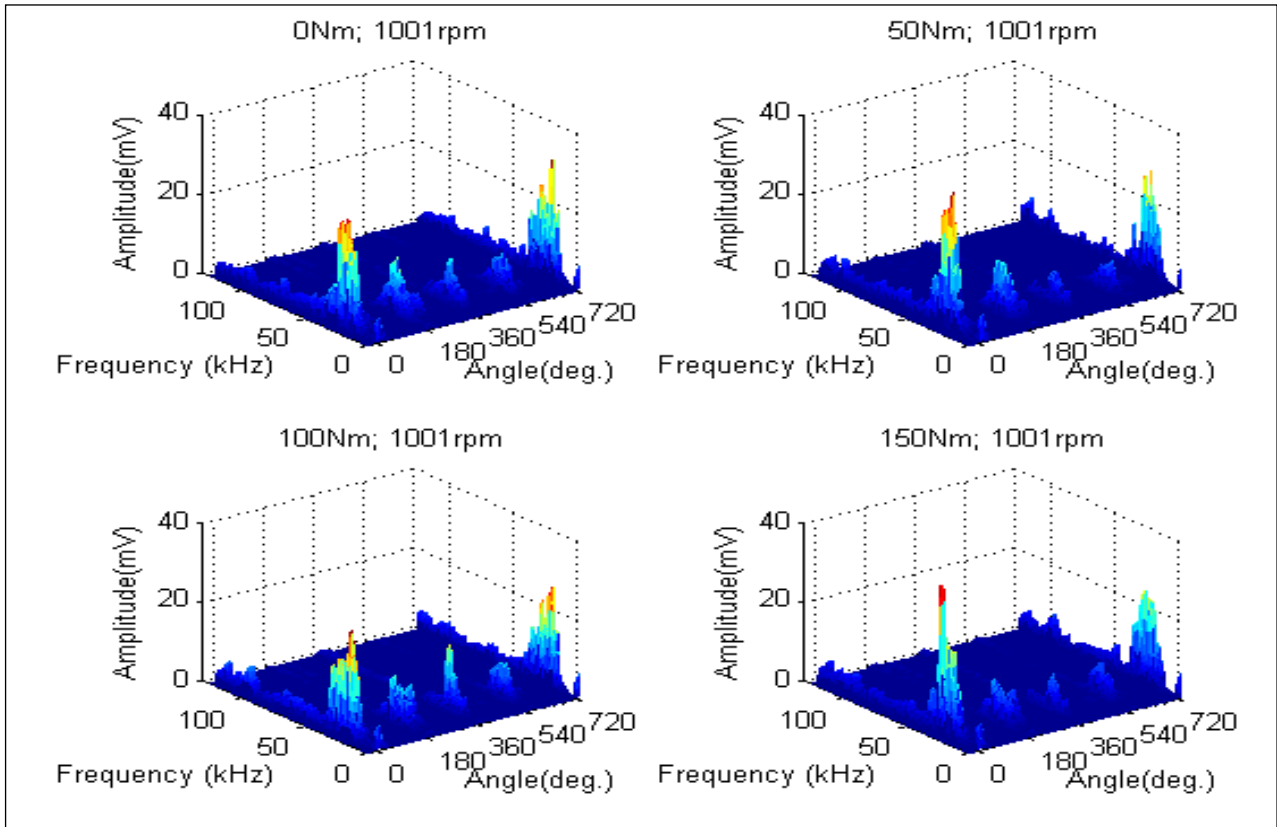


Figure 6.23 Time-frequency domain of raw AE signal from engine running at 1000 rpm with four different loads: 0 Nm, 50 Nm, 100 Nm and 150 Nm (zoomed).

CHAPTER SEVEN

DIESEL ENGINE FUNDAMENTAL ACOUSTIC EMISSION CHARACTERISTICS

This chapter investigates the fundamental characteristics of diesel engine acoustic emission signals, using time-domain, frequency-domain, and other statistical analyses of AE data. Acoustic emission signals for a range of loads and speeds are considered in order to provide a baseline for normal engine characteristics.

Firstly, time-domain characteristic techniques are discussed. Secondly, the power spectrum of the engine AE signal is investigated. Thirdly, statistical parameters are used for detecting and diagnosing simulated faults. An analysis of a number of measured parameters from the engine test rig is then undertaken for the purposes of detecting, diagnosing and assessing the severity of the seeded faults described in Chapter Six: changes in injection pressure and changes in lubricant viscosity, level and temperature.

7.1 Introduction

Research into the AE generated from diesel engines, where the AE stress waves are in the ultrasound region (from 20 kHz up to several gigahertz), is now being undertaken by investigators in a number of UK universities. Work in this field has led to many experimental and theoretical studies into the relationship between engine generated AE and other parameters such as engine type, speed, load and combustion system [1, 6]. The studies tend to focus on the characteristics of the AE wave transmission path. Investigations on many diesel engines of widely varying types and designs have shown that the AE event generated by combustion represents a considerable part of the overall AE events, and the combustion event is highly dependent on the cylinder pressure and rate of change of pressure in the combustion chamber [246].

AE signals can also be characterised by calculating certain statistical parameters such as mean value, standard deviation, skewness and kurtosis or can be further processed to obtain the probability density function and correlation function. In the case of diesel engine AE signal analysis, the correlation function allows the contribution of the combustion event to the total AE level to be calculated.

7.2 Combustion Pressure Event

The pressure in the combustion chamber of a diesel engine has been extensively studied, primarily from the point of view of monitoring engine operating performance, but in recent years there has also been interest in the combustion event and consequent high-frequency AE within the diesel engine.

A typical pressure-crank angle curve for the cylinder pressure in the JCB diesel engine used in this work is shown in Figure 7.1. If the combustion does not occur, then the pressure rises and falls as shown by the curve 'Without firing'. If fuel is injected slightly before top dead centre (TDC), then, after a small delay period, there is rapid combustion during which the pressure quickly rises to a maximum and then falls see curves 'Firing'. The pressure – crank angle waveform is similar for all curves measured, whether on full load, part load or no load and with or without firing. The extra area under the firing curve is a measure of the work done in the cylinder during the combustion stroke.

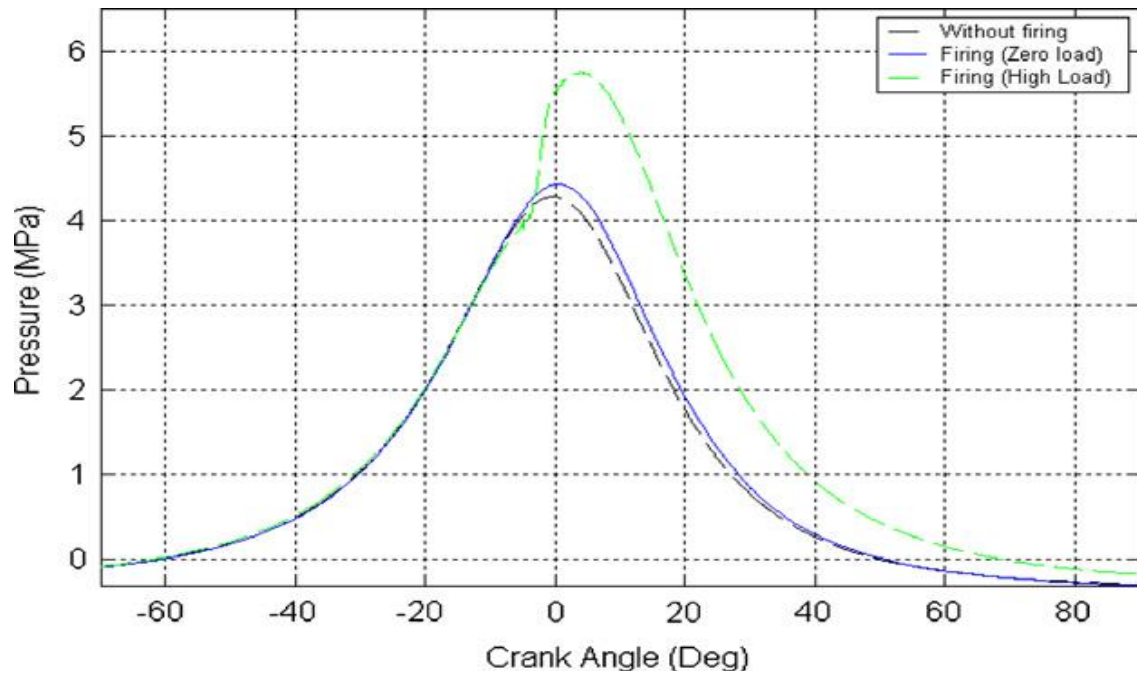


Figure 7.1 Diagram of cylinder pressure vs. crank angle ($0^\circ = \text{TDC}$).

The rapid rise in pressure generates high-frequency components in the excitation force, as shown in Figure 7.2. This figure shows a clear increase in amplitude of the frequency components of excitation above about 250 Hz, when combustion takes place.

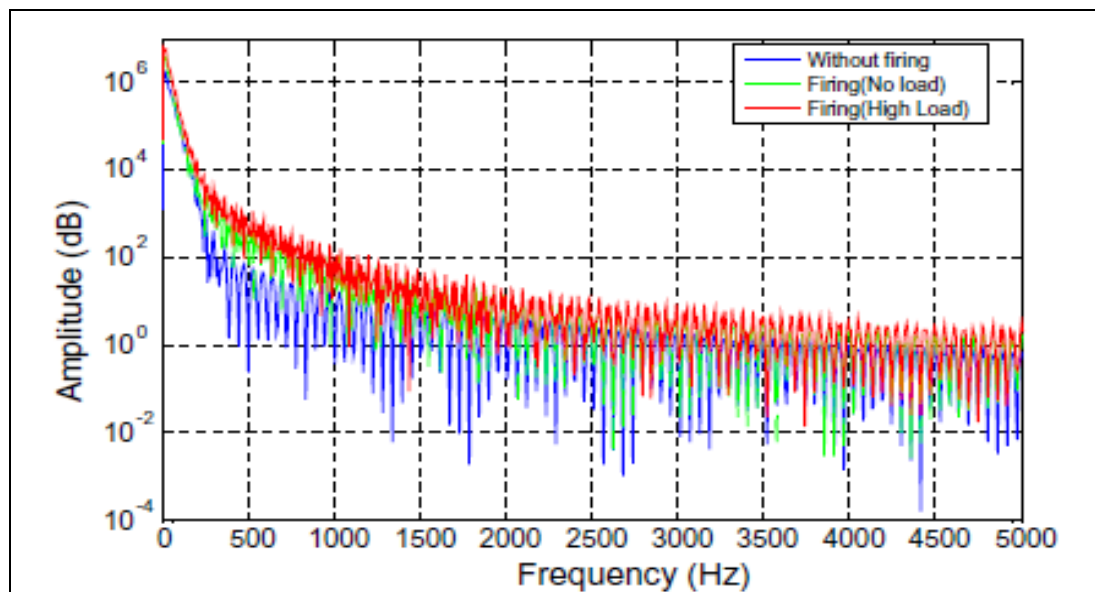


Figure 7.2 Spectrum of cylinder pressure.

Clearly, these high frequency components contain information about the combustion process, particularly its onset and rate of rise. The spectrum of the cylinder pressure initially drops off rapidly, about 45dB per octave, and thus contains little high-frequency energy. The shape of the cylinder pressure curve is similar whether there is firing with no load, some load or high load, the difference being the brief period of rapid pressure rise due to combustion, thus it can be inferred that the increase in high-frequency (above 250 Hz) energy when combustion takes place is due to this rapid increase in pressure when the piston is approaching TDC, after the fuel has been injected.

7.3 Diesel Engine Acoustic Emission Waveform

The output of the AE sensor mounted on the front of the cylinder head (close to cylinder one) of the test engine running at an average speed of 1000 rpm and with no load is shown in Figure 7.3(a). Because the AE waveform was recorded in a laboratory environment without any special considerations or precautions, the higher resonance frequencies were removed by low pass digital filtering [282].

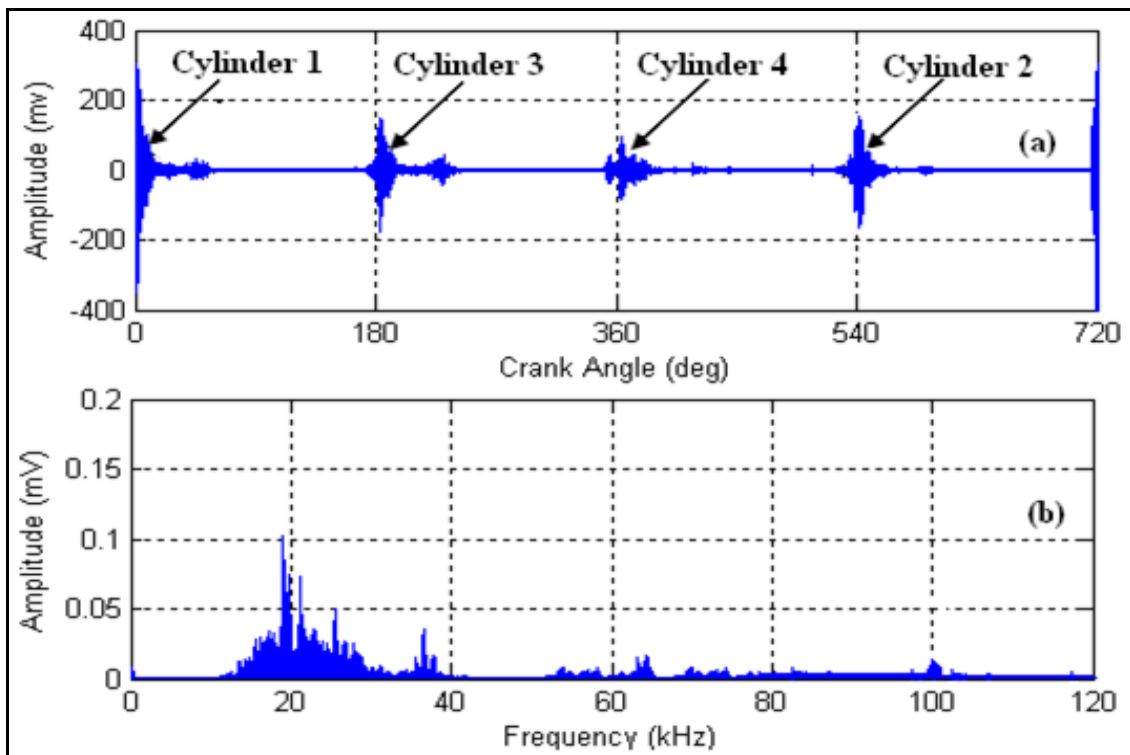


Figure 7.3 Acoustic emission waveform and power spectrum of the diesel engine, AE sensor mounted on the front side of cylinder head (close to cylinder No: 1)

The main feature that could be observed from the acoustic emission waveform are shown in Figure 7.3(a), is the four peaks corresponding to the engine firing sequence and these represent combustion events in the cylinders 1,3,4 and 2 respectively. What makes the waveform complicated and difficult to extract information from is the numerous frequency components superimposed on each other.

In the associated power spectrum, shown in Figure 7.3(b), four peaks can be seen; the first at approximately 19 kHz, the second at approximately 37 kHz, the third at approximately 65 kHz and the fourth at about 100 kHz. The amplitudes of any higher harmonics can be ignored because they contain considerably less energy than the first four leading terms.

As would be expected, the first peak is due to the combustion process and its amplitude is highly dependent on the combustion conditions and the associated peaks to the first peak may be due to gear timing mechanisms. The second peak (37 kHz) is probably due to the closing impact of the valves, which occur twice per crankshaft revolution, every second revolution in each cylinder. By increasing the load the amplitude of both these peaks increases, see Figure 7.4. The third peak at 65 kHz corresponds to the third harmonic of the peak combustion frequency, also increases in amplitude at higher loads. It has been shown that the peaks at 65 and 100 kHz are due to the AE events in cylinder head and may be due to valves impact events or fuel injection [238].

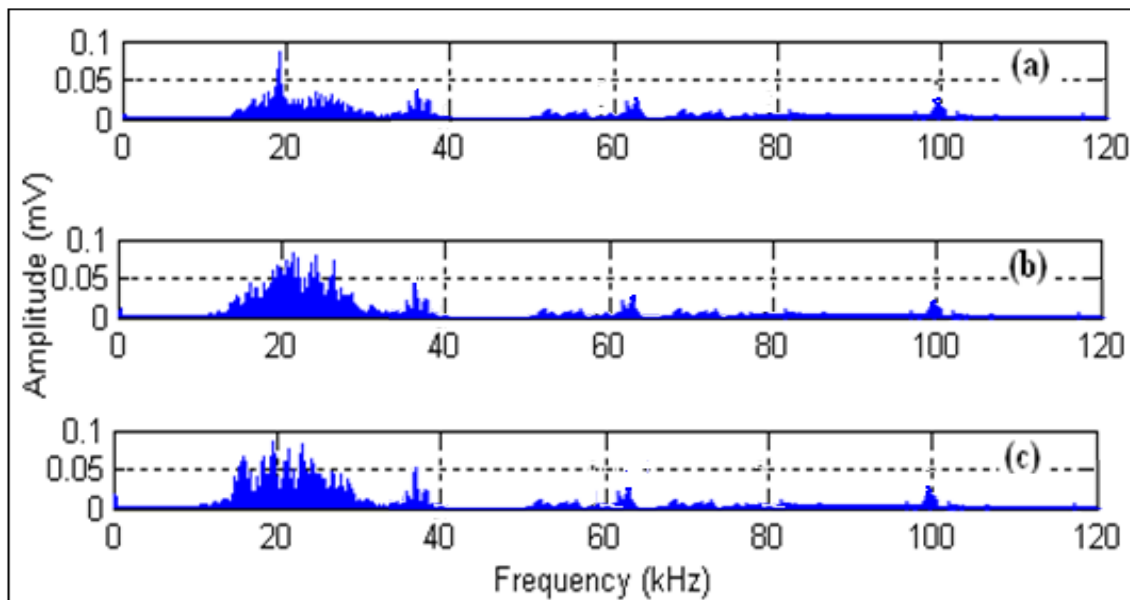


Figure 7.4 AE waveform power spectra of the diesel engine at loads of (a) 50 Nm, (b) 100 Nm, and (c) 150 Nm.

7.3.1 Effect of Operating Conditions on the AE Signal

Each cylinder experiences fuel injection and combustion once for every two complete revolutions of the crankshaft. Thus the number of ‘combustions’ per single revolution of the camshaft will be equal to (number of cylinders)/2. Here there are four cylinders, so there will be two combustion processes during each complete revolution of the camshaft, and the corresponding AE occurrence for 1000 rpm will be at twice the fundamental frequency.

This section reports on how varying the engine rig speed and load affect the characteristics of the AE signals. The engine rig was operated at two speeds, 1000 and 2000 rpm under no load. A Matlab code was written to show the measured AE signal in terms of both the time-domain (expressed as crank angle), and frequency-domain.

Figure 7.5 shows angular domain histories at both speeds with their associated spectra. It can be observed that the amplitudes of the angular-domain wave forms increase as the speed increases. In the frequency domain the amplitude of the peaks also increases with increasing speed. It seems that the peaks stay in much the same places, but the relative amplitudes change. The peak at 19 kHz does not move but it remains at 19 kHz at both 1000 rpm and 2000 rpm. However the peak at about 25 kHz gets a lot bigger at 2000 rpm than at 1000 rpm and dominates the spectrum.

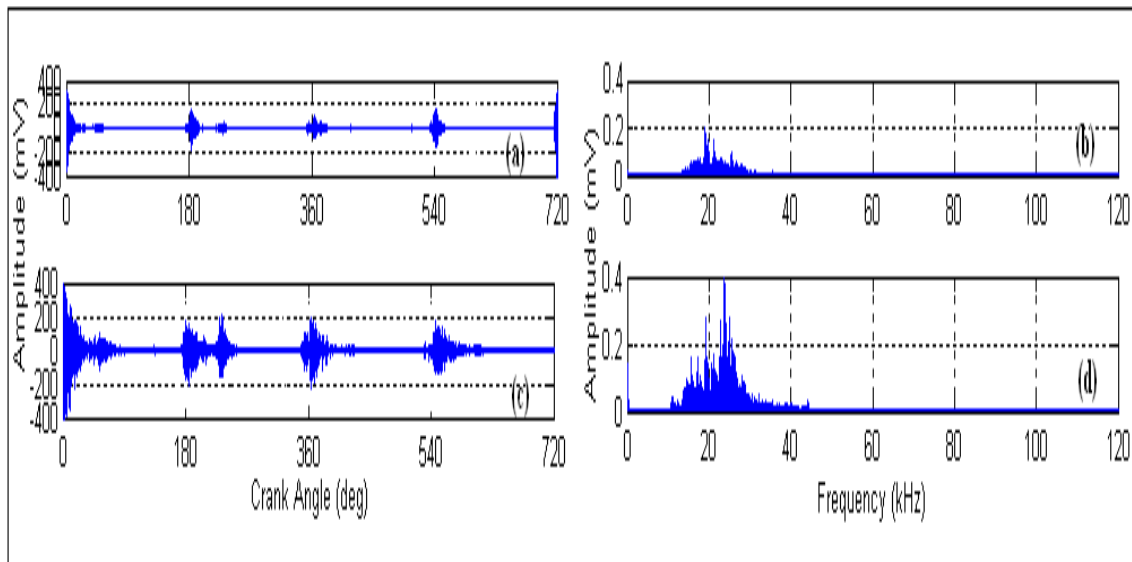


Figure 7.5 Angular domain and frequency domain, respectively, of the AE signal from a diesel engine for engine speeds of (a) 1000 rpm; (b) 1000 rpm power spectrum; (c) 2000 rpm; (d) 2000 rpm power spectrum.

To gain a better understanding of the speed effects, Figure 7.6(a) shows the signals for the two speeds, superimposed on each other. The corresponding AE frequency domain representations are shown in Figure 7.6 (b) and (c) respectively.

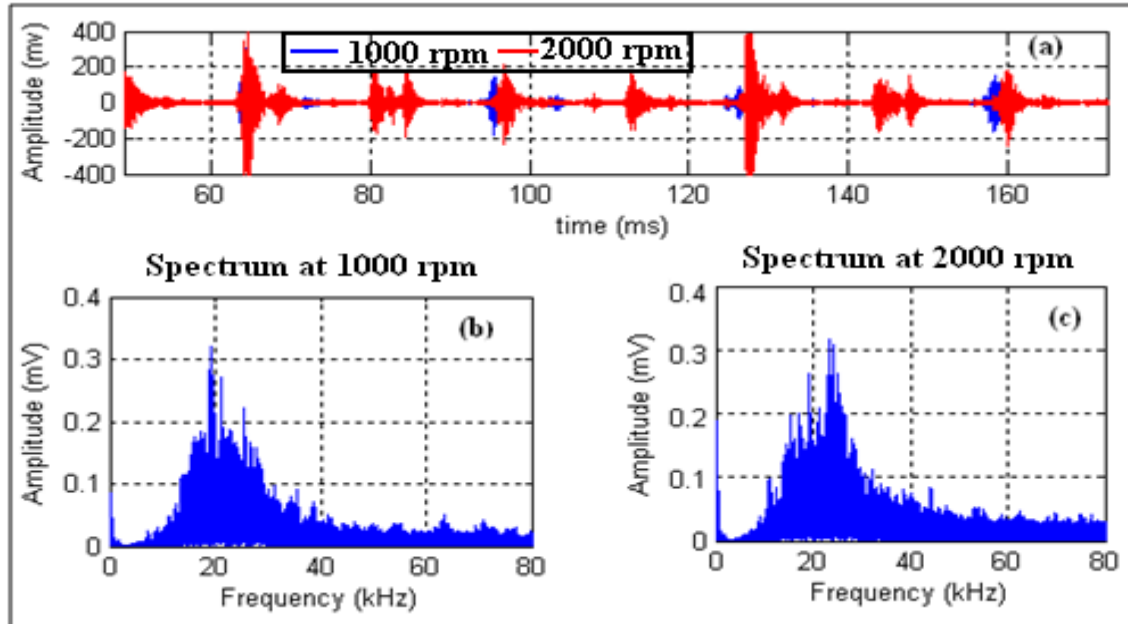


Figure 7.6 Time and power spectra of AE signals from a diesel engine running at 1000 rpm and 2000 rpm.

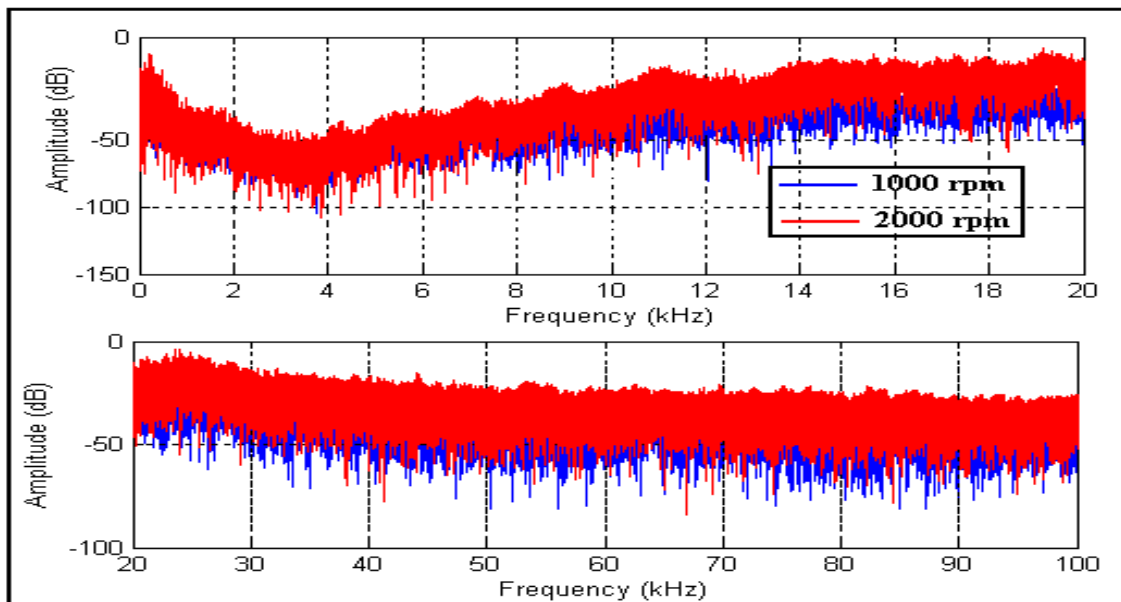


Figure 7.7 Fourier spectrum of the AE signal from a diesel engine running at 1000 rpm and 2000 rpm; up to 20 kHz (upper) and 20 kHz to 100 kHz (below).

Firstly, in Figure 7.6(a), the angular domain analysis of the AE signals is shown for the two engine speeds of 1000 and 2000 rpm, for two complete revolutions (720°) of the crank shaft – about 0.12 seconds and 0.06 seconds duration respectively.

Secondly, the differences in peak amplitudes are obvious; at a speed of 2000 rpm the waveform amplitude is double that at 1000 rpm. This confirms that engine speed has a substantial effect on the measured AE levels. Also, it can be seen from Figure 7.6 that the speed variation does not affect the distinctive cyclical character of the AE waveform.

The spectrum of the AE signal has been divided into two, a lower frequency band –up to 20 kHz - and a higher frequency band from 20 kHz up to 100 kHz, see Figure 7.7. The lower box in Figure 7.7 shows the high frequency portion, above 20 kHz, and reveals clear differences in the signal due to a change in engine speed. The major portion of the AE energy is located in this frequency band. This demonstrates that the higher frequency band dominates the engine AE levels for the combustion event. The spectrum amplitudes increase with the increase of engine speed and more harmonics can be seen in the spectrum. The frequency response of the AE sensor is linear up to approximately 40 kHz, but we can still observe relative amplitudes beyond this frequency.

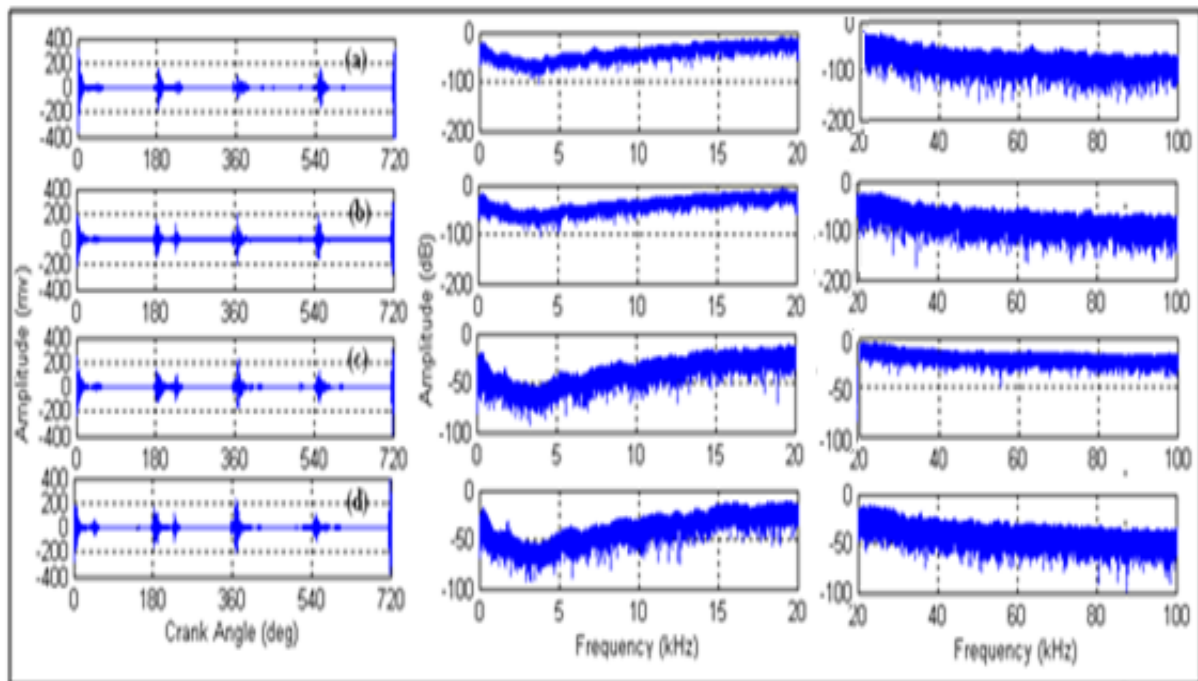


Figure 7.8 AE signals and associated Fourier spectra for the AE from a diesel engine running at 1000 rpm under; (a) no load; (b) 50 Nm; (c) 100 Nm; (d) 150 Nm.

To investigate effects of load variation, the AE signal was recorded when the engine was running at a speed of 1000 rpm, and under four different loads: zero, 50 Nm, 100 Nm and 150 Nm. The recorded AE signals and the associate Fourier spectra are shown in Figure 7.8. The complexity of the AE signals generated by the diesel engine makes the identification of the differences in the AE waveforms in the time-domain, due to different loads, difficult to determine. The amplitude of the spectrum in the higher frequency band, 20 kHz - 100 kHz shows clearer results.

The load of 50 Nm exhibits higher amplitude but fewer transients compared with the case of no load and this agrees with some previous researchers that the AE level is load dependent. By increasing the load to 100 Nm and then to 150 Nm, the amplitude of the AE signals spectrum increased and more transients could be seen in the spectrum in both the lower and higher frequency bands.

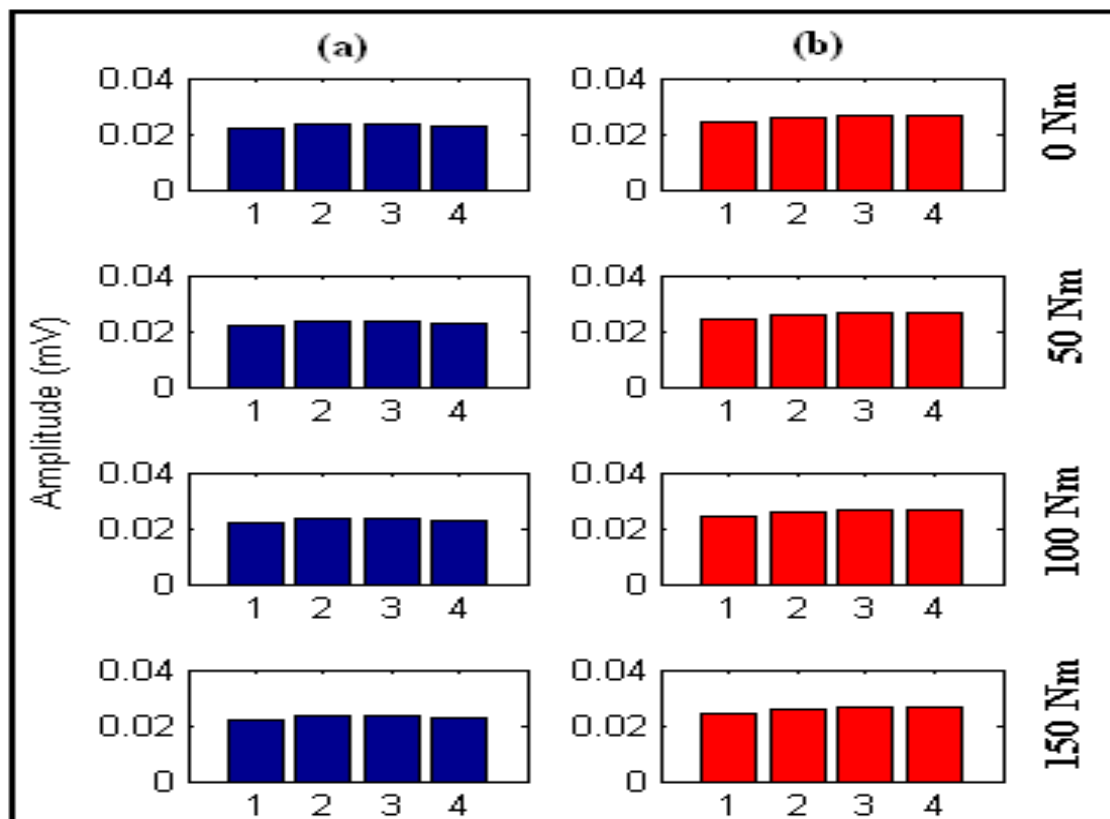


Figure 7.9 Mean value of AE signal for a diesel engine running at (a) 1000 rpm at four different loads and (b) 2000 rpm at four different loads.

Figure 7.9 shows the effect of load variation at different speeds on the RMS of the AE signals. Figure 7.9 confirms that the mean value of AE signal increases with the increase of engine speed (double), however, the relationship between load and the AE signal level is more complex. At low speeds the mean of AE signal level appears largely independent of load, but that at the higher engine speed (2000 rpm) the mean AE signal level appeared to have increased with load (load dependent).

7.4 Data Analysis Using Statistical Parameters

Here the term statistics refers to systematic methods of arranging and describing scientific data and inferring general properties from specific sets of observations. The idea behind testing the engine in this way is to investigate the possibility of utilising AE measurements and simple statistical methods for online condition monitoring. Calculating the RMS values and the variance of the AE signal may give a quick indication of the engine health in a relatively straight-forward way, and information on the engine's health could be assessed by a technician without the need for any special training.

The statistical parameters: mean, standard deviation, variance, kurtosis and skewness are described with their defining equations in Section 4.5.2.1, Time-Domain Analysis. The author wished to assess the use these statistical parameters have in identifying of fault severities, assist in finding solutions for uncertain fault problems and help to avoid high engine maintenance cost through enhanced online monitoring and better identification of unexpected failure.

7.4.1 RMS Value and Variance as Fault Severity Indicators

In this section RMS values and variance of the acoustic emission signals are used to give an indication of fault severity. The engine was tested under four conditions, one with no fault and three different faults commonly found in injectors were introduced, see Table 7.1. Case 1 was with no fault introduced. In case 2 the injection pressure of cylinder 1 was reduced by 35 bars (13%) to 235 bars. Case 3 the injection pressure was increased by 55 bars (20%) to 325 bars. In case 4 the fuel injector was disconnected from the fuel line (full misfire). The engine was tested with each fault under four conditions: with no load, 50 Nm, 100 Nm and a load of 150 Nm, each at speeds of 1000 rpm, 1100 rpm, 1200 rpm and 2000 rpm.

RMS values and variances of the measured AE signals were calculated and averaged for each of the test conditions, see Figures 7.10 and 7.11. The RMS values increased from case 2 through to case 4, and this applies for two speeds and both loads. This increase corresponds to the fault severity increase and could be postulated to the fact that in each case the number of faults increases (mechanical impacts and flow friction etc.) the combustion getting affected more and hence the AE level increased. Richard [283] stated that the variance of the RMS signal could be used as an indicator of combustion quality.

Table 7.1 Summary of faults seeded into the diesel engine

	<i>Case 1</i>	<i>Case 2</i>	<i>Case 3</i>	<i>Case 4</i>
Fault location	N/A	Cylinder 1	Cylinder 1	Cylinder 1
Injection pressure	270 bar	235 bar	325 bar	Full misfire
Description	Healthy condition	Injection pressure reduction	Injection pressure increase	Injector completely disconnected

Figures 7.10 and 7.11 are showing the RMS values and the variance for each case. It can be seen that the faulty cases all have higher variances compared with the healthy case, case 1. Again an increase in variance can be seen as the number (as mentioned before) and severity of the faults increased, and this suggests that this quick simple approach could be used as an indicator for fault severity.

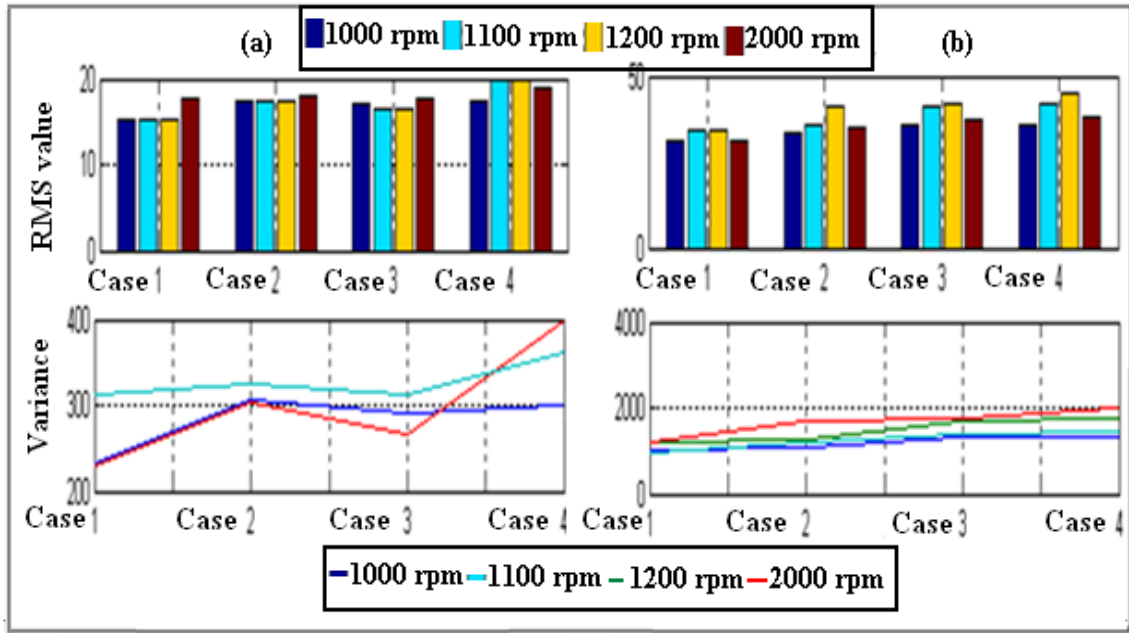


Figure 7.10 AE signals RMS values and the variances (a) no load and four speeds, and (b) 50 Nm load and four speeds

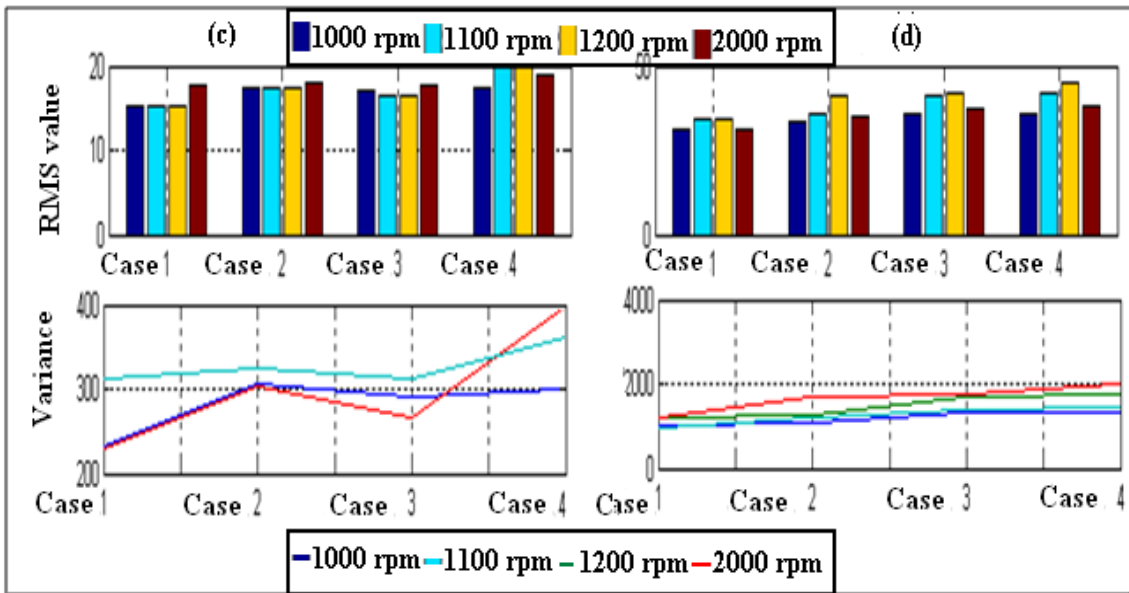


Figure 7.11 AE signals RMS values and the variances (a) four speeds under 100 Nm load and (b) four speeds under 150 Nm load.

7.4.2 Kurtosis as a Tool for Fault Diagnosis

In this section the possibility of detecting and diagnosing fuel injector faults using kurtosis is investigated. In cylinder number 1 fuel injector pressure was altered from a healthy pressure (270 bar), first to 235 bar, 325 bar and then subsequently disconnected. The instantaneous in-cylinder pressure is shown in Figure 7.12. There are clear differences between the peak pressures of the four cases (especially at high load) and, as expected, introducing the fault increases the peak pressure, cause the peak pressure depends on the combustion rate in the initial stages, which is influenced by the amount of fuel taking part in the uncontrolled combustion phase, which in turn is governed by the delay period [284].

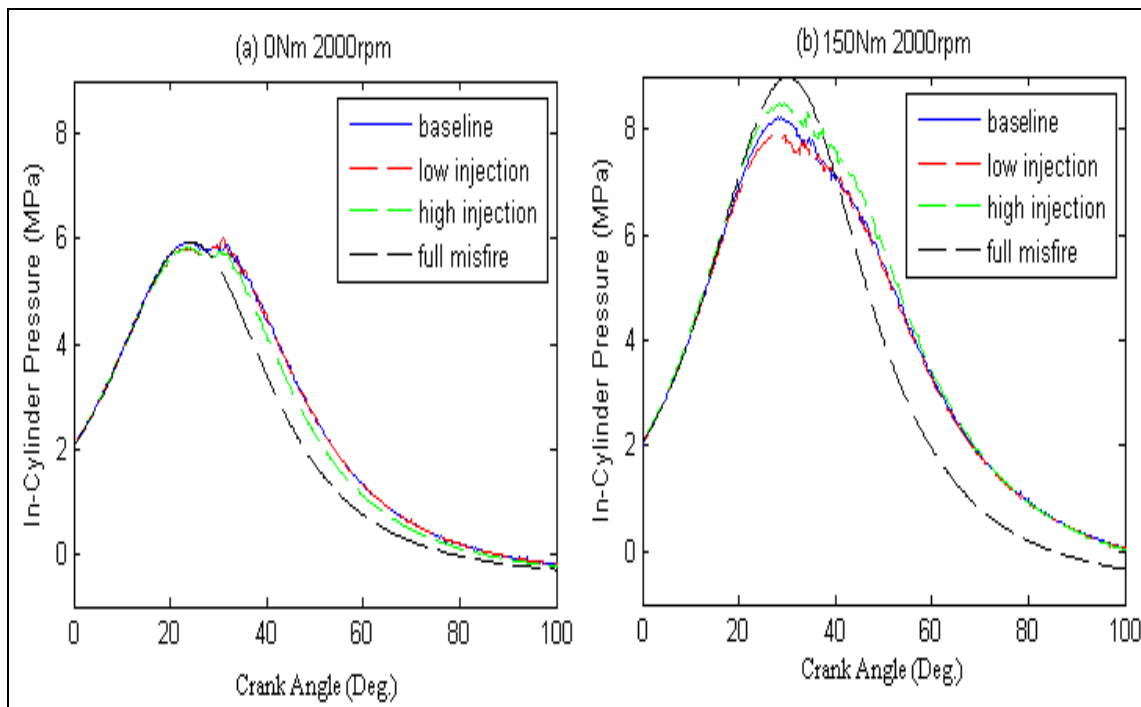


Figure 7.12 In-cylinder pressures of diesel engine cylinder 1 at 2000 rpm, (a) at no load and (b) at 150 Nm load

Figure 7.13 presents a possible detection method whereby faults are found by plotting the kurtosis of the AE signals from the diesel engine against its RMS value.

The spectra of the AE signals in the low frequency band show a clear difference between the AE signal for the healthy and faulty cases. At low frequencies it easy to detect a clear difference see

Figure 7.13. At high frequencies it is more difficult to detect a clear difference, because there is clear signal, but at lower frequencies the differences can be seen clearly.

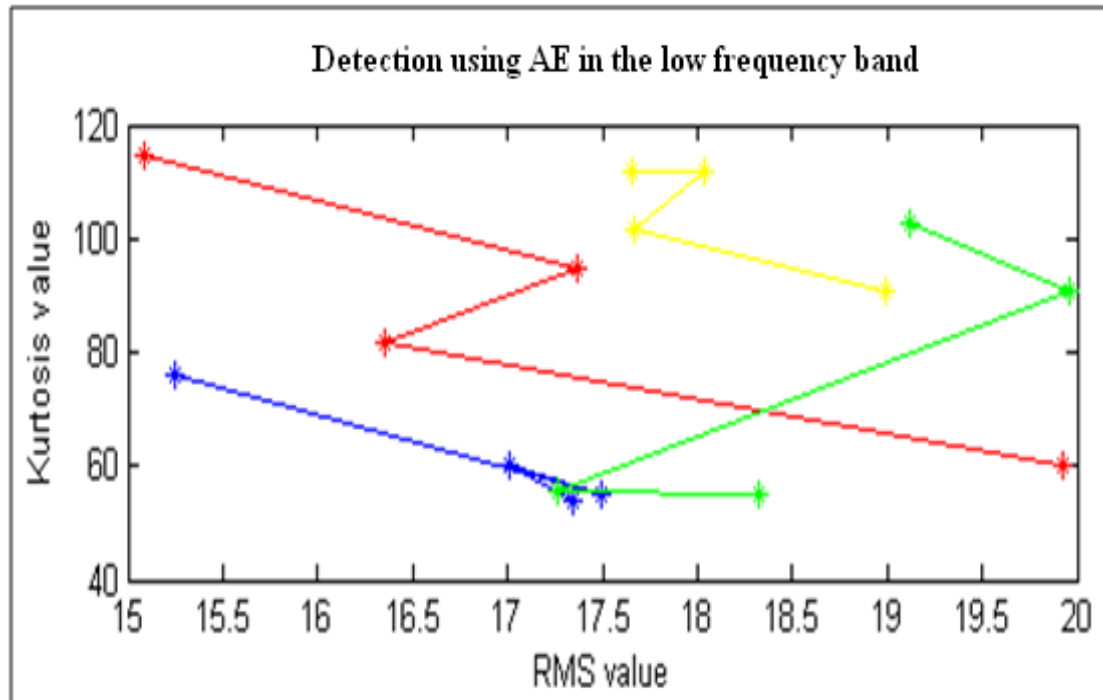


Figure 7.13 Plot of kurtosis against RMS for the AE spectrum below 20 kHz (Blue) 270 bar, (Red) 235 bar, (Green) 325 bar and (yellow) full misfire

7.4.3 Analysis in the Angular-Domain

Angular-domain of the AE signals under the four given loads at (engine speed was fluctuating between 950 and 1000 rpm) are presented in Figures 7.14, 7.15 and 7.16. These show the comparison of healthy AE signals with those obtained with the three seeded faults.

For the reduced injection pressure (-13%), a clear difference can be seen for no load operation just before 360°, see Figure 7.14(a), compared with the other load conditions.

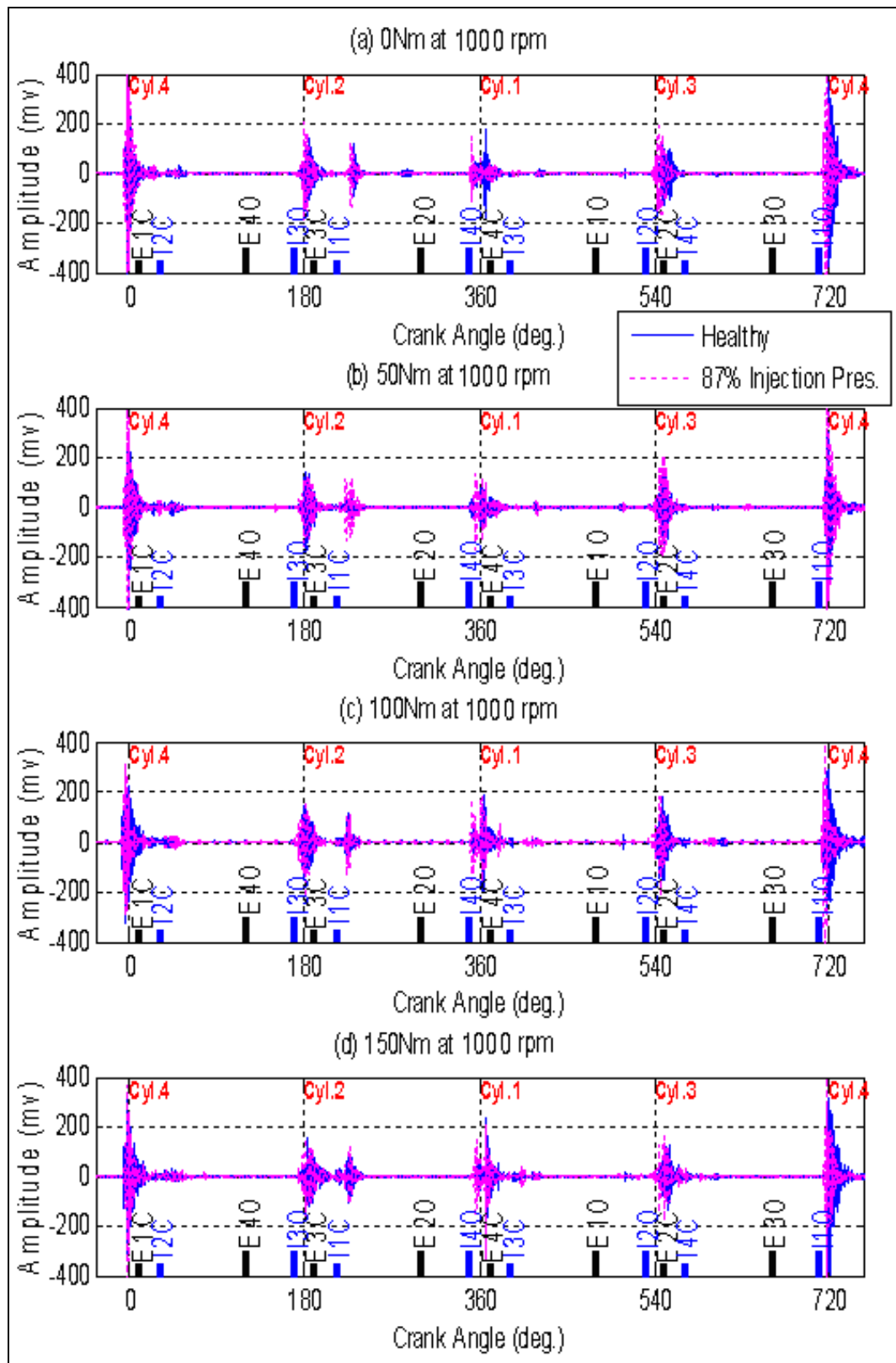


Figure 7.14 AE signals in the angular-domain (87% injection pressure).

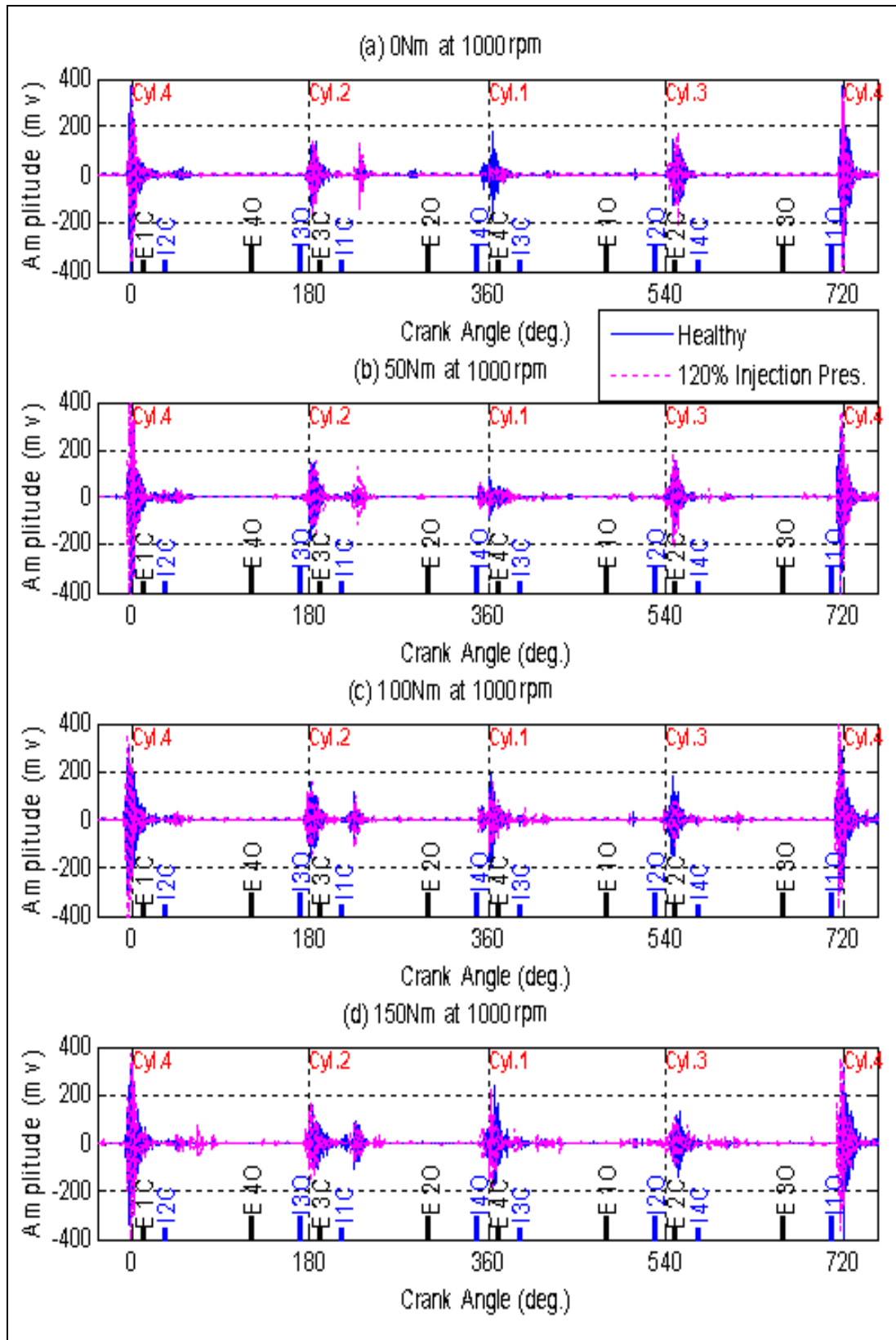


Figure 7.15 AE signals in the angular-domain (120% injection pressure).

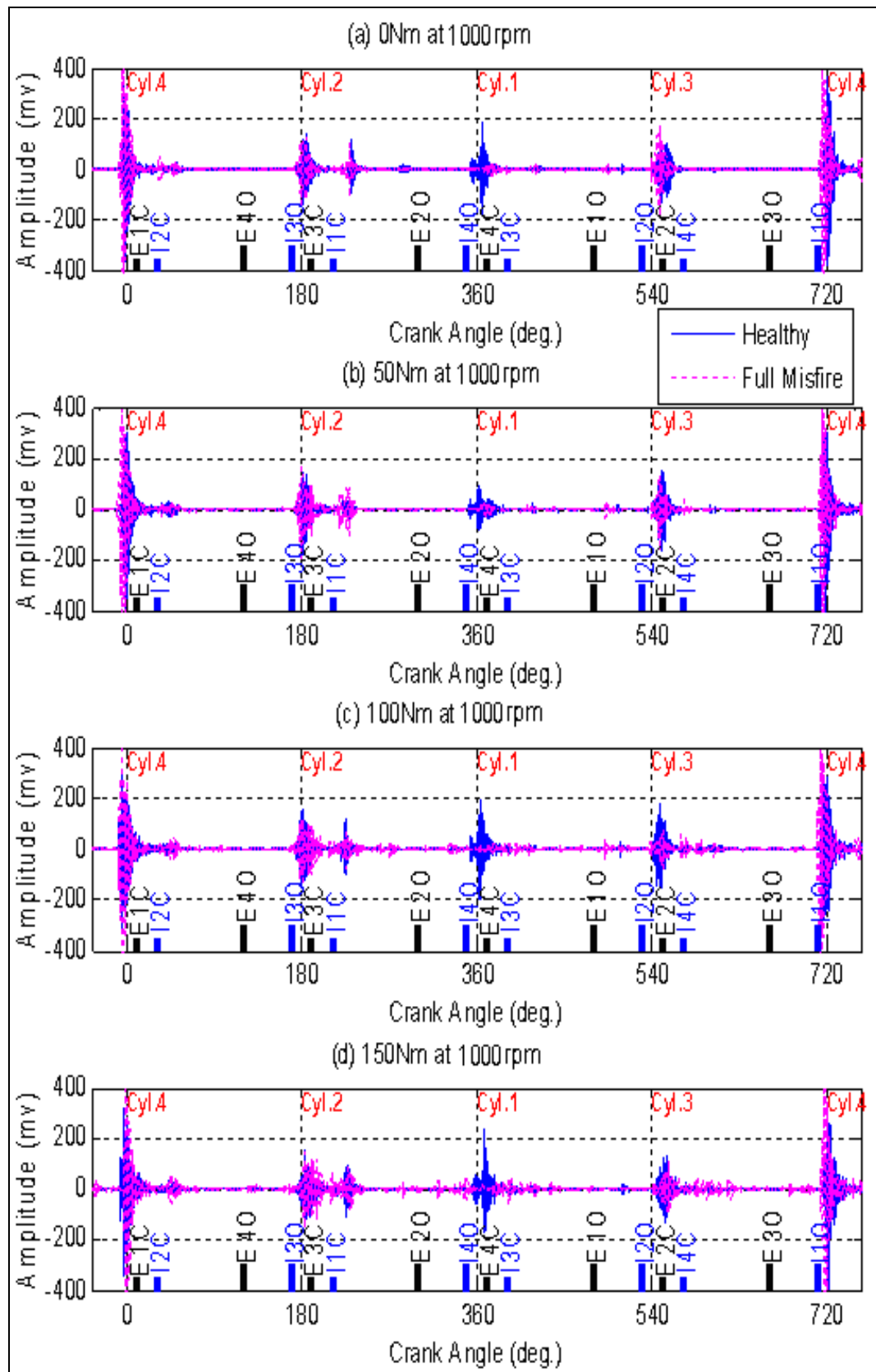


Figure 7.16 AE signals in the angular domain (full misfire)

The rapid transient event of the no load condition indicates an obvious injector valve impact due to the pressure reduction. However, for other load conditions this feature is not so clearly observed in this angular-domain presentation. This shows that more advanced analysis is required to achieve full fault diagnosis.

For the increased injection pressure (+20%), again a clear difference is seen for the no load condition around 360°, see 7.15(a), compared with the other load conditions.

For full misfire the AE signal in Figure 7.16 show the same distinctive and a clear AE event at 360° for all load conditions, that is there is no AE peak and this allows the misfire to be detected straightforwardly in the angular-domain.

7.4.4 Analysis in the Frequency-Domain

The AE signals in the frequency-domain are obtained by applying the Fast Fourier Transformation (FFT) to raw time-domain AE signals. Figures 7.17, 7.18 and 7.19 give spectral comparison for three faulty cases respectively. It can be seen that high AE energy is mainly in a frequency range from 10 kHz to 45 kHz and a clear change can be observed in the spectrum between the healthy and faulty cases.

For the three faulty cases, the main frequency components shift slightly to higher frequency bands. It may indicate that the engine responds with sharper impacts or more violent flow processes, which are basic symptoms of the faulty operation.

However, it is impossible to determine which cylinder has a faulty injector from the spectrum and to differentiate between the three faulty cases.

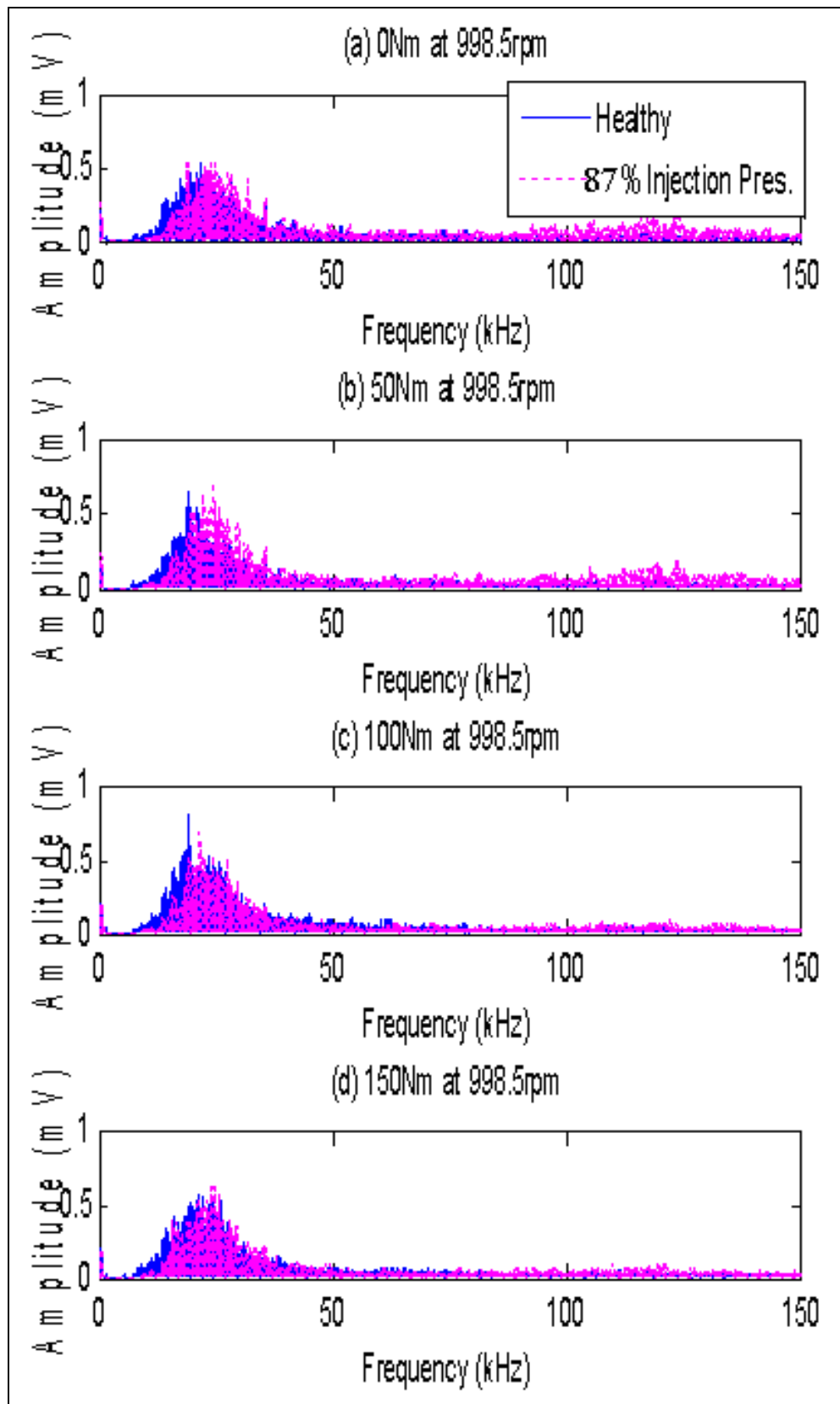


Figure 7.17 Spectra of the AE signals for 87% injection pressure.

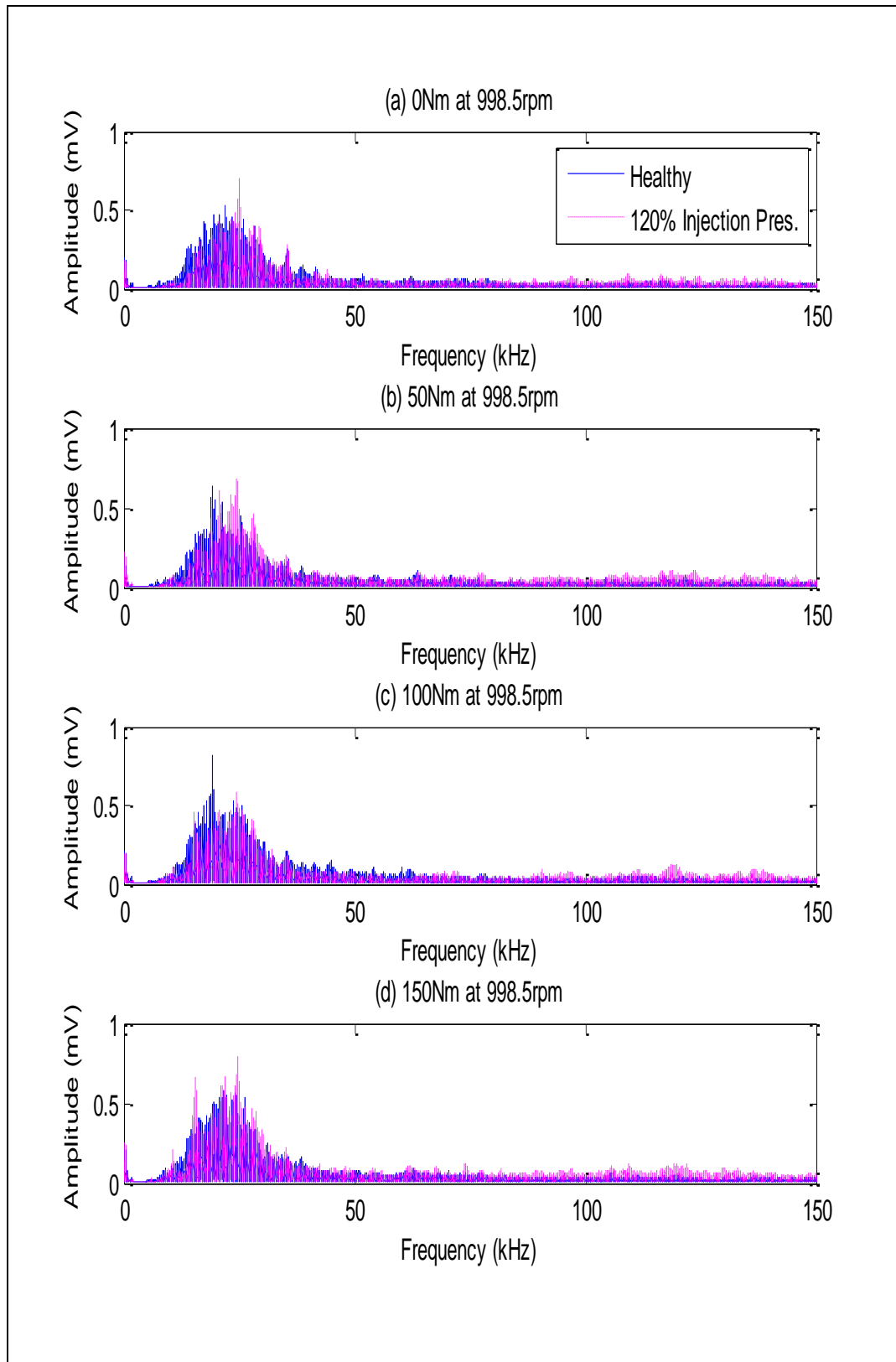


Figure 7.18 Spectra of the AE signals for 120% injection pressure

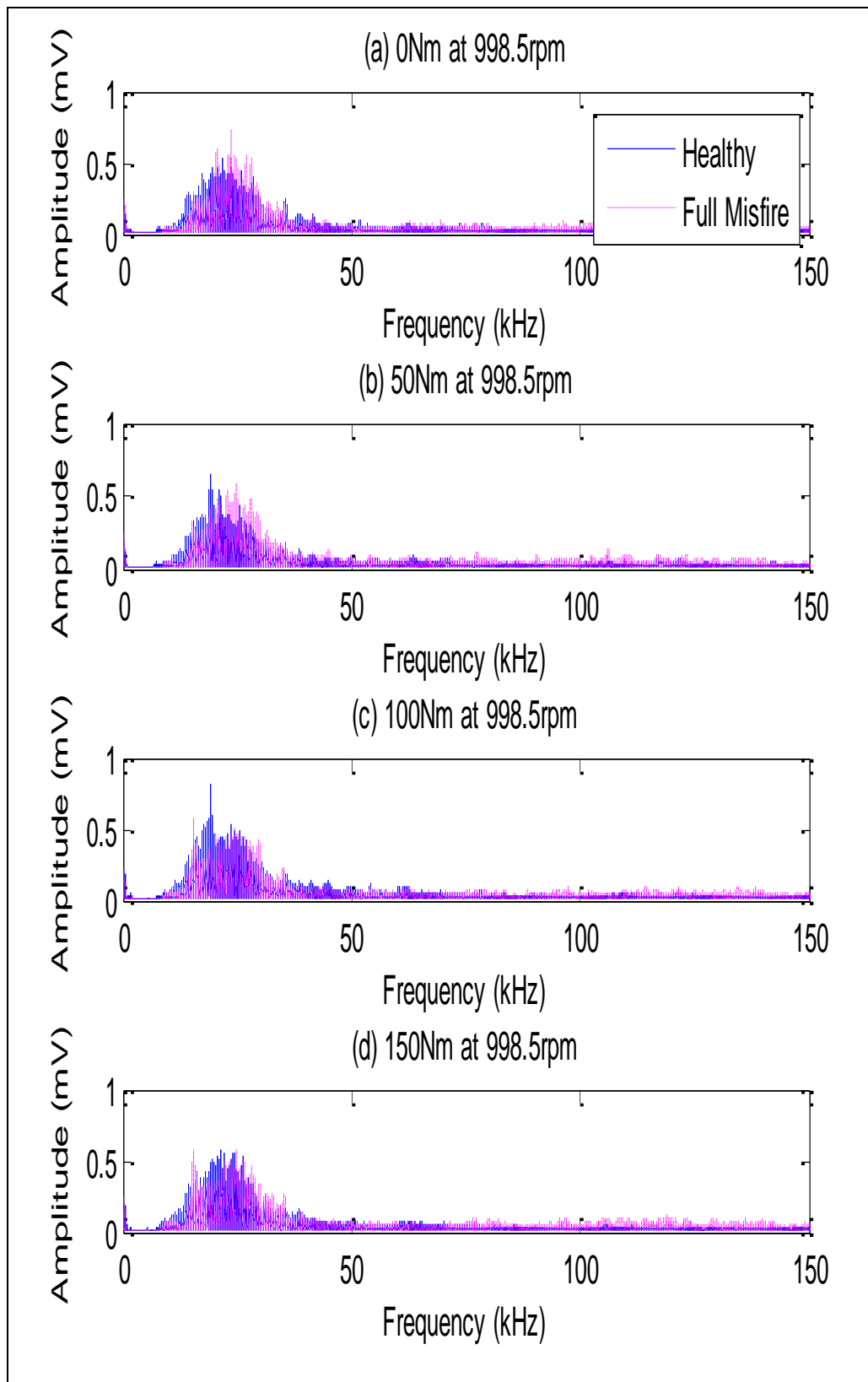


Figure 7.19 Spectra of the AE signals for full misfire

7.4.5 Analysis in the Angular-Frequency Domain

Angular domain analysis shows that AE signals in the angular-domain can diagnose the no load condition but not higher load conditions, whereas spectrum representation allows fault detection for all cases but not diagnosis. To combine the capabilities of both the angular and frequency domains, joint angular-frequency analysis is applied to the AE signals. Previously work [285, 286] has shown that the smoothed Wigner distribution is effective in analysis of injector impact induced vibration. However, recent advances in signal processing show that the wavelet transform is more suitable for the analysis of highly non-stationary signals such as AE from engines. Therefore, the measured AE signals is analysed with a continuous wavelet transform (CWT) using a Morlet wavelet [287].

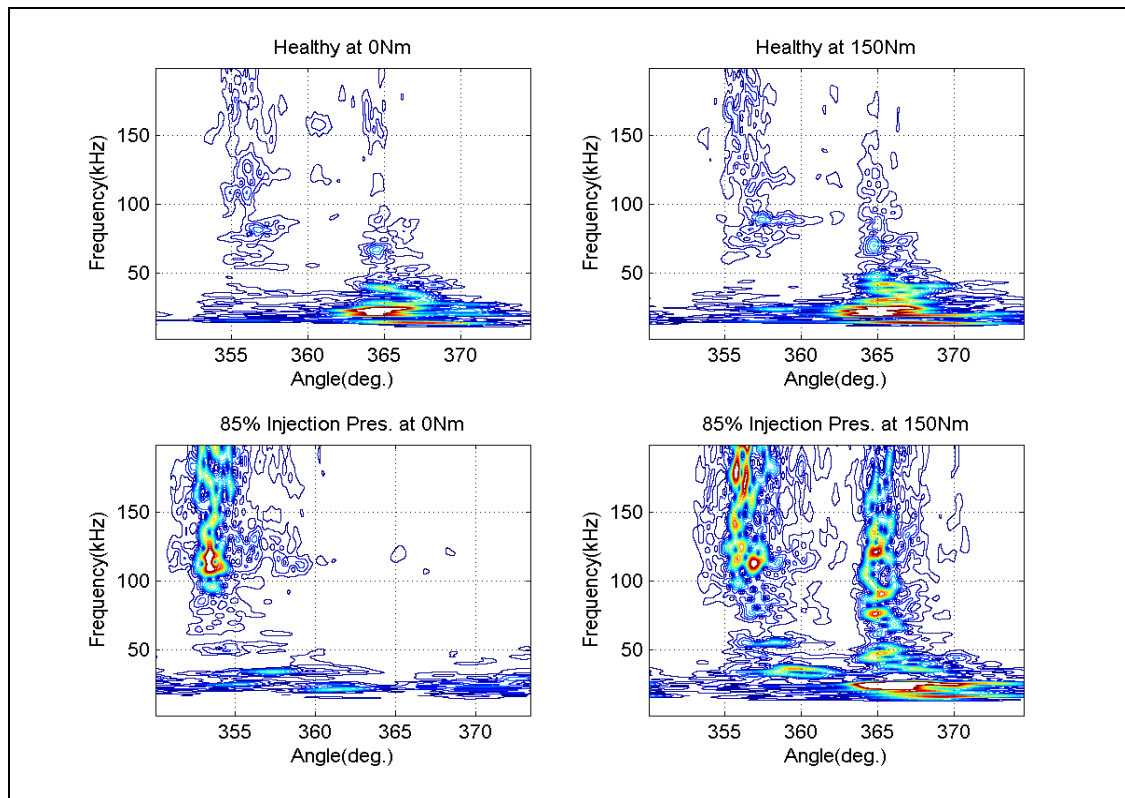


Figure 7.20 Angular-frequency representation of healthy engine and engine with 87% injection pressure

For a more detailed study, CWT results are presented centred on the combustion TDC of cylinder 1. The two graphs in the top of Figure 7.20 show CWT results for a healthy engine under no load and a high load respectively. It can be seen that the combustion AE events occurs around 365° and its

high frequency content increases under high load. In addition, the amplitudes of the spectral peaks also increase. The AE event due to fuel injection happens just after 355° and both its frequency range and amplitude increase with load.

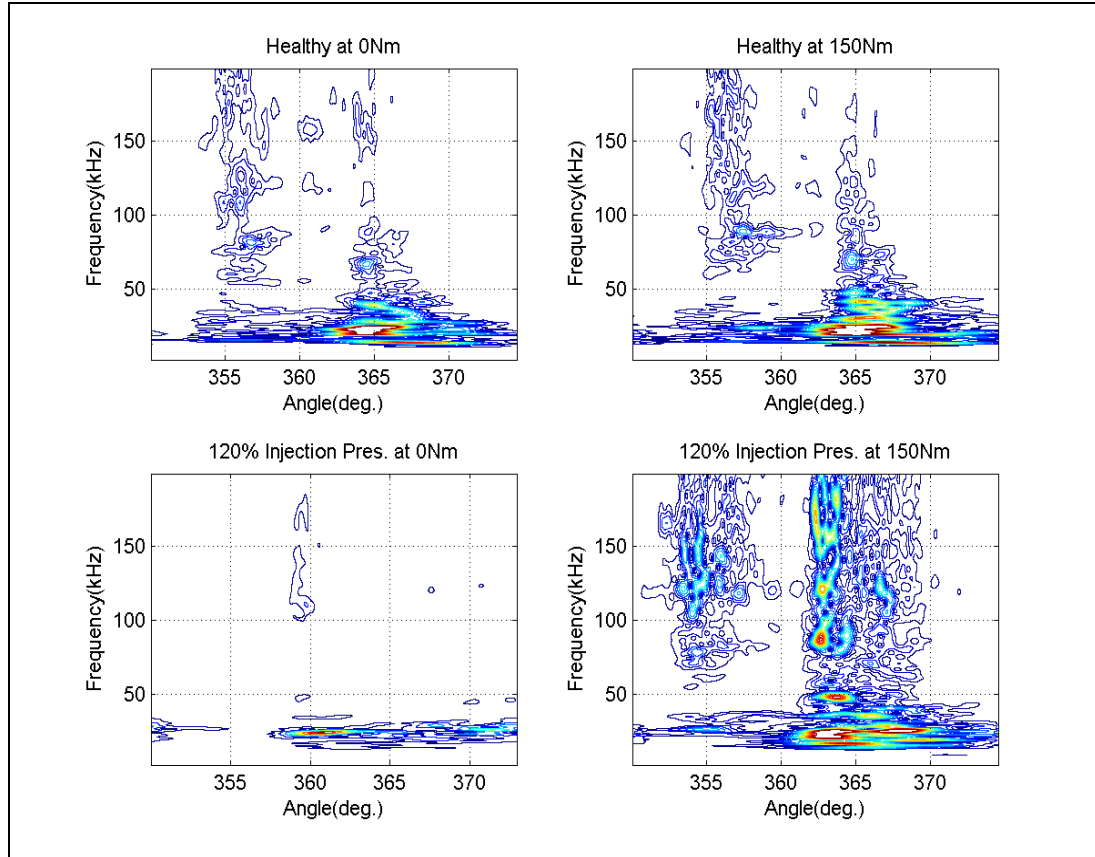


Figure 7.21 Angular-frequency representation of healthy and 120% injection pressure

With the introduction of the small decrease in injection pressure, the CWT results change substantially. CWT results shown in bottom graphs have higher AE amplitudes, indicating higher impact from needle valve opening due to reduced injection pressure. For the no load case, the combustion event is substantially reduced, indicating poor combustion occurring in the cylinder. In contrast, the high load condition show a very high AE combustion event with a much wider frequency range. This shows that the combustion occurs violently because of poor fuel atomization and more fuel is injected caused by reduced injection pressure [281].

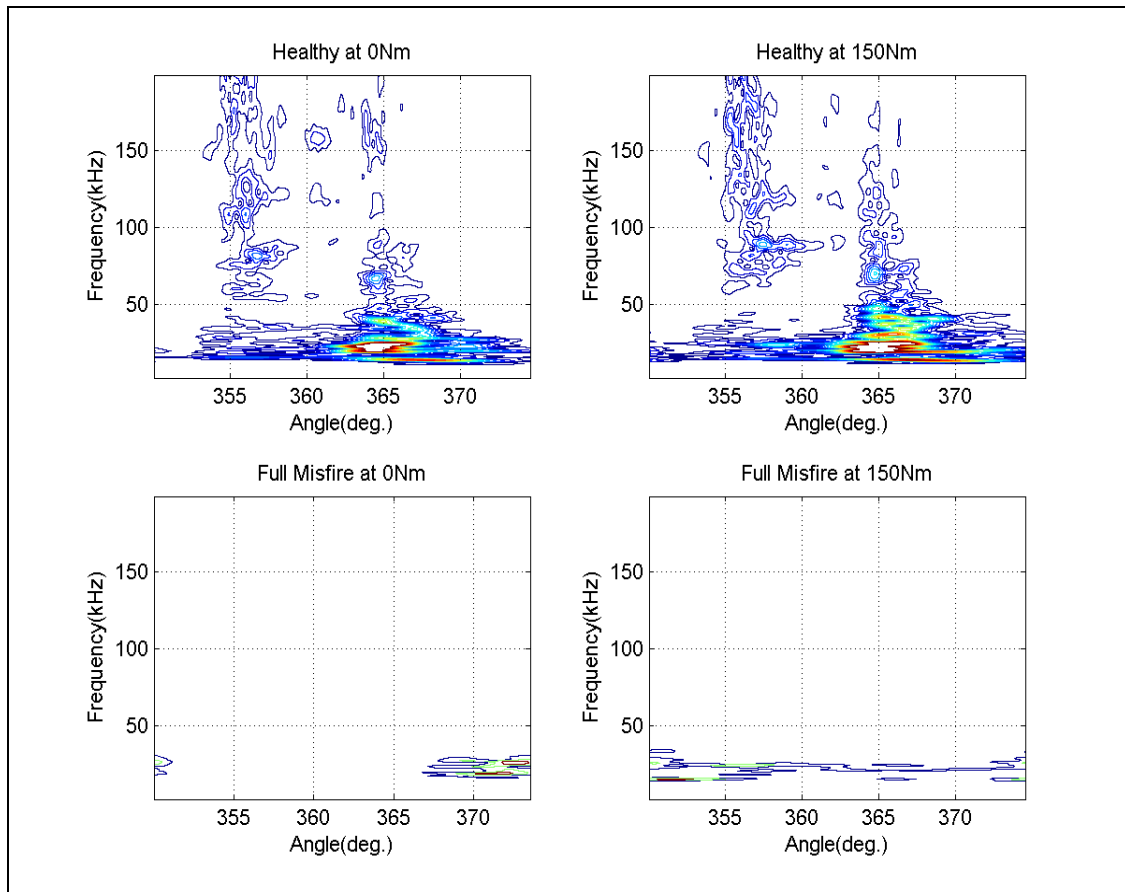


Figure 7.22 Angular-frequency representation of healthy and full misfire

Figure 7.21 shows result of higher injection pressure (120%), CWT results differ substantially from that healthy case. CWT results shown in bottom figures have low AE amplitude at no load and higher amplitude at high load. This indicates lower impact from needle valve opening due to the increased injection pressure. For the zero load case, it shows no combustion AE event around 365° indicating no combustion occurring in the cylinder. In contrast, the high load condition show a very high AE combustion event (good combustion) with extended frequency range. This shows that the combustion occurs weakly because despite good fuel atomization less fuel is injected caused by the increased injection pressure.

These changes in the CWT due to the presence of these faults show that it is possible to differentiate a small injection fault from healthy conditions and successfully diagnose it under both high and low load conditions.

Figure 7.22 present the CWT results for a healthy engine and full misfire for both low and high load conditions. It is obvious that neither the combustion AE event nor injection show on the CWT results and hence this fault can be detected and diagnosed without difficulty.

7.5 Lubrication Monitoring Using Piston Slap Intensity

One of the driving factors for the development of modern diesel engines is engine pollutant emission [280]. The pollutant could be of used oil which ends up in landfills, in sewers, or directly in the environment where it contributes to spoiling freshwater resources and degrading ecosystems. To minimise this aspect of pollution advanced technologies are needed for all aspects of engines, including engine lubrication oil.

The performance of the piston slap in a diesel engine is directly associated with the friction, and wear, which are in turn closely related to engine knock, lubrication oil and fuel. Understanding the relation between engine oil and piston slap intensity is important for developing advanced diesel engines. Many studies identified that liner and its lubrication are not responsible for the greatest proportion of the engine failures. Engine faults encountered included cracked liners and abnormal, excessive wear caused by poor lubricating conditions.

In this section engine lubricating oil condition and quality are evaluated by analysing the acoustic emission signal from the diesel engine in certain frequency bands. Initially the engine was tested using good quality lubricating oil (20W50 type) at the full level (healthy case); subsequently 10% of oil was removed (engine oil level was 90%) and then engine oil level was 110% (10% added), the removed and added oils were measured by the engine capacity from the engine specification, while the engine was run at two speeds (1000 and 2000 rpm) with different loads but at constant coolant temperature ($90\pm 5^{\circ}\text{C}$). The AE signals were measured using an AE sensor mounted on the side of the engine cylinder block.

Simultaneously cylinder pressure data was collected from the 1st cylinder using a combustion pressure sensor. The engine speed was set at two speeds, the acoustic emission was sampled at 2 MHz and 6 segments were collected in each experiment. In the three tests no effects on the cylinder pressure were detected in the time-domain waveforms of the AE signal.

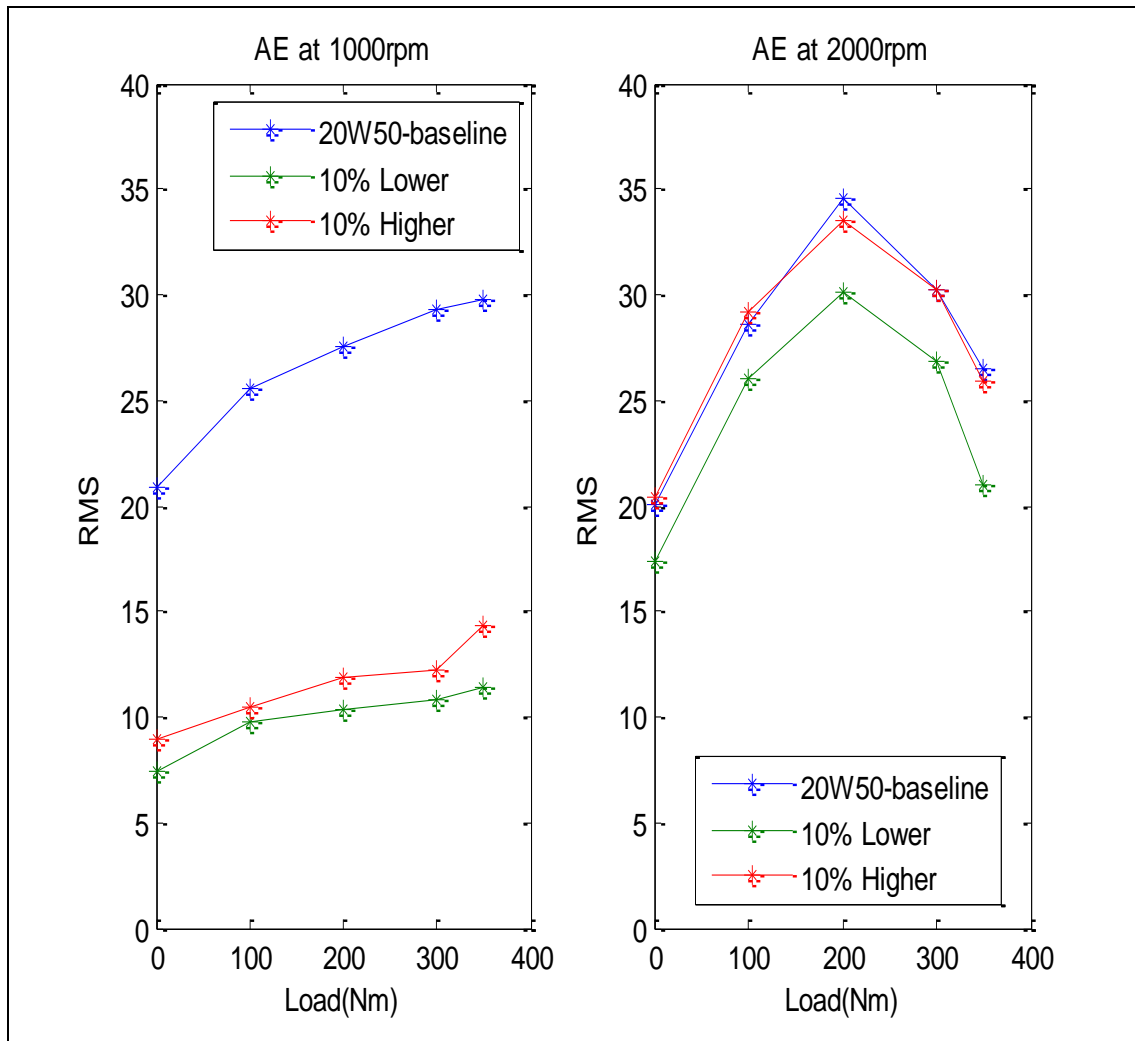


Figure 7.23 RMS of AE signal at two speeds

By taking the RMS values of the signals, some changes could be observed as seen in Figure 7.23. It was found that the RMS values of the frequency band 10 to 50 kHz are affected by the level of the oil. Certain components of the AE signals in this frequency band increased when the oil level was reduced by 10%. It was considered that these changes in amplitude of the components in this frequency band are due to piston slap [282,287].

As can be seen in figure 7.23 there are clearly changes between the baseline and the two oil levels at 1000 rpm. At 2000 rpm there is a smaller but similar change for oil decrease, but nothing significant for the 10% increase.

The component amplitudes in this frequency band were found linearly proportional to the engine speed and load.

7.5.1 Engine Load

Previous studies have shown that piston slap intensity increases when the load is increased. In this study the engine speed was set at 1000rpm and the load was varied from zero to 350 Nm in steps of 100 Nm. The time-averaged RMS values for the frequency band 10 to 50 kHz are shown in Figure 7.24 [286]. The load affects the magnitude of the cylinder pressure, which directly relates to the driving force on the piston, thus increasing engine load and slap intensity.

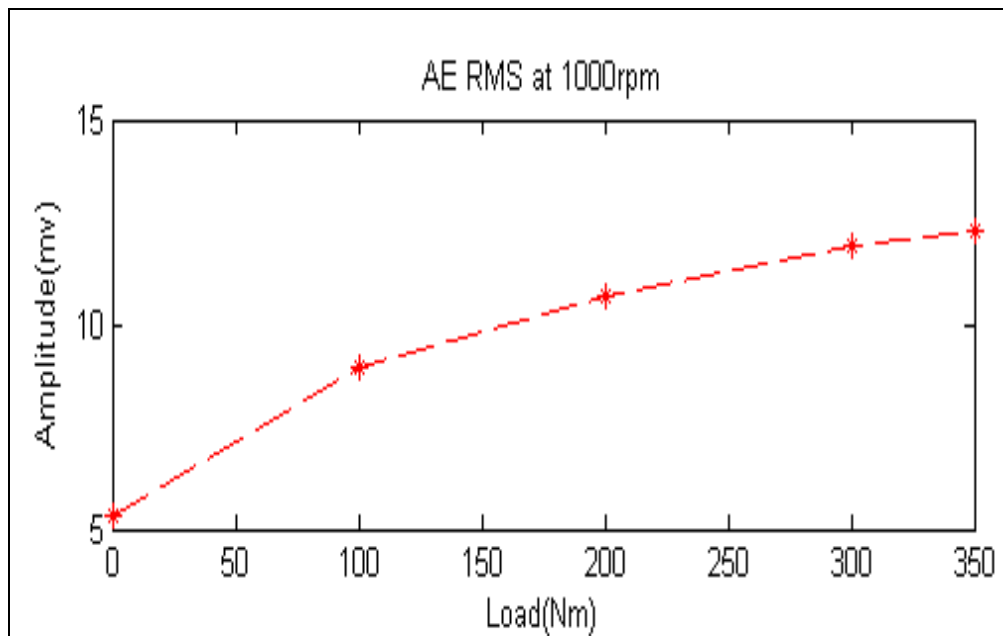


Figure 7.24 RMS value of AE signal 10 kHz to 50 kHz with change in engine load at speed of 1000rpm.

7.5.2 Oil Temperature

Oil temperature was increased from 30°C to 90°C in steps of 5°C (controlled from the panel control, where there is oil temperature indicator and the temperature start measurement when engine starting until engine warmed up by collecting data in each step until 90°C). Figure 7.25 shows the RMS spectral amplitudes of structure-borne stress waves as the oil temperature increased. At an oil temperature 30°C, the viscosity is ~50% higher than for fully warmed up conditions (90°C Oil temperature) [287].

Thus, with cold oil the duty parameter (viscosity*speed/load) in the Stribeck curve [264] is high and there is more possibility for hydrodynamic lubrication than for boundary or mixed lubrication in the piston assembly (see Figure 5.1).

Increasing oil temperature increases piston slap intensity as the result of two effects:

1. Increasing the oil temperature decreases its viscosity dramatically, which provides less damping in the oil film between the piston and the cylinder walls.
2. Increase in oil temperature is accompanied by an increase of cylinder liner temperature, which has the effect of enlarging the clearance between the piston and liner so the motion of the piston would be less restricted, increasing the slap intensity [287].

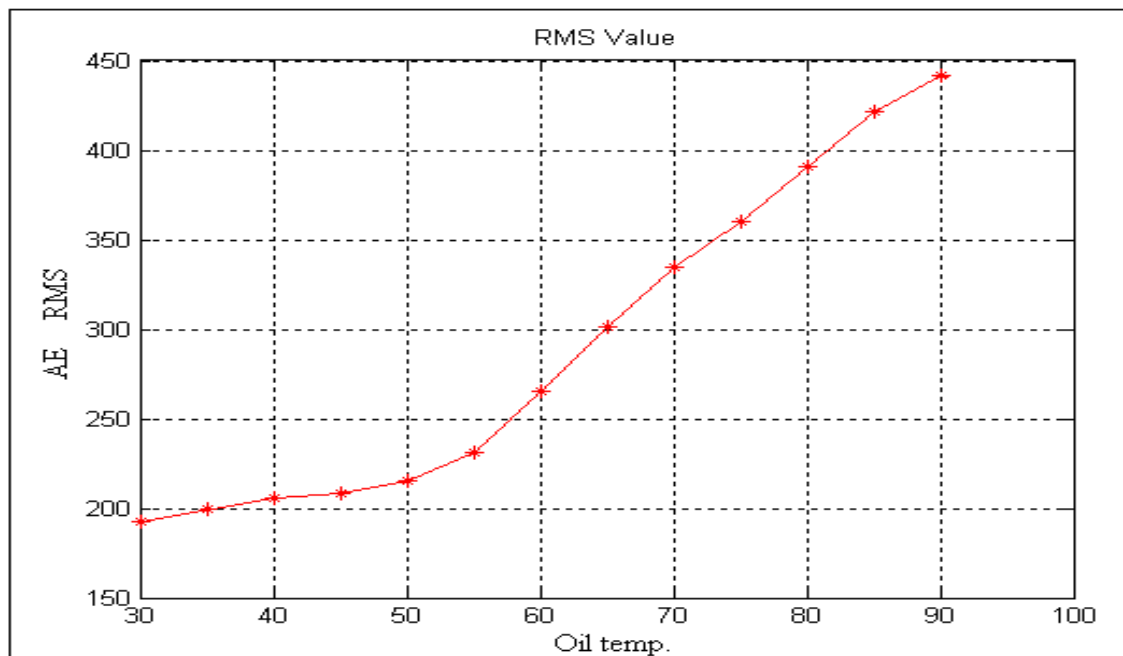


Figure 7.25 Effects of oil temperature on RMS value of AE signal 10 kHz to 50 kHz with change in engine temperature at speed of 1000rp

7.5.3 Engine Speed

The effect of engine speed on piston slap was studied at engine speeds of 1000, 1100, 1200, 1300, and 1400 rpm at a load of 100 Nm. Figure 7.26 shows that increasing engine speed increases the acceleration of the cylinder block. Increasing the speed increases the in-cylinder pressure and the piston's kinetic energy, and these are the reasons for the intensity of impacts being higher [287].

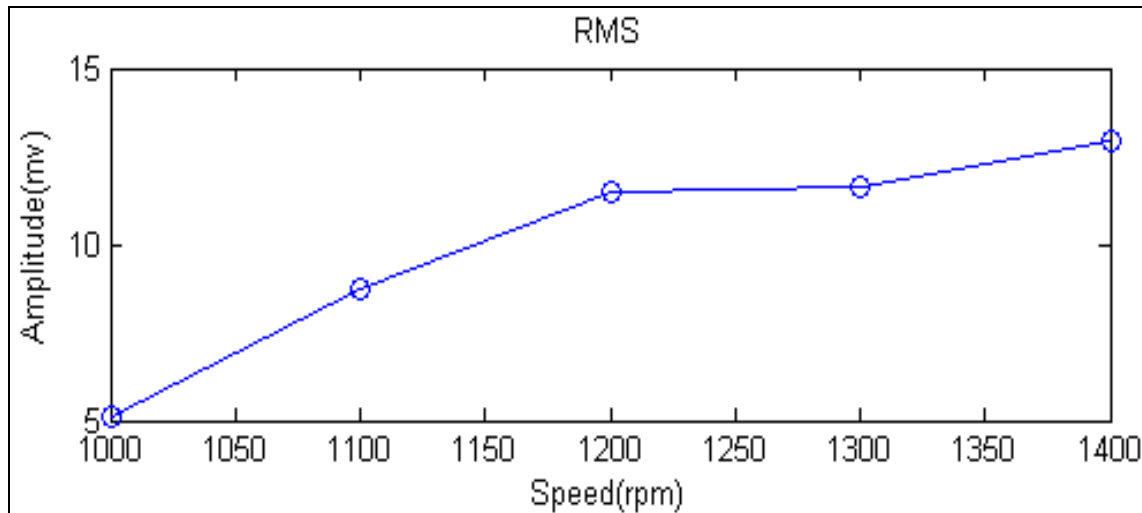


Figure 7.26 Effect of engine speed on RMS value of AE signal 10 kHz to 50 kHz with change in engine speed at constant load of 100 Nm

7.5.4 Oil Type

Engine oil should have certain acceptable properties for satisfactory lubrication of the engine, of which viscosity is one of the most important as it affects the oil's capacity to lubricate effectively.

The effects of oil viscosity on the capacity of piston slap to generate AE signals were investigated by changing the oil viscosity by using two different types of engine oil; 10W-30 and 20W-50. Table 7.2 presents some of their typical and relevant properties. Between oil changes the oil was left to drain for 30 mins and the oil filter was renewed.

The engine speed was set to 1000 rpm, and the AE signals were recorded at different temperatures and engine loadings. Figure 7.27 shows the consequent changes in the AE signal. It was difficult to discern any clear effects on the AE signals as a consequence of changing the oil type using only the mean spectral components [287].

By band pass filtered the signals using a digital band pass filter between 10 and 50 kHz and calculating the RMS values of the signals, clear differences could be observed, see Figure 7.27. The intensity of the impacts is less when using higher viscosity oil, because of its higher damping characteristics.

The RMS values in the case of 20W-50 are less at 200 and 350 Nm but more data would be needed to confirm the intermediate loads. By increasing the oil temperature this effect became less.

Table 7.2 Typical properties of the oils used.

	<i>Typical properties</i>	<i>10W-30</i>	<i>20W-50</i>
1	Viscosity mm^2/s @ 100 C°	11.0	17.5
2	Viscosity mm^2/s @ 40 C°	72	153
3	Viscosity Index	143	125
4	Viscosity, mPa.s - 25 C°	<7000	<9500
5	Viscosity, mPa.s - 20 C°	<7000	<9500
6	Viscosity, mPa.s - 15 C°	<7000	<9500
7	Sulphated Ash, wt.%	1.2	1.2
8	Yield Stress	None	None
9	Total Base #	7.75	7.75

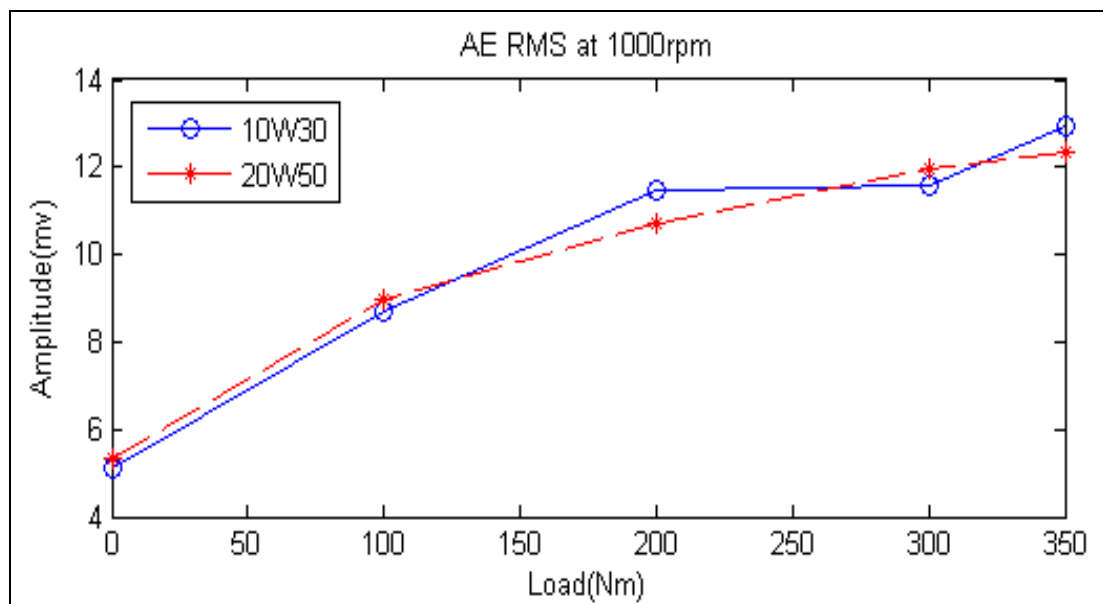


Figure 7.27 Effects of engine oil viscosity on amplitude of AE signal.

7.6 Conventional Techniques: Limitations and Drawbacks

The main drawbacks of the conventional methods of analysis; such as time-domain or angular domain extracted features (see Section 7.4.3), spectral analysis and statistical parameters (see Section 7.4.); is that they give limited information, especially when the sampling frequency is very high as it is in AE data acquisition. The frequency-domain analysis gives only information about the frequency components of the measured signals and in the case of diesel engine AE condition monitoring these frequency components are dominated by the firing frequencies of the engine and its harmonics (as seen in Section 7.4.4). The low frequency band (higher than 20 kHz) is dominated by the combustion event and it is difficult to detect any other AE event sources such as injection process event, exhaust and intake valve event sources. More advanced signal processing techniques have been investigated and applied in this chapter, time-frequency domain analysis using continuous wavelet transform (CWT) see Section 7.4.5.

CHAPTER EIGHT

SIMULATION AND MODEL VALIDATION

This chapter evaluates the models developed using parameters of a healthy four-stroke diesel engine. The mathematical equations are solved numerically in a MATLAB environment to give displacement, speed, acceleration, piston lateral force, gas torque, friction power, indicated power and inertia torque. The model has proved to be useful results, which can be used successfully for fault detection and diagnosis.

8.1 General Concept

Chapter Five developed a mathematical model for the four-stroke diesel engine to predict likely piston slap and friction signatures. The derived mathematical equations now have to be solved. Because the differential equations are both coupled and nonlinear (also some of the many algebraic equations to be solved are highly nonlinear), it is not possible to derive a closed form of solution and numerical methods are used. Importantly, an initial validation of the model is performed by comparing the predicted parameters over the work cycle to a healthy engine.

The method of solving the set of nonlinear and coupled differential equations that make up the model is based on a fourth order Runge-Kutta algorithm [55, 101]. The step size in the algorithm is adaptive, allowing longer steps when the functions to be integrated are smooth and smaller steps when the function changes rapidly. The simulation of the dynamic operation of the engine becomes the solution of repeated simultaneous equations for a number of initial value-boundary problems, corresponding to each element of the system. Knowing the initial values of all variables and the interaction which take place across the boundary of each element during the small time intervals of the iterations, the values of all variables can be determined. This process is repeated successively for the complete work cycle of the engine.

8.2 Influence of Piston Displacement

Piston secondary motion (displacement) in the piston–cylinder gap has a direct influence on cavitation destruction, lubrication, and oil consumption via the cylinder–piston group, on friction losses and cylinder–piston group wear, on engine reliability and on vibration, AE and noise.

Piston displacement occurs under the action of lateral forces. Friction opposes piston motion in the form of: the friction force between piston skirt and cylinder; the friction force between piston rings and pistons; the friction force between piston rings and the cylinder; the friction moment in the piston pin connections; and the friction moment between the connecting rod and connecting rod neck.

It was found that piston displacement takes place according to variation in the forces acting on it. If the sign of the force changes the piston starts to move freely from one wall of the cylinder shell to the opposite.

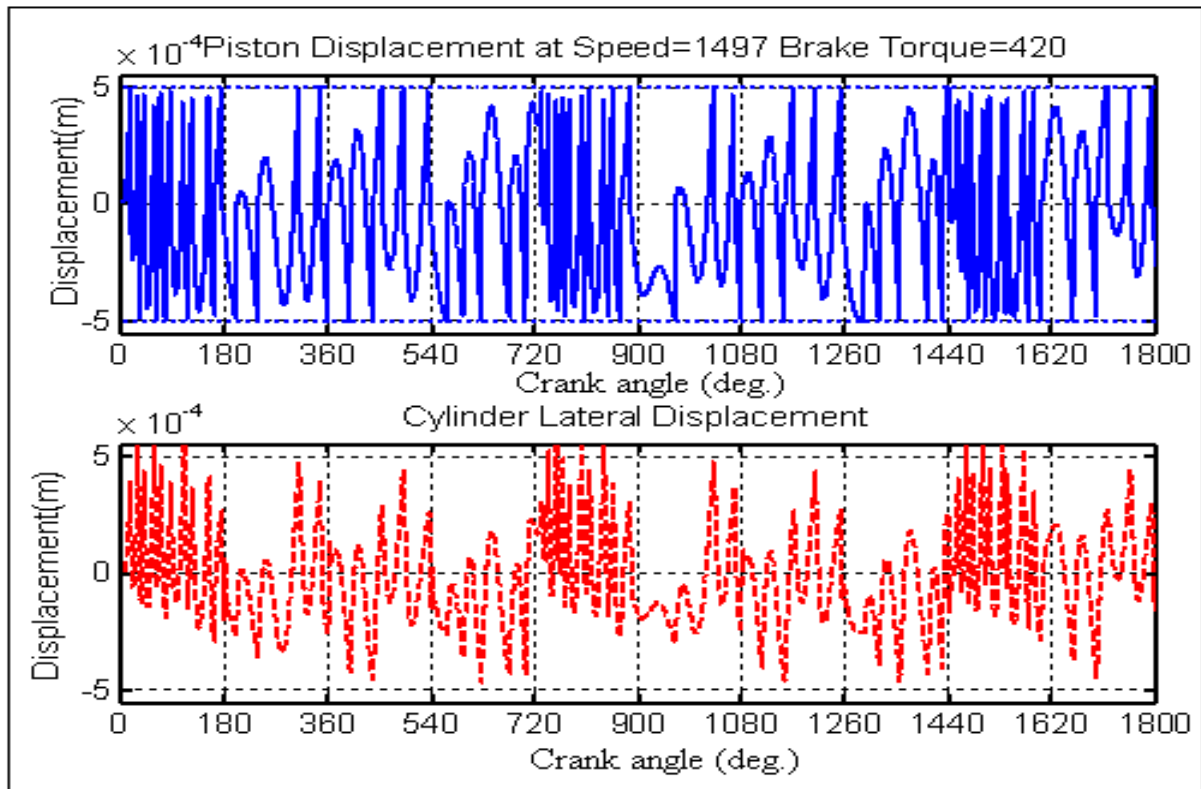


Figure 8.1 Piston lateral displacement and cylinder lateral displacement at engine speed 1497 rpm and brake torque 420 Nm

In this case, the top and bottom edges of the piston start to move simultaneously. Then the bottom edge of the piston skirt outstrips the top edge. Figure 8.1 shows the relative lateral displacements of the piston and cylinder at engine speed of about 1500 rpm and load of 420 Nm. This figure shows experiments results and the environment between the piston skirt and the cylinder liner changes due to the crank rotation and cylinder pressure. As can be seen, the magnitude plot has a high magnitude of about 5 m, and which is the peak found in the frequency spectra of the piston. The first phase of free motion ends when the bottom edge of the skirt comes in contact with the opposite side of the cylinder shell. As soon as the bottom edge closes the gap, the top of the skirt starts to rotate (rollover) relative to the bottom. The rollover takes place with the oil that is squeezed out of the gap being removed by the top edge of the piston skirt. In this way, the radial motion of the piston is a result of a change in the direction of force and it is compound.

Piston free motion cannot be realized simultaneously with a change in the sign of the force (sign as in Equation 5.26). In order for motion to be initiated, it is necessary to overcome frictional forces

including moment resistance. The start of the piston's free lateral motion in the unloaded direction is delayed from the moment of sign change in the force by between 15–20° from the dead centre of the intake stroke, compression stroke, and exhaust stroke.

During the exhaust stroke, the piston is displaced once near the operational TDC. The moment the free lateral motion of the piston begins corresponds to 10–15° after TDC. The whole of the resistance to piston displacement is equivalent to the value of the force at the moment piston free motion begins and depends on stroke and operational mode of the diesel engine.

The resistance forces and moments do not influence the maximum rate of piston displacement, but they do determine the starting moment of piston lateral free motion and hence the end of the displacement: piston impact on the piston shell.

8.3 Influence of Piston Sliding Velocity

Regardless as to whether or not the transmission properties of the cylinder block are understood, further investigation of the signals is still constructive as it may reveal information about the factors which govern the amount of AE generated.

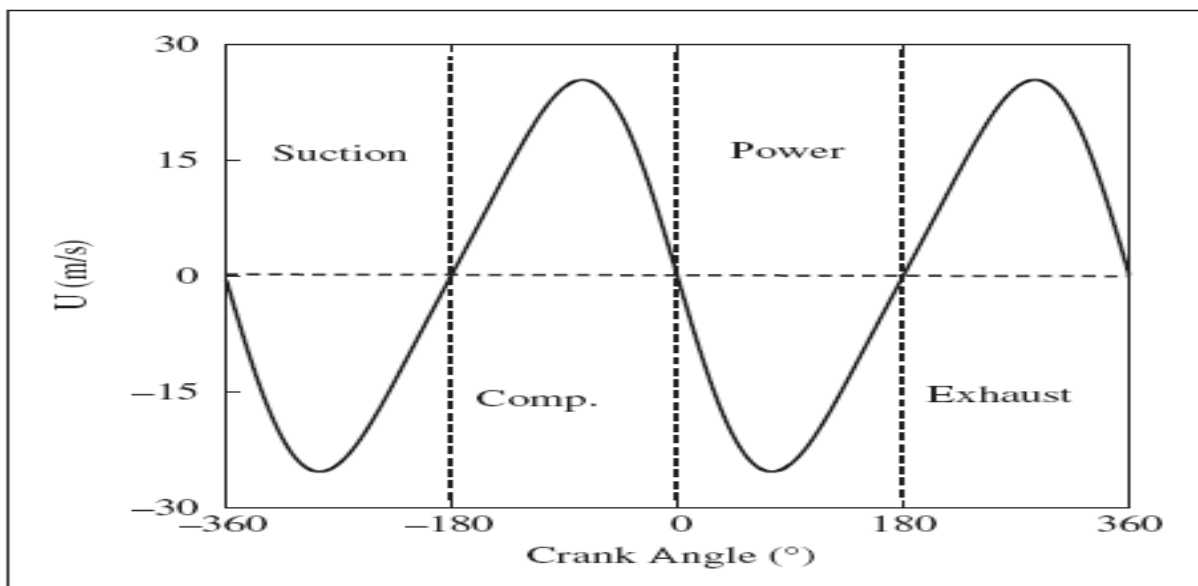


Figure 8.2 Piston sliding velocity at constant engine rpm

The consistency during the cycle of the continuous events proposed to relate to the piston liner contact is seen in Figure 8.2 for data acquired from the AE sensor positioned on the cylinder block.

The plot shows the amount of piston lateral velocity at an engine speed of about 1500 rpm and load of 420 Nm.

Due to the four-stroke cycle, strokes 1 and 3 follow the same motion and similarly strokes 2 and 4 are grouped together. The figure emphasises that AE activity is related to piston velocity. It is also clear that there is a distinction between the directions of piston velocity; at a given piston displacement the AE energy is greater for velocity towards the cylinder head than towards the crankshaft.

The piston trajectories for cylinders 1 and 3 are essentially the same although the engine firing order dictates that the trajectory for cylinder 3 is 180 degrees out of phase with cylinder 1. The firing order further determines that cylinder 2 follows the same trajectory with cylinder 3, although 360 degrees out of phase in terms of the engine cycle, and similarly cylinder 4 and cylinder 1 are 360 degrees out of phase.

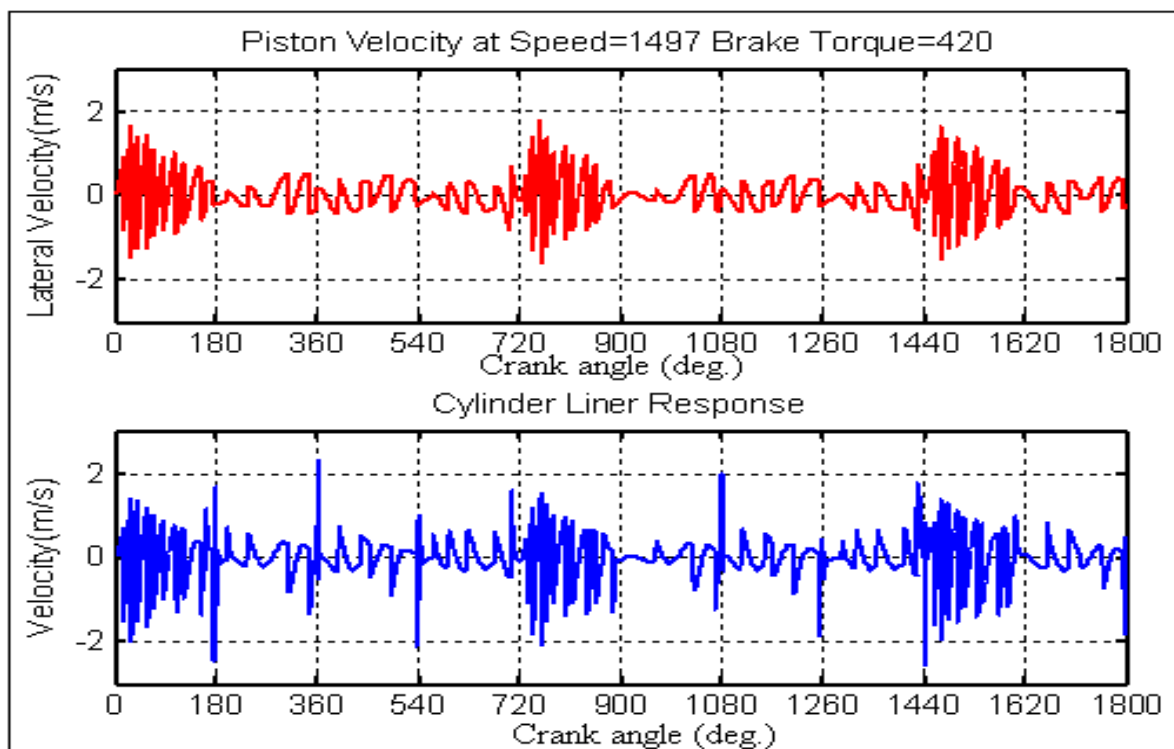


Figure 8.3 Piston lateral velocity and cylinder liner response at engine speed 1497 rpm and brake torque 420 Nm

Burst-type AE events, are noted as occurring at maximum piston speeds when the direction of piston acceleration changes and also at certain angles on the piston upstroke.

The precise origins of these AE events are not known. One possibility is that they occur due to disruption of piston liner contact as the direction of piston acceleration changes; another is that they result from impacts caused by movement of the pushrod tappets.

There are also two possible explanations identified for the difference in the amount of AE generated between acceleration directions. Firstly, the direction of acceleration may impact upon the piston ring dynamics causing a change in the tribological behaviour and consequently a change in the AE generation properties. This is obviously dependent upon the AE generation being sensitive to changes in piston sliding contact behaviour, this has been shown in other applications and, for instance, different AE generation characteristics have been observed for different contact areas at the head-slider/disk interface in HDDs [250, 251]. This explanation also relies on the AE measured at the centre-line of a cylinder being dominated by the piston liner interaction in that particular cylinder.

The second explanation concerns cross-cylinder propagation. Given the apparent relationship between piston speed and AE activity the effects of any cross-cylinder propagation will be most obvious when the piston velocities for cylinders 2 and 3 are greater than for cylinder 1. The piston kinematics is such that these circumstances occur when the direction of the piston in cylinder 1 accelerates towards the crank. This provides a possible explanation for what seemingly appeared to be an acceleration related feature. The issue of cross-cylinder propagation is significant as it suggests that to achieve monitoring of specific cylinders it may be necessary to develop spatial reconstitution techniques to decompose the signal into its constituent parts.

Considering that the AE measured at the centre-line of any cylinder will likely involve contributions from each of the four cylinders comparisons which related AE activity to solely the motion of the piston in one cylinder will be inaccurate. Rather, the AE data should be compared to a combination to varying extents (depending upon their relative importance) of all the piston motions. Determination of each cylinders contribution would require knowledge of the complicated transmission properties of the cylinder block and of the source AE levels and phases at each piston liner contact. The complexity of this task limits what can be achieved here and instead the mean piston speed of all four pistons is used as an approximation. No distinction is made between

directions of piston speed since the objective is to compare the AE activity with the overall piston speed characteristics. It is observed that the mean piston speed resembles more accurately the profile of the AE energy during the cycle than the individual cylinder piston speed, which may imply that it offers a more realistic representation of the signal composition.

The principal observation from tests on the engine is that AE activity appears to be generated from piston liner contact and that the selection of sensor position greatly affects the measured strength of this activity. Furthermore, it has also been established that for this activity there is a relationship between piston velocity and the amount of AE generated.

8.4 Influence of Cylinder Block Displacement

The cylinder block is one of the major structures of a diesel engine; it generates AE due to combustion gas pressure, oil film pressures and friction on the piston skirt and in the crankshaft bearings. AE analysis of cylinder block is helpful for analysing the AE characteristics of the whole engine.

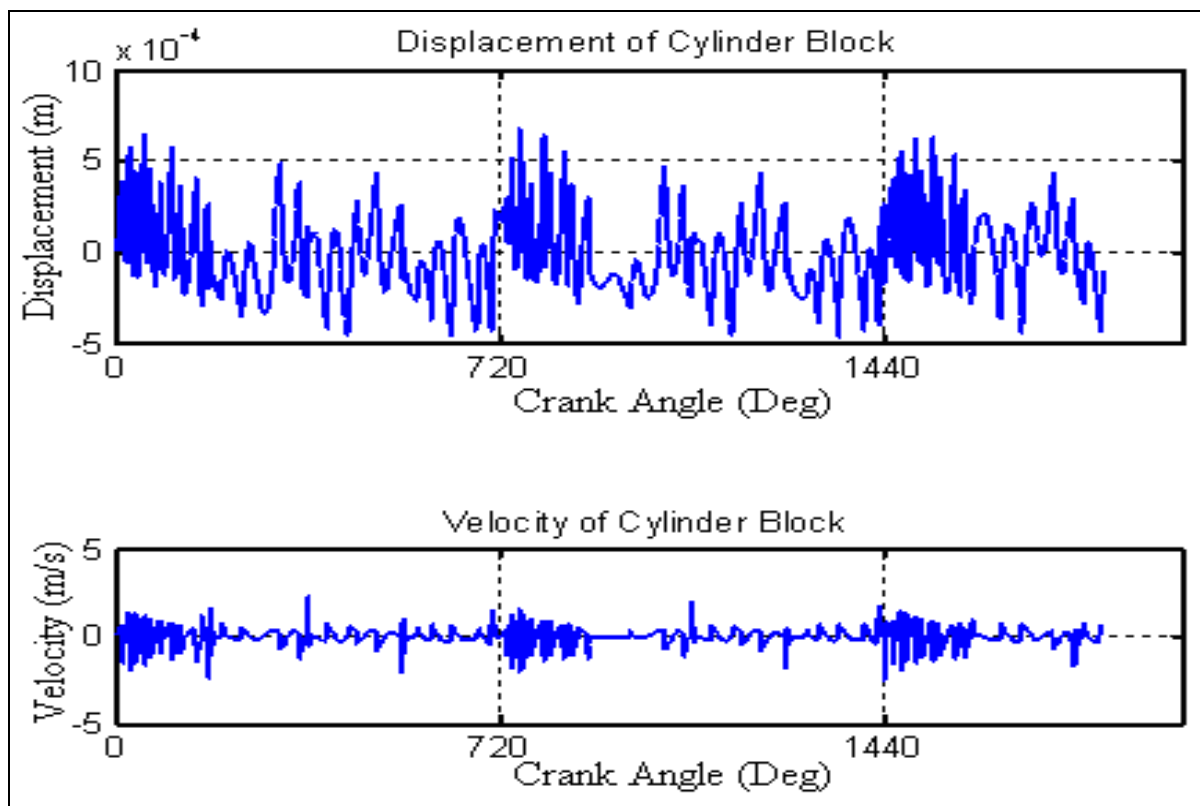


Figure 8.4 Displacement and velocity of cylinder block.

The AE sensor position on the engine cylinder block that produced the largest AE signal was the upper position, followed by the lower and then the mid position. This indicates that AE propagation from the liner to the external surface of the cylinder block occurs best above the water jacket (in this study we mounted the AE sensor above the water jacket).

Figure 8.4 shows the data collected from the AE sensor that was mounted on the upper side of the engine block. This data provides a way of identifying the existence of piston slap and friction, and their intensities; however it is deficient in representing the dynamics of the piston.

From the figure 8.4, a distinct peak is observed at approximately 33 degree ATDC and it is considered that the peak is caused by piston slap. Also, the magnitude of the peak is an indication of the intensity of impact. These observations mean the cylinder block displacement data can be used as a tool in identifying the existence of piston slap (by finding acceleration), and measuring intensity effects due to changes in different engine parameters.

Thus when analysing piston slap data the results will be represented in terms of engine block displacement. Also, oil film thickness measurements can be used when applicable in discerning the dynamics of the piston.

8.5 Engine Friction Measurement

Due to the importance of friction losses in a diesel engine, we have developed a method to measure engine friction loss with high accuracy. In spite of its importance and past endeavours to measure engine friction, its accurate measurement is not easy since the amount of friction is relatively small compared with power dissipated in the brakes or cylinder pressure, and so on. Accurate measurements of the piston assembly friction are an especially difficult and challenging problem and friction measurement of the piston assembly under firing condition remains a challenging problem.

8.5.1 Engine Friction using Conventional Technique

The Indicated power (IP), Brake power (BP) and Friction power (FP) for two engine oils 25w-50 and 10w-30 for an engine operating at eight different test conditions are given in Table 8.1. It was observed that there was a rise in engine friction with the increase in engine speed (rpm) for all conditions, which indicates that speed is one of the most important factors for engine friction. Other parameters on which engine friction depend are engine load, oil viscosity, oil temperature etc.

However, in this case the engine oil temperature was controlled ($90\pm5^{\circ}\text{C}$) for both lubricants so the effect of engine lubricant temperature on friction can be ignored.

Table 8.1 Indicated power (IP), Brake power (BP) and Friction power (FP) for 25w-50 and 10w-30 oils under prescribed engine operating conditions

Engine Speed rpm	Torque Nm	IP (kW)		BP (kW)		FP (kW)	
		Oil 20w-50	Oil 10w-30	Oil 20w-50	Oil 10w30	Oil 20w-50	Oil 10w-30
1000	50	7.31	7.76	5.22	5.24	2.09	2.52
1000	100	11.78	12.38	10.46	10.51	1.32	1.87
1000	200	22.75	22.87	20.91	20.96	1.84	1.91
1000	300	34.58	34.24	31.42	31.41	3.16	2.83
2000	50	20.89	20.44	10.55	10.49	10.34	9.95
2000	100	31.48	31.12	20.98	20.94	10.50	10.18
2000	200	50.60	48.85	41.78	41.83	8.83	7.02
2000	300	68.81	68.20	62.83	62.95	5.98	5.25

At high speed and low load engine friction power is significantly higher (four to five times as great) compared to low speed and low load because the piston ring assembly and bearings are operating predominantly in the hydrodynamic lubrication regime and there is a strong dependence of hydrodynamic friction on engine speed (and oil viscosity). This strengthens the argument that the contribution of hydrodynamic friction in an engine is higher than the boundary and mixed lubrication friction. At low speed, for all load levels (engine operating in boundary and mixed lubrication regime) it was observed that there is marginal change in engine friction between the oils.

$$\text{BP} = \text{IP} - \text{FP} \quad (8.1)$$

At high speed, high load the friction power is reduced to a level comparable to the low speed, high load condition; this may be explained with the help of the well-known fact that the contribution of friction as a percentage of indicated power output reduces as load increases, which is also shown in

Figure 8.5. It may also be decided that the shearing of the oil film's sub-layers would be easier at high speed and high load which helps friction reduction.

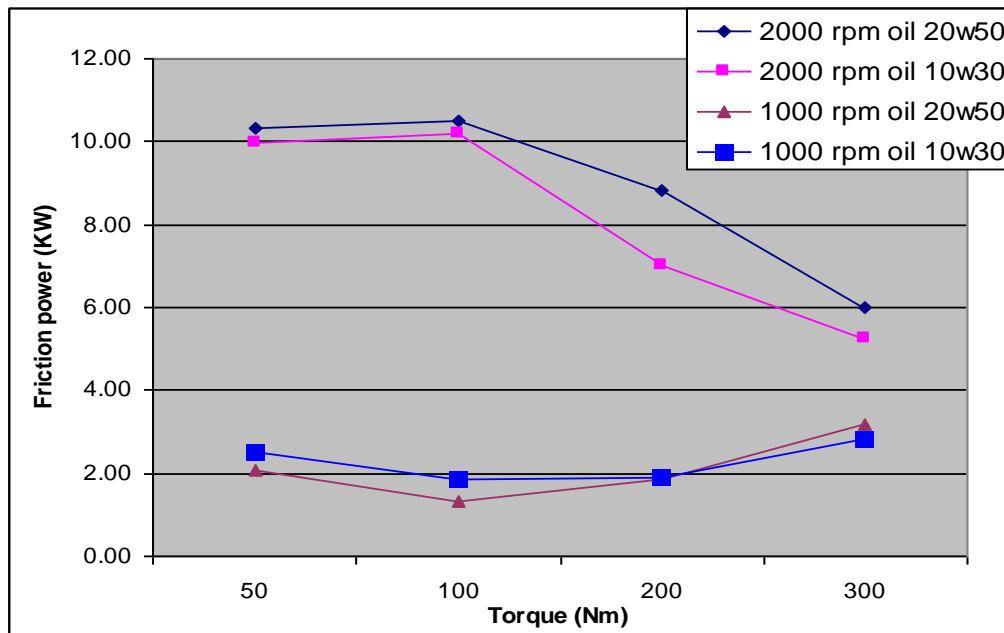


Figure 8.5 Engine friction power at different operating conditions with lubricating oils of 20w-50 and 10w-30.

8.5.2 Brake Specific Fuel Consumption

The brake specific fuel consumption is defined as the fuel flow rate per unit power output. It is desirable to obtain a lower value of BSFC meaning that the engine used less fuel to produce the same amount of work. This is one of the most important parameters for engine development.

Brake specific fuel consumption (BSFC) was calculated at an engine speed of 2000 rpm for loads applied to the engine for both engine lubricants, see Table 8.2. The percentage reduction in BSFC obtained with changing the lubricant to one of lower viscosity was also calculated. Results indicate that there is significant reduction of fuel consumption of an engine when lower viscosity grade oil was used. Similar trends were observed for gasoline test vehicle during a chassis dynamometer study [288].

As we saw in the previous section engine friction power can be reduced by using a lower viscosity grade oil at high speed and at all load points without affecting the engine adversely, which also corroborated by the BSFC results and which showed fuel saving of approximately 2%.

Table 8.2 Brake specific fuel consumption (g/(kW.hr)) of an engine operating at 2000 rpm and different loads (torque)

Torque (Nm)	BSFC (g/(kW.hr))		% Reduction due to change in oil
	10W30	20W50	
50	367.30	372.27	1.33
100	269.74	275.22	1.99
200	256.65	259.26	1.01
300	231.46	234.04	1.10

8.5.3 Friction Measurement Using AE

Friction in the piston assembly is the most complex as large variations in the speed and load occur over a single cycle. Friction arises because both the piston rings and the piston skirt rub against the cylinder liner. The rings are loaded against the liner through pre-tension and under the effect of the in-cylinder pressure. The skirt will tend to lean against the liner as a result of the reaction of the connecting rod. It is generally assumed that the piston skirt is in the hydrodynamic region of the lubricating oil throughout the engine cycle. The piston rings have a more complex operation and when the piston is at mid-stroke, hydrodynamic lubrication occurs.

As the piston approaches TDC or BDC, the reduction in speed causes the oil film to break down. At TDC combustion, this is enhanced by the build-up of the cylinder pressure, which increases the loading further. This has been observed by measuring the frictional force acting on the cylinder liner; a spike is seen around TDC and BDC, characteristic of a move into the mixed and boundary-lubrication regimes. Overall, piston friction occurs mainly in the hydrodynamic regime and is therefore highly sensitive to the lubricant viscosity.

Figure 8.5 shows the indicated power vs load for two speeds and the two types of oil. An increase of engine speed means an increase in power for a given load, and an increase in load for a given speed also means an increase in power. There appeared to be very little change in power with change in oil. The rate of increase of power appears to be slightly larger for the higher engine speed.

Figure 8.6 shows engine friction power vs load for two speeds and the two types of oil. It can be seen that friction power is greater at the higher speed and for the range considered speed has a more pronounced effect on the friction power than load. This may show that the increase in cylinder pressure (i.e. load) does not lead to as much increase in friction as an increase in cylinder speed. This means that the high peaks of the thrust force at TDC, shown in Figures 8.2 and 8.3, result in less friction and hence less AE effect, than speed changes.

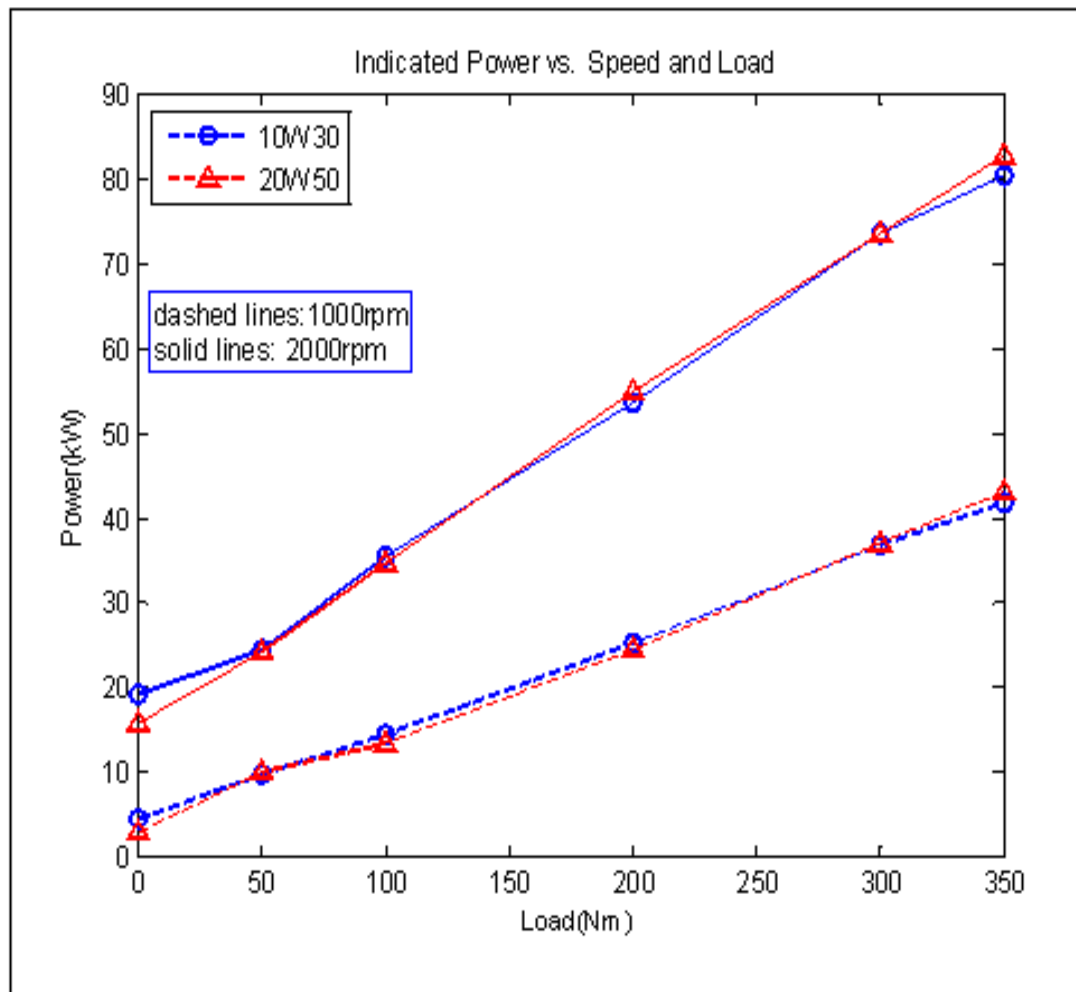


Figure 8.6 Indicated power vs. load at engine speeds 1000 rpm and 2000 rpm with lubricating oils of 20w-50 and 10w-30

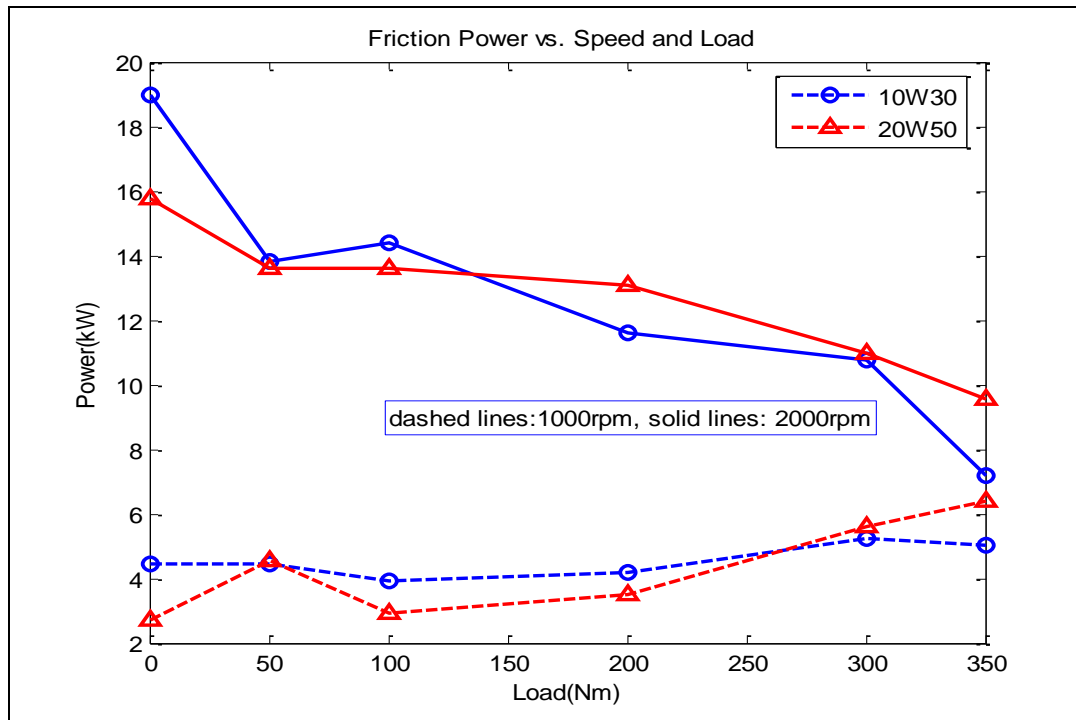


Figure 8.7 Friction power vs. load at engine speeds 1000 rpm and 2000 rpm with lubricating oils of 20w-50 and 10w-30

The results in Figure 8.5 show clearly that the low quality oil consumes more power than the other. This confirms that oil quality has a significant influence on engine performance. It is difficult to differentiate between the oil type in the results for friction power, although 20W50 shows marginally less friction power in the load range of from 50Nm to 250Nm at 1000 rpm (see Figure 8.6), which is to be expected because it has higher viscosity. During the tests, the oil and water temperatures were maintained at $90 \pm 5^\circ\text{C}$.

There are many sources of mechanical friction losses beside piston assembly friction (such as main bearings, water pump, oil pump, etc.).

Figure 8.7 shows the relative friction power vs. load curves at two different engine speeds 1000 rpm and 2000 rpm with lubricating oils of 20w-50 and 10w-30. In these tests the friction losses of the water pump, oil pump, and other mechanical parts are taken into account. The friction of the water pump and the timing chain are included in the camshaft assembly loss. The oil pump friction is included in the crankshaft assembly loss. In Figure 8.7, the piston assembly friction is responsible for about 45% of the total engine friction losses, (see Section 4.2.2). As expected, the crankshaft

assembly friction loss increased with increasing engine speed. This means that the dominant friction mechanism of the crankshaft assembly was in the hydrodynamic region.

The camshaft assembly friction losses also increased, as the engine speed increased, but not as strongly as for the crankshaft assembly. This can be explained because the main lubrication regime of the camshaft assembly is boundary or mixed lubrication. The friction losses of the piston assembly decrease with increasing speed in the low speed regions but increase in the high speed regions. That is, as expected, at low engine speeds the piston assembly friction shows that the boundary and mixed lubrication characteristics are dominant. However, as the engine speed becomes higher, the dominant lubrication mechanism is converted to hydrodynamic. From these considerations it can be deduced that the hydrodynamic friction force between two states (between two regions/regimes of the oil), would be different and can affect such piston dynamics such as slap and secondary motion.

While examining the friction results it is important to bear in mind that the measured piston assembly frictional force is the summation of four main components: two compressions rings, an oil control ring, and the piston skirt. Therefore a change in a variable may produce different and even conflicting effects for each component. For example at moderate lubricant temperatures the piston skirt operates in the hydrodynamic regime whereas the piston rings operate in the boundary to hydrodynamic lubrication regimes. Any increase in lubricant temperature would bring the piston ring lubrication conditions more towards boundary, increasing the friction loss whereas decrease in viscosity would reduce the friction contribution from the piston skirt owing to a reduction in shear loss.

At low oil temperatures at the start of the power stroke the piston assembly friction is high because of severe lubrication conditions, resulting in boundary lubrication but, as the piston picks up velocity, just before and after mid-stroke, the friction decreases owing to a high entraining velocity dragging more lubricant into the piston–liner interface.

Thus the piston–liner interface enters the hydrodynamic lubrication regime. At mid-stroke, the entraining velocity is high and under hydrodynamic lubrication conditions, this results in an increase in friction due to a high shear rate. A similar picture can be seen for other piston strokes.

At high temperature, because of severe lubrication conditions, a sharp rise in friction can be usual at the start of the power stroke. Also the friction at the start and end of each stroke is high as the film thickness in this region is relatively small because of a low entraining velocity and low lubricant viscosity, but at mid-strokes there is a slight decrease in friction. One of the main factors

responsible for the difference in friction loss during upward and downward piston strokes is the flow and availability of lubricant on the liner surface, as the piston uncovers and covers the liner. The flow and availability of lubricant is also dependent on the engine speed. The friction contribution from skirt–liner interaction is mainly due to shear loss, as evidenced by a continuous decrease in power loss as lubricant temperature increases at any engine speed.

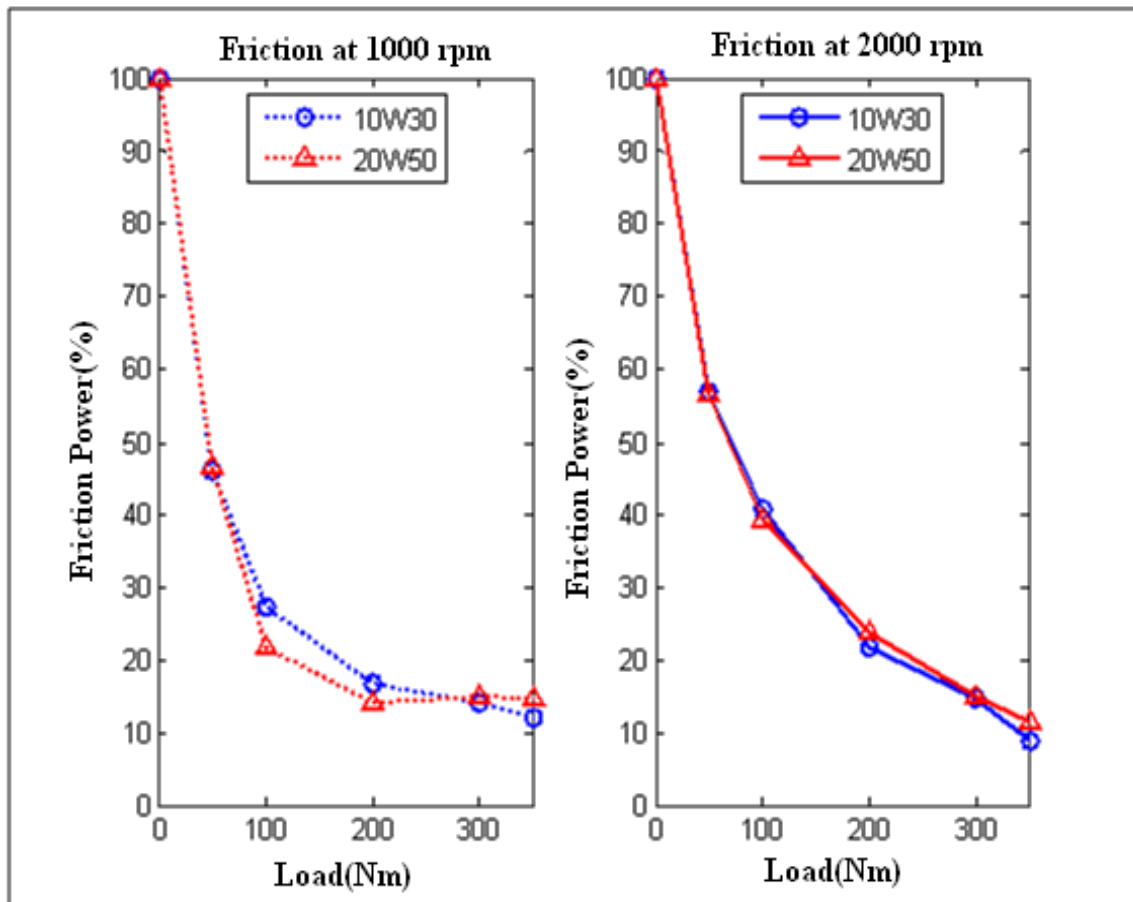


Figure 8.8 Relative friction power vs. load at two different engine speeds 1000 rpm and 2000 rpm with lubricating oils of 20w-50 and 10w-30

8.5.4 Indicated Mean Effective Pressure Measurements

The Indicated Mean Effective Pressure (IMEP) method can determine the piston assembly friction force from the measured cylinder pressure, the connecting rod force, and the piston assembly inertia

force. For the measurement of the connecting rod force and the piston assembly inertia force, information about the piston dynamics is needed.

The measured piston friction force cannot provide any information about the lubrication mechanism. That is, the measured piston assembly friction using the IMEP method includes lots of information, such as piston viscous lubrication friction components, mixed lubrication friction components, and piston skirt friction. In addition the friction measurements using the IMEP method result in a very accurate measurement of forces acting on the complete piston assembly, but it is necessary to include the piston assembly inertial force and assume that the zero degree is the engine TDC position, the start of the power stroke. The sudden change in the sign of the frictional force at the end of each stroke is due to the change in the direction of piston travel. It was seen that, at low lubricant temperatures, there is a slight drift at the end of the compression stroke (between 675 and 720 degrees), causing the frictional force to cross the zero datum line slightly. The effect was reduced considerably at higher lubricant temperatures.

Figure 8.8 is for a lubricant temperature of about 90°C, because of severe lubrication conditions a sharp rise in friction can be seen at the start of the power stroke. Also the friction at the start and end of each stroke is high as the film thickness in this region is relatively small because of a low entraining velocity and low lubricant viscosity but at mid-stroke there is a slight decrease in friction. At any engine operating condition, the maximum friction takes place at the start of the power stroke as the lubrication condition at this point is in the boundary regime owing to the peak combustion pressure. At the end and start of each stroke the piston–liner friction is more towards boundary lubrication, whereas at mid-stroke it is generally hydrodynamic because of the relatively high entraining velocity.

Some factors affecting IMEP are [289]:

1. Compression ratio,
2. Air/fuel ratio,
3. Volumetric efficiency,
4. Ignition timing,
5. Valve timing and lift, and
6. Air pressure and temperature.

In the IMEP method, the piston pin friction force was neglected when calculating the piston friction force from the measured pressure force, connecting rod force, and the inertia force. The piston pin

exerts a frictional force on the piston assembly and affects the piston friction force and dynamics. However, it is very difficult to measure the piston pin friction force.

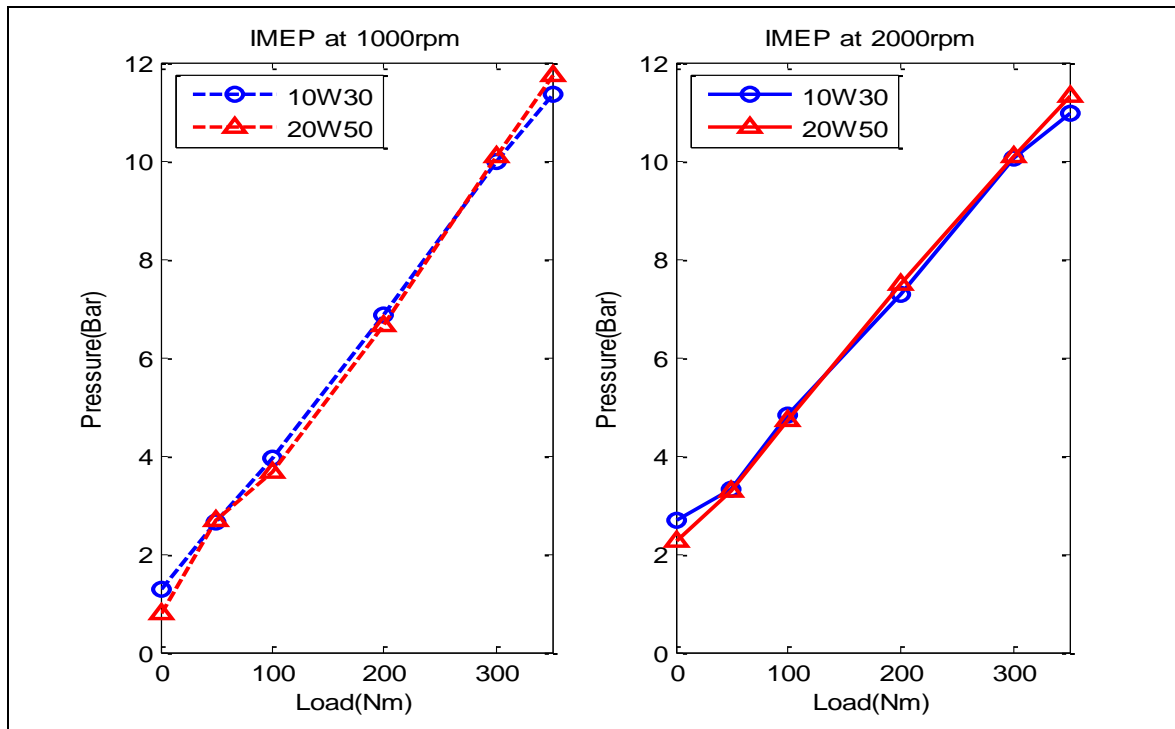


Figure 8.9 IMEP vs. load at two different engine speeds 1000 rpm and 2000 rpm with lubricating oils of 20w-50 and 10w-30

8.6 Lateral Force on Piston

The lateral force transmitted from the wrist-pin to the piston is defined by the lateral force balance on the wrist-pin (see Figure 5.4). This force, combined with the lateral pressure force around combustion TDC, drives the piston's lateral motion while its interaction with the cylinder bore constrains it, and supports the driving force. The contribution of gravity is negligible.

The lateral displacement and lateral impact velocity of the piston are initially unknown, and solved for iteratively based on satisfying a lateral force balance on the piston. The piston tilt significantly impacts both the lateral pressure force generated around combustion TDC, and the piston-cylinder bore clearance distribution.

During the intake and exhaust strokes there are significant fluctuations in the wrist-pin force due to the wrist-pin and connecting rod inertias, and corresponding fluctuations in the cylinder force due to

these plus the added effect of piston inertia. These fluctuations are due to the fact that at light loads, the component's lateral inertias are significant and the elastic piston tends to bounce on the rigid cylinder bore during piston slap. It is expected that, in the physical system, oil would significantly damp out this motion. At higher loads, the piston's tendency to bounce is significantly reduced as the piston's inertia becomes negligible compared to the large driving force.

As shown in Figure 8.9 (upper one), the force supported at the piston-cylinder bore interface is essentially a function of combustion chamber pressure and connecting-rod angle. In the absence of a significant amount of interference, variations in the side force driving the piston's motion, from the ideal function of pressure force are:

1. Piston and wrist-pin axial inertias lead to a difference between the pressure force on the piston, and the axial force on the connecting-rod. The balance of combustion chamber pressure and component inertias can significantly shift the timing of mid-stroke piston slap during the intake and exhaust strokes.
2. The angle at which the connecting rod acts generates a lateral force from the axial load.
3. Connecting rod inertia and wrist-pin friction shift the moment balance on the connecting rod, altering the angle of action of the connecting rod force and the resulting lateral force on the connecting rod. The wrist-pin friction does not significantly impact the lateral force transmitted to the piston. Connecting rod inertia can significantly shift the timing of mid-stroke piston slap, and in high speed, low load running conditions, increasing component inertias significantly change the lateral force as they become more significant compared to the pressure load.
4. The wrist-pin lateral inertia introduces further fluctuations in the lateral force. These fluctuations, and those due to lateral motion of the connecting rod small end, are dependent on the detailed piston cylinder bore interface interactions, and can be considered to represent a significant source of uncertainty in the motion of the system.
5. The lateral component of the combustion chamber pressure force can become significant around combustion TDC, but is highly dependent on piston tilt.

The side force driving the piston's motion is the side force that must be generated at the piston cylinder bore interface by the net lateral force on the piston. The piston's inertia introduces additional fluctuations to the piston cylinder bore interface force, and the translation of the piston

across the cylinder during piston slap interrupts this force, particularly in the upper section of the cylinder bore where there are significant clearances.

Piston slap begins to occur when the side force driving the piston's motion changes sign. The timing of this sign changes and tends to occur for two reasons:

1. The axial force transmitted through the components changes sign. This tends to occur at mid-stroke during the intake and exhaust strokes as the inertia and pressure force terms balance, but may also occur in the compression or expansion strokes at high speed, low load running conditions. The exact timing is dependent on the pressure trace.
2. The connecting-rod angle changes sign. The timing of this is a function of the engine's geometry, and for an engine with no crankshaft offset will be 0° , 180° , 360° and 540° crank angle. There is a small shift in this timing due to the fact that the wrist-pin connecting rod force does not lie along the connecting rod axis.

There is a small delay between the initiation of piston slap, and the piston actually leaving the cylinder bore surface. The piston may then translate freely across the cylinder, during which time there is no piston cylinder bore interface force, before making contact with the other side of the cylinder bore. In cases where there is an interference fit, the piston will remain in contact with both sides of the cylinder bore throughout this process. It is possible, even without an interference fit, for the piston to remain partly in contact with each side of the cylinder bore if there is sufficient tilt.

There are many uncertainties in the interface force at the piston cylinder bore which affect the detailed distribution of the force. These uncertainties include [289]:

1. Local surface geometry,
2. Asperity contact force,
3. Friction coefficient, and
4. Oil film thickness.

The impact force on the major thrust side is considerably larger than the corresponding values on the minor thrust side. This is because the offset position of the wrist-pin creates a larger clearance on the major thrust side, thus the impact velocity is greater there. This is analogous to a ball falling upon an oily plate from a greater height resulting in a larger impact force. It can be observed that, on the major thrust side, the contact force attains its maximum value at the maximum combustion pressure.

As the contact force dramatically decreases on the major thrust side, the corresponding value on the minor thrust side begins to increase at around the crank angle of 60° , which is nearly one-third of

piston travel in the down-stroke sense. From the Figure 8.9 we can see that at the TDC a lateral displacement has resulted in an almost aligned piston orientation (see figure for the crank angle of 0°). As the piston moves downwards, the lateral displacement increases dramatically with rising pressure towards the major thrust side, culminating in a lateral displacement, and a corresponding tilt towards the major thrust side.

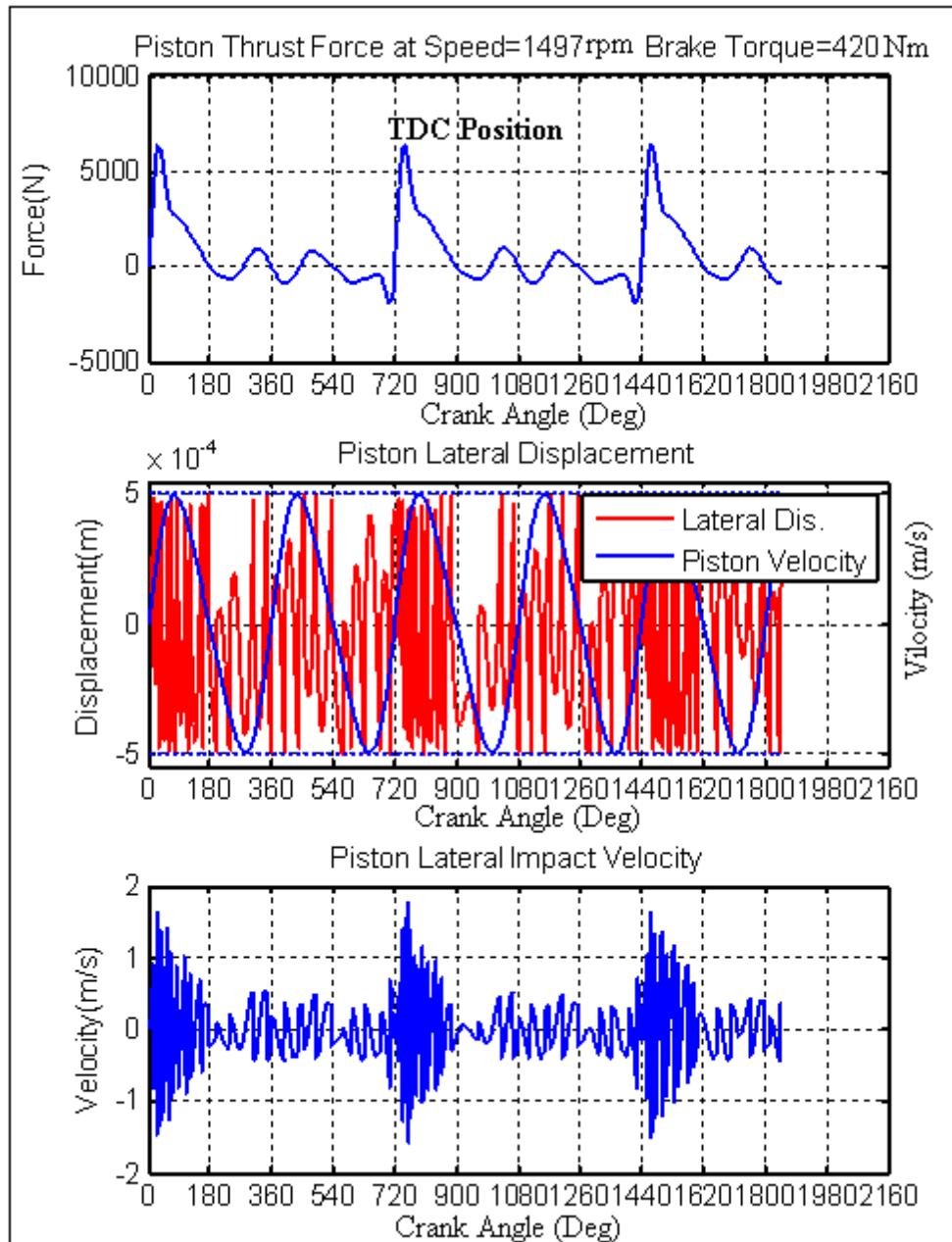


Figure 8.10 Piston lateral force, lateral displacement and lateral impact velocity.

These motions are responsible for the high thrust force. After combustion (maximum pressure) the piston tilting motion reverses in deal with rapid emergence of clearance on the major thrust side (i.e. a reduction in rigid body approach with respect to the major thrust side). The piston continues in this manner, where the combination of lateral minor thrust and reversal of tilting motion away from the major thrust side leads to the diminution of the gap on the minor thrust side, and this is the reason for the emergence of increasing contact forces on the minor thrust side. From mid-cycle, at 90° crank-angle, the lateral motion reverses to one approaching the minor thrust side. This is indicated in Figure 8.9 by the negative values of lateral displacement. At the same time, the tilt angle is generally reducing, until a totally aligned configuration is observed at the BDC, as expected. This is where the few undulations in the tilt angle are due to increased lubricant reactions due to the approach of the piston towards cylinder bore on the minor thrust side.

On the upstroke of the piston from BDC (i.e. for crank-angles greater than 180°) the piston aligns itself to the minor thrust side with small tilt angles due to low combustion pressures. The inertial dynamics of the engine displaces the piston laterally towards the major thrust side. At 360° the power stroke cycle is complete. The tilt angle and the corresponding lateral displacement values at 0° and 360° should ideally be the same, if the transient analysis is to yield a repeatable cycle. It is clear that a number of such cycles should be included in the transient analysis but due to the computational time and memory constraints, it was clear that such an undertaking was impractical and that a clear picture of transient contact behaviour should emerge with the initial analysis. Any further extension of the analysis can only lead to refinement of the results in a quantitative sense, but not for the fundamental understanding of the physical phenomena.

8.7 Influence of Gas Torque on the Piston

The gas torque signal is a very important signal for power train control. The gas torque is affected by many different sources such as fuel injection, air quantity, oil temperature and so on. The maximum torque value represents the maximum pressure in the cylinder during the combustion stroke.

As a consequence of the large fluctuations in engine torque during the cycle, the variations in the rotational speed are obvious in Figure 8.10; the sudden drop in the piston velocity and its subsequent increase can be linked with the negative and positive peaks of the gas torque. The amplitudes of the cyclic speed fluctuations tend to increase as the mean engine speed decreases owing to the fact that at low engine speed the cycle time is long and the engine deceleration at the

end of the compression stroke is dominant and vice versa. This is a very important criterion in making compromises between the flywheel size, the engine speed of response and the engine low idle speed limit.

As shown in Figure 8.10, the cylinder pressure is quite similar at different engine speeds. The combustion pressure can result in significant radial deformation of the piston, relative to the piston cylinder bore clearance, particularly close to combustion TDC. The upper portion of the piston is deformed outwards, while the lower portion bends in the soft, central portion of the skirt bends further inwards than the more rigid outer edge. Pressure deformation becomes significant over the compression and expansion strokes.

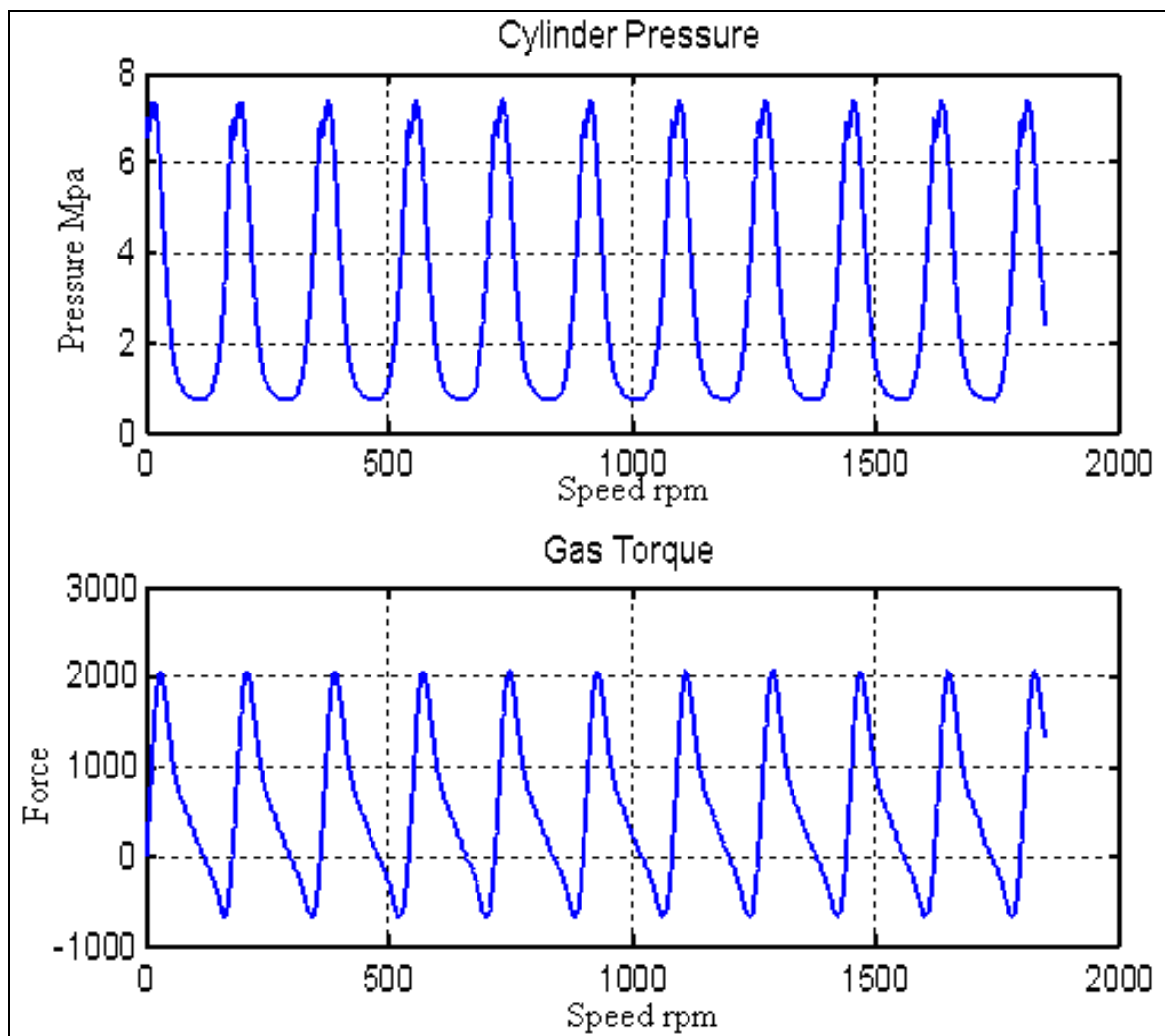


Figure 8.11 Cylinder pressure and gas torque.

Thus, the effect of engine speed on the friction force of the piston assembly is complicated by the effect of engine speed on cylinder pressure, in addition to the direct dependence on engine speed. Basically, it is known that the gas pressure behind a ring provides the major contribution to the sealing force. Thus, in the case of the top compression ring the gases in the combustion chamber pass down the clearance space between the piston crown land and the cylinder liner and then into the top ring groove to load the rear face of the ring. Thus, this top groove pressure affects the piston ring assembly friction since the high groove pressure exerts piston ring side force and increases the normal load of the ring against the cylinder liner. It is usual in lubrication analyses of piston ring packs to assume that the pressure in the top ring groove is at all times equal to the combustion chamber pressure.

8.8 Influence of Inertia and Gas Torques on the Piston

The inertia of the engine will affect its performance. For real-time monitoring and control of the engine the torque produced by a cylinder will have two components, the gas pressure torque and the reciprocating inertia torque. The gas pressure torque depends, almost exclusively, on the engine load and could vary from cylinder to cylinder even under steady-state operating conditions. The reciprocating inertia torque depends only on engine speed and is fairly uniform for all cylinders. Under steady-state operating conditions, the total torque corresponding to a given cylinder, may be considered a periodic function of time (crank angle). Figure 8.11 represents the resultant inertia and gas torques throughout the cycle for several engine speeds. As expected, the inertia torque has the same magnitude at any engine speeds. The resultant torque between gas and inertia has similar fluctuations at different engine speeds as seen in the figure.

The resulting friction force of the piston assembly can be computed using information concerning the pressure force, the connecting rod force, and the inertial forces of the connecting rod and piston assembly. The friction torque can be calculated from the measured inertia torque and the gas pressure torque.

From Figure 8.11 the axial inertia result in significant radial deformation of the piston, relative to the piston cylinder bore clearance, particularly at TDC and BDC. Negative axial acceleration results in a positive axial inertia force, deforming the piston upwards. The lower portion of the skirt is deformed outwards while the crown bends inwards, and the soft, central portion of the skirt bends further outwards than the more rigid outer edges.

Although the values of inertia torque and pressure torque are zero, the friction torque at each crank angle is the resultant torque generated by inertia, cylinder pressure, and friction. Thus, the inertia and pressure torque influence the instantaneous torque at each crank angle and therefore, the inertia and gas pressure torque must be considered to allow the friction torque information to be extracted from the measured torque at each crank angle. The total inertia torque is just the sum of linear inertia torque and angular inertia torque.

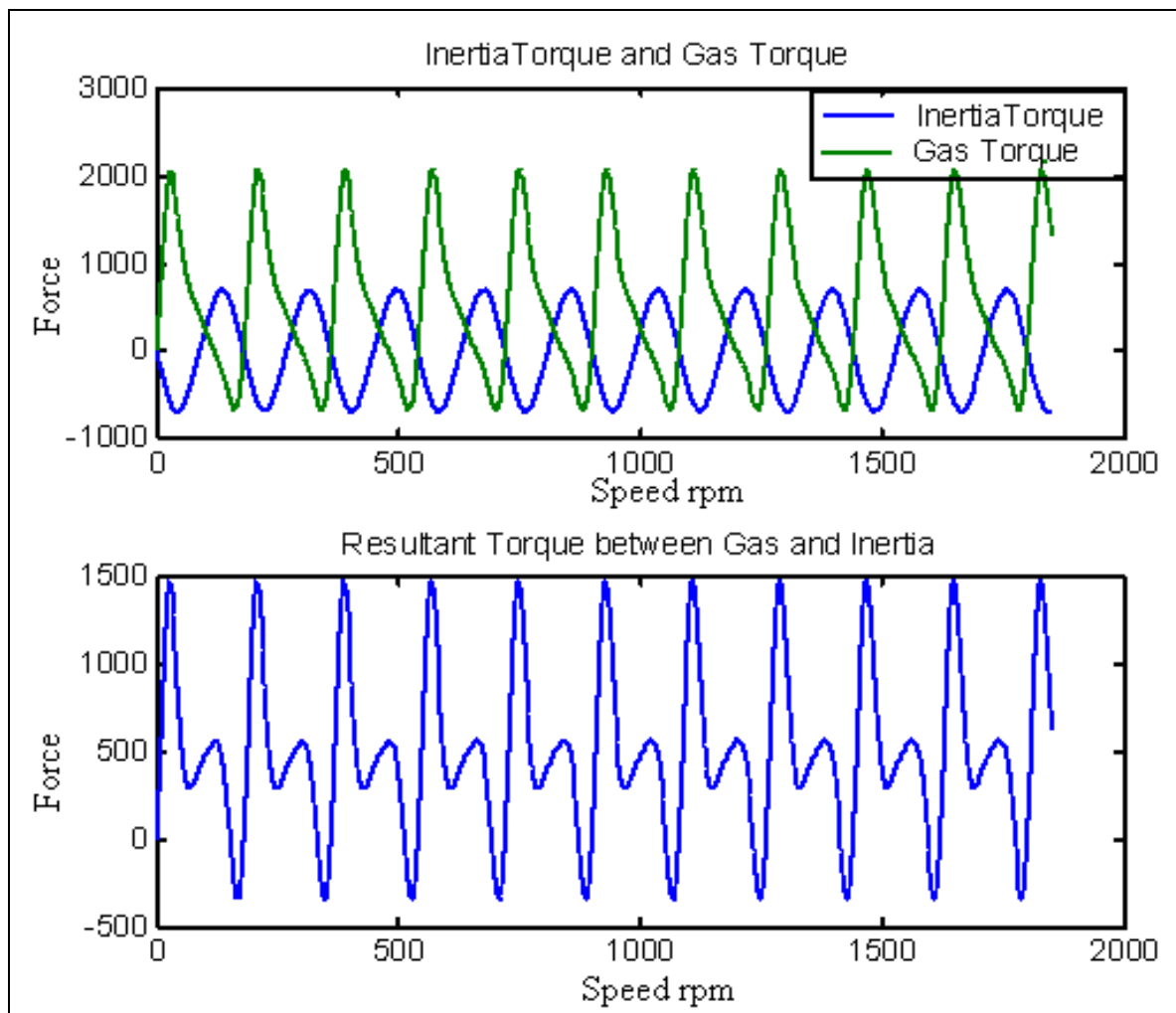


Figure 8.12 Inertia, gas and resultant torques.

8.9 Lubricant Chemistry

Lubricants are the result of a base stock which can be of either mineral or organic origin and a collection of additives which represent only a small fraction of the final product [67]. Diesel engine

oil viscosities are highly dependent on the temperature and decrease exponentially with increasing temperature [289]. The relationship between the viscosity and the temperature is quantified by the viscosity index (VI) which is an arbitrary scale assessing the change in viscosity between 30 °C and 100 °C. Ideally the scale of the VI should be 0–100 °C. To perform satisfactorily in an engine oils now should have VI levels above 150. To achieve this, additives known as viscosity modifiers or viscosity index improvers can be used. These are polymeric molecules that have a temperature-dependent structure; at low temperatures, they coil into a ball and have little effect on the fluid viscosity but, at high temperatures, they uncoil and become surrounded by oil and considerably increase the oil viscosity. Figure 8.12 shows the kinematic viscosity–temperature relationships for two oil types. As can be seen their viscosities decrease similarly with increasing temperature. 10W-30 type decreases much less with increasing temperature compared with 20W-50.

There are some important additives which are designed to improve boundary-lubrication characteristics, reducing the friction coefficient on the extreme left-hand section of the Stribeck curve (Figure 5.1). These molecules have a polar constituent that attaches to the lubricated surface, while organic chains in the molecule absorb a layer of oil. They are very effective at reducing friction in boundary lubrication as long as the temperature does not rise so as to cause decomposition of the molecule or desorption of oil on the surface. Some other additives necessary in lubricating oils are sometimes used.

To calculate the viscosity of a given lubricant at any temperature the Vogel equation (8.2) may be used for straight weight oils.

$$\nu = k \cdot \exp\left(\frac{\theta_1}{\theta_2 + T}\right) \quad (8.2)$$

Where k , θ_1 and θ_2 are constants determined for each lubricant with units of cSt for k and °C for θ_1 and θ_2 . T is the temperature of the lubricant in °C, and ν is the kinematic viscosity at the desired temperature in cSt.

There were differences in results which may be due to operating conditions (loading, temperatures, soot contamination, etc.) and which highlight the difficulty of performing accurate testing in this area.

Figure 8.12 indicates the effect of temperature on the oil viscosity of the two test engine oils. The oil viscosity is much lower when it is warmer. As shown in Figure 8.12 at 30°C the oil viscosity

could be ten times higher than for fully warmed up conditions (90°C). Thus, with hot oil the duty parameter (viscosity*speed/load) in the Stribeck curve is reduced and there is a greater possibility for boundary or mixed lubrication than for hydrodynamic lubrication in the piston assembly friction.

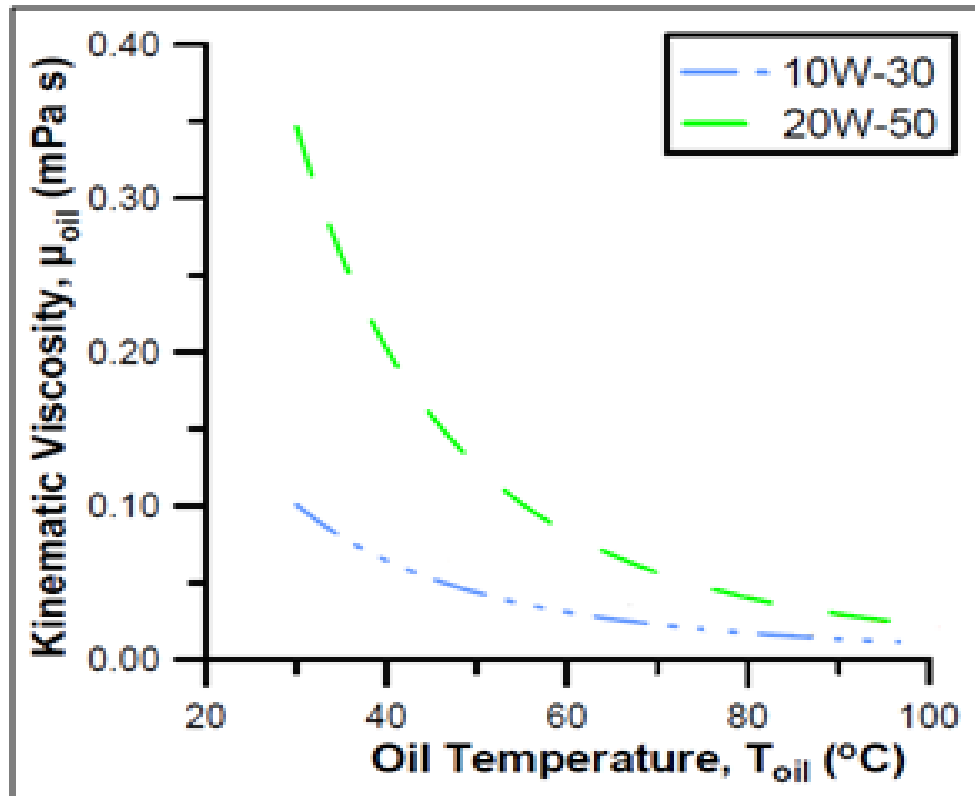


Figure 8.13 Kinematic viscosities vs. oil temperature for the two types of lubricating oil [287].

8.10 Piston and Wrist-Pin Motion

8.10.1 Lateral Motion

The lateral motion of the piston is driven by the wrist-pin lateral force, and constrained by the piston cylinder bore interface. The side force is essentially a function of the axial pressure load on the piston and the connecting rod angle, with shifts due to component inertias. It is expected that the side force on the piston will change sign for two reasons:

1. When the connecting rod angle changes sign, which for an engine with no crankshaft offset is at 0, 180, 360 and 540 crank angle degrees.

2. When the axial load on the connecting rod changes from compression to tension, which is determined by the pressure trace and component inertias, and typically occurs about mid-stroke during the intake and exhaust strokes.

8.10.2 Tilt

Piston tilt is determined by the moment balance on the piston, about the wrist-pin axis. The wrist-pin friction moment tends to drive piston rotational motion approaching combustion TDC, while the friction and normal moments at the piston cylinder bore interface, combined with the piston's rotational inertia, determine the tilt during intake and exhaust strokes. All four are significant during combustion. In some cases, particularly when there is wrist-pin offset, the combustion chamber pressure moment will also significantly affect piston tilt around combustion TDC, and can be used to counter-act the wrist-pin moment.

Approaching combustion TDC, the connecting rod is rotating clockwise (negative), and drives both the wrist-pin and the piston to rotate clockwise, decreasing piston tilt. The large loads on the wrist-pin bearings at this point result in a large negative moment being applied to the piston. At TDC the side force on the piston goes to zero and piston slap is initiated. As the piston travels across the cylinder bore it rotates rapidly clockwise until contact is made on the upper portion of the skirt, generating a very large positive moment, which in turn results in rapid, anticlockwise rotation of the piston and brief oscillation until the tilt reaches a stable positive tilt.

Piston tilt throughout the rest of the cycle is determined by the balance of normal and friction moments created at the piston cylinder bore interface, and the piston's rotational inertia. This balance is very sensitive to the point of action of the normal force at the piston cylinder bore interface, which in turn is dependent on the local geometry.

Oscillations occur as the piston hits the cylinder bore at an angle, and then rotates, over correcting, to find its balance point. To complicate matters further, the piston profile is significantly changed by radial deformation due to combustion chamber pressure, axial inertia, and contact with the cylinder bore.

As can be seen in Figure 8.13, in the absence of significant wrist-pin and pressure moments, the "stable" piston tilt (neglecting oscillations) is a function of:

1. Deformed piston geometry: The location of the minimum clearance point and the slope of the profile determine the amount of tilt required to shift the point of action of the contact force,

2. Cylinder bore geometry: The average cylinder bore gradient, over the load bearing area of the piston, significantly contributes to piston tilt, and
3. Piston cylinder bore friction coefficient: Around combustion TDC, the significant friction moments generated affect piston tilt, while throughout the rest of the cycle it was found to have very little effect.

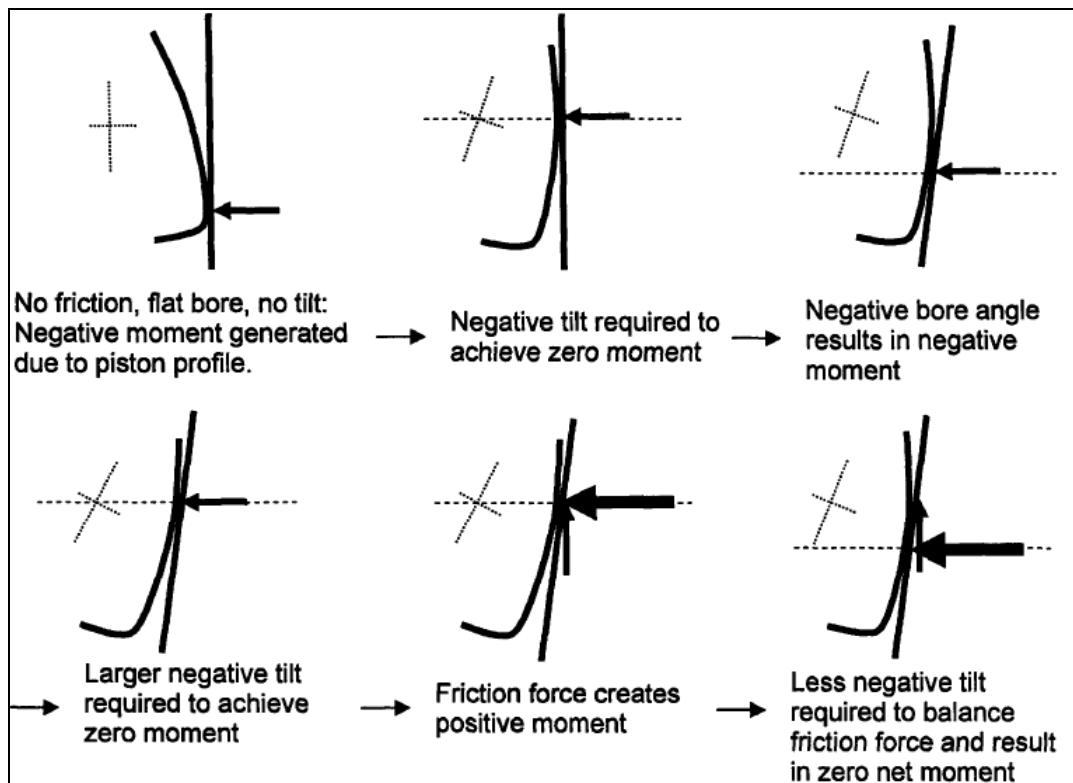


Figure 8.14 Stable piston tilts [289].

8.11 Summary

Fuel economy of large, diesel engines is critical performance metric for engine manufacturers. Demands for increased fuel economy are coupled with corresponding improvements in engine performance, durability, and emissions. One method of improving fuel economy is to reduce the losses due to mechanical friction within the engine. Mechanical friction accounts for between 10% and 15% of the indicated work output of the engine. Reductions in mechanical friction directly improve engine thermal efficiency and fuel economy.

The angular motion of the piston is driven by the friction moments at the piston wrist pin and piston cylinder bore interfaces, and the moments generated by the pressure force and piston cylinder bore side force. In the absence of wrist-pin offset, the wrist-pin friction moment dominates this moment balance approaching combustion TDC until piston slap occurs, at which point the piston interactions with the cylinder bore also becomes significant. Away from combustion TDC, where the loads transmitted through the system are much smaller, the piston is essentially searching for a stable position on the cylinder bore where the side force and friction force moments will balance. The oil film thickness plays a significant role in piston tilt, effectively changing the geometry constraining piston motion, and resulting in larger tilt, particularly during piston slap and an increase in land contact at combustion TDC.

Accurate determination of the friction generated at the piston cylinder bore interface continues to pose a significant challenge. The oil film thickness can have a significant effect on reducing friction generation at the piston cylinder bore interface, but the accuracy of these results come into question when we compare the different surface representations, particularly approaching combustion TDC and throughout the expansion stroke, where there significant variations in the friction predicted.

The net normal force generated by the piston cylinder bore interface is relatively by the lateral wrist-pin force, the proportion of it that can be supported by hydrodynamic vs. asperity contact pressure is not. At small clearances, small variations in surface geometry or piston deformation may result in significant variations in the hydrodynamic and asperity contact pressure, and corresponding changes in the resulting contact friction.

Further investigation is required to determine the degree of accuracy that can be placed on friction predictions.

CHAPTER NINE

CONCLUSIONS AND RECOMMENDATIONS FOR FUTURE WORK

This chapter summarises the research work described in this thesis achievements and relates them to the objectives as defined in section 1.5.2. The key conclusion is that useful information for detecting and diagnosing faults can be extracted from the acoustic emission signals from a diesel engine, in a normal laboratory environment without the necessity for any testing. More importantly most of the used techniques and signal processing methods are inexpensive and their limitations and drawbacks are well defined.

The chapter ends by addressing areas of future work that would helpfully extend some of the main topics such as the mathematical model developed in this thesis.

9.1 Review of Research Objectives and Achievements

9.1.1 Overview

The primary incentive for the work in this thesis has been to address the growing requirement for a system that can monitor running conditions at the piston assembly and cylinder liner contact in four-stroke diesel engines. The possibility of achieving this through analysis of non-intrusive AE measurements has been investigated since prior work indicated a sound technical basis. AE monitoring has previously been found to be an effectual tool for examination of other engine processes [61, 67, 73, 85-109], furthermore, the friction and wear processes expected to occur at the piston, rings and liner contact and slap impact occur at piston skirt and liner contact are known AE generating sources [129-140] and finally, it has been shown that AE signals propagate from the internal liner surface to the external engine surfaces where measurements can be made [111].

In this work a number of tests were conducted on a JCB four-stroke diesel engine where the effect on AE generation at the piston, rings and liner contact of parameters such as piston sliding speed, piston skirt friction, piston impact forces and lubricating oil were evaluated in order to clarify and understand the AE source mechanisms.

Discussions of results from the separate tests have been presented in the previous Chapters. The conclusions from all chapters are brought together in this Chapter to clarify what has been achieved. Overall conclusions regarding monitoring of the diesel engine are then drawn and implications for application towards engine monitoring are discussed. This Chapter closes with recommendations for future work.

9.1.2 Objectives and Achievements

The achievements of this research are outlined in this section. The research focused on the diesel engine condition monitoring via the analysis of its acoustic emission signals. Both theoretical and experimental work was carried out. A variety of signal processing techniques were used to extract useful information from the generated AE signals about the engine condition and to detect and diagnose certain quantified seeded faults. This was achieved in a typical untreated engineering laboratory. The main achievements of this work are presented below in the same order they appear in Section 1.5.

Objective 1: To review condition monitoring of diesel engines.

Achievement 1: A review of CM generally and for diesel engines in particular was presented in Chapter 1, Section 1.4 preceded by a general introduction to the procedure for implementing a diagnostic system.

Objective 2: To review the diesel engine's principal faults and practical condition monitoring techniques used to monitor and evaluate these faults.

Achievement 2: A review of the CM of the diesel engine and engine fundamentals were presented in Chapter 2, Section 2.4 preceded by a general introduction to the field of CM. An overview of the frequency of occurrence of the principal diesel engine faults was given in Subsection 2.4.1, followed by an introduction to the CM techniques most commonly used to detect and diagnose these faults.

Objective 3: To study diesel engine AE sources and to investigate what information can be extracted from AE measurements regarding engine operation. This necessitates an evaluation of AE signals acquired from the AE sensor with the aim of correlating features in the AE signals to actual events occurring within the engine.

Achievement 3: A review of AE generation and how it can be measured and analysis to provide information useful for CM of diesel engines was presented in Chapter 3. The use of AE for engine CM has been found to offer greater diagnostic capabilities than comparable techniques, due to higher spatial resolutions and signal-to-noise ratios.

Objective 4: To study specifically AE signals arising from the lubrication condition, which is a key element of engine operation and impacts upon engine performance, emissions and reliability and, importantly, is an event which presently lacks a suitable monitoring tool even though a number of techniques have been used in the past. The influence of other engine parameters such as engine speed, load and temperature will be also investigated in order to develop understanding of the source mechanisms responsible for AE generation, and thereby of the aspects of interfacial behaviour which can be monitored.

Achievement 4: The diesel engine as an AE system was introduced in Chapter 4, Section 4.3. The major sources of the acoustic emission signals were presented and discussed in Section 4.3.1, 4.3.2 and 4.3.3, emphasis being given to mechanical impact and friction events generated AE. Section 4.5

discusses the AE measurements and compares the three basic signal processing techniques used for AE data processing: time domain, frequency domain and the time-frequency domain. It is considered useful to provide a brief review of other approaches AE signal processing.

Objective 5: To develop a mathematical model of the diesel engine to be used for CM. The experimental results will be used to verify the model prediction.

Achievement 5: The main concern in this model was the dynamics of the pistons. In Chapter 5 a mathematical model is developed for the numerical simulation of the behaviour of the diesel engine used in the test rig. The model consists of piston equations (displacement equation, speed equation and acceleration equation) and governing equations (piston motion equation, piston ring normal and friction forces, wrist-pin friction equation, cylinder liner support equation, and skirt liner friction equation). The information gained from such simulations can be used to help develop more advanced models for the CM.

Objective 6: To introduce specific quantified faults into the engine and both measure and predict the effects on engine performance.

Achievement 6: A description of the test rig was given in Chapter 6. This included the specifications for the particular diesel engine used and details of the measuring equipment and test system see Figure 6.2.

It was decided in Section 6.6 that, given the relative frequency found in the literature review, the faults that would be introduced in to the engine would be reduction and increase of injection pressure (and a disconnected fuel pipe), and changes in the quality, level and temperature of the oil in the engine. These faults would, of course, influence the combustion process, the pressure pulse it generated and the timing of the impacts of the injection process. The problem which the research programme was to address was whether or not the consequent changes in the AE signal from the engine could be reliably detected and used to diagnose the fault.

AE sensor for the measurement of the AE signal from the engine were integrated with the existing test rig, including the conventional condition monitoring instrumentation already being used; cylinder pressure and injection line pressure.

Objective 7: To apply signal processing methods and techniques (time, frequency and time-frequency domain analysis) to extract fault features for early fault detection and compare their performance.

Achievement 7: Several signal processing methods were applied to the data collected from the AE sensor. Although initial emphasis was focused upon time-domain analysis, data was also examined in the frequency and time-frequency domains. Each of the three processing methods was evaluated for its usefulness in fault detection, diagnosis and assessment of severity level. Attention was also given to the practical implications of the use of the various methods. The results from the AE signal analysis is presented in Chapter 7.

Not only can features from the time domain be relatively directly interpreted, and this is a major benefit of this means of analysis, but they can be used for immediate fault diagnosis. Frequency analysis of the acoustic emission signals while useful for detection of injector faults in misfiring. More advanced means for signal processing included the use of CWT in Chapter 7.

Objective 8: To allow the advanced CM techniques investigated and developed in this thesis to be used for demonstration in educational and training purposes concerning diesel engines.

Achievement 8: A wide variety of computer simulated codes and advance measurement techniques were developed and prepared in this research work, as tools for diesel engine CM. For example the ability of continuous Wavelet Transform (CWT) was presented in Section 7.4.5. Outside the University of Huddersfield there are a number of students and professionals world-wide who have expressed an interest in the work.

Objective 9: On the basis of the investigation conducted in this work to provide useful information to guide future research in this field.

Achievement 9: In this field of research there remains much for any subsequent researcher to undertake. In particular, the development of the mathematical model and application of new signal processing techniques, to further extend this work to CM and fault detection and diagnosis of diesel engines. Suggestions are listed below, in proposed possible future work.

Finally, the author has been able to make a number of presentations and publish a number of papers.

1. **F. Elamin**, Y. Fan, F. Gu and A. Ball, Detection of diesel engine valve clearance by acoustic emission. In: Proceedings of Computing and Engineering Annual Researchers' Conference 2009: CEARC'09. University of Huddersfield, Huddersfield, pp. 7-13. ISBN 9781862180857.
2. **F. Elamin**, F. Yibo, F. Gu and A. Ball (2010) Diesel Engine Valve Clearance Detection Using Acoustic Emission. Journal of Advances in Mechanical Engineering, 2010. ISSN 1687-8132.
3. **F. Elamin**, O. Glikes, F. Gu, A. Ball (2010) The Analysis of Acoustic Emission Signals from the Cylinder Head of a Diesel Engine for Fault Detection. In: CM 2010 and MFPT 2010: The Seventh International Conference on Condition Monitoring and Machinery Failure Prevention Technologies, 22-24 June 2010, Stratford-upon-Avon, UK.
4. **F. Elamin**, F. Yibo, F. Gu and A. Ball (2010) Detection of Diesel Engine Injector Faults Using Acoustic Emissions. In: COMADEM 2010: Advances in Maintenance and Condition Diagnosis Technologies towards Sustainable Society, 28th June-2nd July 2010, Nara, Japan.
5. **F. Elamin**, F. Gu and A. Ball (2010) Diesel Engine Injector Faults Detection Using Acoustic Emissions Technique. Journal of Modern Applied Science, 44 (9). pp. 3-13. ISSN 1913-1844
6. **F. Elamin**, F. Gu and A. Ball (2010) Online Monitoring of Engine Oil Quality Based on AE Signal Analysis. In: School of Computing and Engineering Researchers' Conference, University of Huddersfield 2010, 3rd December 2010, Huddersfield, UK.
7. D. Singh, **F. Elamin**, F. Gu, O. Gilkes, J. Fieldhouse, A. Jain, N. Singh, and S. Singal (2010) Study of friction characteristics of a diesel engine running on different viscosity grade engine oils using conventional and acoustic emissions technique. In: 7th International Conference on Industrial Tribology (ICIT 2010), 2nd - 4th December 2010, Ranchi, India.
8. **F. Elamin**, F. Gu and A. Ball (2011) Diesel engine lubricating oil condition and performance monitoring using acoustic emission measurements. In: 24th International Congress on Condition Monitoring and Diagnostics Engineering Management (COMADEM 2011), 30th May - 1st June 2011, Stavanger, Norway.

9.2 Conclusions

This work has established that continuous AE activity in signal acquired from the cylinder block is related to sliding contact. The potential benefits of this research have important consequence. Particularly considering that the current method assessing piston running condition in engine is limited to the periodic inspections and oil analysis.

On the basis of this research, AE monitoring offers diagnostic information that may be exploited to offer monitoring of engine condition and performance. The question is about finding the way of extracting this information from the signals. The main aim of the analytical methods used in this work was to characterise changes in the signals to aid understanding of the AE source. However, it is possible that these methods can also be used as the basis of a monitoring system. For instance, in the tests conducted on the engine, the AE energy of the signals, where friction was the predominant source as it clearly increased as running conditions deteriorated. Similarly, the gradient of the engine load verses AE energy relation increased. These parameters could be collected where then trended over time or evaluated against a predetermined knowledge archive in order to identify running condition.

However, since these diagnostic features are based on the measured AE amplitude the information they provide is inherently qualitative. For example the AE amplitude is a function not only of the intensity of source mechanism but also of the source-sensor transmission and the sensor response characteristics.

9.2.1 Conclusions Relating to AE Measurement Statistical Parameters

It was found that conventional time-domain statistical parameters such as RMS, mean and variance, for diesel engine AE signals served as good condition indicators.

Abnormal engine behaviour could be detected as these parameters deviated from baseline values which make these parameters suitable for online CM. However, two problems were found to be associated with the use of these parameters. They are sensitive to many different events from different sources and this often requires further investigation to attain a diagnosis. This drawback might be overcome, in certain circumstances, by signal averaging and/or using appropriate filtering. Frequency-domain analysis gives information concerning the frequency components of the measured AE signals and, because the energy content of these frequency components are dominated by the combustion event of the engine which, while it gives a good indication about the combustion process swamps other sources with a relatively much lower energy content. Certain frequency

bands are associated with certain engine events, i.e. piston slap excitations are in the frequency band of 15 to 35 kHz. Higher order statistics as Kurtosis is one of useful statistical parameter to give a quick indication of engine health.

9.2.2 Conclusions Relating to Time Representation

Conclusion 1: Engine operation conditions affect the AE intensity, generally, an increase in either engine speed or load leads to a corresponding increase in the AE. In terms of AE sources, increase in engine load appears to have a stronger effect than a corresponding increase in speed; this will increase the accuracy for fault detection such as small faults.

Conclusion 2: The variation of the AE peak amplitude with change of the amount of fuel injected into the cylinder relative to the healthy condition confirms a method for injector fault detection. Injector faults such as low pressure, high pressure and disconnected injector (misfire) can be clearly detected and diagnosed, and the cylinder where the fault is occurring can be identified. These types of faults can be easily identified on different cylinders with the same sensor position.

The detection of such faults avoid the engine running under faulty conditions which may lead to high fuel consumption, high levels of emissions, and increased engine noise and vibration which may lead to further mechanical problems.

Conclusion 3: The work has shown that a wide range of engine faults can be successfully detected and diagnosed using a limited number of sensors and simple time- and frequency-domain analysis of the AE wave. The time-domain analysis offers clear and powerful detection and diagnosis of most injector faults compared with frequency analysis which give a clear detection only in the case of a blocked injector.

Conclusion 4: It has been shown that for injector fault detection based on AE waveforms, the identifying feature in case of reducing injection pressure is an increase in the pressure peak in the cylinder due to increased fuel injected and timing change in the combustion process.

9.2.3 Conclusions Relating to Time-Frequency Representation

Time-frequency analysis techniques, whether linear or bilinear, are capable of presenting the results in either two or three dimensional plots in which the time, frequency and amplitude information can be observed. Unfortunately, in the case of diesel engine AE signals their capabilities are limited due to complexity of the signals. Based upon the results in Chapter 6, the CWT was found to be able to detect high frequency short time transient signals and its higher frequency range gives good condition monitoring information. It was applied to detect certain engine faults, because most of the engine faults occur as transient such as injection and piston slap impacts. These transients could be captured using the ability of CWT to capture impacts, and calculating the energy content of these transient impacts could be a good condition monitoring.

9.3 Overall Conclusions Regarding Monitoring of Diesel Engine

This work has established that continuous AE activity in the signals acquired from the cylinder block of a four-stroke diesel engine is related to sliding contact at the piston assembly liner contact.

Conclusion 1: Wear component would be expected to be a factor since the condition and profile of pistons are important elements that affect piston frictional behaviour.

Conclusion 2: A further concern from commercial application of AE monitoring may be the complexity and reliability of the AE measurement hardware. Experience gained from this project suggests that sensors of sufficient robustness for long-term application are available (wideband sensor was installed on engine for several running hours with no obvious deterioration in sensor construction or response). Moreover, piezoelectric type sensors are already applied on the cylinder block of some engines to detect the occurrence of knock conditions. A further issue is the sophistication of DAQ hardware required as the high sampling rate necessary for raw AE acquisition may be excessive for incorporation within a mixed sensor array. However, the use of RMS AE reduces the sampling frequency to a more acceptable level and this work has shown that such measurements are an adequate base from which to evaluate piston running condition.

Conclusion 3: The diagnostic information can be obtained without the need for intrusive measurements or expensive engine modifications. It therefore represents a new and promising

opportunity which may be of significant benefit to users of JCB heavy duty engine and one which complements existing monitoring systems.

Conclusion 4: In addition AE measurements can be made on an on-line basis and are therefore available for potential integration into engine management systems. This means that as well as early diagnosis of problems the information may be used to adjust operating conditions so as to optimise operating costs or component lifetimes.

9.4 Contribution to Knowledge

The work conducted by the author and described by this thesis included several aspects that are novel and not previously implemented by other researchers or practitioners. A summary of these aspects is given below.

Contribution 1: The author believes that the application of AE for detection and diagnosis of friction in heavy duty diesel engine faults is novel (Chapter 8). No work has been found in the literature that describes the use of the analysis for CM of heavy duty diesel engine using AE data, either experimentally or using a mathematical model.

Contribution 2: The author believes that the use of CWT techniques for the analysis of the acoustic emission spectrum for a heavy duty diesel engine monitoring for CM is novel (Chapter 7) as no reports in the literature have been found using CWT for fault detection and fault diagnoses for heavy duty diesel engine.

Contribution 3: The author believes that the application of lubrication monitoring by AE in order to detect piston slap intensity (Chapter 8) has not previously been employed for heavy duty diesel engine.

9.5 Recommendations for Future Work

Although diesel engine CM has been a topic of study over the past few years, it is still an open field and many problems have still to be resolved. This thesis has dealt with some of them, but the author identifies the following possible directions for future research. There are several areas in which further research is recommended, including aspects of dynamic modelling, signature recovery.

Recommendation 1: In the modern diesel engines major AE sources such as piston slap and combustion process are reasonably well understood and controlled. However, some minor sources such as wear due to decrease of oil film thickness, cavitation and lubrication blow by need to be modelled and a better understanding of these sources is required.

Recommendation 2: Integration of AE measurement based system with measurements taken directly from the engine, such as vibration and Instantaneous Angular Speed (IAS), could be very useful in building a reliable diesel CM system.

Recommendation 3: The investigations using the AE waveform predicted by the model could be extended to investigate the capabilities of piston cylinder bore friction coefficients as a function of axial position.

Recommendation 4: Induce scuffing conditions. In this work scuffing was not considered, therefore, although AE monitoring has been shown to be sensitive to changes in lubrication condition, the ability to detect scuffing cannot be confirmed. In order to induce scuffing the cylinder should be starved of lubricant for a longer period of time and action should be taken to prevent an oil mist entering the cylinder via the scavenge ports. If this fails to induce scuffing, water injection should be considered as a means to aid the removal of lubricating oil from the sliding surfaces.

Recommendation 5: Investigate Blind Source Separation and Independent Component Analysis techniques as possible new robust feature extraction methods.

Recommendation 6: The exploration of more advanced techniques such as AE classifications using neural networks to detect and diagnose engine faults at an early stage.

Recommendation 7: Combine the methods developed here with other CM methods, such as the noise from the engine system, to improve detection performance and increase information about the engine condition.

Recommendation 8: Test other diesel engines types, to see if trends occur in AE measurements, where engine size, injection type, turbo size are varying. These would be the transparent to AE to build-up online commercial system of AE for CM.

Recommendation 9: Investigation of how the findings of this work can be applied towards engine monitoring and management. This will likely involve the development of signal processing techniques to improve the accuracy, efficiency and robustness of the analysis. These may also be more amenable to automation and integration with engine management systems. Particular application is foreseen as an element of a cylinder lubrication control system for the purpose of optimising oil dosage rates.

Recommendation 10: Long-term testing over a wider range of engine and correlation with engine performance and maintenance activities would allow a knowledge archive to be developed of the changes in AE activity during the service life of a cylinder and piston and of the features which characterise various running conditions.

REFERENCES

- 1 Romberg T., Black J., Ledwidge T., 1996. Signal Processing for Industrial Diagnostics, John Wiley & Sons Ltd, ISBN 0 471 96166 3.
- 2 Hydrocarbon Processing Monthly Magazine, “Boutique Diesel in the On-road Market”. March 2006.
- 3 Gopinath, O. (1999). Diagnostic Classifier Ensembles: Enforcing Diversity for Reliability. PhD thesis, Sheffield University, UK.
- 4 Ball, A D., and Gu, F. (1995). A Basis for the Vibration monitoring of Diesel Fuel Injector, Journal of Maintenance, Vol. 10, No. 2, pp 24 - 30.
- 5 Claudio, A. H. (1994). Multi-sensor Approach to the Diagnostics of Reciprocating Compressor. PhD, thesis University of Arkansas at Little Rock.
- 6 Davies. A. (1998). Handbook of Condition Monitoring, Techniques and Methodology. Chapman & Hall, Thomson Science, London, UK, ISBN, 0 41261320 4.
- 7 Baydar, N, (2000). The Vibro-acoustic Monitoring of Gearboxes. Eng. D. Thesis, Manchester University, Manchester, UK.
- 8 SKF Condition Monitoring (1998). Utilising Vibration Monitoring as a planning Tool for a Predictive Maintenance Programme, Technical Paper, Denmark, & (CM101D).
- 9 Heinz, B., and John, J. (1996). Reciprocating Compressors, Operation & Maintenance. Butterworth-Heinemann, Gulf Company, Houston, TX. ISBN 0-88415-525-0.
- 10 Beattie A. G. (1983) “Acoustic emission principles and instrumentation”, J. Acoustic. Emission. , 2:95-128.6y.
- 11 Acoustic Emission Testing. Non-destructive Testing Handbook. American Society for Non-destructive Testing (ASNT). Vol. 6. Third Edition.
- 12 Chen, B., and Sperling, D., “Analysis of Auto Industry and Consumer Response to Regulation and Technological Change”, Case study of light duty vehicle in Europe. June 2004. Institute of Transportation Studies, University of California. UCD-ITS-RR-04-14
- 13 Automotive Industry Data, Warwick, CV34 4JP, UK (2010).
- 14 Health Effects Institute, “Diesel Exhaust: A Critical Analysis of Emissions, Exposure and Health Effects (A Special Report of Diesel Working Group)”, Health Effects Institute, Cambridge, MA. 1995.
- 15 Walzer, P., “Future Power Plants for Cars”, SAE Paper No: 2001-01-3192.
- 16 R. Gennish. Diesel engine performance and condition monitoring using exhaust gas pressure. PhD Thesis, Manchester University, 2007.
- 17 Stone R., 1999. Introduction to Internal Combustion Engines. Macmillian, 3th edition Pennsylvania.
- 18 Arques P., 1989. Parametrical Assessment of Damage for Diesel fuel Injection Systems. Seminar on Diesel Fuel Injection System of Institution of Mechanical Engineers. Birmingham Grande Bretagne.

- 19 Dilpiaz, G. and Rivola, A., 1997. Condition monitoring and diagnostics in automatic machines: Comparison of vibration analysis techniques. *Mechanical System and Signal Processing*, 11(1), 53-73.
- 20 Gu F., Ball A. D., 1995 Diesel Injector Dynamic Modelling and Estimation of Injection Parameters from Impact Response. Part 1: Modelling and Analysis of Injector Impacts. *Proc Institution of Mechanical Engineers. Proc Inst. Mech. Eng., Part D (J. Automob. Eng.)*, Vol. 210, pp. 293-302.
- 21 Gu F., Ball A. D., 1995. Diesel Injector Dynamic Modelling and Estimation of Injection Parameters from Impact Response. Part 2: Prediction of Injection Parameters from Monitored Vibration, *Proc Institution of Mechanical Engineers, Proc. Inst. Mech. Eng. , Part D (J. Automob. Eng.)*, Vol. 210, pp. 303-312.
- 22 Molinaro F., Castanie F. 1995. Signal Processing Pattern Classification Techniques to Improve Knock Detection in Spark Ignition Engines. *Mechanical Systems and Signal Processing*, Volume 9, Issue 1, January 1995, Pages 51-62.
- 23 Thomas J., Dubuisson B., 1997, Agens M., Peltier D., Engine Knock Detection from Vibration Signals Using Pattern Recognition, *International Journal of Mechanical* 32-5- pp. 431-439.
- 24 Grimmelius H., Meiler P., Maas H., Bonnier B., Grevink J., Kuilenburg R., 1999. Three State-of-the-Art Methods for Condition Monitoring. *IEEE Transactions on Industrial Electronics*, Vol. 46, no. 2, 1999.
- 25 Beck, J. Johnson, J. 1984. The Application of Analytical Ferrography and Spectroscopy to Detect Normal and Abnormal Diesel Engine Wear. *SAE paper 841371*.
- 26 Liu, Y. Liu, Z. Xie, Y. Yao, Z. 2000, Research on an On-line Wear Condition Monitoring System for Marine Diesel Engine. *Tribology International*, 33-12, Pages 829-835.
- 27 Galley. J.C. and Powel. J.D., "Fuel-air Ratio Determination from Cylinder Pressure Time Histories", *Transaction of the ASME*, 107, December 1985.
- 28 Gassenfeit, E.H. and Powel, J.D., "Algorithms for Air-Fuel Ratio Estimation using Neural Combustion Engine Cylinder Pressure", *SAE Paper No: 890300*, 1989.
- 29 Anastasia, C.M. and Pestana, G.W., "A Cylinder Pressure Sensor for Closed loop Engine Control", *SAE Paper No: 870288*, 1987.
- 30 Leonhardt, S., Ludwig, C. and Schwarz, R., "Real-time Supervision for Diesel Engine Injection Control", *Control Engineering Practice*, 3(7):1003-1010, 1995.
- 31 Fog, T.L., Larsen, J. and Hansen, L.K., "Training and Evaluation of Neural Networks for multivariate Time Series Processing", In *Proceedings of IEEE International Conference on Neural Networks*, Perth, Australia November 1995.
- 32 Kawamura, Y., Shinshi, M., Sato, H., Takahashi, M. and Iriyama, M., "Control through Individual Cylinder Pressure Detection" *SAE Paper No: 881779*, 1988.
- 33 Pestana, G.W., "Engine Control Methods using Combustion Pressure Feedback", *SAE Paper No: 890758*, 1989.
- 34 Russel, M.F. and Haworth, R., "Combustion Noise from High Speed Direct Injection Diesel Engines", *SAE Paper No: 850973*, 1985.

- 35 Ben Sasi, A., Albarbar, A., Soobramaney, P., Gu, F., Ball, A., 2003. Diesel Engine Condition Monitoring Using Instantaneous Angular Speed Extracted From the Alternator Output Voltage, COMDIT International Conference, Oxford, UK. 2003.
- 36 Sood, A., Frieland, C., Fahs, A., 1985. Engine Fault Analysis: Part I- Statistical Methods. IEEE Transactions on Industrial Electronics, IE-32(4), 294-300.
- 37 Sood, A., Fahs, A., Henein, N., Engine Fault Analysis: Part II- Parameter Estimation Approach. IEEE Transactions on Industrial Electronics, IE-32(4), 301-307, 1985.
- 38 Kim, Y., Rizzoni, G., Samimy, B., Wang, Y., 1995. Analysis and processing of Shaft Angular Velocity Signals in Rotating Machinery for Diagnostic Applications, IEEE International Conference on Acoustic Speech and Signal Processing USA, 5-2971-0749-8411.
- 39 Jianguo, Y., Lijun, P., Zhihua, W., Yichen Z., Xinping, Y., 2001. Fault Detection in a Diesel Engine by Analysing the Instantaneous Angular Speed Mechanical Systems and Signal Processing, 15-3,549-564.
- 40 Gu, F., Liu, S., Ball, A., 1999. The On-line Detection of Engine Misfire at Low Speed Using Multiple Feature Fusion with Fuzzy Pattern Recognition, Research Group Report, Maintenance Engineering Department, University of Manchester, UK.
- 41 Peters, R., 2002. Machine & Systems Condition Monitoring Series ‘‘The Noise & Acoustic Monitoring Handbook’’ First edition Coxmoor publishing company, ISBN 1 901892 04 2.
- 42 Mucklow, P., 1970. The Results of Two Tests Applying Acoustic Diagnosis to Gas Turbine Engines, Internal Report Rolls-Royce Ltd, Derby.
- 43 Schmillen, K., Wolschendorf, J., 1989. Cycle-to-Cycle Variations of Combustion Noise in Diesel Engines. SAE Paper 890129, 60-69.
- 44 Aouichi, A., Herrmann, M., 1989. Diesel Engine Noise and Internal Excitation Mechanisms, SAE, Paper, pp. 71-85, 890132.
- 45 Izumi, K., 1988. Research on Effects and Control of Noise in Japan, Journal of Sound and Vibration. 127(3), 401-404.
- 46 Chaudhri, R., 1991 Development and Application of Machine Health Monitoring Techniques for Reciprocating Machines, Proceeding of COMADEM, pp.475-479.
- 47 Ball, A. D, Gu, F. And Li, W., 2000, The Condition Monitoring of Diesel Engine using Acoustic Measurements--Part 2: Fault Detection and Diagnosis, SAE Technical Paper Series 2000-01-0368.
- 48 Gu, F., Li, W., Ball, A. D. And Leung, A. Y, 2000, The Condition Monitoring of Diesel engines using Acoustic Measurements--Part 1: Acoustic Modelling of the Engine and Representation of the Acoustic Characteristics, SAE Paper. 2000-01-0730.
- 49 Hadden, S., Hulls, L., Sutphin, E., 1976. Non-Contact Diagnosis of Internal Combustion Engine Faults Through Remote Sensing. SAE paper, 760146.
- 50 Gill, A., 1988. Design Choices for 1990S Low Emission Diesel Engines, SAE paper, 880350.
- 51 Khair, M., Bykowaski, B., 1992. Design and Development of Catalytic Converters for Diesels, SAE paper 921677.

- 52 Hartman, P., Plee, S., Bennethum, J., 1991. Diesel Smoke Measurement and Control Using an In-Cylinder Optical Sensor, SAER paper, 910723.
- 53 Klingen, H., Roth, P., 1991. Real-Time Measurements of Soot Particles at the Exhaust Valve of a Diesel Engine, SAE paper, 912667.
- 54 Corcione, F., Vaglieco, B., 1994. Cycle Resolved Measurements of Diesel Particulate by Optical Techniques, SAE paper, 941948.
- 55 Smallwood, G., Clavel, D., Gareau, Sawchuk, R., Snelling, D., Witze, P., Axelsson, B., Bachalo, W., Gulder, O., 2002 Concurrent Quantitative Laser-Induced Incandescence and Smps Measurements of EGR Effects on Particulate Emissions From a TDI Diesel Engine, SAE paper, 2002-01-2715.
- 56 Soliman, A., Rizzoni, G., Krishnaswami, V., 1995. The Effect of Engine Misfire on Exhaust Emission Levels in Spark Ignition Engines, SAE paper, 950480.
- 57 Holroyd, T., Randall, N., 1993. Use of Acoustic Emission for Machine Condition Monitoring, British Journal of NDT, 35(2).
- 58 Fog, T., Brown E., Hansen, H., Madsen, L., Sorensen, P., Hansen, E., Steel, J., Reuben, R., Pedersen, P., 1988. Exhaust Valve Leakage Detection in Large Marine Diesel Engines, 11th International Congress and Exhibition on Condition Monitoring and Diagnostic Engineering Management COMADEM, Launceston, Tasmania, 269-278.
- 59 El-Ghamary, M., Reuben, R., Steel, J., 2003. The Development of Automated Pattern Recognition and Statistical Feature Isolation Techniques for the Diagnosis of Reciprocating Machinery Faults Using Acoustic Emission, Journal of Mechanical Systems and Signal Processing, 17(4), 805-823.
- 60 Reuben, R. L. Role of acoustic emission in industrial condition monitoring. International Journal of COMADEM, 1998, 1(4), pp. 35-46.
- 61 Steel, J. A. and Reuben, R. L. Recent developments in monitoring of engines using acoustic emission. The Journal of Strain Analysis for Engineering Design, 2005, 40(1), pp. 45-57.
- 62 Pollock, A. A. Classical wave theory in practical AE testing. Progress in Acoustic Emission III – Japanese Society of Non-Destructive Testing, 1986, pp. 708-721.
- 63 Bagnoli, S., Capitani, R., Citti, P. Comparison of accelerometer and acoustic emission signals as diagnostic tools in assessing bearing damage. Proc. of 2nd Intl. Conference on Condition Monitoring, London, UK, 24-25th May 1988, 10, pp. 117-125.
- 64 Neill, G. D., Benzie, S., Gill, J. D., Sandford, P. M., Brown, E. R., Steel, J. A. and Reuben, R. L. The relative merits of acoustic emission and acceleration monitoring for the detection of bearing defects. Proc. 11th Intl. Conference on Condition Monitoring and Diagnostic Engineering Management, COMADEM, Launceston, Australia, 8-11 December 1998, pp. 651-661.
- 65 Tandon, N. and Choudhury, A. A review of vibration and acoustic measurement methods for the detection of defects in rolling element bearings. Tribology International, 1999, 32(8), pp. 469-480.
- 66 Fog, T. L. Condition monitoring and fault diagnosis in marine diesel engines. PhD Thesis, Danish Technical University, August 1998.

- 67 El-Ghamry, M. H., Brown, E. R., Ferguson, I., Gill, J. D., Reuben, R. L., Steel, J. A., Scaife, M. and Middleton, S. Gaseous air-fuel quality identification for a spark ignition gas engine using acoustic emission analysis. Proc. 11th Intl. Conference on Condition Monitoring and Diagnostic Engineering Management, COMADEM, Launceston, Australia, 8-11 December 1998, pp. 235-244.
- 68 Gill, J. D., Brown, E. R., Twite, M., Horner, G., Reuben, R. L. and Steel, J. A. Monitoring of a large reciprocating compressor. Proc. 11th Intl. Conference on Condition Monitoring and Diagnostic Engineering Management, COMADEM, Launceston, Australia, 8-11 December 1998, pp. 317-326.
- 69 Sikorska, J. Z. and Hodkiewicz, M. Comparison of acoustic emission, vibration and dynamic pressure measurements for detecting change in flow conditions on a centrifugal pump. Proc. 18th Intl. Congress on Condition Monitoring and Diagnostic Engineering Management, COMADEM, Cranfield, UK, 31 August-2 September 2005, pp. 171-181.
- 70 Singh, A., Houser, D. R. and Vijayakar, S. Early detection of gear pitting. Proc. of 7th ASME Intl. Power Transmission and Gearing Conference, San Diego, USA, 6-9 October 1996, 88, pp. 673-678.
- 71 Siores, E. and Negro, A. A. Condition monitoring of a gearbox using acoustic emission testing. Materials Evaluation, 1997, 52(2), pp. 183-187.
- 72 Tandon, N. and Mata, S. Detection of defects in gears by acoustic emission measurements. Journal of Acoustic Emission, 1999, 17(1-2), pp. 23-27.
- 73 Fog, T. L., Brown, E. R., Hansen, H. S., Madsen, L. B., Sorensen, P., Hansen, E. R., Steel, J. A., Reuben, R. L. and Pedersen, P. S. Exhaust valve leakage detection in large marine diesel engines. Proc. 11th Intl. Conference on Condition Monitoring and Diagnostic Engineering Management, COMADEM, Launceston, Australia, 8-11 December 1998, pp. 269-278.
- 74 Long, B. R. and Boutin, K. D. Enhancing the process of diesel engine condition monitoring. Proc. of the 18th Annual Fall Technical Conference of the ASME Internal Combustion Engine Division, Fairborn, USA, 20-23 October 1996, 27(1), pp. 61-68.
- 75 Autar, R. K. An automated diagnostic expert system for diesel engines. Transactions of the ASME: Journal of Engineering for Gas Turbines and Power, 1996, 118(3), pp. 673-679.
- 76 Sasaki, S. Vibration monitoring for wear condition of cylinder liner and piston ring in marine diesel engine. Proc. of 6th Intl. Symposium on Marine Engineering, ISME, Tokyo, Japan, 23-17 October 2000, 2, pp. 556-561.
- 77 Cole, P. and Gautrey, S. Acoustic emission experience with AE monitoring of new vessels during initial proof test. Proc. of 26th Conference on Acoustic Emission Testing, EWGAE, Berlin, Germany, 15-17 September 2004, pp. 75-81.
- 78 Rogers, L. M. Structural and engineering monitoring by acoustic emission methods – fundamentals and applications. Report: Lloyd's Register: Technical Investigation Department, 2001, 80 pages.
- 79 Paulson, P. O. Continuous acoustic monitoring of suspension bridges and cable stays. Structural Materials Technology III: An NDT Conference, Proc. of The Intl. Society for Optical Engineering, SPIE, San Antonio, USA, 31 March-2 April 1998, 3400(26), pp. 205-213.

- 80 Caneva, C., Pampallona, A. and Viskovic, S. Acoustic emission to assess the structural condition of bronze statues. Case of the “Nike” of Brescia. Proc. of 26th Conference on Acoustic Emission Testing, EWGAE, Berlin, Germany, 15-17 September 2004, pp. 567-574.
- 81 Schwalbe, H-J., Bamfaste, G. and Franke, R. P. Non-destructive and non-invasive observation of friction and wear of human joints and of fracture initiation by acoustic emission. Proc. of the IMechE, Part H; Journal of Engineering in Medicine, 1999, 213(1), pp. 41-48.
- 82 Rosner, S. and Kikuta, S. B. Ultrasound acoustic detection of cavitation events in water conducting elements of Norway spruce wood. Proc. of 26th Conference on Acoustic Emission Testing, EWGAE, Berlin, Germany, 15-17 September 2004, pp. 149-156.
- 83 West, D., Venkatesan, G., Tewfik, A., Buckley, K., and Kaveh, M. Detection and modelling of acoustic emissions for fault diagnostics. Proc. 8th IEEE Signal Processing Workshop on Statistical Signal and Array Processing, SSAP, Corfu, Greece, 24-26 June 1996, pp. 303-306.
- 84 Buckley, K., Venkatesan, G., West, D. and Kaveh, M. Detection and characterization of cracks for failure monitoring and diagnostics. Proc. IEEE Intl. Conference on Acoustics, Speech and Signal Processing, ICASSP, Atlanta, USA, 7-10 May 1996, pp. 2738-2741.
- 85 Gill, J. D., Reuben, R. L., Scaife, M., Brown, E. R. and Steel, J. A. Detection of diesel engine faults using acoustic emission. Proc. 2nd Intl. Conference: Planned Maintenance, Reliability and Quality, Oxford, England, 2-3 April 1998, 1, pp. 57-61.
- 86 Gill, J. D., Reuben, R. L., Steel, J. A., Scaife, M. W. and Asquith, J. A study of small HSDI diesel engine fuel injection equipment faults using acoustic emission. Journal of Acoustic Emission, 2000, 18, pp. 96-101.
- 87 Berjger, A. An investigation of acoustic emission in fuel injection. Proc. of 3rd European Conference of Young Research and Science Workers in Transport and Telecommunications, TRANSCOM, Žilina, Slovakia, 29-30 June 1999, 7, pp. 135-138.
- 88 Bialkowski, M. T., Pekdemir, T., Reuben, R. L., Brautsch, M., Towers, D. P. and Elsbett, G. Preliminary approach towards a CDI system modification operating on neat rapeseed oil. 31st Intl. Scientific Conference on Internal Combustion Engines, KONES, Wroclaw, Poland, 4-7 September 2005, 12(1-2), 14 p.
- 89 Godinez, V., Finlayson, R. D., Miller, R. K. and Carlos, M. F. AE characterization of cavitation and detonation in combustion engines. Proc. of Acoustic Emission Working Group Meeting, AEWG-43, Seattle, USA, 18-19 July 2000.
- 90 Frances, A. K., Gill, J. D., Reuben, R. L. and Steel, J. A. Practical application of AE monitoring to diesel engines. Proc. 17th Intl. Conference on Condition Monitoring and Diagnostic Engineering Management, COMADEM, Cambridge, UK, 23-25 August 2004, pp. 325-333.
- 91 Chandroth, G. O., Sharkey, A. J. C and Sharkey, N. E. Cylinder pressures and vibration in internal combustion engine condition monitoring. Proc. 12th Intl. Congress on Condition Monitoring and Diagnostic Engineering Management, COMADEM, Sunderland, UK, 7-9 July 1999, pp. 141-151.

- 92 Sharkey, A. J. C., Chandroth, G. O. and Sharkey, N. E. Acoustic emission, cylinder pressure and vibration: a multisensor approach to robust fault diagnosis. Proc. IEEE-INNS-ENNS Intl. Joint Conference on Neural Networks, Como, Italy, 24-27 July 2000, 6, pp. 223-228.
- 93 El-Ghamry, M., Steel, J. A., Reuben, R. L. and Fog, T. L. Indirect measurement of indicated power from diesel engines using acoustic emission. Mechanical Systems and Signal Processing, 2005, 19(4), pp. 751-765.
- 94 Grossmann, G. and Voss, A. Influence of the lube oil feed rate on the wear rate of liners of two stroke diesel engines. Proc. of the 21st Intl. Congress on Combustion Engines, CIMAC, Interlaken, Switzerland, 15 May 1995.
- 95 Randall, R. B., Ren, Y. and Ngu, H. Diesel engine cylinder pressure reconstruction. Proc. 21st Intl. Seminar of Modal Analysis (ISMA 23), Leuven, Belgium, 18-20 September 1996, 2, pp. 847-856.
- 96 Gao, Y. and Randall, R. B. Reconstruction of diesel engine cylinder pressure using a time domain smoothing technique. Mechanical Systems and Signal Processing, 1999, 13(5), pp. 709-722.
- 97 Zurita, G., Ågren, A., Randall, R. B. and Gao, Y. Reconstruction of cylinder pressure time trace on a six-cylinder engine from acceleration measurements. Proc. 23rd Intl. Seminar of Modal Analysis (ISMA 23), Leuven, Belgium, 10-12 September 1998, 3, pp. 1387-1394.
- 98 Gu, F., Jacob, P. J. and Ball, A. D. A RPF neural network model for cylinder pressure reconstruction in internal combustion engines. IEEE Colloquium on Modelling and Signal Processing for Fault Diagnosis, Leicester, UK, 18 September 1996, pp. 4/1-4/11.
- 99 Gu, F., Jacob, P. J. and Ball, A. D. Non-parametric models in the monitoring of engine performance and condition. Part 2: non-intrusive estimation of diesel engine cylinder pressure and its use in fault detection. Proc. of the IMechE Part D: Journal of Automotive Engineering, 1999, 213(2), pp. 135-143.
- 100 Citron, S. J., O'Higgins, J. E. and Chen, L. Y. Cylinder by cylinder engine pressure and pressure torque waveform determination utilizing speed fluctuations. SAE Intl. Congress and Exposition, Detroit, USA, 27 February - 3 March 1989, SAE Paper 890486, pp. 131-145.
- 101 Lida, K., Akishino, K. and Kido, K. IMEP estimation from instantaneous crankshaft torque variation. February 1990, SAE Paper 900617.
- 102 Brown, T. S. and Neill, W. S. Determination of engine cylinder pressures from crankshaft speed fluctuations. SAE Intl. Congress and Exposition, Detroit, USA, 22-26 February 1992, SAE Paper 920463, pp. 61-69.
- 103 Mauer, G. and Watts, R. J. On-line cylinder diagnostics on combustion engines by noncontact torque and speed measurements. SAE Intl. Congress & Exposition, Detroit, USA, 27 February - 3 March, 1989, SP-771-Sensor and Actuators, SAE Paper 890485, pp. 123-130.
- 104 Shimuza, T. Research for abnormal condition diagnosis on diesel engine. Proc. of 6th Intl. Symposium on Marine Engineering, ISME, Tokyo, Japan, 23-27 October 2000, 1, pp. 316-323.
- 105 Fog, T. L., Hansen, L. K., Larsen, J., Hansen, H. S., Madsen, L. B., Sørensen, P., Hansen, E. R. and Pedersen P. S. On condition monitoring of exhaust valves in marine diesel engines.

- Proc. IEEE Workshop on Neural Networks for Signal Processing IX, Piscataway, USA, 23-25 August 1999, pp. 554-563.
- 106 Friis-Hansen, A. and Fog, T. L. Monitoring exhaust valve leaks and misfire in marine diesel engines. Proc. 14th Intl. Conference on Condition Monitoring and Diagnostic Engineering Management, COMADEM, Manchester, UK, 4-6 September 2001, pp. 641-648.
 - 107 El-Ghamry, M., Reuben, R. L. and Steel, J. A. The development of automated pattern recognition and statistical feature isolation techniques for the diagnosis of reciprocating machinery faults using acoustic emission. Mechanical Systems and Signal Processing, 2003, 17(4), pp. 805-823.
 - 108 Frances, A. K., Gill, J. D., Reuben, R. L. and Steel, J. A. Investigation into identification of faults in small HSDI diesel engine using acoustic emission. Proc. of 26th Conference on Acoustic Emission Testing, EWGAE, Berlin, Germany, 15-17 September 2004, pp. 357-369.
 - 109 Frances, A. K., Gill, J. D., Reuben, R. L. and Steel, J. A. A study of the variability of acoustic emission signals from a medium size marine diesel engine under service conditions. Proc. 16th Intl. Congress on Condition Monitoring and Diagnostic Engineering Management, COMADEM, Växjö, Sweden, 27-29 August 2003, pp. 503-512.
 - 110 Gill, J. D., Douglas, R. M., Neo, Y. D., Reuben, R. L. and Steel, J. A. Examination of plate valve behaviour in a small reciprocating compressor using acoustic emission. Journal of Acoustic Emission, 2000, 18, pp. 96-101.
 - 111 Nivesrangsan, P. Multi-source, multi-sensor approaches to diesel engine monitoring using acoustic emission. PhD thesis, Heriot-Watt University, Edinburgh, UK, December 2004.
 - 112 Nivesrangsan, P., Steel, J. A. and Reuben, R. L. AE mapping of engines for spatially located time series. Mechanical Systems and Signal Processing, 2005, 19(5), pp. 1034-1054.
 - 113 Nivesrangsan, P., Steel, J. A. and Reuben, R. L. Acoustic emission mapping of diesel engines for spatially located time series – Part II: Spatial reconstitution. Mechanical Systems and Signal Processing. 2007, 21(2), pp. 1084-1102.
 - 114 Nivesrangsan, P., Steel, J. A. and Reuben, R. L. Source location of acoustic emission in diesel engines. Mechanical Systems and Signal Processing, 2007, 21(2), 1103-1114.
 - 115 Pontoppidan, N. H. and Sigurdsson, S. Independent components in acoustic emission energy signals from large diesel engines. Accepted for publication in International Journal of COMADEM, 2006.
 - 116 Sigurdsson, S., Pontoppidan, N. H. and Larsen, J. Supervised and unsupervised condition monitoring of non-stationary acoustic emission signals. Proc. 18th Intl. Congress on Condition Monitoring and Diagnostic Engineering Management, COMADEM, Cranfield, UK, 31 August - 2 September 2005, pp. 535-541.
 - 117 Pontoppidan, N. H. and Douglas, R. M. Event alignment, warping between running speeds. Proc. 17th Intl. Conference on Condition Monitoring and Diagnostic Engineering Management, COMADEM, Cambridge, UK, 23-25 August 2004, pp. 621-628.
 - 118 Pontoppidan, N. H. and Larsen, J. Non-stationary condition monitoring through event alignment. Proc. IEEE Workshop on Machine Learning for Signal Processing, MLSP, São Luís, Brazil, 29 September - 1 October 2004, pp. 499-508.

- 119 Pontoppidan, N. H. and Larsen, J. Unsupervised condition change detection in large diesel engines. Proc. 2003 IEEE Workshop on Neural Networks for Signal Processing, NSSP, Toulouse, France, 17-19 September 2003, pp. 565-574.
- 120 Pontoppidan, N. H., Larsen, J. and Fog, T.L. Independent component analysis for detection of condition changes in large diesels. Proc. 16th Intl. Conference on Condition Monitoring and Diagnostic Engineering Management, COMADEM, Växjö, Sweden, 27-29 August 2003, pp. 493-502.
- 121 Carlton, J. S. Techniques for ship and machinery failure investigation and performance assessment. Greek CIMAC Association Seminar, Athens, Greece, 3 April 2003.
- 122 Grabec, P. and Leskovar, P. Acoustic emission of a cutting process. Ultrasonic, 1977, 15 (1), pp. 17-20.
- 123 Iwata, K. and Moriwaki, T. Application of acoustic emission measurement to in-process sensing of tool wear. Annals of CIRP 26, 1977, 26(1-2), pp. 19-23.
- 124 Dornfeld, D. A. and Kannatey-Asibu, E. Acoustic emission during orthogonal metal cutting. International Journal of Mechanical Sciences, 1980, 22(5), pp. 285-296.
- 125 Saini, D. P. and Park, Y. J. A quantitative model of acoustic emissions in orthogonal cutting operations. Journal of Materials Processing Technology, 1996, 58(?), pp. 343-350.
- 126 Carolan, T. A., Kidd, S. R., Hand, D. P., Wilcox, S. J., Wilkinson, P., Barton, J. S., Jones, J. D. C. and Reuben, R. L. Acoustic emission monitoring of tool wear during face milling of steels and aluminium alloys using a fibre optic sensor. 1. Energy analysis. Proc. of the IMechE Part B2: Journal of Engineering Manufacture, 1997, 211(4) pp. 299-309.
- 127 Hwang, T. W., Whintont, E. P., Hsu, N. N., Hsu, Blessing, G. V. and Evans, C. J. Acoustic emission monitoring of high speed grinding of silicon nitride. Ultrasonic, 2000, 38(1-8), pp. 614-619.
- 128 Jayakumar, T., Mukhopadhyay, C. K., Venugopal, S., Mannan, S. L. and Raj, N. A review of the application of acoustic emission techniques for monitoring forming and grinding processes. Journal of Materials Processing Technology, 2005, 159(1), pp. 48-61.
- 129 Belyi, V. A., Kholodilov, O. V. and Sviridyonok, A. I. Acoustic spectrometry as used for the evaluation of tribological systems. Wear, 1981, 69(3), pp. 309-319.
- 130 McBride, S. L., Boness, R. J., Sobczyk, M. and Viner, M. R. Acoustic emission from lubricated and unlubricated rubbing surfaces. Journal of Acoustic Emission, 1989, 8(1-2), pp. 192-196.
- 131 Boness, R. J., McBride, S. L. and Sobczyk, M. Wear studies using acoustic emission techniques. Tribology International, 1990, 23(5), pp. 291-295.
- 132 Boness, R. J. and McBride, S. L. Adhesive and abrasive wear studies using acoustic emission. Wear, 1991, 149(1-2), pp. 41-53.
- 133 Jiaa, C. L. and Dornfeld, D. A. Experimental studies of sliding friction and wear via acoustic emission signal analysis. Wear, 1990, 139(2), pp. 403-423.
- 134 Hamchi, J. and Klamecki, B. E. Acoustic emission monitoring of the wear process. Wear, 1991, 145(1), pp. 1-27.
- 135 Klamecki, B. E. and Hanchi, J. Wear process description based on acoustic emission. Transactions of ASME: Journal of Tribology, 1990, 112(3), pp. 469-476.

- 136 Diei, E. N. Investigation of the milling process using acoustic emission signal analysis. PhD thesis, University of California, Berkeley, USA, 1985.
- 137 Lingard, S. and Ng, K. K. An investigation of acoustic emission in sliding friction and wear of metals. *Wear*, 1989, 130(2), pp. 367-379.
- 138 Lingard, S., Yu, C. W. and Yau, C.F. Sliding wear studies using acoustic emission. *Wear*, 1993, 162-164(1), pp. 597-604.
- 139 Mechefske, C. K. Monitoring sliding wear using acoustic emission. Proceedings of 14th Intl. Conference on Condition Monitoring and Diagnostic Engineering Management, COMADEM, Manchester, UK, 4-6 September 2001, pp. 57-65.
- 140 Boness, R. J. Measurements of wear and acoustic emission from fuel-wetted surfaces. *Wear*, 1993, 162-164(1), pp. 703-705.
- 141 Price, E. D., Lees, A. W. and Friswell, M. I. Detection of severe sliding and pitting fatigue wear regimes through the use of broadband acoustic emission. *Proc. of the IMechE, Part J; Journal of Engineering Tribology*, 2005, 219(2), pp. 85-98.
- 142 Shuster, M., Combs, D., Karrip, K. and Burke, D. Piston ring cylinder liner scuffing phenomenon studies using acoustic emission technique. *Proc. of CEC/SAE Spring Fuels & Lubricants Meeting and Exposition*, Paris, France, 2000, pp. 901-913.
- 143 Kita, T., Kogure, K., Mitsuya, Y. and Nakanishi, T. New method of detecting contact between floating-head and disk. *IEEE Transactions on Magnetics*, 1980, MAG-16(5), pp. 873-875.
- 144 Khurshudov, A. G. and Talke, F. E. A study of sub-ambient pressure tri-pad sliders using acoustic emission. *Transactions of ASME: Journal of Tribology*, 1998, 120(1), pp. 54-59.
- 145 Ravikiran, A., Low, T. S. Estimation of lubricant thickness on a magnetic hard disk using acoustic emission. *Review of Scientific Instruments*, 2000, 71(4), pp. 1915-1916.
- 146 Liew, T. Y. F., Chai, M. C., Weerasooriya, S. and Low, T. S. Head-disk interaction of proximity sliders studied by the acoustic emission probe, the dynamic height tester, and the laser Doppler vibrometer. *IEEE Transactions on Magnetics*, 1997, 33(5), pp. 3175-3177.
- 147 Zhu, Y-L., Liu, B., Li, Y-H., and Leng, Q-F. Slider-disk interaction and its effect on the flying performance of slider. *IEEE Transactions on Magnetics*, 1999, 35(5), pp. 2403-240.
- 148 Benson, R. C., Chiang, C. and Talke, F. E. The dynamics of slider bearings during contacts between slider and disk. *IBM Journal of Research and Development*, 1989, 33(1), pp. 2-14.
- 149 Ravikiran, A., Liew, T. and Low, T. S. Effect of disk acceleration on the generation of acoustic emission signal at the head-disk interface. *Journal of Applied Physics*, 1999, 85(8), pp. 5612-5614.
- 150 Liu, Y., Jiaa, C. L. and Eltoukhy, A. Acoustic emission study of lubricant effect on proximity contact recording. *IEEE Transactions on Magnetics*, 1997, 33(5), pp. 3160-3162.
- 151 Tanaka, H., Yonemura, S. and Tokisue, H. Slider dynamics during continuous contact with textured and smooth disks in ultra low flying height. *IEEE Transactions on Magnetics*, 2001, 37(2), pp. 906-911.
- 152 Sharma, V., Talke, F. E. and Ng, Q. Tribological investigations of tri-pad sliders. *IEEE Transactions on Magnetics*, 1996, 32(5), pp. 3651-3653.

- 153 Benson, R. C., Sundaram, R. and Talke, F. E. A study of the acoustic emission from slider/disk interface in a 5¼ inch hard disk drive. STLE Special Publication 25: Tribology and Mechanics of Magnetic Storage System, 1988, pp. 87-93.
- 154 Xu, J., Tokisue, H. and Kawakubo, Y. Study on soft-particle intrusion in a head/disk interface of load/unload drives. IEEE Transactions on Magnetics, 2000, 36(5), pp. 2745-2747.
- 155 Briggs, J. C., Chang, M-K., and Tse, M. K. High frequency slider vibrations during asperity impacts in rigid magnetic disk system. Advanced Information Storage Systems, 1992, 4, pp. 181-194.
- 156 Matsuoka, K., Taniguchi, K. and Nakakita, M. In-situ wear monitoring of slider and disk using acoustic emission. Transactions of ASME: Journal of Tribology, 2001, 123(1), pp. 175-180.
- 157 McMillan, T. C. and Talke, F. E. Identification of slider/disk contacts using the energy of the acoustic emission signal. IEEE Transactions of Magnetics, 1998, 34(4), pp. 1819-1821.
- 158 O'Brien, K. and Harris, D. Head/disk interface contact detection using a refined acoustic emission technique. ASME: Journal of Tribology, 1996, 118(3), pp. 539-542.
- 159 Ganapathi, S. K., Donovan, M. and Hsia, Y. T. Contact force measurements at the head/disk interface for contact recording heads in magnetic recording. Proc. of the SPIE- The International Society for Optical Engineering, 1996, 2604, pp. 236-243.
- 160 Matsuoka, K., Forrest, D. and Tse, M. K. On-line wear monitoring using acoustic emission. Wear, 1993, 162-164(1), pp. 605-610.
- 161 Matsuoka, K., Taniguchi, K. and Ueno, Y. Evaluation technique of head/tape contact using acoustic emission. ASME: Journal of Tribology, 1996, 120(2), pp. 259-265.
- 162 Bhushan, B., Wu, Y. and Tambe, N. S. Sliding contact energy measurement using a calibrated acoustic emission transducer. IEEE Transactions on Magnetics, 2003, 39(2), pp. 881-887.
- 163 Toutountzakis, T. and Mba, D. Observation of acoustic emission activity during gear defect diagnosis. NDT and E International, 2003, 36(7), pp. 471-477.
- 164 Tan, C. K. and Mba, D. The source of acoustic emission during meshing of spur gears. Proc. of 26th Conference on Acoustic Emission Testing, EWGAE, Berlin, Germany, 15-17 September 2004, pp. 469-474.
- 165 Tan, C. K. and Mba, D. Identification of the acoustic emission source during a comparative study on diagnosis of a spur gearbox. Tribology International, 2005, 38(5), pp. 469-480.
- 166 Sentoku, H. AE in tooth surface failure process of spur gears. Journal of Acoustic Emission, 1998, 16(1-4), pp. S19-S24.
- 167 Toutountzakis, T. Tan, C. K. and Mba, D. Application of acoustic emission to seeded gear fault detection. NDT&E International, 2005, 38(1), pp. 27-36.
- 168 Miettinen, J. and Siekkinen, V. Acoustic emission in monitoring sliding contact behaviour. Wear, 1995, 181-183(2), pp. 897-900.
- 169 Ferguson, I. G., Gill, J. D., Reuben, R. L., Steel, J. A., Brown, E. R. and Roosch, E. Condition monitoring of rotating seals using acoustic emission. Proc. of the 23rd European

- Conference on Acoustic Emission testing, EWGAE, Vienna, Austria, 6-8 May 1998, pp. 281-286.
- 170 Douglas, R. M., Beugné, S., Jenkins, M. D., Frances, A. K., Steel, J. A., Reuben R. L. and Kew, P. A. Monitoring of gas turbine operating parameters using acoustic emission. Proc. of 26th Conference on Acoustic Emission Testing, EWGAE, Berlin, Germany, 15-17 September 2004, pp. 455-466.
 - 171 Sato, I. Rotating machinery diagnosis with acoustic emission techniques. Electrical Engineering in Japan, 1990, 100(2), pp. 115-127.
 - 172 Board, D. B. Stress wave analysis of turbine engine faults. Proc. IEEE Aerospace Conference, Big Sky, USA, 18-25 March 2000, 6, pp. 79-95.
 - 173 Hall, L. D. and Mba, D. Diagnosis of continuous rotor-stator rubbing in large scale turbine units using acoustic emissions. Ultrasonic, 2004, 41(9), pp. 765-783.
 - 174 Miettinen, J. The influence of the running parameters on the acoustic emission of grease lubricated rolling bearings, Maintenance & Asset Management, 2001, 16(2), pp. 7-11.
 - 175 Miettinen, J. and Andersson, P. Acoustic emission of rolling bearings lubricated with contaminated grease. Tribology International, 2000, 33(11), pp. 777-787.
 - 176 Miettinen, J., Andersson, P. and Wikström, V. Analysis of grease lubrication of rolling bearings using acoustic emission measurement. Proc. of the IMechE Part J: Journal of Engineering Tribology. 2001, 215(6), pp. 535-544.
 - 177 Dornfeld, D. and Handy, C. Slip detection using acoustic emission signal analysis. Proc. of 1987 IEEE Intl. Conference on Robotics and Automation, Raleigh, USA, 30 March - 3 April 1987, pp. 1868-1875.
 - 178 R.M. Douglas, P. Nivesrangsan, A.I.F. Robertson, E.R. Brown, J.A. Steel, R.L. Reuben and T.L. Fog. Acoustic Emission as a Tool to Reveal Diesel Injector Performance. In Rao et al. [2004], pages 316–324. ISBN 0-9541307-1-5.
 - 179 G.D. Neill, S. Benzie, J.D. Gill, P.M. Sandford, E.R. Brown, J.A. Steel, and R.L. Reuben. The relative merits of acoustic emission and acceleration monitoring for detection of bearing faults. COMADEM, 1998.
 - 180 T. Fog, L.K. Hansen, J. Larsen, H.S. Hansen, L.B. Madsen, P. Sørensen, E.R. Hansen and P.S. Pedersen. On condition monitoring of exhaust valve in marine diesel engines. In Y. H. Hu, J. Larsen, E. Wilson, and S. Douglas, editors, Proceedings of the IEEE Workshop on Neural Networks for Signal Processing IX, pages 225–234, Piscataway, New Jersey, 1999. IEEE.
 - 181 AEWATT Project Consortium. Deliverable 3, specification of preliminary sensor array. Technical report, 2003b.
 - 182 P. Nivesrangsan, J.A. Steel, R.L. Reuben, Acoustic emission mapping of diesel engine for spatially located time series, Mechanical System and Signal Processing 19 (2005)1034-1054.
 - 183 H.L. Dunegan. A New Acoustic Emission Technique for Detecting and Locating Growing Cracks in Complex Structures. Technical Report 5, DECI Inc., San Juan Capistrano, CA, US, May 2000.
 - 184 Stepanishen, P. (1998). Transient Radiation. pp 119-126. In: Crocker, M. J. ed. Handbook of Acoustics. New York: John Wiley & Sons, ISBN 047125293X.
 - 185 Cho S. H., Ahn, S. T. Kim Y. H 2002, “A simple model to estimate the impact force induced by piston slap”, Journal of sound and vibrations, vol.255, pp. 229-242.

- 186 Ungar E.E. and Ross D. 1965 Vibration and noise due to piston slap in reciprocating machinery, *Journal of Sound and Vibrations*, 2, 132-146, 1965.
- 187 Griffiths W. J., Skorecki J. 1964. Some aspects of vibration of a single cylinder diesel engine, *Journal of sound and vibration* 1,345-364.1964.
- 188 Fielding, B. j. and Skorecki, J., 1969, Identification of mechanical sources of noise in a diesel engine, *Proceedings of the institute of Mechanical Engineers*, 184,859-874.1969.
- 189 Haddad S. 1995 "Theoretical treatment of piston motion in I.C. piston engine for the prediction of piston slap excitation", *Mech. Mach. Theory*, Vol. 30, No. 2, pp. 253-269.
- 190 Haddad S., Tjan K. T., 1995,"An analytical study of offset piston and crankshaft designs and the effect of oil film on piston slap excitation in a diesel", *Mech. Mach. Theory*, Vol. 30, No. 2, pp. 271-284.
- 191 D' Agostino V., Guida D., Ruggiero A. 2000 "A Four Stroke Engine Friction Model, *Proc. Of Amietri Int. Tribology Conference, AITC, L'Aquila, Italy*.
- 192 Lewis, R. Dwyer-Joyce R. S. and Josey, G. Investigation of wear mechanisms occurring in passenger car diesel engine inlet valves and seat inserts. *SAE paper 1999-01-1216*, 1999.
- 193 Lewis, R., Dwyer-Joyce, R. S. and Josey, G. Design and development of a bench test-rig for investigating diesel engine inlet valve and seat wear. *Trans. Mech. Eng-IE Aust*, 2000, 24(1), 39-46.
- 194 Lewis, R., Dwyer-Joyce, R. S. An experimental approach to solving valve and seat inserts wear problems. *Proceedings of the 27th Leeds-Lyon Symposium on Tribology*, Elsevier Tribology Series No. 39, 2001 (Elsevier, Amsterdam), pp. 629-640.
- 195 Wang, Y. S., Narasimhan, S., Larson, J. M., Larson, J. E. and Barber, G. C. The effect of operating conditions on heavy duty engine valve seat wear. *Wear*, 1996, 201, 15-25.
- 196 Pope, J. Techniques used in achieving a high specific airflow for high-output medium-speed diesel engines. *Trans. ASME, J. Engng for Power*, 1967, 89, 265-275.
- 197 Bradbury, C.H. "The Measurement and Interpretation of Machinery Noise with Special Reference to Oil Engines" *Proc. Inst. Mech. Engrs.*, 1952-53, Vol.1B, pp.1-18.
- 198 Mercy, K.R. "Analysis of the Basic Noise Sources in the Diesel Engine ", *A.S.M.E. Paper No.55-OGP-4*, March 1955.
- 199 McGeehan, J. A., 1978, "Literature Review of the Effects of Piston Ring Friction and Lubricating Oil Viscosity on Fuel Economy," *SAE Paper 780673*.
- 200 Rogowski, A. R., 1961, "Method of Measuring the Instantaneous Friction of Piston Friction of Piston Rings in a Firing Engine," *SAE Paper 379F*.
- 201 Cleveland, A. E. and Bishop, I. N., 1960 "Several Possible Paths to Improved Part-load Economy of Spark-Ignition Engines, " *SAE Paper 150A*.
- 202 Bishop, I. N., 1965, "Effect of Design Variables on Friction and Economy," *SAE Paper 812A*.
- 203 Ricardo, H. and Hempson, J. G. G., 1968, *The High Speed Internal Combustion Engine*, 5th ed., Blackie, London, pp. 139-141.
- 204 Ting, L. L., 1985, "A Review of Present Information on Piston Ring Tribology," *SAE Paper 852355*.
- 205 Patton, K. J., Nitschke, R. G., and Heywood, J. B., 1989, "Development and Evaluation of a Friction Model for Spark-Ignition Engines," *SAE Paper 890836*.
- 206 Kovach, J. T., Tsakiris, E. A., and Wong, L. T., 1982, "Engine Friction Reduction for Improved Fuel Economy," *SAE Paper 820085*.
- 207 Hami, K., et al., 1990, "Development of a Friction Prediction Model for High Performance Engines," *Lubr. Eng.*, 47, No. 7, pp. 567-573.

- 208 Winterbone, D. E., and Tennant, D. W. H., 1981, "The Vibration of Friction and Combustion Rates During Diesel Engine Transients," SAE Paper 810339.
- 209 Wade, W. R., et al., 1984, "Combustion, Friction and Fuel Tolerance Improvements for the IDI Diesel Engine," SAE Paper 840515.
- 210 Cullen, J. A., Dixon, R. F., and Ma, J., 1996, "Plastic Oil Rings for Diesel Engines: A Preliminary Evaluation," SAE Paper 960049.
- 211 Taylor, C. M., 1991, "Valve Train Lubrication Analysis," Vehicle Tribology, Proc. 17th Leeds-Lyon Symposium on Tribology, Elsevier, Amsterdam, pp. 119–131.
- 212 Ball, W. F., Jackson, N. S., Pilley, A. D., and Porter, B. C., 1986, "The Friction of a 1.6 Liter Automotive Engine-Gasoline and Diesel," SAE Paper 860418.
- 213 Baniasad, M. S. and Emes, M. R., 1998, "Design and Development of Method of Valve-Train Friction Measurement," SAE Paper 980572.
- 214 Craig, R. C., King, W. H., and Appeldoorn, J. K. Oil film thickness in bearing of a fired engine, part II: the bearing, as a capacitor. SAE paper 821250, 1982.
- 215 Choi, J. K., Lee, J. H., and Han, D. C. Oil film thickness in engine main bearings: comparison between calculation and experiment by total capacitance method. SAE paper 922345, 1992.
- 216 Choi, J. K., Min, B. S., and Han, D. C. Effect of oil aeration rate on the minimum oil film thickness and reliability of engine bearing. SAE paper 932785, 1993.
- 217 Bates, T. W. and Benwell, S. Effect of oil Rheology on journal bearing performance part 3 – Newtonian oils in the connecting rod bearing of an operating engine. SAE paper 880679, 1988.
- 218 Filowitz, M. S., King, W. H., and Appeldoorn, J. K. Oil film thickness in a bearing of a fired engine. SAE paper 820511, 1982.
- 219 Bates, T. W., Williamson, J. A., Spearot, J. A., and Murphy, C. K. A correlation between engine oil rheology and oil film thickness in engine journal bearing. SAE paper 860376, 1986.
- 220 Spearot, J. A. and Murphy, C. K. A comparison of the total capacitance and total resistance techniques for measuring the thickness of journal bearing oil operating engine. SAE paper 880680, 1988.
- 221 Suzuki, S., Ozasa, T., Yamamoto, M., Nozawa, Y., Noda, T., and Ohori, M. bearings. Temperature distribution and lubrication characteristics of connecting rod big end SAE paper 953550, 1995.
- 222 Choi, J. K., Min, B. S., and Han, D. C. Effect of oil aeration rate on the Minimum oil film thickness and reliability of engine bearing. SAE paper 932785, 1993.
- 223 Choi, J. K., Min, B. S., and Oh, D. Y. A study on the friction characteristics of engine bearing and cam/tappet contacts from the measurement of temperature and oil film thickness. SAE paper 952472, 1995.
- 224 Cho, M. R., Han, D. C., and Choi, J. K. Oil film thickness in engine connecting rod bearing with consideration of thermal effects: comparison between theory and experiment. ASME J. Tribol. 1999, 121, 901–907.
- 225 Irani, K., Pekkari, M., and Angstrom, H. E. Oil film thickness measurement in the middle main bearing of a six-cylinder supercharged 9 litre diesel engine using capacitive transducers. Wear, 1997, 29–33.
- 226 Masuda, T. A measurement of oil film pressure distribution in connecting rod bearing with test rig. Tribol. Trans., 1992, 35(1), 71–76.
- 227 Schilowitz, A. M. and Waters, J. L. Oil film thickness in a bearing of a fired engine – part IV: measurements in a vehicle on the road. SAE paper 861561, 1986.

- 228 Mihara, Y., Hayashi, T., Nakamura, M., and Someya, T. Q5 Development of measuring method for oil film pressure of engine main bearing by thin film sensor. JSAE, 1995, 125–130.
- 229 Helena, R., Antti, V., Simo, V., Ari, H., Markku, K., Ingmar, S., Juha, V., Ari, L., and Juhani, M. Oil film pressure measurement in journal bearing tests by using an optical sensor. 35th Leeds-Lyon Symposium on Tribology, Leeds, 2008.
- 230 Warrens, C., Jefferies, A. C., Mufti, R. A., Lamb, G. D., Guiducci, A. E., and Smith, A. G. Effect of oil rheology and chemistry on journal-bearing friction and wear. Proc. IMechE, Part J: J. Engineering Tribology, 2007, 222(J3), 441–450.
- 231 Mufti, R. A., Warrens, C., Lamb, G. D., and Jefferies, A. C. Effect of oil formulation on engine journal bearing performance. Additive 2007, Application for future transport, London, UK, 2007.
- 232 Mufti, R. A., Warrens, C., Lamb, G. D., Guiducci, A. E., and Jefferies, A. C. Effect of viscosity modifiers on the Q6 bearing load carrying capacity of crankcase lubricants. In Proceedings of the IMechE Tribology 2006: Surface Engineering and Tribology for Future Engines and Drivelines, London, UK, 2006.
- 233 Tanaka, M. Journal bearing performance under starved lubrication. Tribol. Int., 2000, 33, 259–264.
- 234 Cerrato, R., Gozzelino, R., and Ricci, R. A single cylinder engine for crankshaft bearings and piston friction losses measurement. SAE paper 841295, 1984.
- 235 Syverud, T. Experimental investigation of the temperature fade in the cavitation zone of full journal bearings. Tribol Int., 2001, 34, 859–870.
- 236 Sinanoglu, C., Nair, F., and Karamis, M. B. Effects of shaft surface texture on journal bearing pressure distribution. J. Mater. Process. Technol., 2005, 168, 344–353.
- 237 Sorab, J., Korce, S., Brower, C. L., and Hammer, W. G. Friction reducing potential of low viscosity engine oils in bearings. SAE paper 962033, 1996.
- 238 Tseregounis, S. I., Viola, M. B., and Paranjpe, R. S. Determination of bearing oil film thickness (BOFT) for various engine oils in an automotive gasoline engine using capacitance measurements and analytical predictions. SAE paper 982661, 1998.
- 239 Unlu, B. S. and Atik, E. Determination of friction coefficient in journal bearings. J. Mater. Des., 2007, 28, 973–977.
- 240 Stewart, R. M., and Selby, T. W., 1977, “The Relationship between Oil Viscosity and Engine Performance-A Literature Search” SAE Paper 770372.
- 241 Cullen, J. A., and Frodsham, G. A., 1997, “Reduced Cross Section Compression Rings for Diesel Engines,” SAE Paper 971146.
- 242 Yang, S. L. Siow, Y. K., Teo, C. Y. Numerical Study of LDI Combustor with Discrete jet swirlers using Reynolds stress Model. J. Engineering for Gas and Turbine Power, July 2003.
- 243 F. Gu, A.D. Ball, Diesel injector dynamic modelling and estimation of injection parameters from impact response. Part I; modelling and analysis of injector impacts, Proceedings of the Institution of Mechanical Engineers, Part D: Journal of Automobile Engineering 210 (4) (1996) 293-302.
- 244 F. Gu, A.D. Ball, K.K. Rao, Diesel injector dynamic modelling and estimation of injection parameters from impact response. Part II: prediction of injection parameters from monitored vibration, Proceedings of the Institution of Mechanical Engineers, Part D: Journal of Automobile Engineering 210 (4) (1996) 303-312.

- 245 J.D. Gill, R.L. Reuben, J.A. Steel, A study of small HSDI diesel engine fuel injection equipment faults using acoustic emission, in: proceedings of the EWGAE 2000, 24th European Conference on Acoustic Emission Testing, Paris, May 2000, pp.281-286.
- 246 Jeng, Y.-R. Theoretical analysis of piston ring lubrication. Part I-fully flooded lubrication. STLE, Tribology Trans., 1992, 35(4), 707-714.
- 247 Miller, R.K. and McIntire, P., Acoustic Emission Testing, Vol. 5, 2nd Ed. Non-destructive Testing Handbook, American Society for Non-destructive Testing, 1987, pp. 275-310.
- 248 Miller, R.K. and McIntire, P., Acoustic Emission Testing, Vol. 5, 2nd Ed. Non-destructive Testing Handbook, American Society for Non-destructive Testing, 1987, pp. 417-443.
- 249 Brown, E. R., Reuben, R. L., Neill, G. D. and Steel, J. A. Acoustic emission source discrimination using a piezopolymer based sensor. Materials Evaluation, 1998, 57(5), pp. 515-520.
- 250 Hsu, N. N., Simmons, J. A. and Hardy, S. C. An approach to acoustic emission signal analysis – theory and experiment. Materials Evaluation, 1977, 35(10), pp. 100-106.
- 251 Hsu, N. N. and Breckenbridge, F. R. Characterisation and calibration of acoustic emission sensors. Materials Evaluation, 1981, 39(1), pp. 60-68.
- 252 Beattie, A. G. and Jaramillo, R. A. The measurement of energy in acoustic emission. Review of Scientific Instruments, 1974, 45(3), pp. 352-357.
- 253 Bagnoli, S., Capitani, R., Citti, P. Comparison of accelerometer and acoustic emission signals as diagnostic tools in assessing bearing damage. Proc. of 2nd Intl. Conference on Condition Monitoring, London, UK, 24-25th May 1988, 10, pp. 117-125.
- 254 Welch, P.S.D. The use of fast Fourier transform for the estimation of power spectra: a method based on time averaging over short, modified periodograms. IEEE Transactions Audio Electro acoustics, 1967, Vol. AU-15, pp. 70-73.
- 255 Newland, D. E. (1994a) Wavelet analysis of vibration, Part 2: wavelet map. Journal of Vibration and Acoustics, Vol.116, 417-425.
- 256 Newland, D. E. (1994b) Wavelet analysis of vibration, Part I: theory. Journal of Vibration and Acoustics, Vol.116, 409-416.
- 257 Peng, Z. K. & CHU, F. L. (2004) Application of the wavelet transform in machine condition monitoring and fault diagnostics: a review with bibliography. Mechanical System and Signal Processing, Vol.18, 199-221.
- 258 Qi, G. (2000) Wavelet-based AE characterization of composite materials. NDT & E International, 33, 133.
- 259 Jeong, H. (2001) Analysis of plate wave propagation in anisotropic laminates using a wavelet transform. NDT & E International, Vol.34, 185-190.
- 260 Ding, Y., Reuben, R. L. & Steel, J. A. (2004) A new method for waveform analysis for estimating AE wave arrival times using wavelet decomposition. NDT & E International, 37, 279-290.
- 261 J. P. Ryan. Impact analysis of piston slap in a spark ignition engine. Master Thesis, Massachusetts Institute of Technology, August 1993.
- 262 Dursunkaya, Z., Keribar, R. and Ganapathy. V. (1994), A Model of Piston Secondary Motion and Elastohydrodynamic Skirt Lubrication, Journal of Tribology, Transactions of the ASME, 116 (4), 777-785.
- 263 Myoungjin Kim, Friction Force Measurement and Analysis of the Rotating Liner Engine. PhD Thesis, University of Texas, August 2005.

- 264 Nakada, M., "Piston and Piston Ring Tribology and Fuel Economy," Proceedings of Internal Tribology Conference, Yokohama, 1993.
- 265 Haddad, S. D. And Howard, D. A., "Analysis of Piston-Induced Noise and Assessment of Some Methods of Control in Diesel Engines," SAE Paper 800517, 1980.
- 266 Ohta, K., Irie Y., Yamamoto, K., and Ishikawa, H., "Piston Slap Induces Noise and Vibration of Internal Combustion Engines (1st Report, Theoretical Analysis and Simulation), "SAE Paper 870990, 1987.
- 267 Amann, C. A., "Engineering the Spark Ignition Engine System—The Piston Rings Cylinder Wall Interface," Prepared for the XXII FISITA Congress, Dearborn, MI/ Washington, D. C., September 25-30, 1988.
- 268 Rohrl, M., "Affecting Diesel Engine Noise by the Piston," SAE Paper 750799, 1979.
- 269 Whitacre, J.P., "Automotive Gasoline Engine Piston Noise, Sources and Solutions, "SAE paper 901491, 1990.
- 270 Vora, K. C., and Ghosh, B., " Vibration Due to Piston Slap and Combustion in Gasoline and Diesel Engines, "SAE Paper 911060, 1991.
- 271 Patir, N. and Cheng, H. S., (1978), An Average Flow Model for Determining Effects of Three-Dimensional Roughness on Partial Hydrodynamic Lubrication, Journal of Lubrication Technology, Transactions of the ASME, 100,12-17.
- 272 Zhu, D., Cheng, H. S., Arai, T. and Hamai, K. (1992), Numerical Analysis for Piston Skirt in Mixed Lubrication. Part I: Basic Modelling, Journal of Tribology, Transactions of the ASME, 114 (3), 553-562.
- 273 Zhu, D., Cheng, H. S., Arai, T. and Hamai, K. (1993), Numerical Analysis for Piston Skirt in Mixed Lubrication. Part II: Deformation Considerations, Journal of Tribology, Transactions of the ASME, 115, 125-133.
- 274 Ball, A D. (2000). Reciprocating Engines and Compressors. Maintenance Engineering M12, section 11, Course Notes, University of Manchester, Manchester, England.
- 275 Li, D.F, Rhode, S.M, and Ezzat, H.A., "An Automotive Piston Lubrication Model," ASLE Transactions, Vol. 26, No. 2, pp. 151-160, 1983.
- 276 L. Moughon. Effects of piston design and lubricant selection on reciprocating engine friction. Master Thesis, Massachusetts Institute of Technology, Jun 2006.
- 277 Namazian, M., and Heywood, J.B., "Flow in the Piston-Cylinder-Ring Crevices of a Spark Ignition Engine: Effect on Hydrocarbon Emissions, Efficiency and Power." SAE 820088, 1982.
- 278 Bruel & Kjaer., Transducer & Conditioning, Company Catalogue, Spectres Group, Denmark, 1997
- 279 National Instrument Company, "Lab Windows/CVI User Manual, Version 5.5. Internet", London, UK, 2000.
- 280 Physical Acoustic Corporation, PCI-2 based AE system user's manual, 2003, pp 27.
- 281 Chiollaz M., Faver B., 1993. Engine Noise Characterisation with Wigner-Ville Time-Frequency Analysis. Journal of Mechanical Systems and Signal Processing. 75,375-400.
- 282 Hong, Z., Bing, H., 2004. Analysis of Engine Front Noise Using Sound Intensity Techniques. Mechanical Systems and Signal Processing Journal, 19(2005) 213-221.
- 283 Richard, B., Heiberger, H., Heiberger, R., Holland, B., 2004 An Introduction to Statistical Methods and Data Analysis. Duxbury, fourth edition. ISBN: 0387402705.
- 284 Heywood, J.B. 1998. Internal Combustion Engines Fundamentals, Mc Graw Hill International Edition, Singapore.

- 285 Wowk, V., 1991. Machinery Vibration Measurement and Analysis. McGraw Hill.
- 286 Bendat, J., 1995. The Hilbert Transform and Applications to Correlation Measurements. Bruel & Kjaer Naerum, Denmark.
- 287 Teraguchi, S., Suzuki, W., Takiguchi M., 2001. Effects of Lubricating Oil Supply on Reductions of Piston Slap Vibration and Piston Friction, SAE Technical Paper Series 2001-01-0566.
- 288 D.Singh, N.Singh, A.K.Jain, V.K.Chibber & Mukesh Saxena, "Effect of Engine Oil Viscosity on Fuel Economy", Paper presented and published in proceedings of 5th International Conference on Industrial Tribology-06, Indian Institute of Science, Bangalore (IISc), 30th Nov- 2nd Dec 2006.
- 289 Fiona McClure Numerical Modelling of Piston Secondary Motion and Skirt Lubrication in Internal Combustion Engines. PhD Thesis, Massachusetts Institute of Technology. September 2007.